

<https://doi.org/10.15388/vu.thesis.172>

<https://orcid.org/0000-0003-3628-6373>

VILNIUS UNIVERSITY

CENTER FOR PHYSICAL SCIENCES AND TECHNOLOGY

Tadas

BARTULEVIČIUS

# Compact high pulse energy fiber laser systems for industrial and scientific applications

**DOCTORAL DISSERTATION**

Natural Sciences,

Physics (N 002)

---

VILNIUS 2021

This dissertation was written between 2016 and 2020 at the Department of Laser Technologies of the Center for Physical Sciences and Technology and the company Ekspla. The research was supported by the Research Council of Lithuania.

**Academic supervisor:**

**Dr. Andrejus Michailovas** (Center for Physical Sciences and Technology, Natural Sciences, Physics, N 002).

**Dissertation Defence Panel:**

**Chairman – Dr. Gediminas Račiukaitis** (Center for Physical Sciences and Technology, Natural Sciences, Physics, N 002).

**Members:**

**Assoc. Prof. Dr. Rytis Butkus** (Vilnius University, Natural Sciences, Physics, N 002).

**Prof. Dr. Artūras Jukna** (Vilnius Gediminas Technical University, Natural Sciences, Physics – N 002).

**Dr. Mangirdas Malinauskas** (Vilnius University, Natural Sciences, Physics, N 002).

**Prof. Dr. Valdas Pašiškevičius** (KTH Royal Institute of Technology, Natural Sciences, Physics – N 002).

The dissertation shall be defended at a public meeting of the Dissertation Defence Panel at 15:00 on 7th June 2021 in the hall of FTMC Institute of Physics.

Address: Savanoriu Ave. 231, LT-02300 Vilnius, Lithuania

Tel. +370 5 264 8884; e-mail: [office@ftmc.lt](mailto:office@ftmc.lt)

The text of this dissertation can be accessed at the libraries of Center for Physical Sciences and Technology and Vilnius University, as well as on the website of Vilnius University:

[www.vu.lt/lt/naujienos/ivykiu-kalendorius](http://www.vu.lt/lt/naujienos/ivykiu-kalendorius)

<https://doi.org/10.15388/vu.thesis.172>

<https://orcid.org/0000-0003-3628-6373>

VILNIAUS UNIVERSITETAS  
FIZINIŲ IR TECHNOLOGIJOS MOKSLŲ CENTRAS

Tadas  
BARTULEVIČIUS

# Kompaktiškos didelės impulsų energijos šviesolaidinės lazerinės sistemos industriniams ir moksliniams taikymams

**DAKTARO DISERTACIJA**

Gamtos mokslai,  
Fizika (N 002)

---

VILNIUS 2021

Disertacija rengta 2016–2020 metais Fizinių ir technologijos mokslų centro Lazerinių technologijų skyriuje ir kompanijoje Ekspla. Mokslinius tyrimus rėmė Lietuvos mokslo taryba.

**Mokslinis vadovas:**

**Dr. Andrejus Michailovas** (Fizinių ir technologijos mokslų centras, gamtos mokslai, fizika, N 002).

**Gynimo taryba:**

**Pirmininkas – dr. Gediminas Račiukaitis** (Fizinių ir technologijos mokslų centras, gamtos mokslai, fizika, N 002).

**Nariai:**

**Doc. dr. Rytis Butkus** (Vilniaus universitetas, gamtos mokslai, fizika, N 002).

**Prof. dr. Artūras Jukna** (Vilniaus Gedimino technikos universitetas, gamtos mokslai, fizika, N 002).

**Dr. Mangirdas Malinauskas** (Vilniaus universitetas, gamtos mokslai, fizika, N 002).

**Prof. dr. Valdas Pašiškevičius** (Švedijos Karališkasis technologijų institutas, gamtos mokslai, fizika, N 002).

Disertacija ginama viešame Gynimo tarybos posėdyje 2021 m. birželio mėn. 7 d. 15:00 val. FTMC Fizikos instituto salėje.

Adresas: Savanorių pr. 231, LT-02300 Vilnius, Lietuva

Tel. +370 5 264 8884; el. paštas: office@ftmc.lt

Disertaciją galima peržiūrėti Fizinių ir technologijos mokslų centro bei Vilniaus universiteto bibliotekose ir VU interneto svetainėje adresu:

<https://www.vu.lt/naujienos/ivykiu-kalendorius>

# CONTENTS

CONTENTS.....	5
ACKNOWLEDGEMENTS.....	8
LIST OF ABBREVIATIONS.....	9
INTRODUCTION.....	10
SCIENTIFIC NOVELTY.....	13
PRACTICAL VALUE.....	13
STATEMENTS TO DEFEND.....	14
AUTHOR'S CONTRIBUTION.....	15
CO-AUTHORS' CONTRIBUTION.....	15
SCIENTIFIC PAPERS.....	16
PATENTS.....	17
CONFERENCE PRESENTATIONS.....	17
THE STRUCTURE OF THE THESIS.....	18
CHAPTER ONE.....	20
1.1 Literature review.....	20
1.1.1 Ultrashort pulse generation in fiber oscillators.....	20
1.1.2 Control of ultrashort pulse spectral characteristics.....	25
1.1.3 Laser technologies for fiber chirped pulse amplification systems.....	29
1.2 High-quality femtosecond pulses from a compact FCPA system based on a CFBG stretcher and CVBG compressor with matched dispersion profiles.....	32
1.2.1 Ultrashort pulse generation in all-in-fiber oscillator and nonlinear pulse spectrum broadening.....	32
1.2.2 Experimental fiber chirped pulse amplification system.....	34
1.2.3 Precise dispersion compensation between CFBG and CVBG.....	36
1.2.4 Characterization of experimental ultrashort pulse FCPA system.....	38
Summary of the results.....	40
CHAPTER TWO.....	42
2.1 Literature review.....	42
2.1.1 High-energy and moderate average power fiber lasers.....	42

2.1.2 Compressed ultrashort pulse quality enhancement and techniques for nonlinear phase-shift compensation .....	44
2.1.3 The influence of photodarkening effect in fiber amplifiers .....	49
2.2 Compact high-energy and moderate average power FCPA system .....	50
2.2.1 Experimental FCPA system based on a CFBG stretcher and CVBG compressor with matched dispersion profile.....	50
2.2.2 Examination of ultrashort pulses and nonlinear phase-shift compensation by applying second-order and third-order dispersion.....	54
2.2.3 Characterization of high-energy ultrashort pulses delivered from FCPA system .....	58
2.2.4 High-energy FCPA system optimized for solid-state Yb:YAG amplifier ....	60
2.2.5 Optimization of a single-mode fiber amplifier configuration and minimization of photodarkening effect.....	61
Summary of the results .....	65
CHAPTER THREE.....	67
3.1 Literature review.....	67
3.1.1 Fiber technology for high-power applications .....	67
3.1.2 High-power fiber laser systems .....	72
3.1.3 Sophisticated techniques for realization of extremely-high average power levels in fiber laser systems.....	74
3.1.4 High-power high pulse repetition rate FCPA systems .....	77
3.2 The realization of high-power FCPA systems .....	78
3.2.1 High-power FCPA system with LMA fiber power amplifier operating in a single-pulse regime .....	79
3.2.2 Pulse repetition rate multiplier and GHz burst formation.....	82
3.2.3 High-power GHz intra-burst repetition rate FCPA system with LMA fiber power amplifier .....	85
Summary of the results .....	91
CHAPTER FOUR.....	93
4.1 Literature review.....	93
4.1.1 Applications of the laser systems generating high repetition rate bursts of laser pulses .....	93
4.1.2 Techniques providing high repetition rate bursts of laser pulses .....	96

4.2 The development of the technique to synthesize ultra-high PRR burst of ultrashort pulses .....	100
4.2.1 The description and operation of the active fiber loop .....	101
4.2.2 FCPA system with implemented active fiber loop .....	105
4.2.3 The demonstration of 217 GHz intra-burst PRR burst.....	108
Summary of the results .....	109
CONCLUSIONS.....	110
SANTRAUKA .....	112
Ižanga .....	112
Mokslinis naujumas .....	114
Praktinė nauda.....	115
Ginamieji teiginiai.....	116
Autoriaus indėlis .....	117
Diskusija ir rezultatų apžvalga.....	117
Kompaktiška FCPA sistema, naudojanti CFBG impulsų plėstuvą ir CVBG impulsų spaustuvą su suderintais dispersijos profiliais.....	117
Kompaktiškas didelės energijos femtosekundinis šviesolaidinis lazeris su CFBG impulsų plėstuvu ir CVBG impulsų spaustuvu .....	120
Didelės vidutinės galios šviesolaidinis lazeris .....	123
Gigahercinio impulsų pasikartojimo dažnio ultratrumpųjų impulsų paketų sintezavimo metodas .....	124
Išvados .....	126
CURRICULUM VITAE .....	128
About the author .....	128
Apie autorių .....	128
BIBLIOGRAPHY .....	129
COPIES OF PUBLICATIONS.....	148

## ACKNOWLEDGEMENTS

First of all, I am most grateful to my academic supervisor Dr. Andrejus Michailovas for providing excellent conditions for the research and work at laser manufacturing company Ekspla.

I express my gratitude to former academic advisor Dr. Nerijus Rusteika for sharing his experience and consultation for the big part of my studies.

Special thanks to Dr. Rokas Danilevičius for being the first person to read the draft of my thesis, consulting me and giving me valuable insights into my work.

Thanks to Virginija Petrauskienė for the aid examining the literature and considerate remarks during the preparation of the scientific publication.

Thanks to my fellows and colleagues Karolis Madeikis and Laurynas Veselis for the remarkable time spent together these past years of PhD studies. I really appreciated your company and it will never be forgotten!

Thanks to my colleagues Dr. Karolis Viskontas, Raimundas Burokas, Aivaras Kazakevičius and the rest of the group at Ekspla for the friendly atmosphere and pleasant conversations at coffee breaks.

Last but certainly not least, I want to thank my parents, Birutė and Linas, who taught me from an early age to seek for the highest goals in life, brother Tomas and my lovely fiancée Agnė for unconditional love and support. Thanks to you, this work has reached the light of day.

## LIST OF ABBREVIATIONS

AOM	acousto-optic modulator
ANDi	all-normal dispersion
ASE	amplified spontaneous emission
AWG	arbitrary waveform generator
ACF	autocorrelation function
CCC	chirally-coupled core
CFBG	chirped fiber Bragg grating
CPA	chirped pulse amplification
CVBG	chirped volume Bragg grating
DPA	divided-pulse amplification
FCPA	fiber chirped pulse amplification
FTL	Fourier transform-limited
FROG	frequency-resolved optical gating
FWHM	full width half maximum
GD	group delay
GDD	group delay dispersion
GVD	group velocity dispersion
YDF	ytterbium-doped fiber
YAG	yttrium aluminum garnet
LMA	large-mode-area
LPF	large-pitch fiber
OPO	optical parametric oscillators
PCF	photonic crystal fiber
PTR	photo-thermo-refractive
PRR	pulse repetition rate
SHG	second harmonic generation
SPM	self-phase modulation
SESAM	semiconductor saturable absorber mirror
TEC	thermoelectric cooler
TOD	third-order dispersion
TMI	transverse mode instability
VBG	volume Bragg grating
WDM	wavelength-division multiplexer

## INTRODUCTION

Fiber lasers have number of features that differentiate them from the other laser technologies and give superior performance. Fiber lasers provide good thermal management and allows efficient cooling due to high surface area to volume ratio. Waveguide properties of the fiber reduce or eliminate thermal distortion typically resulting in an excellent beam quality. Inhomogeneously broadened active-ion emission and absorption spectra produced by the amorphous nature of the glass host enables fiber lasers to be wavelength-tunable and operate from continuous-wave operation to ultra-short pulse generation. Low transmission losses, small quantum defect and high gain makes fiber lasers suitable for average power scaling to multi-kW level in the single transverse mode regime [1] and reaching record wall-plug efficiencies [2,3]. Furthermore, versatile fiber technology allows compact designs of the fiber lasers because most common fibers can be bent and coiled.

Fiber laser sources are attractive for a wide array of applications in science and industry due to aforementioned optical fiber properties. In industry high-power fiber lasers are mostly used for various material processing, such as welding, drilling and cutting, they are kW-level continuous wave [4] or Q-switched lasers, generating intense nanosecond pulses [5]. Many applications in metrology as precision optical ranging [6] or pump-probe experiment [7] involving time-dependent phenomena require short pulse durations. Microscopic methods based on two-photon or multi-photon excitation fluorescence for imaging biological tissues require ultrashort pulse duration and relatively low nJ-level pulse energy [8,9]. Similar laser radiation, in terms of pulse duration and energy level, is used for the generation of broadband surface-emitted THz radiation [10].

However, a number of advanced applications are demanding higher average powers of tens of Watts and pulse energies from tens to hundreds of  $\mu\text{J}$  from these ultrashort pulse sources, e.g., laser material micro-processing [11], nonlinear spectroscopy [12], generation of X-ray radiation [13] and efficient parametric wavelength conversion [14,15]. Average power scaling of the laser can be achieved by the implementation of high-power pump source modules and novel gain media designs [16] or coherent combination of the laser beams [17].

Different fiber laser systems operating at high-power levels from continuous wave regime to ultrashort pulses face different effects limiting the output laser parameters. High energy operation in ultrashort fiber lasers

is limited due to small saturation energy and relatively small fiber core diameters compared to solid-state laser counterparts. The design of fiber lasers delivering high peak-power pulses is challenging due to the impact of nonlinear effects, arising from long interaction length and small mode area of the gain fibers, which limit the amplification of ultrashort optical pulses in fiber amplifiers. Self-phase modulation is the most dominant nonlinear effect originated from the optical Kerr-effect. Other nonlinear effects such as self-focusing and Raman scattering must be avoided together with self-phase modulation to prevent from undesired pulse distortions. To mitigate these detrimental effects in solid-state lasers the chirped pulse amplification (CPA) technique was proposed [18].

The combination of chirped pulse amplification and large mode area fibers may be employed in ultrashort pulse fiber laser systems which produce record-high pulse energies of around 1 mJ [19]. Recently, a fiber-based ultrafast CPA system has been demonstrated delivering 10.4 kW average output power and maintaining ultrashort pulse duration of 254 fs after the pulse compression [20]. It demonstrated the feasibility of realization of high-power fiber-based CPA system utilizing coherent beam combining and with the potential to derive average-power scalability of this technology up to 100 kW level suitable for future applications in particle acceleration [21,22]. That was the highest average-power realized by ultrafast laser system to the date of the publication. Constantly, new records of the average power and pulse energy of the radiation generated by the fiber lasers are achieved by improving fiber technology, developing new methods and avoiding detrimental nonlinear effects.

One of the main goals of this thesis was to build a compact and robust high energy  $\mu\text{J}$ -level femtosecond fiber chirped pulse amplification (FCPA) system utilizing a core-pumped single-mode polarization-maintaining Yb-doped fiber amplifier and operating at 1.03  $\mu\text{m}$  center wavelength. Special attention was paid to maintain a compact laser design realizing all-in-fiber laser configuration and a novel FCPA scheme based on a chirped fiber Bragg grating stretcher and a small foot print chirped volume Bragg grating compressor. The dispersion profiles of chirped fiber Bragg grating stretcher and chirped volume Bragg grating compressor were matched in order to realize high fidelity transform-limited ultrashort laser pulses at the output of the system. The aim of this work was the optimization of the fiber CPA system and the compensation of the accumulated nonlinear phase-shifts of  $>1$  rad which is the conventional nonlinear limit for traditional CPA systems in order to achieve high temporal quality femtosecond pulses. The mitigation

of photodarkening effect, recognized as the limiting factor on the lifetime and reliability of fiber amplifiers pumped with high intensity radiation, was investigated in this work both numerically and experimentally. Gathered experience was used for the realization of a high-power ultrashort pulse fiber lasers. Pulse energy extracted directly from large-mode-area fiber amplifier has a sufficiently clear technological limit, due to the fact that the fiber core cannot be enlarged as much as desired. Thus, laser operating regimes that imitate higher pulse energies by generating burst of pulses, were developed and demonstrated first in MHz burst regime [23], later in GHz intra-burst regime [24]. The development of new method allowing the expansion of the regimes of the laser operation generating gigahertz repetition rate bursts of pulses is presented in this thesis. This invention may open new avenues in science and industry.

## SCIENTIFIC NOVELTY

The scientific novelty of this work lies on the successfully demonstrated laser technologies which allowed the realization of compact fiber chirped pulse amplification systems generating high-energy ultrashort pulses and burst of pulses:

1. A compact fiber chirped pulse amplification system exploiting a tandem of a chirped fiber Bragg grating stretcher and a chirped volume Bragg grating compressor with matched dispersion profiles, realizing high fidelity transform-limited ultrashort laser pulses at the output of the system was proposed and experimentally demonstrated. Such high quality of compressed ultrashort pulse temporal profile using this pulse stretching/compression configuration was achieved for the first time. This configuration of fiber chirped pulse amplification system opens path to truly compact and robust high-energy femtosecond fiber lasers.
2. High pulse energy (10  $\mu\text{J}$ ) was achieved from a compact environmentally stable all-in-fiber chirped pulse amplification system utilizing an optimized core-pumped single-mode hybrid fiber amplifier consisting of ytterbium doped fibers with different concentrations.
3. The realization of high-power ultrashort pulse fiber laser generating gigahertz repetition rate bursts of pulses was based on the implementation of the pulse repetition rate multiplier of cascaded fiber couplers and large-mode-area cladding-pumped Yb-doped fiber power amplifiers, which allowed to expand the regimes of the laser operation and thus to increase the pulse/burst energies and to scale the average output power.
4. A new method to synthesize ultra-high repetition rate bursts of ultrashort laser pulses containing any number of pulses within a burst with identical pulse separation and adjustable amplitude was presented and experimentally demonstrated for the first time.

## PRACTICAL VALUE

The improvement of fiber technologies and development of new techniques enable the creation of novel laser architectures and realization of compact,

robust and environmentally stable ultrashort pulse fiber lasers. Furthermore, the newly developed methods allow to expand the regimes of the laser operation and the application of such laser sources. The implementation of high-energy ultrashort pulse fiber lasers has a great demand in science and industry.

This work has a practical value in several aspects:

1. Evident ultrashort pulse temporal quality improvement in fiber chirped pulse amplification system based on the use of a chirped fiber Bragg grating stretcher and a chirped volume Bragg grating compressor with matched dispersion profiles allows to implement this technology to laser systems manufactured by the company Ekspla.
2. The optimization of fiber amplifiers and the achievement of high pulse energy allowed to implement fiber laser as a seed source in a high-power high-energy system based on a hybrid fiber and solid-state laser technologies in the company Ekspla.
3. A novel method to synthesize ultra-high repetition rate bursts of laser pulses was successfully demonstrated and enabled the development of laser systems suitable for laser material micro-processing applications and pumping wavelength-tunable laser systems.

## STATEMENTS TO DEFEND

- S1. The exploit of dispersion elements (fiber chirped Bragg grating stretcher and chirped volume Bragg grating compressor) with matched dispersion profiles in a fiber chirped pulse amplification system enables the generation of high fidelity laser pulses of a duration less than 300 fs at high compression ratio of  $\sim 1100$ .
- S2. A single-mode fiber amplifier consisting of two different concentrations and lengths ytterbium doped fibers enables the minimization of a photodarkening effect in a fiber amplifier and realization of very high 10  $\mu\text{J}$  pulse energy and 26 MW peak power compact femtosecond fiber chirped pulse amplification system despite the accumulated large  $> 1\pi$  rad nonlinear phase-shift.
- S3. The realization of gigahertz intra-burst repetition rates, the formation of the bursts and the control of the shape of the burst amplitude envelope allows to expand the regimes of the laser operation and thus to increase the pulse/burst energies, from 1.5  $\mu\text{J}$  in single-pulse

operation regime to 30  $\mu\text{J}$  in burst regime, produced by the high-power fiber laser utilizing single-mode cladding-pumped large-mode-area (11  $\mu\text{m}$  core diameter) Yb-doped fiber power amplifier.

- S4. Ultra-high repetition rate ( $>2$  GHz) bursts of ultrashort laser pulses containing any number of pulses in a burst with identical pulse separation and adjustable amplitude can be synthesized using a new method based on the use of an active fiber loop.

### AUTHOR'S CONTRIBUTION

Author constructed all laser systems described in A1-A4 articles, P1 patent and contributed to experimental investigation preparing P2 patent. The author suggested valuable ideas and performed the realization of the experimental setups presented in A3 publication, proposed technical solutions for development of the new method to synthesize ultra-high repetition rate bursts of ultrashort laser pulses described in A4 article and P1 patent. The author prepared the manuscripts of A1-A4 articles. Furthermore, author performed numerical simulations and theoretical analysis of the research presented in the proposed articles and this thesis.

### CO-AUTHORS' CONTRIBUTION

- Dr. Andrejus Michailovas was a supervisor of the author's PhD studies, provided excellent conditions for the research and suggested significant ideas for the work published in A4 article and organized the process of P1 and P2 patenting.
- Dr. Nerijus Rusteika suggested ideas and organized the research published in A1 and A2 articles. Furthermore, Nerijus provided consultation and shared his experience for the big part of the PhD studies.
- Dr. Saulius Frankinas was an initiator of experimental investigations of fiber chirped pulse amplification systems using chirped fiber Bragg grating stretcher and chirped volume Bragg grating compressor. Saulius advised on experimental work presented in A1.
- Vadim Smirnov and Ruslan Vasilyeu shared their expertise and insights about chirped volume Bragg grating technology presented in A1.

- Dr. Francois Trepanier supervised the manufacturing process of chirped fiber Bragg grating which was matched to chirped volume Bragg grating and provided experimentally measured group delay traces of a chirped volume Bragg grating and a chirped fiber Bragg grating presented in A1.
- Virginija Petrauskienė examined the literature review presented in A4 publication. Also, Virginija has done valuable work in making the descriptions of P1 and P2 patents.
- Dr. Rokas Danilevičius programmed a source code of theoretical methods used in modelling software which was further developed by the author of this thesis. Rokas advised on various numerical simulation issues.
- PhD stud. Karolis Madeikis and PhD stud. Laurynas Veselis advised on various issues of laser technology and shared their experience in performing experimental work.

## SCIENTIFIC PAPERS

Publications related to the topic of the thesis:

- A1. **T. Bartulevicius**, S. Frankinas, A. Michailovas, R. Vasilyeu, V. Smirnov, F. Trepanier, and N. Rusteika, “Compact fiber CPA system based on a CFBG stretcher and CVBG compressor with matched dispersion profile,” *Opt. Express* **25**, 19856-19862 (2017). DOI: 10.1364/OE.25.019856.
- A2. **T. Bartulevicius**, L. Veselis, K. Madeikis, A. Michailovas, and N. Rusteika, “Compact femtosecond 10  $\mu$ J pulse energy fiber laser with a CFBG stretcher and CVBG compressor,” *Opt. Fiber Technol.* **45**, 77-80 (2018). DOI: 10.1016/j.yofte.2018.06.006.
- A3. **T. Bartulevičius**, K. Madeikis, L. Veselis, A. Michailovas, “Compact high-power GHz intra-burst repetition rate all-in-fiber CPA system with LMA fiber power amplifier,” *Proc. SPIE* **11260**, 112602F (2020). DOI: 10.1117/12.2545665.
- A4. **T. Bartulevicius**, K. Madeikis, L. Veselis, V. Petrauskiene, and A. Michailovas, “Active fiber loop for synthesizing GHz bursts of equidistant ultrashort pulses,” *Opt. Express* **28**, 13059-13067 (2020). DOI: 10.1364/OE.389056.

Other publications:

- A5. S. Frankinas, **T. Bartulevicius**, A. Michailovas, N. Rusteika, “Investigation of all-in-fiber Yb doped femtosecond fiber oscillator for generation of parabolic pulses in normal dispersion fiber amplifier,” *Optical Fiber Technology* **36**, 366–369 (2017). DOI: 10.1016/j.yofte.2017.05.012.
- A6. L. Veselis, **T. Bartulevicius**, K. Madeikis, A. Michailovas, and N. Rusteika, “Compact 20 W femtosecond laser system based on fiber laser seeder, Yb:YAG rod amplifier and chirped volume Bragg grating compressor,” *Opt. Express* **26**, 31873-31879 (2018). DOI: 10.1364/OE.26.031873.

## PATENTS

- P1. A. Michailovas, **T. Bartulevicius**, *Method for generating gigahertz bursts of pulses and laser apparatus thereof*. International publication number: WO 2021/059003 A1.
- P2. A. Michailovas, K. Madeikis, **T. Bartulevicius**, *Lazeris netiesinei mikroskopijai*. Application number: LT2020 526.

## CONFERENCE PRESENTATIONS

- C1. **T. Bartulevičius**, L. Veselis, K. Madeikis, A. Michailovas, and N. Rusteika, “Compact High Energy Femtosecond Fiber Laser with a CFBG Stretcher and CVBG Compressor,” 18th International Conference on Laser Optics “ICLO 2018”, St. Petersburg, Russia, June 4-8, 2018 (oral presentation).
- C2. **T. Bartulevičius**, L. Veselis, K. Madeikis, A. Michailovas, and N. Rusteika, “Compact High Energy Femtosecond Fiber Laser Source with a CFBG Stretcher and CVBG Compressor for Microfabrication Applications,” 19th International Symposium on Laser Precision Microfabrication “LPM 2018”, Edinburgh, Scotland, June 25-28, 2018 (poster presentation).
- C3. **T. Bartulevičius**, L. Veselis, K. Madeikis, A. Michailovas, and N. Rusteika, “The Optimization of Pulse Compression for Compact High Energy Femtosecond Fiber Laser with CVBG Compressor,” 8th EPS-QEOD Europhoton Conference “Solid-State, Fibre and Waveguide Coherent Light Sources“, Barcelona, Spain, September 2-7, 2018 (poster presentation).

- C4. **T. Bartulevičius**, L. Veselis, K. Madeikis, A. Michailovas, N. Rusteika, “Kompaktiškas didelės impulsų energijos femtosekundinis šviesolaidinis lazeris su čirpuotos šviesolaidinės Brego gardelės plėstuvu ir čirpuotos tūrinės Brego gardelės spaustuvu,” annual Conference of FTMC PhD Students and Young Researchers FizTech 2018, Vilnius, Lithuania, October 17-18, 2018 (oral presentation).
- C5. **T. Bartulevičius**, L. Veselis, K. Madeikis, A. Michailovas, and N. Rusteika, “The Optimization of Compact High Energy Fiber CPA System for Bio-Imaging Applications,” CLEO® / Europe – EQEC, Munich, Germany, June 23-27, 2019 (poster presentation).
- C6. **T. Bartulevičius**, L. Veselis, K. Madeikis, A. Michailovas, “The Optimization of Compact High Energy Fiber CPA System for Bio-Imaging Applications,” Siegman International Summer School on Lasers 2019, Rochester, United States, July 27 – August 03, 2019 (poster presentation).
- C7. **T. Bartulevičius**, L. Veselis, K. Madeikis, A. Michailovas, “Kompaktiško didelės impulsų energijos femtosekundinio šviesolaidinio lazerio parametrų optimizavimas,” 43-oji Lietuvos nacionalinė fizikos konferencija “LNFK 43”, Kaunas, Lithuania, October 3-5, 2019 (oral presentation).
- C8. **T. Bartulevičius**, L. Veselis, K. Madeikis, A. Michailovas, “Gigahercinių impulsų paketų realizacija šviesolaidiniame lazeryje,” annual Conference of FTMC PhD Students and Young Researchers FizTech 2019, Vilnius, Lithuania, October 23-24, 2019 (oral presentation).
- C9. **T. Bartulevičius**, K. Madeikis, L. Veselis, A. Michailovas, “Compact high-power GHz intra-burst repetition rate all-in-fiber CPA system with LMA fiber power amplifier,” SPIE LASE 2020, San Francisco, United States, February 1-6, 2020 (poster presentation).

## THE STRUCTURE OF THE THESIS

The material of the thesis is divided into 4 main parts. First, literature review related to the topic of the research is presented at the beginning of each chapter. Chapter 1 is dedicated to a realization of a compact fiber chirped pulse amplification system. An approach of high-energy fiber laser demonstration is presented in Chapter 2. Chapter 3 is devoted to high-power fiber lasers and the expansion of the regimes of the laser operation by a generation of ultra-high repetition rate bursts of ultrashort laser pulses.

Finally, a new method to synthesize ultra-high repetition rate bursts of ultrashort laser pulses is described in Chapter 4.

## CHAPTER ONE

The literature review of this chapter is dedicated to discuss of proposed and mostly used methods, configurations and technologies for ultrashort pulse generation in ytterbium-doped fiber oscillators. The control of spectral characteristics and spectral shaping techniques of ultrashort pulses in single-mode fibers are also introduced. Furthermore, the implementation of chirped pulse amplification technique and different technological approaches for pulse stretching and compression in fiber laser systems are reviewed.

The experimental realization of ultrashort pulse generation and amplification in fiber chirped pulse amplification system utilizing a chirped fiber Bragg grating stretcher and a chirped volume Bragg grating compressor with matched dispersion profiles is presented in the experimental section of this chapter.

### 1.1 Literature review

#### 1.1.1 Ultrashort pulse generation in fiber oscillators

Ultrashort laser pulses can be generated in ytterbium-doped fiber oscillators initiating passive mode-locking and realizing two mostly used cavity designs of Fabry-Perot (linear) type [25] and fiber ring configuration [26]. A new type of fiber oscillator, so-called Mamyshev oscillator, was recently proposed and quickly attracted the interest of the researchers [27,28].

Passive mode-locking in fiber ring configuration of fiber oscillators can be achieved by employing fiber-optic nonlinear effect as the nonlinear polarization rotation phenomenon [29] or implementing a nonlinear amplifying fiber loop mirror [26,30]. During the evolution of the nonlinear polarization rotation, the peak and the wings of the pulses exhibit different transmission levels due to different polarization states which leads to the intensity discrimination and narrowing of the pulse. Thus, an artificial saturable absorber is formed using nonlinear polarization rotation effect together with a polarizer in the fiber ring setup. This absorber is very fast, as nonlinear polarization rotation is originated from optical Kerr effect, and suitable for the passive mode-locking of ultrashort laser pulses.

Another type of artificial absorber is based on the use of a nonlinear amplifying fiber loop mirror in which the amplification, shaping and stabilization of a circulating ultrashort pulses are performed [26,30]. In this

case, main fiber loop is connected with a nonlinear amplifying fiber loop mirror by a fiber coupler to form a figure-of-eight cavity. The fiber coupler divides the pulse into two equal replicas that propagate in a loop in opposite directions. These two pulse replicas accumulate different nonlinear phase shift due to different level of the pulse amplification. A sufficiently large phase shift occurs for pulses of certain peak power and after one round-trip in the loop these pulses interfere at the coupler and are not returned to the original but transmitted to the other output of the coupler. In this way a nonlinear amplifying fiber loop mirror behaves as an artificial saturable absorber and the other part of the loop provides the cavity for oscillation.

In fiber ring oscillators self-starting operation can be initiated from noise when the power level inside the cavity surpasses a threshold of mode-locking regime. In addition, an oscillator can be constructed from all-fiber components realizing a monolithic design. However, in practice this type of fiber oscillator is susceptible for the mechanical and temperature fluctuations due to the use of non-polarization maintaining optical fibers which makes it difficult to use such oscillator in harsh environmental conditions. The modifications of this method using polarization-maintaining fibers are still under development [31,32].

Mamyshev oscillator can be distinguished as a new type of fiber oscillator that has a great potential to become a widely used fiber-optic laser technology for ultrashort pulse generation in the future. The operation of this type of oscillator is based on a close interplay of pulse amplification, nonlinear spectral broadening due to self-phase modulation (SPM) and pulse filtering effect of two non-overlapping spectral filters. The pulse propagating in the resonator is amplified in the fiber amplifiers to a certain energy sufficient for spectral broadening in a nonlinear medium (either a passive or a rare earth ion-doped fiber) between each filter. These filters pass only those wavelengths that have been newly generated due to SPM. Spectral modulations occur between those filters during pulse propagation and a stable periodic pulse evolution at a certain pulse energy is ensured. In such a way strong effective saturable absorption is provided by Mamyshev regenerator mechanism [33]. The parameters of the generated pulses highly depend on the separation of the spectral band-pass filters. Higher pulse energy and the bandwidth could be ensured by a larger separation of spectral filters. Mamyshev oscillator can support huge nonlinear phase shifts, as high as  $\sim 60\pi$  rad, and greater peak powers achieved directly from the oscillator than in other fiber oscillator technologies, reaching MW peak power level [28,34,35].

Mamyshev oscillator can be realized in both ring and linear type cavity designs of the oscillator [27,36,37]. A completely all-in-fiber design of the oscillator is complicated but can also be realized [36,37]. The biggest challenge for Mamyshev oscillators is self-starting which is not achievable in most cases. Several methods for starting Mamyshev oscillators have been proposed, as the use of an external saturable absorber mirror for mode-lock initiation [37], a pump diode modulation [36] or the incorporation of an auxiliary cavity [38]. By solving self-starting problems, Mamyshev oscillators can become a powerful tool for generating ultrashort laser pulses, enabling outstanding performance levels and new applications [34].

The third, forementioned, cavity design of the fiber oscillator is Fabry-Perot (linear) type. This type of fiber oscillator is used in the experiments described in this thesis, so an overview of ultrashort pulse generation, passive mode-locking regimes and pulse evolution is briefly discussed.

Passive mode-locking in the linear design of fiber oscillator is achieved by incorporating saturable absorber in the cavity. Many saturable absorbers made of novel materials were used in fiber oscillators for passive mode-locking, e.g., carbon nanotube [39], graphene [40], perovskite [41], transition metal dichalcogenides [42] or topological materials [43]. Unfortunately, most of these demonstrations were realized with erbium-doped fiber oscillators at 1.5  $\mu\text{m}$  central wavelength. For ytterbium-doped fiber oscillators semiconductor saturable absorber mirror (SESAM) technology still outperform above-mentioned approaches [44,45]. Semiconductor saturable absorbers are characterized by long-term degradation of their properties [46]. However, a good performance of a fiber oscillator can be assured reaching up to tens of thousands of working hours by choosing a particular oscillator configuration and SESAM structure.

Semiconductor saturable absorber mirror is an element that can respond instantaneously to a change of the incident light intensity – it selectively absorbs low-intensity light and transmit light which has sufficiently high intensity. When a saturable absorber is bleached, the high-intensity light fluctuation is amplified in a laser cavity and further shaped in time, leading to the formation of bandwidth-limited mode-locked pulse. Stable passive mode-locking in ytterbium-doped fiber (YDF) oscillator can be ensured by adjusting the interplay of gain, nonlinearity and dispersion. The normal dispersion of the cavity in ytterbium-doped oscillators should be compensated for the stable ultrashort pulse generation. Different mode-locking regimes can be realized depending on the net value of group velocity dispersion (GVD) in the cavity. All-normal dispersion, similariton and

stretched pulse (dispersion managed) mode-locking regimes can be initiated in YDF oscillators.

All-normal dispersion (ANDi) oscillator has no negative dispersion element inside the cavity, so the net GVD is very high and positive [47]. The dispersion is managed by the use of a narrow bandwidth filter which plays an essential role in pulse formation. The pulse spectrum is broadened due to self-phase modulation, when a pulse of a sufficiently high peak power propagates in a nonlinear medium inside the cavity. The pulse and the pulse spectrum are narrowed when it passes through a narrow band-pass spectral filter. The Gaussian-like spectral filter could lead not only to pulse width management but also to spectral shaping and amplitude modulation by attenuating the wings more than the central part of the pulse. The spectrum is broadened significantly at a further stage of pulse propagation after the filter and a structured profile with steep edges is developed due to strong self-phase modulation. After that, the narrow band-pass filter cuts down the edges of the spectrum and restores pulse envelope and spectral shape to its initial form.

Pulses generated by ANDi oscillator are strongly chirped but can be well compressed outside the laser cavity to a sub-100 fs pulse duration [48]. The output parameters strongly depend on the total cavity dispersion, the spectral filter bandwidth and the total accumulated nonlinear phase-shift over one round-trip. This type of oscillator can tolerate large variation of gain and loss during the process of pulse evolution. Most importantly, all-normal dispersion fiber oscillator can be constructed using strictly all-fiber polarization-maintaining components which leads to a simple, compact, robust and maintenance-free fiber laser design [49,50].

Similariton fiber oscillator contain negative dispersion element and the net GVD of the cavity is high and positive [51,52]. The negative dispersion element is used for the dispersion management and pulse temporal compression. The pulse remains positively chirped during all propagation in the cavity, despite the chirp being reduced by the element of the negative dispersion. Pulse envelope and a spectrum evolve to a parabolic shape with a linear positive chirp during the pulse propagation in the cavity. Similariton oscillators have a quadratic phase profile over the pulse which is a significant feature for this type of oscillators. Pulses which have a parabolic intensity profile and a quadratic phase profile can be amplified in the gain medium very effectively as they are resistant to wave-breaking [51]. For this reason, this type of pulses is eligible for energy scaling in the fiber

amplifiers [53,54]. Unfortunately, the realization of pulses which have perfect parabolic intensity profile is quite difficult in practice.

The pulse generation in the oscillator of stretched (or dispersion managed) pulses is very similar to that of similariton [55]. In this case, net GVD is close to zero. First, the temporal and spectral widths of the pulse increase by propagating through the passive and ytterbium-doped fibers due to the interplay of GVD and nonlinearity. After the element of negative dispersion, pulse becomes negatively chirped leading to spectral and temporal compressions after the pulse propagation in a cavity of a positive dispersion. The mode-locked pulse during the propagation in the cavity experiences periodic stretching and compression. After each round trip, the temporal envelope of the pulse and the pulse spectrum repeats themselves resulting in soliton-like pulse formation. This type of pulse is known as dispersion managed soliton or stretched pulse, since conventional soliton pulse cannot be generated for a wavelength around 1  $\mu\text{m}$ . Stretched pulse fiber oscillators can provide shorter pulse durations than the other forementioned fiber oscillators, as short as 30 fs and pulse energies of a few nJ [56].

Compensation of a positive dispersion in similariton and stretched pulse fiber oscillators can be realized by using dispersion elements with negative dispersion such as a pair of prisms or diffraction gratings [52,56]. However, such an oscillator configuration is not practical because the oscillator becomes sensitive to mechanical perturbations due to the use of free-space components and is not robust and compact. Alternative solution for normal dispersion compensation is the implementation of photonic crystal fiber inside the cavity [57]. However, this solution is also not very practical as a rather long photonic crystal fiber must be used for dispersion compensation. In this case, the total length of the resonator is increased due to the use of an optical fiber of a certain length and limits the maximum possible repetition rate of the generated pulses. Chirped fiber Bragg grating is the best solution for the dispersion compensation, as it can provide either low or very high negative dispersion without increasing the size of a cavity [25,58]. Furthermore, a compact, robust and maintenance-free fiber laser design can be constructed using strictly all-fiber polarization-maintaining components.

## 1.1.2 Control of ultrashort pulse spectral characteristics

Various formation techniques of ultrashort pulse and its spectrum outside the fiber oscillator may enable not only shorter pulse duration at the system output but also higher pulse energy, what is required for many applications.

Self-phase modulation induced pulse spectrum broadening in a single-mode fiber is one of the main techniques used in fiber lasers for realization of ultrashort laser pulses [59]. This method is also applied in the experimental fiber laser systems described in this thesis. Due to the self-phase modulation, spectrum of the bandwidth limited pulse is enriched with new spectral components during the pulse propagation in a single-mode optical fiber. This broadening of pulse spectrum strongly depends on the nonlinear properties and the length of the optical fiber as well as the initial pulse parameters such as peak intensity and pulse duration. During propagation, different level of pulse spectrum broadening and spectral shaping can be obtained resulting in altered Fourier transform-limited (FTL) pulse duration at the output of the system. Two cases of pulse propagation and pulse spectrum formation are shown in Fig. 1.1.1., as an example. Numerical simulation of the pulse spectrum formation during pulse propagation in a single-mode optical fiber is provided here. A rectangular-like shape of the pulse spectrum with strong modulations can be formed when intense (1655 W peak intensity) initial Gaussian-like pulse of sufficiently narrow spectral width of 0.31 nm (the duration of a pulse – 5 ps)

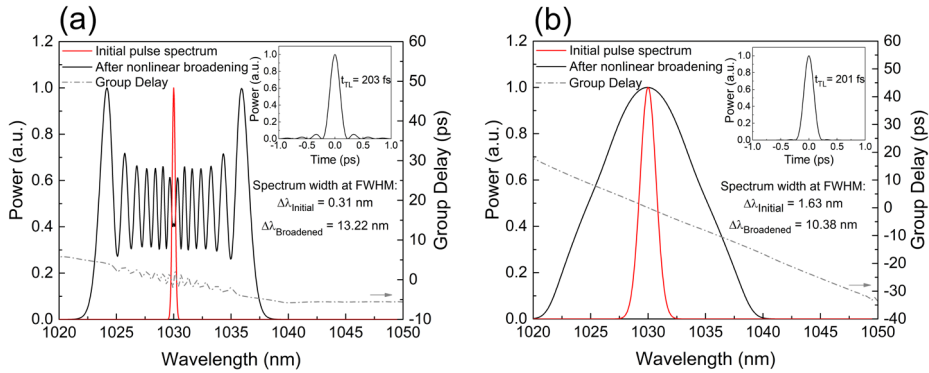


**Fig. 1.1.1.** Numerical simulation of the rectangular-like (a) and triangular-like (b) pulse spectrum formation during pulse propagation in a single-mode optical fiber. Initial pulse spectrum (red line), after nonlinear spectral broadening (black line). Numerically simulated group delay trace after nonlinear spectral broadening (grey dash-dotted line). Inset: An envelope of a Fourier transform-limited pulse.

propagate through 10 m long passive single-mode (6  $\mu\text{m}$  diameter) optical fiber (Fig. 1.1.1. (a)). At certain initial pulse parameters (initial pulse spectrum width at full width half maximum (FWHM) of 1.63 nm, 1 ps pulse duration, 404 W peak intensity), a triangular-like pulse spectrum is formed after pulse propagation in a sufficiently long 50 m of optical fiber (Fig. 1.1.1. (b)). The interplay of self-phase modulation and normal dispersion of the material resulted in pulse formation of a linear chirp over the entire pulse spectrum, as seen in Fig. 1.1.1 (b). These shaped pulses could be compressed by introducing an anomalous group velocity dispersion to a duration of 201 fs. An envelope of a transform-limited pulse is showed in the inset of Fig. 1.1.1. In a case of a rectangular-like pulse spectrum, the pulses could also be compressed to a similar pulse duration of 203 fs. However, the compressed pulses of the same energy would have lower peak power due to the rectangular-like pulse spectrum shape and visible group delay distortions. It can be seen that due to the nonlinear pulse propagation and self-phase modulation in a single-mode optical fiber, a completely different shapes of pulse spectrum could be obtained. These illustrations showed that the pulse duration depends not only on the bandwidth of the pulse but on its spectral shape as well.

On the other hand, self-phase modulation occurring in the amplification stage of chirped pulses is generally undesirable because it contributes an additional nonlinear phase-shifts that result in the compressed pulse quality degradation [60]. Accumulated nonlinear phase-shift can be characterized by the intensity dependent parameter named B-integral which is equal to the integral of the maximum phase shift over the path of the pulse propagation [61]. In conventional chirped pulse amplification systems, it is assumed that the accumulated nonlinear phase-shift in the system should be below 1 rad so that the pulse can be compressed without significant distortions [60]. This nonlinear phenomenon will be encountered more in detail in the following sections of this thesis.

Higher pulse energies or better compressed pulse quality can be achieved by using parabolic shape pulse spectrum formation in fiber laser systems. Parabolic pulses can be generated in a similariton fiber oscillator, mentioned in the previous section. Also, such pulses can be formed outside the oscillator from initial Fourier transform-limited pulses under certain amplification and pulse propagation conditions under the influence of self-phase modulation and normal material dispersion [62]. Such a method for parabolic pulse realization can be called a passive method, whereas only certain initial conditions and chosen experimental laser configuration is

used. The control of the pulse spectrum shape could also be introduced using active spectral amplitude shaping by applying a liquid crystal spatial light modulator in fiber-based chirped pulse amplification system [63]. The method of parabolic pulse shaping and amplification allowed significant performance improvement to overcome nonlinearity limitations of conventional fiber CPA systems. In a demonstrated system, high-intensity high temporal quality pulses of a few hundred femtosecond duration were achieved despite the large (16 rad) accumulated nonlinear phase-shift. Such level of accumulated nonlinear phase-shift could not be managed using initial Gaussian-like pulse shape. On the other hand, introduced system was complex enough and lost its main advantage of fiber laser if all-in-fiber design is desired.

More sophisticated method based on spectral combination of ultrashort laser pulses for the increase of pulse peak power was reported [64]. In a described system, two spectrally and temporally separated pulses were generated in the pulse stretcher of a chirped pulse amplification system. These two pulses were amplified and then coherently recombined in the pulse compressor. Using this method, a single short pulse was produced from the two pulses. The obtained power of combined pulse was 1.7 times larger than the sum of the peak powers of each individual pulse. This demonstrated approach of spectral combination of ultrashort laser pulses required free space elements, as diffraction grating based pulse stretcher and compressor, which must have been aligned with high accuracy. Coherent spectral combining of femtosecond optical pulses from multiple parallel fiber CPA channels was also proposed [65]. This technique enabled ultrashort pulse amplification with an aggregate spectrum significantly exceeding amplification bandwidths of each individual fiber amplifier. This method could be particularly useful in systems that delivers ultra-high intensity laser pulses that can optically damage critical elements of the system and could lead to multi-mJ fiber laser sources with high average powers.

The range of application of ultrashort pulse lasers can be extended by realizing an optically synchronized dual-wavelength fiber laser source [66]. All-in-fiber laser design could be used to seed both high-energy femtosecond ytterbium-doped and picosecond neodymium-doped amplifiers. This approach eliminates the necessity of pulse synchronization between two laser outputs and enables the simplification of the system. Schematic representation of the constructed optically synchronized dual-wavelength fiber laser source is shown in Fig. 1.1.2. Pulse spectrum shaping and spectral

filtering techniques were used for the construction of such fiber laser source.

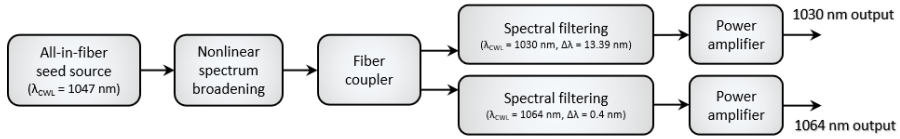


**Fig. 1.1.2.** Schematic representation of the constructed optically synchronized dual-wavelength fiber laser source

Numerical simulation of pulse spectrum of optically synchronized dual-wavelength fiber laser source is provided in Fig. 1.1.3., together with experimental results. Numerical simulation and experimental results had a very good agreement. A passively mode-locked all-in-fiber oscillator operating at 1047 nm center wavelength was used for pulse generation. The pulse spectrum was broadened due to self-phase modulation in single-mode passive fiber to overlap the gain spectra of ytterbium and neodymium-doped laser amplifiers (Fig. 1.1.3.). Spectrally broadened pulses were divided into

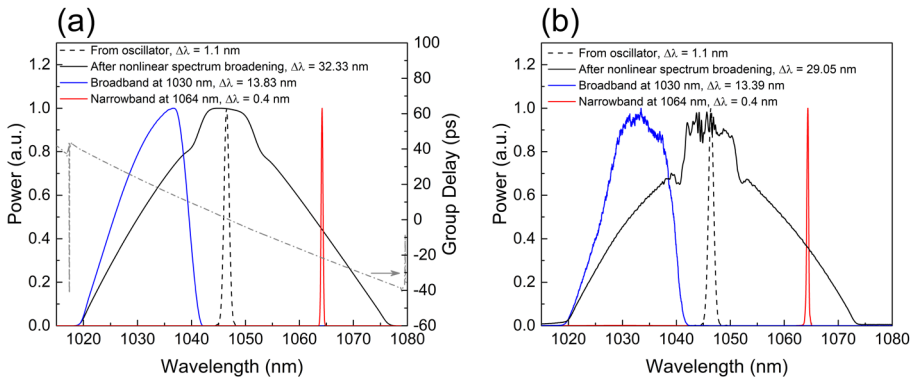


**Fig. 1.1.3.** Numerically simulated (a) and experimentally measured (b) pulse spectra of optically synchronized dual-wavelength fiber laser source. Pulse spectrum: from oscillator (black dashed line), after nonlinear spectrum broadening (black line), broadband output at 1030 nm (blue line), narrowband output at 1064 nm (red line). Numerically simulated group delay trace after nonlinear spectrum broadening (grey dash-dotted line).

two outputs by the fiber coupler. The narrowband 1064 nm output for the neodymium-doped amplifier was obtained using a Gaussian-like spectral filter of 0.4 nm spectral bandwidth. A pulse spectrum of  $\sim 13$  nm bandwidth at FWHM centered at  $\sim 1030$  nm was formed in another optically synchronized fiber laser output. Broadband pulse spectrum corresponded to a transform-limited pulse duration of  $< 200$  fs. Pulses may be successfully compressed in a pulse compressor because it has a linear chirp over the

entire pulse spectrum as seen in Fig. 1.1.3(a). Pulses were stretched in time and amplified in fiber amplifiers reaching the energies required for effective further pulse amplification in solid-state ytterbium and neodymium-doped power amplifiers.

As it has been seen, the formation of pulse spectrum may enable to achieve higher pulse energies or even may extend the range of application of ultrashort pulse lasers by realizing an optically synchronized dual-wavelength fiber laser source. Though, most importantly for femtosecond lasers, it allows ultrashort pulse durations of several hundred femtoseconds to be achieved in conventional fiber CPA systems.

### **1.1.3 Laser technologies for fiber chirped pulse amplification systems**

This section is dedicated for the introduction of laser technologies used in fiber chirped pulse amplification systems. Different technological approaches could be used for temporal pulse stretching and compression that enable high intensity femtosecond pulses at the output of the system. The desired requirements for the technologies used in FCPA systems are compactness, reliability, simplicity and, most importantly, good achievable pulse quality.

Direct amplification of high energy ultrashort pulses in fiber amplifiers is limited by nonlinear effects due to long interaction length and small mode area of the gain fibers. Chirped pulse amplification is a powerful technique to mitigate nonlinear effects [18]. FCPA technique allows achieving significantly higher pulse energies by reducing nonlinear effects in a gain fiber by stretching initial pulse and compressing the pulse after the amplification. Pulse stretching and compressing in CPA systems can be conveniently realized using diffraction gratings [67,68]. This approach has major advantage that properly designed stretcher and compressor have exactly compensated dispersion profiles and high-quality compressed pulses could be achieved at the output of the laser system. By using this technology, initial pulses can be stretched in time to durations of few nanoseconds. This allows to minimize nonlinear effects and achieve record-high pulse energies of around 1 mJ-level from the FCPA system [19]. However, the pulse temporal stretching is usually practically limited to hundreds of picoseconds as stretching and compressing beyond this duration becomes impractical due to the large dimensions of diffraction gratings in stretcher and compressor of FCPA system. Furthermore, diffraction grating based pulse stretcher and compressor are susceptible to mechanical and thermal perturbations. A

quality of compressed pulse temporal profile as well as spatial beam profile strongly depends on precise alignment of the optical elements [69]. In addition, chirped pulses need to be coupled back to a fiber after pulse stretcher, which is not a very practical solution, as the stability and accuracy of the implemented optomechanical units need to be ensured. Therefore, when applied to fiber laser systems diffraction grating based CPA approach negates their important advantage in compactness and robustness. For these reasons, much effort has been devoted to develop alternative technologies for temporal stretching and compressing of pulses that can be easily integrated into a fiber laser. One of the simplest ways is to use single-mode optical fiber as a pulse stretcher that elongates pulses in time due to the chromatic dispersion of material. Using a sufficiently long fiber of several hundred meters pulses can be stretched to a duration of several hundred picoseconds [18,70]. However, in this case, a mismatch of the third-order dispersion (TOD) between the fiber stretcher and the diffraction grating compressor is obtained, because the contributions of TOD are of the same sign. It significantly reduces achievable peak intensity and quality of the compressed pulses in the FCPA system [70]. Hollow photonic crystal fibers can be used for pulse compression [71]. However, such fibers have a relatively small dispersion per unit length that limits the maximum ratio of stretched and compressed pulse durations. As a result, the achievable pulse energy is lower comparing with the systems based on diffraction grating compressors.

Major achievement in making the FCPA systems more robust and compact was a substitute of diffraction grating based pulse stretcher by a chirped fiber Bragg grating (CFBG) [72]. The technology of chirped fiber Bragg grating has greatly reduced the dimensions of the pulse stretcher as it is produced in the core of the fiber and the CFBG itself is several centimeters in length and can be placed next to the fiber or other micro-optical components of the system. The CFBG can be manufactured to have parameters that perfectly match to the configuration of the pulse compressor and compensate the higher order dispersion of FCPA system. A system configuration using CFBG as a pulse stretcher and diffraction grating based compressor is the most widely used in FCPA systems. Diffraction grating compressor, however, remained the limiting factor in realization of truly compact and robust fiber laser system. On the other hand, the size of the diffraction grating based compressor depends on the line density of the grating. For this reason, manufacturing technologies are being developed that allow the production of efficient diffraction gratings with higher line

density in order to achieve smaller compressor dimensions for the same achievable amount of group delay dispersion.

Another breakthrough was accomplished when large aperture chirped volume Bragg grating (CVBG) was introduced as a pulse stretcher and compressor in femtosecond FCPA system [73]. This idea was proposed long time ago [74]. However, due to the lack of holographic materials it was not implemented until volume Bragg gratings (VBGs) based on Photo-Thermo-Refractive (PTR) glass were developed [75]. VBGs holographically fabricated in PTR glass have several key advantages: unrestricted life time, stability to harsh environmental conditions and high diffraction efficiency. On top of it, PTR glass has a low absorption coefficient that enables its usage for compression of high power/energy ultrashort pulses. Over the last several years parameters of CVBGs were significantly improved [76], which led in an increased efficiency of CVBGs combined with a nearly diffraction limited beam quality. Chirped volume Bragg grating can stretch pulses to a duration of few hundred picoseconds and recompress them to femtosecond duration in only a few centimeters of glass. The use of CVBG as a pulse stretcher and compressor has practical advantage over the diffraction grating based systems due to compactness, simplicity of alignment, efficiency and robustness [75–77]. All the reasons mentioned above triggered extensive development of novel laser designs. Several CVBG based FCPA systems for the most common wavelengths, such as 1  $\mu\text{m}$  (ytterbium-doped fiber) [77,78], 1.56  $\mu\text{m}$  (erbium-doped fiber) [76,79], 2.05  $\mu\text{m}$  (thulium/holmium-doped fiber) [80,81], were demonstrated. Two historic milestones were recently achieved for PTR glass based CVBGs: compression of more than 100 W power beam [78] and 100 mJ pulses [82].

FCPA systems based solely on CVBG element for pulse stretching and compression have several drawbacks as these systems require additional dispersion compensation to eliminate the residual dispersion of the fiber [77]. Compensation of dispersion in the system is inconvenient and requires an addition of the fiber with opposite sign of dispersion. To minimize the recompressed pulse duration a cut back of the fiber while monitoring pulse duration is required. Furthermore, using CVBG as a pulse stretcher, chirped pulses have to be coupled back to a fiber and in that case sophisticated optomechanical units are preferred.

To overcome the limitations of FCPA systems based solely on CVBG, an alternative ultrafast fiber laser configuration using CFBG as a pulse stretcher and CVBG as a pulse compressor was proposed [83,84]. However, compressed pulses were not transform-limited and had temporal pedestal due

to the imprecise dispersion compensation between CFBG and CVBG. In the next section of this chapter, a compact FCPA system consisting of CVBG compressor and CFBG stretcher which was manufactured with matched dispersion profile in order to achieve high fidelity femtosecond pulses is presented.

## 1.2 High-quality femtosecond pulses from a compact FCPA system based on a CFBG stretcher and CVBG compressor with matched dispersion profiles

Material related to this section was published in A1

In this section, the main focus is paid on the generation of high-quality ultrashort pulses in a fiber oscillator and the realization of a novel FCPA system exploiting a tandem of a chirped fiber Bragg grating (CFBG) stretcher and a chirped volume Bragg grating (CVBG) compressor with matched dispersion profiles. The main goal was to check the dispersion matching in the system and to achieve high-quality compressed pulses of a duration of less than 300 femtoseconds. FCPA system provided relatively low (nJ-level) energy ultrashort pulses that nonlinear effect would not distort the envelope of the compressed pulses. Demonstration of microjoule level pulses from FCPA system is a subject of Chapter 2 of this thesis.

### 1.2.1 Ultrashort pulse generation in all-in-fiber oscillator and nonlinear pulse spectrum broadening

The experimental setup of all-in-fiber oscillator, together with the segment of nonlinear pulse spectrum broadening is showed in Fig. 1.2.1.

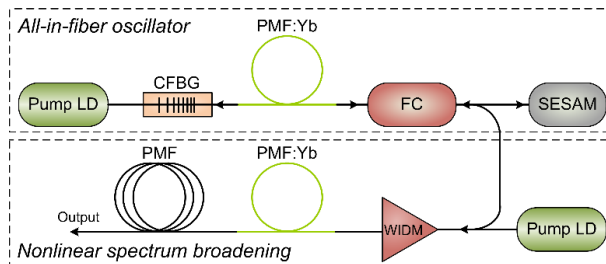


**Fig. 1.2.1.** Schematic setup of all-in-fiber oscillator and nonlinear spectrum broadening. LD - laser diode, CFBG - chirped fiber Bragg grating, PMF:Yb - ytterbium doped polarization maintaining single-mode fiber, FC - fiber coupler, SESAM - semiconductor saturable absorber mirror, WIDM - hybrid wavelength-division multiplexer - isolator, PMF - polarization maintaining single-mode fiber.

All-in-fiber passively mode-locked oscillator of a linear type cavity design was used for generation of ultrashort laser pulses. The resonator of the oscillator consisted of a chirped fiber Bragg grating, a segment of ytterbium doped single-mode fiber, a fiber coupler and a semiconductor saturable absorber mirror. The CFBG operated as a rear mirror of the resonator forming a pulse spectrum and as a dispersion element which compensated the normal dispersion of the optical fibers in the cavity. Total cavity dispersion of the experimental oscillator was estimated to be about  $-0.1 \text{ ps}^2$ . In such oscillator, temporal and spectral properties of a mode-locked pulse experienced periodic stretching and compression and repeated itself after each round trip, thus resulting in a soliton-like pulse formation. A semiconductor saturable absorber mirror operated as another rear mirror of the resonator which ensured stable self-starting mode-locking regime. Ytterbium-doped single-mode fiber was pumped by a single-mode laser diode (976 nm) and the radiation of the laser diode was directed in the cavity through CFBG. Ultrashort laser pulses generated by the oscillator were outcoupled by a fiber coupler which also acted as a polarizer in the resonator. All the components used in the cavity were polarization-maintaining which ensured reliable, robust and maintenance-free operation of the fiber oscillator. The fiber oscillator described in this work generated nearly transform-limited laser pulses of 3.77 nm bandwidth (Fig. 1.2.2.) operating at 1029.4 nm center wavelength and 53 MHz pulse repetition rate.

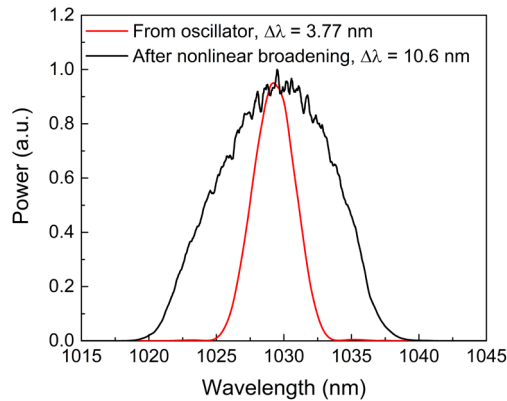


**Fig. 1.2.2.** Pulse spectrum: output from the all-in-fiber oscillator (red line) and after nonlinear spectrum broadening (black line).

The pulses from the oscillator were amplified in a single-mode fiber amplifier to an energy of  $\sim 300 \text{ pJ}$ . The stage of nonlinear spectrum broadening consisted of fiber amplifier and 30 meters long passive single-

mode fiber (Fig. 1.2.1.). During the pulse propagation in a relatively long fiber, the pulse spectrum was broadened to a bandwidth of 10.6 nm at FWHM (Fig. 1.2.2.) due to self-phase modulation and the pulse duration increased to approximately 13 ps due to the effect of material dispersion. Pulse spectrum is broad enough to provide a pulse duration of less than 300 fs at the output of the system after pulse compression.

## 1.2.2 Experimental fiber chirped pulse amplification system

Schematic representation of the experimental FCPA system is depicted in Fig. 1.2.3. The main parts of the system were all-in-fiber seed source (described in previous section), CFBG stretcher, power amplification stage and CVBG compressor. Seed source, CFBG stretcher and fiber amplifier were fusion spliced to a monolithic FCPA system. Linearly up-chirped pulses from the seed source were down-chirped to about 230 ps duration by using CFBG stretcher (*TeraXion*) with group delay dispersion (GDD)  $\beta_2$  of  $-13.65 \text{ ps}^2$ .

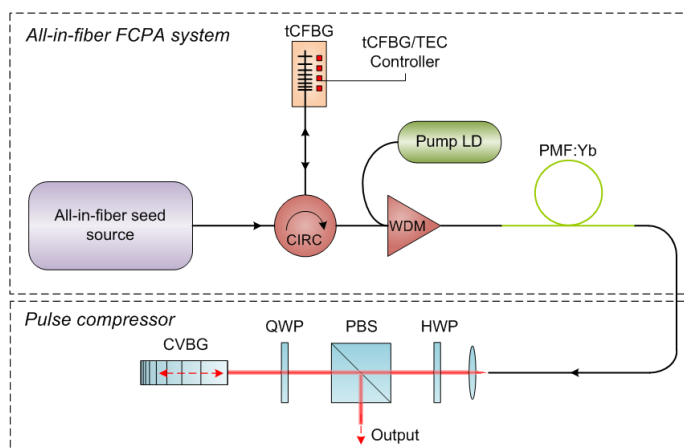


**Fig. 1.2.3.** Schematic representation of the experimental FCPA system with CFBG stretcher and CVBG pulse compressor. CIRC - optical circulator, tCFBG - thermally tunable CFBG module, WDM - wavelength-division multiplexer, LD - laser diode, PMF:Yb - ytterbium doped polarization maintaining single-mode fiber, HWP - half-wave plate, PBS - polarization beam splitter, QWP - quarter-wave plate, CVBG - chirped volume Bragg grating. Adapted with permission from [A1].

Temporal envelope of the stretched pulses was measured using a photodiode with 35 ps response time and a 20 GHz bandwidth oscilloscope. Temporal shape of the stretched pulses is shown in Fig. 1.2.4.

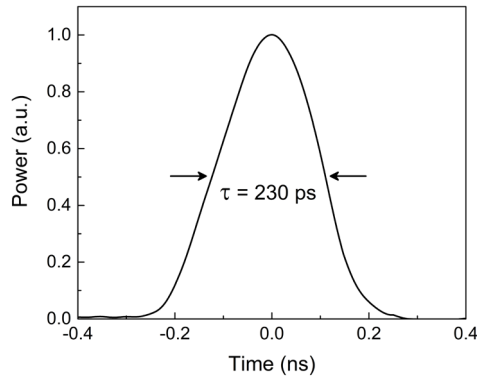


**Fig. 1.2.4.** Temporal envelope of the stretched pulses.

After CFBG chirped laser pulses were combined with pump radiation from the single-mode laser diode (976 nm) by wavelength-division multiplexer and amplified in a single-mode Yb-doped fiber amplifier. Chirped pulses were amplified up to 4.85 nJ energy (257 mW average power). Total power gain of the system was 13.3 dB. After the amplifier pulses were compressed in free space by CVBG compressor (*OptiGrate*). The output of the system was arranged by separating incident and reflected beams using quarter wave-plate (QWP) and polarizing beam splitter (PBS), as shown in the Fig. 1.2.3. Average power of the system after pulse compression was 223 mW, which corresponded to 87% efficiency of CVBG compressor. A few nanojoule pulse energy was sufficient for further pulse characterization and nonlinear effects in the fiber amplifier were negligible.

Dispersion-matched CFBG was placed in thermal unit (produced by *TeraXion*) for dispersion fine-tuning. Temperature distribution along CFBG was controlled by thermoelectric cooler (TEC) elements which enabled the tunability of GDD and optimization of compressed pulse duration without requirement to change length of the fiber in the system.

The use of CFBG stretcher ensured all-in-fiber configuration of FCPA system. Further, a small footprint (5 cm in length and 5x5 mm of clear aperture) CVBG element simplified the design of the pulse compressor and made it as compact as possible. For comparison, in a 1600 l/mm diffraction grating compressor operating at Littrow configuration, an optical path of 40 cm between the diffraction gratings would be required to achieve similar value of GDD. This is a few times larger value in distance, excluding the physical dimensions of the other compressor elements.

### 1.2.3 Precise dispersion compensation between CFBG and CVBG

The key novelty in the described FCPA system is the use of CFBG and CVBG elements in tandem as well as dispersion matching between these elements. Below the details of producing these elements are described.

CVBG was designed for this application aiming at several important points: efficiency above 85%, spectral bandwidth supporting pulses <300 fs along with stretching up to ~500 ps. Manufactured grating had diffraction efficiency >85% for more than 20 nm spectral bandwidth (Fig. 1.2.5.).

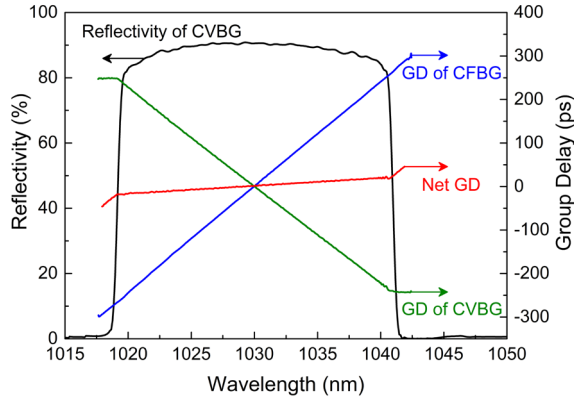


**Fig. 1.2.5.** Experimentally measured and smoothed (~0.3 nm smoothing) GD traces of CVBG (green line), CFBG (blue line) and their net GD trace (red line). The black curve shows measured reflectivity profile of CVBG. Adapted with permission from [A1].

It also had linear stretching factor of ~22 ps/nm. Nearly diffraction limited beam quality was measured by reflection from both sides of this grating. It confirms that CVBG can be used in both orientations providing positive and negative dispersion.

The mismatch of chromatic dispersion profiles between stretcher and compressor might lead to temporal distortion of compressed pulses. In this work, a custom CFBG stretcher was produced with its dispersion profile designed to compensate dispersion profile of CVBG as well as residual dispersion of the FCPA system approximately equal to 1 ps<sup>2</sup> (equivalent to 50 m of fused silica fiber). First, dispersion profile of CVBG element with clear aperture of 5x5 mm was measured by using a homemade high-resolution interferometric group delay measurement system. From this dispersion profile and estimated additional dispersion in the FCPA system, the matched CFBG design was computed and the parameters were sent to a UV based CFBG manufacturing station. Following inscription of the CFBG

in the fiber, its dispersion profile was measured and compared against the target dispersion to validate its performance. Measured group delay (GD) traces of CVBG and CFBG, as well as their net GD trace are presented in Fig. 1.2.5. The delay of the different spectral components has close to linear dependence on wavelength for both CFBG and CVBG. Total GD for CVBG was  $\sim 500$  ps in its reflection bandwidth range of 1019-1041 nm with shorter wavelengths being delayed in respect to the longer ones (normal dispersion). CFBG had similar total GD in the same bandwidth but with opposite sign (anomalous dispersion). Net GD trace had a slightly rising slope (anomalous dispersion) in order to compensate residual dispersion of the FCPA system.

The group delay traces plotted in Fig. 1.2.5. are characterized by a close to linear dependence on wavelength but are not completely linear. In order to highlight the characteristic differences of the GD traces, the linear slope must be eliminated. Experimentally measured GD traces of CVBG, CFBG and their net GD trace with eliminated linear slope is showed in Fig. 1.2.6. It can be seen that GD trace of CFBG perfectly reproduces the trace of CVBG, only with an opposite sign, which indicates that the dispersion profile of CFBG was successfully matched to this of CVBG. The net GD value is close to zero at all wavelengths, which means that spectral phase will be compensated after pulse stretching and compression.

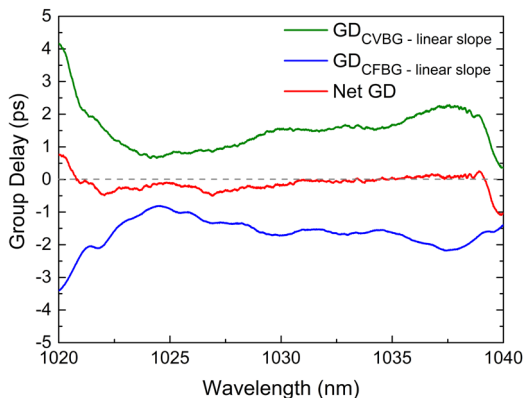


**Fig. 1.2.6.** Experimentally measured GD traces of CVBG (green line), CFBG (blue line) and their net GD trace (red line) with eliminated linear slope.

Envelopes of the numerically calculated compressed pulses using experimentally measured GD traces for calculations are presented in Fig. 1.2.7. In the case of dispersion matching between CFBG and CVBG, a high temporal quality 224 fs pulse was obtained. The need for dispersion

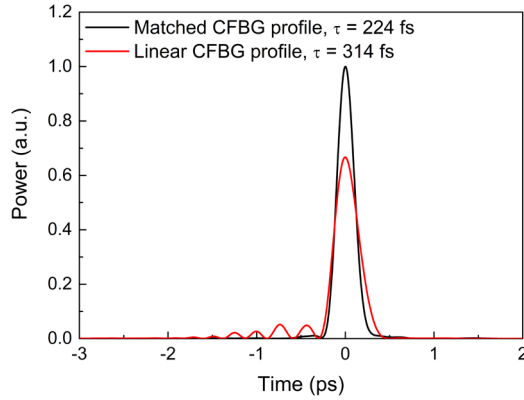


**Fig. 1.2.7.** Envelopes of the numerically calculated compressed pulses using: experimentally measured GD trace of CVBG and experimentally measured GD trace (matched profile) of CFBG (black line); experimentally measured GD trace of CVBG and linear GD trace (linear profile) of CFBG (red line), for calculations.

matching becomes apparent after numerical calculations using the experimental GD profile of CVBG and the linear CFBG profile. In this case, the pulse peak intensity is almost 30 percent lower, the duration is longer (314 fs) and the temporal envelope is distorted, characterized by the trail of side pulses (Fig. 1.2.7).

Thus, the technological limitations that prevent the recording of a completely linear dispersion profile in a CVBG can be overcome by matching the dispersion profile using a high-precision CFBG.

#### 1.2.4 Characterization of experimental ultrashort pulse FCPA system

The outlook of the developed experimental fiber chirped pulse amplification system consisting of CVBG compressor and CFBG stretcher with matched dispersion profile was presented in section 1.2.2. The main experimental measurements validating the realization of high-quality ultrashort pulses using this novel fiber laser design is presented this section.

The compressed pulse duration in FCPA system was fine-tuned by temperature gradient along the fiber Bragg grating stretcher which was placed in thermal platform. At first, pulse compression was investigated when the temperature along CFBG was set constant (60°C). Measured autocorrelation trace had a width of 1.42 ps (FWHM), which corresponded to 1.01 ps pulse duration for Gaussian-shaped pulses. Then TEC temperatures along CFBG were optimized to minimize pulse duration after the compressor. Only linear temperature gradient was required in order to

reach minimal width (301 fs) of the autocorrelation function. Both autocorrelation traces are shown in Fig. 1.2.8 with corresponding temperature distributions along CFBG depicted in the inset of the figure. GDD additionally induced due to thermal gradient of 15°C per 50 mm of CFBG length, was estimated around 0.072 ps<sup>2</sup> (equivalent to 3.6 m of fused silica fiber).

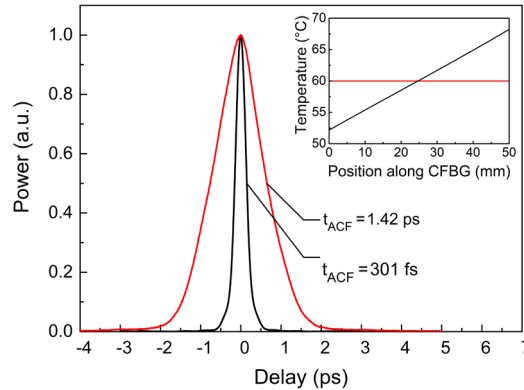


**Fig. 1.2.8.** Measured autocorrelation traces of compressed pulses after CVBG with a constant nominal temperature along CFBG (red line) and with an optimized temperature gradient applied along CFBG (black line). Inset: corresponding temperature distributions along CFBG. Adapted with permission from [A1].

Optimally compressed pulses were further characterized using second harmonic generation (SHG) frequency-resolved optical gating (FROG) autocorrelation method. The pulse duration retrieved by FROG algorithm (*Swamp Optics*) was equal to 208 fs (Fig. 1.2.9(a)). FROG retrieval was

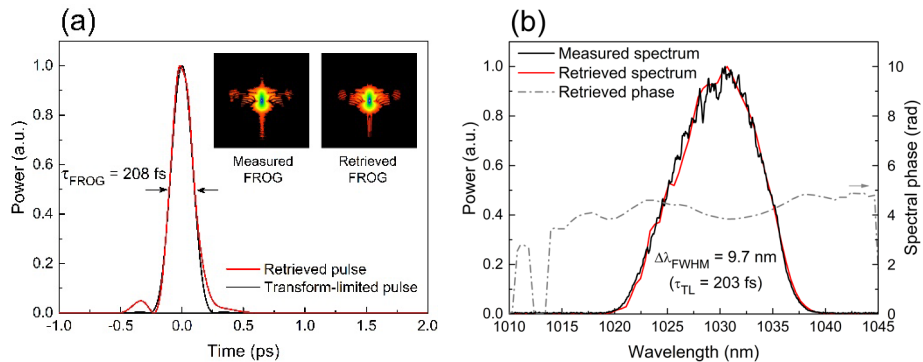


**Fig. 1.2.9.** a) Envelope of the compressed pulse retrieved from SHG FROG measurement in comparison with Fourier transform-limited pulse shape derived from the measured spectrum. Inset: measured and retrieved FROG traces. b) Experimental pulse spectrum from the FCPA system in comparison with retrieved spectrum and retrieved spectral phase from FROG measurement. Adapted with permission from [A1].

performed on a  $256 \times 256$  grid and yielded an error of 0.19%. Experimental pulse spectrum after the FCPA system is depicted in Fig. 1.2.9(b) and compared with spectrum and its phase retrieved from the FROG measurement. Fourier transform-limited pulse duration derived from the spectrum was 203 fs. Close match between FTL and retrieved pulse duration proved that CVBG dispersion profile was successfully matched to that of CVBG. This is also confirmed by a small residual spectral phase ( $< \pm 0.5$  rad) retrieved from the FROG measurement. Pulse contrast defined as the ratio of energy in main pulse to the energy of side pulses was  $>90\%$ . Excellent temporal quality of the compressed pulses was achieved despite high pulse compression ratio of  $\sim 1100$  in the described FCPA system.

Beam quality at the output of the system was measured by performing z-scan of the beam. The beam quality parameter  $M^2$  was estimated from the beam radius change along the propagation axis with best fit yielding  $M^2 \sim 1.06$ , indicating excellent beam quality (Fig. 1.2.10). This was achieved due to the high optical homogeneity of photo-thermo-refractive glass of CVBG as well as the precise control of Bragg grating geometry.

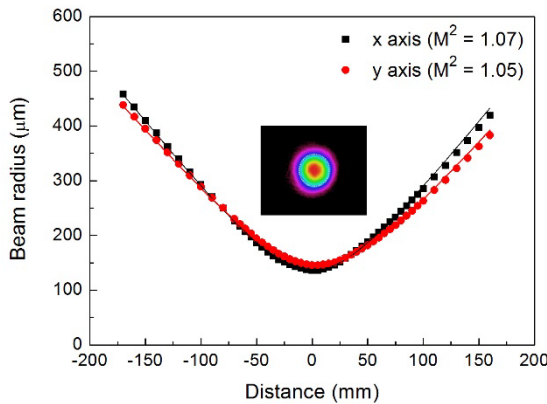


**Fig. 1.2.10.** Dependence of  $4\sigma$  beam radius at the output of the FCPA system versus the distance from the waist location for both directions perpendicular to the axis of propagation. Inset: beam profile at the waist position. Adapted with permission from [A1].

## Summary of the results

In this work a compact fiber chirped pulse amplification system exploiting tandem of a chirped volume Bragg grating compressor and a chirped fiber Bragg grating stretcher with matched dispersion profiles was demonstrated. Chirped pulses of 230 ps duration were amplified in Yb-doped fiber amplifier and compressed down to 208 fs duration pulses corresponding to a

compression ratio of  $\sim 1100$ . Pulse contrast defined as the ratio of energy in main pulse to the energy of side pulses was  $>90\%$  declaring high-quality ultrashort pulses obtained at the output of the system. This novel FCPA configuration opens path to truly compact and robust high energy femtosecond fiber lasers.

## CHAPTER TWO

This chapter is devoted to high-energy and moderate average power fiber lasers. First of all, the definition of high-energy fiber laser is provided. The nonlinear phase-shift compensation mechanisms that allow to achieve higher pulse energy in the fiber laser system are described in the literature review of this chapter. An overview of the photodarkening effect, recognized as the limiting factor on the lifetime and reliability of fiber amplifiers pumped with high-intensity laser diode radiation, is provided.

The demonstration of 10  $\mu\text{J}$  pulse energy sub-W average power femtosecond FCPA system utilizing Yb-doped single-mode fiber amplifier is presented in the experimental section of this chapter. Nonlinear phase-shift of  $>1\pi$  rad compensation mechanism and the minimization of photodarkening effect in a fiber amplifier are also described there.

### 2.1 Literature review

#### 2.1.1 High-energy and moderate average power fiber lasers

Fiber lasers can provide laser pulses from pJ to mJ energy. The definition of high-energy fiber laser must be introduced. This definition can be related to the laser-induced damage threshold of the fiber output. The theoretical optical damage threshold of the surface on air/glass interface for silica glass is about 10  $\text{GW}/\text{cm}^2$  for a single pulse of 10 ns duration at 1064 nm [85]. Pulse duration, energy and fiber core diameter are the main parameters needed for the evaluation of the optical damage threshold of the fiber. This value scales with the duration of a pulse and can be re-calculated for the energy level of a single pulse required for the damage of the single-mode fiber amplifier which is described in this chapter [86]. Optical damage threshold would be about 66  $\text{GW}/\text{cm}^2$  and  $\sim 14.5$   $\mu\text{J}$  energy limit for a 230 ps duration single pulse, in a case of 11  $\mu\text{m}$  core diameter Yb-doped single-mode fiber amplifier. However, defects in the fiber material, doping level of ytterbium and germanium ions, surface quality and cleanliness can lower the theoretical damage threshold significantly. Furthermore, the practically safe limit must be at least 2-3 times lower than the theoretical limit since the surface is exposed to many pulses over time. Considering these factors, the maximum pulse energy value for the safe laser operation utilizing a small mode area fiber amplifier is about 2  $\mu\text{J}$ . This could be defined as a lower limit of the pulse energy specification for a single-mode high-energy fiber

laser. Certainly, this value would be higher for larger core fiber amplifiers and the definition is adapted for a particular case.

Special fiber terminator such as end-cap may be used to expand a laser beam at the glass/air surface as the end-caps contain no waveguide, decreasing the energy density and protecting the output of the fiber [87]. Small pieces of few hundred micrometers in length of coreless fibers can be spliced to single-mode fiber ends and serve like the end-caps. Further, larger pieces of glass can be spliced by using glass welding technology with CO<sub>2</sub> laser if larger beam expansion on the glass surface is desired. For high-energy applications, the surface of an end-cap is covered with an anti-reflective dielectric coating which increases the optical damage threshold.

The main goal of the work introduced in this chapter is the realization of high-energy level sub-W average power femtosecond FCPA system based on the novel architecture using CFBG stretcher and CVBG compressor with matched dispersion profiles described in Chapter 1. High temporal quality pulses of less than 300 fs duration were desired from this system. One of the biggest challenges achieving high-quality high-energy pulses was the management of the accumulated nonlinear phase-shift as a small mode area single-mode Yb-doped fiber was used in the main amplification stage.

Yb-doped fiber amplifiers feature extremely good optical-to-optical conversion efficiency of ~80% and, hence, can assure the delivery of high-energy femtosecond pulses as it was expected from this fiber laser system. High-brightness single-mode laser diode radiation (976 nm) was implemented for efficient core-pumping of the fiber amplifier. These laser diodes must have a very good spatial beam quality for the laser radiation to be effectively coupled into a single-mode fiber of a numerical aperture value equal to 0.12. Such high-brightness laser diodes have recently become commercially available and the average power of such sources is currently limited to about 1 W. Relatively low average power of the pump is the main factor limiting the average power to sub-W level at the output of fiber laser using this pumping design. However, the use of compact single-mode laser diodes is a major achievement that allows to minimize the dimensions of FCPA system by eliminating of lower-brightness high-power and larger footprint laser diodes. Compact laser source could decrease system complexity, dimensions, price and be more attractive for certain applications. Further, high-energy sub-W average power femtosecond FCPA system could be used for nonlinear applications, in particular bio-imaging, where high average power is not required and is even harmful [88–91],

efficient parametric wavelength conversion [92] and as a seed source in high-power high-energy femtosecond CPA laser systems [93].

Past time, various fiber laser systems were introduced for the most common wavelengths delivering similar pulse parameters as targeted in the system presented in this chapter:  $\mu\text{J}$ -level energy and few hundred femtosecond pulse duration [81,94–98]. Demonstrated systems generated laser pulses in a range of 0.5-5  $\mu\text{J}$  energy and pulse durations from 160 fs to 711 fs. The average power of laser radiation ranged from 0.5 W to 21 W. All systems were based on chirped pulse amplification and the use of relatively high-power (tens of Watts) multimode low-brightness laser diodes for the pumping of fiber amplifiers. For this reason, demonstrated fiber systems were complex and lacked compactness and simplicity desired for fiber lasers. For FCPA systems that have delivered 0.5 W output power [81,96–98], the usage of high-power laser diodes was not the optimal option. FCPA system, which is presented in the experimental section of this chapter, confirmed that. High-energy femtosecond pulses were delivered from this system using high-brightness single-mode (low-power) laser diodes for core-pumping fiber amplifier. High-power laser diodes are most useful for high-power fiber laser systems with an output power reaching tens or hundreds of watts. The review of the technologies for high-power fiber laser operation is discussed in Chapter 3 of this thesis.

Amplification of ultrashort pulses and high-energy realization is limited by nonlinear effects. An excessive uncompensated nonlinear phase-shift may result in distorted temporal pulse envelope after pulse compression. Fortunately, undesired nonlinear phase-shift could be partly compensated introducing various techniques presented in the next section.

### **2.1.2 Compressed ultrashort pulse quality enhancement and techniques for nonlinear phase-shift compensation**

Nonlinear effects limit the maximum achievable pulse quality and energy from the fiber lasers. FCPA technique and parabolic shape pulse spectrum formation introduced in Chapter 1 can help to mitigate these effects. However, self-phase modulation occurring in the amplification stage of chirped pulses contributes an additional nonlinear phase-shift that result in the compressed pulse quality degradation. Hence, dispersion matching and control of a nonlinear phase-shift are essential for high-energy femtosecond fiber lasers. This section reviews compressed ultrashort pulse quality enhancement techniques and partial compensation of a nonlinear phase-shift

in order to achieve better compressed pulse quality or even higher pulse energy from nonlinear FCPA systems.

It was described that significant compressed pulse distortion occurs in FCPA systems for the accumulated nonlinear phase-shift above 1 rad [60]. A detailed investigation showed that the spectral phase induced by the self-phase modulation can be partly compensated using normal dispersion in chirped pulse amplification system [99]. This technique was demonstrated for few designs of FCPA systems employing different stretching and compressing elements. Demonstrated methodology was particularly useful in systems using static (hardly tunable) dispersive elements such as CVBG. The change of normal dispersion was introduced by varying the length of the fiber in the system. Significant pulse quality enhancement was demonstrated in the systems that accumulated  $\sim 10$  rad nonlinear phase-shift. The effect of the phase compensation above and below the optimum nonlinear phase-shift values were presented. It should be noted, that higher nonlinear phase-shift (B-integral values) are permitted at larger bandwidth of the pulse. Thus, phase compensation mechanisms are particularly important in systems that aim to obtain compressed pulse durations of less than 300 fs.

Nonlinear phase-shift could be partly compensated by using not only positive second-order dispersion but third-order dispersion as well [100,101]. Stretcher and compressor in CPA system can be designed to have residual TOD that is used to compensate the nonlinear phase-shift accumulated in the system. Using this technique, high-quality 30  $\mu$ J pulse energy, 240 fs duration pulses were achieved despite large accumulated nonlinear phase-shift of  $17\pi$  rad [102]. In another demonstrated FCPA system based on 40  $\mu$ m core-diameter photonic crystal Yb-doped fiber amplifier, 650 fs pulse duration and 100  $\mu$ J energy laser pulses were obtained after compression by forming asymmetric pulses in temporal and spectral domain [103]. The disadvantage of such method is that the system is optimized for a certain pulse energy and the pulse quality is decreased not only for the higher pulse energies due to the uncompensated part of the nonlinear phase-shift but also for the lower pulse energies due to the dispersion mismatch.

Residual nonlinear phase shift can also be used to compensate the dispersion mismatch in the system in order to improve the pulse quality [104]. A certain amount of fiber with negative TOD was implemented to reduce the total value of TOD in the system. High-quality (90% of total energy contained in the main pulse) 10  $\mu$ J energy pulses were obtained at the output of the system.

The demonstrated techniques where nonlinear phase-shift was compensated by positive second-order or even third-order dispersion are inconvenient because it requires a cut back of the fiber inside the fiber laser system for optimization of the pulse duration after pulse compression. To overcome this inconvenient phase compensation mechanism, alternative technique using temperature tunable CFBG unit was proposed [83,105]. The positive second-order dispersion required for nonlinear-phase compensation was induced by a linear temperature distribution along the CFBG stretcher. By using the second or the third-order dispersion for nonlinear phase-shift compensation, the nonlinear phase-shift is only partially compensated. The uncompensated higher-order spectral phase can be reduced by applying nonlinear temperature gradient along the CFBG stretcher. A significant compressed pulse quality improvement was achieved by lowering the uncompressed pulse pedestal and shortening pulse duration by 50%, compared with the case where constant or linear temperature distribution along CFBG was applied [105]. It showed the possibility that higher-order dispersion parameter can be compensated by using more sophisticated temperature distributions. However, careful temperature distribution management and advanced technological units for the control of the temperature along the CFBG would be required.

Forementioned methods that uses second and/or third-order dispersion for nonlinear phase-shift compensation by using an additionally implemented fiber or special design of the stretcher and compressor in the FCPA system can be defined as passive compensation methods. The compressed pulse quality in nonlinear FCPA systems can also be improved by implementing active techniques based on the use of programmable spatial light modulators. This approach was presented in section 1.1.2 by introducing the control of the pulse spectrum shape for parabolic pulse formation, the management of spectral phase and compressed pulse quality [63]. The implementation of a spatial light modulator in FCPA system allowed active modulation of the pulse amplitude and phase (or phase only) of the initial pulse for the enhancement of compressed pulse quality [106,107]. This sophisticated technique together with an adaptive feedback loop monitoring the compressed pulses makes it possible to compensate for any effect of phase modulation in the fiber and to obtain ideal transform-limited or user-defined shape pulses at the output of the system. In the demonstrated system using spectral-phase pre-shaping, high-quality 65  $\mu\text{J}$  energy pulses with a duration of 800 fs were produced after the pulse compression. The peak intensity of

the measured autocorrelation was 3.4 times higher compared to the case of unshaped pulses [106].

Similar pulse shaping technology using the acousto-optic programmable dispersive filter based on co-propagating acousto-optic interaction can be implemented in CPA system [108]. The experimental implementation of an acousto-optic programmable dispersive filter in CPA system allowed to compensate the phase distortions and the gain narrowing in the amplifier and enabled the generation of 17 fs duration transform-limited pulses at the output of the system.

Methods for the active control of the pulse amplitude and phase are very useful for the management of the compressed pulses and can be employed for different applications in ultrafast science and technology. However, this approach significantly increases the complexity and cost of the system which may be unacceptable for compact stand-alone fiber lasers.

F CPA systems operating under high nonlinear conditions are highly sensitive to the slightest spectral, phase and temporal envelope modulations of chirped pulses [109–111]. Such modulations are amplified and strongly distort the phase characteristics of the compressed pulses by forming a pedestal or satellite pulses. During amplification and nonlinear propagation in the optical fiber, intensity of the initial amplitude modulation increases. These modulations ultimately lead to the appearance of phase modulation and a decrease in pulse contrast. Thus, low pulse quality at the input of the amplifier and large accumulated nonlinear phase-shift (B integral) result in lower pulse quality at the system output. Strongly increased modulation, due to the optical Kerr effect in the fiber amplifier, can even result in a pulse breakdown or energy exchange between the main and side pulses. Spectral or phase distortions can be caused by the spectral response of non-ideal fiber-optical components, especially by the low-quality pulse stretchers used in F CPA systems or can originally be generated in the oscillators [112]. Weak modulations can never be avoided in real laser systems, thus the quality of the components used in the laser must be very high and the accumulated nonlinear phase-shift preferred to be as low as possible in order to generate high-quality and high-contrast ultrashort pulses.

The illustration of compressed pulse quality degradation in nonlinear F CPA system utilizing low-quality CFBG stretcher which had a modulated phase profile is provided in Fig. 2.1.1. Measured autocorrelation trace of low-contrast compressed pulses is shown in log scale. The appearance of side pulses was caused by initial group delay modulations of CFBG stretcher (depicted in the inset of the Fig. 2.1.1.) and the influence of high gain and

accumulated large nonlinear phase-shift in the power amplifier. Numerical simulation was performed using an experimentally measured group delay trace for pulse stretching in time. The pulses were amplified in a single-mode fiber amplifier where a nonlinear phase-shift of  $2\pi$  rad was accumulated. The compressed pulses had the same low pulse contrast with observable side pulses at the same time positions as in the experimentally measured autocorrelation trace (Fig. 2.1.1.). A good agreement of numerical simulation and experimental measurement confirmed the origin of the compressed pulse quality degradation.

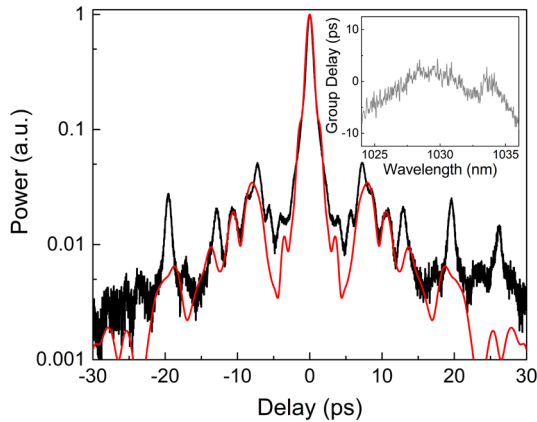


**Fig. 2.1.1.** Measured (black line) and numerically simulated (red line) autocorrelation traces of compressed pulses from FCPA system using CFBG pulse stretcher which had a modulated phase profile. Inset: experimentally measured group delay trace with eliminated linear slope of CFBG for the evident presentation of GD modulations.

Temporal contrast enhancement of high-energy laser pulses can be achieved using a proposed technique based on spectral filtration of self-phase-modulation broadened spectrum [113]. Using this method, low temporal contrast initial pulses were amplified and pulse spectrum broadened due to the effect of self-phase modulation. Spectrally broadened pulses were filtered using super-Gaussian filter by passing just one sidelobe of the spectrum which had a smooth envelope and corresponded to a very short pulse with strongly improved contrast. Experimentally measured temporal contrast of the pulse was enhanced by at least seven orders of magnitude. Unfortunately, this method may not be suitable for all technological applications, as it results in a shift of central wavelength of pulse spectrum. In a demonstrated system, initial central wavelength of 1030 nm was shifted to a 1060 nm spectral region of about 20 nm

bandwidth. The gain bandwidth of the laser amplifier must be wide enough to support further pulse amplification at such case of spectral shift.

In conclusion, the generation of ultrashort high-energy laser pulses in FCPA systems is limited by the nonlinear effects resulting in pulse quality degradation after pulse compression. This makes the development of such laser systems extremely difficult. Presented techniques can help to increase pulse quality and contrast by compensating these effects. However, some methods can be too complex for the commercial fiber systems. As it has been shown in this section, the most important thing for the design of high-energy FCPA systems remains the use of extremely high-quality fiber-optical components that would not degrade the phase characteristics of ultrashort pulses. The regime of laser operation is preferred which accumulate nonlinear phase-shift as low as possible as well.

### **2.1.3 The influence of photodarkening effect in fiber amplifiers**

The photodarkening effect is recognized as one of the limiting factors of high-energy FCPA systems, especially pumped by high-intensity laser diode radiation. This effect reduces the lifetime and reliability of fiber amplifiers and it must be mitigated for the desired laser operation.

The photodarkening effect is described as light-induced optical losses which occur in silica fibers doped with different rare earth ions, including ytterbium-doped fibers. The optical losses are supposedly resulted by the formation of color centers in glass, which increase the level of the loss and reduce the output power from the laser. Unfortunately, the mechanism of the color center formation in silicate glass fibers is not fully investigated and explained to this date. It was observed that photodarkening rate depends on the inversion of ytterbium ions, concluding that 3 to 4 excited ions create one color center responsible for the induced losses [114]. Detailed research of the effect showed that photodarkening is not uniformly distributed over the cross-section and the length of the Yb-doped fiber [115,116]. Further, the optimization of the core composition can efficiently reduce the photodarkening in Yb-doped fiber amplifiers [117]. The certain concentrations of ytterbium ions and co-dopants of the fiber core as aluminum and phosphorous [117,118], cerium [119] or sodium [120] can significantly reduce the light-induced optical losses or even eliminate them. The development and improvement of new designs of rare-earth-ion-doped fibers that are more resistant to the photodarkening effect are always on demand for high-power and high-energy fiber laser systems [121].

The influence of UV exposure and heat treatment for the effect of photobleaching, defined as a reduction of light-induced optical losses, was presented [122,123]. The laser radiation characteristics can be fully restored by exposing the fiber with UV radiation or heating it over 200<sup>0</sup>C for a certain amount of time. However, these methods are usually used for the scientific investigation of the photodarkening and photobleaching effects and are not practically applicable in commercial laser systems.

The level of light-induced optical losses strongly depends on the laser configuration and design of fiber amplifiers. The main goal presented in this chapter is not to investigate the nature of the effect but to optimize the Yb-doped fiber amplifier configuration implemented in FCPA system that enables the minimization of the photodarkening and realization of a stable and efficient high-energy operation of a fiber laser.

## **2.2 Compact high-energy and moderate average power FCPA system**

Material related to this section was published in A2

A compact 10  $\mu$ J pulse energy, sub-W average power and 349 fs pulse duration FCPA system utilizing a core-pumped single-mode Yb-doped fiber amplifier and a matched pair of CFBG stretcher and CVBG compressor is presented in this section. Partial nonlinear phase-shift of  $>1\pi$  rad compensation mechanism was demonstrated by using the second-order and the third-order dispersion which was induced by temperature distribution along the CFBG stretcher in order to improve the compressed pulse quality. The optimization of a single-mode fiber amplifier consisting of ytterbium doped fibers with different concentrations enabled the minimization of a photodarkening effect and realization of a stable operation of a fiber laser.

### **2.2.1 Experimental FCPA system based on a CFBG stretcher and CVBG compressor with matched dispersion profile**

On the basis of the work presented in Chapter 1, the developed high-quality femtosecond fiber laser was used as a front-end for building a high-energy FCPA system. The experimental setup of the developed high-energy FCPA system is illustrated in Fig. 2.2.1. The already described front-end consisted

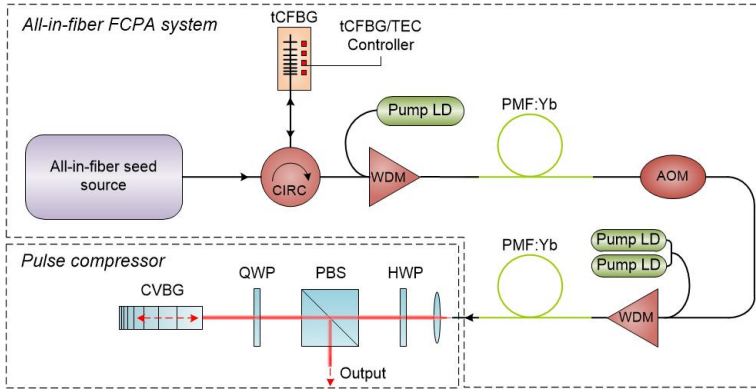


**Fig. 2.2.1.** Schematic presentation of the high-energy FCPA system. CIRC - optical circulator, tCFBG - thermally tunable CFBG module, WDM - wavelength-division multiplexer, LD - laser diode, PMF:Yb – ytterbium-doped polarization maintaining single-mode fiber, AOM - acousto-optic modulator, HWP - half-wave plate, PBS - polarization beam splitter, QWP - quarter-wave plate, CVBG - chirped volume Bragg grating.

of all-in-fiber seed source (passively mode-locked oscillator and a stage of nonlinear pulse spectrum broadening), CFBG stretcher (*TeraXion*) and a fiber amplifier pumped by a single-mode laser diode.

The parameters of the laser radiation from the all-in-fiber front-end are summarized here as a reminder. Linearly up-chirped pulses of 13 ps duration from the seed source (1029.4 nm central wavelength, 10.6 nm pulse spectrum bandwidth at FWHM, 53 MHz pulse repetition rate) were down-chirped to about 230 ps pulse duration by using a CFBG stretcher with group delay dispersion of  $\beta_2 = -13.65 \text{ ps}^2$ . Thermal tuning of the CFBG was used for fine dispersion control. Chirped laser pulses were combined with pump radiation from a single-mode laser diode (976 nm) by wavelength-division multiplexer and amplified in a core-pumped single-mode Yb-doped fiber amplifier up to 7.8 nJ pulse energy. A detailed description of this fiber seed source can be found in section 1.2 of this thesis.

Pulse repetition rate was reduced using a fiber-coupled acousto-optic modulator (AOM) before the power amplifier enabling pulse amplification from nanojoule to microjoule energy level. The brightness of pump radiation was doubled by using incoherent polarization beam combination technique of two single-mode laser diodes. Resulting 1.4 W pump power was coupled to the 11  $\mu\text{m}$  core of the Yb-doped truly single-mode fiber (0.3 m length) which produced high pump power density of  $\sim 3 \text{ MW/cm}^2$ . For comparison, pump power of  $\sim 200 \text{ W}$  would be required to reach the same intensity for the scenario of the cladding coupling in 125  $\mu\text{m}$  diameter fiber. A small mode area ( $\sim 100 \mu\text{m}^2$ ) pump radiation of 1.4 W gave high power density in the

core of the fiber and enabled high gain in relatively short fiber amplifier. Moreover, high absorption Yb-doped fiber was used (ytterbium doping concentration was estimated to be about  $7 \cdot 10^{25} \text{ m}^{-3}$ ) to obtain efficient high-energy operation. All FCPA system, except the compressor, was monolithically fusion spliced realizing a robust and environmentally stable design of the laser. Amplified pulses were compressed in the free space CVBG compressor and out-coupled from the laser by separating incident and reflected beams using a quarter wave-plate (QWP) and a polarizing beam splitter (PBS), as shown in Fig. 2.2.1.

Beam quality at the output of the system was measured by performing z-scan at  $\mu\text{J}$ -level pulse energy. Incident beam diameter at the input of the CVBG was about 1.1 mm (at  $1/e^2$  level). Measured beam quality parameter  $M^2 \sim 1.06$  in directions perpendicular to the propagation axis was close to the diffraction limit indicating excellent beam spatial properties (Fig. 2.2.2), as it could be expected from a single-mode fiber amplifier. The spatial beam properties were not distorted in the CVBG compressor operating at the highest pulse energy of 10  $\mu\text{J}$  which indicated a good optical homogeneity of photo-thermo-refractive glass as well as a precise control of geometry of the holographically recorded chirped Bragg grating.

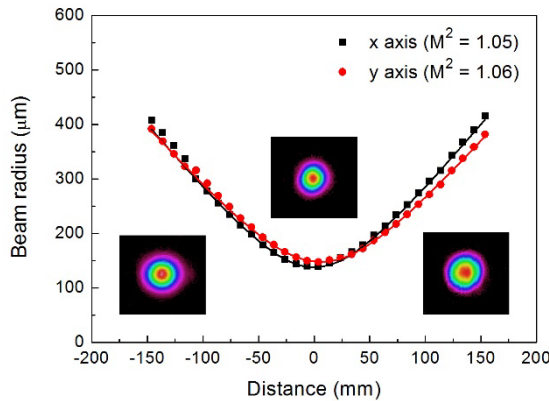


**Fig. 2.2.2.** Measurement of the beam quality parameter  $M^2$  ( $4\sigma$ ) for both directions perpendicular to the axis of propagation at the output of the high energy FCPA system. Insets: beam intensity profiles at three different positions from the waist location.

Dependence of average output power and pulse energy on the pulse repetition rate is shown in Fig. 2.2.3. At 10.6 MHz pulse repetition rate average power of 658 mW was measured after compressor corresponding to 62 nJ pulse energy. Although, average output power was reduced by less

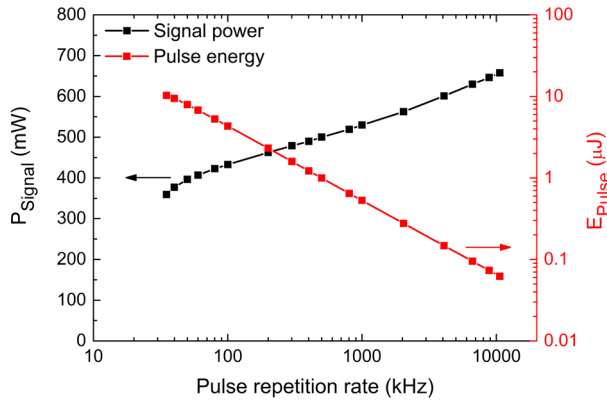


**Fig. 2.2.3.** Dependence of average amplified signal power (left axis) and pulse energy (right axis) after pulse compressor on pulse repetition rate. Highest pulse energy of  $10 \mu\text{J}$  was achieved at lowest pulse repetition rate of 35 kHz.

than two times to 359 mW though seed power after AOM coupled to the amplifier was reduced from 47 mW at 10.6 MHz to 0.16 mW at 35 kHz pulse repetition rate. Weak dependence of average output power on seed input power manifested high level of saturation in the single-mode fiber amplifier. Highest pulse energy of  $10 \mu\text{J}$  after the compressor was obtained at 35 kHz pulse repetition rate corresponding to 26 MW peak power and a total gain of 34.8 dB in the power amplifier.

Finally, a compact high-energy and moderate average power femtosecond FCPA system was constructed. Robustness and environmental stability of the fiber laser was achieved by the design choices: only polarization maintaining fiber was used in the laser system and the laser was monolithically fusion spliced. Very compact air-cooled setup was obtained by the use of compact single-mode laser diodes and a versatile fiber technology which allows fibers to be bent and coiled. The entire fiber laser system, together with the necessary laser control electronics and power supply units was placed in a housing of only  $45 \times 43.6 \times 13.3 \text{ cm}^3$  footprint. The use of a CVBG compressor enabled the construction of the small footprint laser head (output collimator, isolator and CVBG) of approximately  $15 \times 7 \times 7 \text{ cm}^3$  in size. Laser systems based on solid-state laser technologies delivering similar high-energy ultrashort pulse parameters are at least few times larger and can reach even table-top sizes.

## 2.2.2 Examination of ultrashort pulses and nonlinear phase-shift compensation by applying second-order and third-order dispersion

Compressed ultrashort pulse quality can be enhanced by compensating nonlinear phase-shift that occur due to high nonlinearities in fibers at high-energy laser operation. Partial nonlinear phase-shift compensation mechanism by the appliance of second-order and third-order dispersion which was induced by the temperature distribution along the CFBG stretcher is presented in this section.

Pulse compression quality was examined at different output pulse energies using second harmonic non-collinear autocorrelator. Measured widths (FWHM) of autocorrelation functions (ACF) at different pulse energies are shown in Fig. 2.2.4. ACF widths of the Fourier transform-limited pulses were calculated from experimental pulse spectra and are

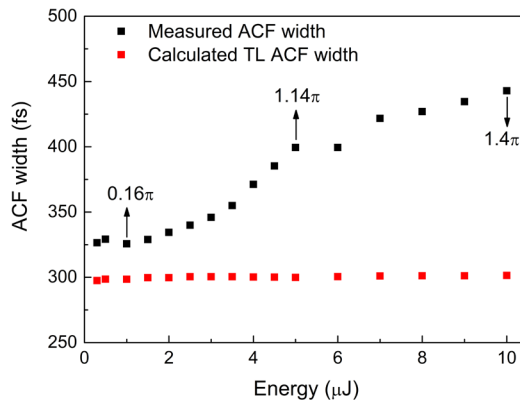


**Fig. 2.2.4.** Width (FWHM) of autocorrelation function of laser pulses at different energies in comparison with FTL pulse autocorrelation function width. Accumulated nonlinear phase-shift in a single-mode amplification stage at three different pulse energies is indicated in the picture.

shown at the same graph. For pulse energies below 2  $\mu\text{J}$ , FTL and measured ACF widths were similar,  $\sim 300$  fs and  $\sim 330$  fs respectively. Assuming Gaussian pulse shape at low pulse energies, this corresponded to pulse duration of  $\sim 240$  fs. For pulse energies above 2  $\mu\text{J}$ , FTL and measured ACF widths differed significantly. This could be attributed to the accumulation of nonlinear phase which cannot be completely compensated in the system. Accumulated nonlinear phase-shift was partly compensated by changing dispersion of CFBG stretcher. When pulse energy was increased, a linear

temperature gradient of  $13^{\circ}\text{C}$  per 50 mm of CFBG length was applied to achieve the shortest pulse duration. Optimal thermally induced GDD was estimated to be  $0.077\text{ ps}^2$  for  $10\text{ }\mu\text{J}$  pulse energy. When the dispersion curve of the CFBG is changed by the temperature gradient along the CFBG length, the third-order dispersion of the CFBG is changed too. However, the change of the TOD with the linear temperature distribution implemented in this work was very low, estimated to be  $-0.00012\text{ ps}^3$  and did not affect the compressed pulse.

The results of numerical simulation on how induced TOD (and GDD) values affect pulse temporal envelope and duration is presented in Fig. 2.2.5.

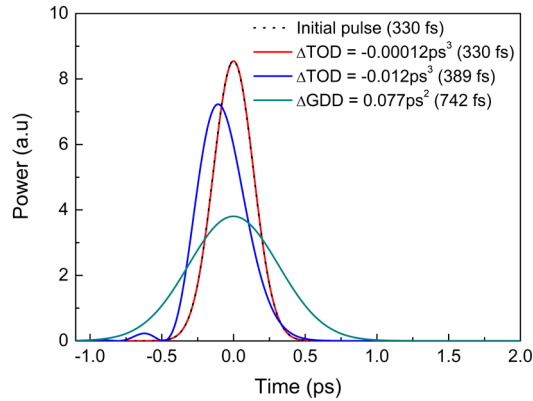


**Fig. 2.2.5.** The numerically simulated pulse temporal envelopes at different conditions of induced certain values of TOD and GDD:  $\Delta\text{TOD} = -0.00012\text{ ps}^3$  (red curve),  $\Delta\text{TOD} = -0.012\text{ ps}^3$  (blue curve),  $\Delta\text{GDD} = -0.077\text{ ps}^2$  (dark cyan curve).

First, Gaussian-like 330 fs duration initial pulse was simulated (black dotted curve in Fig. 2.2.5.) and TOD value of  $-0.00012\text{ ps}^3$  was applied on that pulse (red curve). No change in pulse quality or pulse duration was observed. Then a hundred times larger value of TOD was taken ( $-0.012\text{ ps}^3$ ) in order to show that this value would have an influence to the quality of the pulse (blue curve). The peak power of the pulse was reduced by  $\sim 15\%$  and pulse quality resulted in the increase of a pulse duration to 389 fs and the slight change of the pulse shape. In addition, the estimated value of GDD ( $\sim 0.077\text{ ps}^2$ ) was applied on the initial pulse to show that the model has a good agreement with the experimental data. With this change of GDD value, the pulse duration increased to 742 fs (dark cyan curve) which would give  $\sim 1.05\text{ ps}$  ACF width and has a good agreement to experimentally measured ACF shown in Fig. 2.2.6 (blue curve). There is a small difference in pulse duration between the simulated and the experimentally measured results

because of the slightly different initial pulse shape and a duration. Nevertheless, this numerical simulation was intended to illustrate that the estimated TOD value of  $-0.00012 \text{ ps}^3$  does not affect pulse quality and is too small to compensate the nonlinear phase-shift.

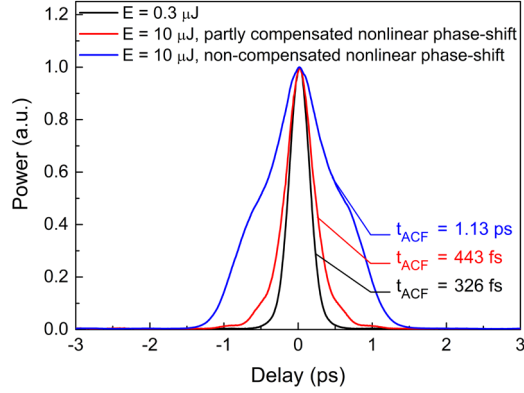


**Fig. 2.2.6.** Measured autocorrelation traces of compressed pulses with non-compensated nonlinear phase (blue line) and partly compensated nonlinear phase (red line) at  $10 \mu\text{J}$  pulse energy in comparison with measured  $0.3 \mu\text{J}$  pulse energy autocorrelation trace (black line).

Accumulated nonlinear phase-shift, characterized by B-integral, was estimated to be  $1.4\pi$  rad for  $10 \mu\text{J}$  pulse energy using phase-compensation relation derived in [99]. Accumulated nonlinear phase-shift, estimated using the compensating temperature gradient values at three different pulse energies was indicated in Fig. 2.2.4 by arrows. Measured autocorrelation traces of the compressed pulses after CVBG with non-compensated nonlinear phase and partly compensated nonlinear phase at  $10 \mu\text{J}$  pulse energy is shown in Fig. 2.2.6. The partially compensated nonlinear phase-shift enabled to achieve a higher temporal quality and a higher peak power of the pulse.

In previous experiments the nonlinear phase-shift was not completely compensated as it would require the appliance of higher order dispersion in the system. Just a second-order dispersion was used for the partial compensation in that demonstration. The further compensation of residual nonlinear phase-shift was demonstrated by using third-order dispersion which was induced by the nonlinear temperature distribution along the CFBG stretcher.

Measured autocorrelation traces of compressed  $10 \mu\text{J}$  energy pulses with different applied temperature distributions along the CFBG and induced TOD values for the further compensation of nonlinear phase-shift is depicted

in Fig. 2.2.7. A case of optimally compressed pulses using a linear temperature distribution along CFBG stretcher was chosen as a reference.

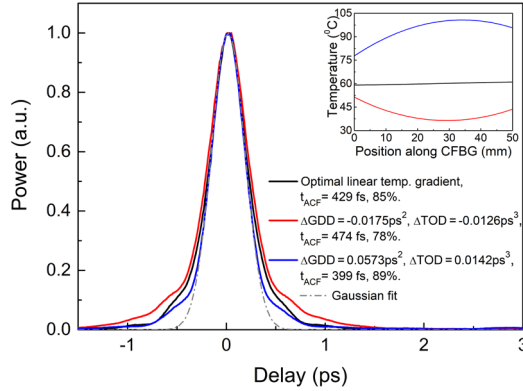


**Fig. 2.2.7.** Measured autocorrelation traces of compressed 10  $\mu$ J energy pulses with different induced TOD values for the further compensation of nonlinear phase-shift. Cases of an optimal linear temperature distribution along CFBG (black line) and nonlinear temperature gradient (red and blue lines) are provided. Inset: corresponding temperature distributions along CFBG.

Two cases of different nonlinear temperature gradients inducing the TOD values of the opposite sign is provided. For optimization of the pulse compression the change of GDD, together with TOD, was required which was estimated and is provided in Fig. 2.2.7. Better pulse quality was achieved using nonlinear temperature gradient which induced  $\Delta TOD = 0.0142 \text{ ps}^3$  and  $\Delta GDD = 0.0573 \text{ ps}^2$  values, compared to the case of optimized linear temperature distribution. A FWHM width of the ACF was slightly reduced from initial 429 fs to 399 fs, resulting in a decreased pulse duration of  $\sim 283$  fs for a Gaussian-like pulse. Enhanced pulse quality can be described by the reduction of uncompressed pulse pedestal. It was defined comparing the area under the curve of the compressed pulse to the area under the Gaussian-like envelope of the approximation. Evaluation showed that the reduction of the pulse pedestal increased this quality parameter by 4% which resulted to the slight increase of the pulse peak power as well. The case of nonlinear temperature distribution which induced TOD value of the opposite sign (red curve in Fig. 2.2.7.) provided degradation of the pulse quality by the increase of pulse duration and larger uncompressed pulse pedestal. The further demonstration of this effect and induced dispersion values were limited by the maximal temperature gradient that could be induced in the CFBG unit.

These experimental measurements showed that the nonlinear phase-shift can be successfully compensated using a positive value of second-order dispersion and further diminished by the additionally induced TOD. High-energy and peak power ultrashort pulse operation would be complicated without this pulse quality enhancement mechanism.

### 2.2.3 Characterization of high-energy ultrashort pulses delivered from FCPA system

The characterization of high-energy ultrashort pulses delivered from a compact FCPA system is presented in this section. Optimized pulse temporal and spectral characteristics from a very similar FCPA system which can be used as a seed source in high-power high-energy femtosecond CPA laser systems based on solid-state Yb:YAG amplifier is also discussed.

The output pulse duration after the CVBG compressor from the FCPA system, described in the section 2.2.1, was also measured using SHG FROG method at 1  $\mu\text{J}$  and 10  $\mu\text{J}$  pulse energies. Pulse envelopes retrieved by FROG algorithm (*Swamp Optics*) are shown in Fig. 2.2.8. FROG retrieval yielded a retrieval error of 0.1% and was performed on a  $1024 \times 1024$  grid. Retrieved pulse durations were 247 fs for 1  $\mu\text{J}$  and 349 fs for 10  $\mu\text{J}$  pulse energies. Fourier transform-limited pulse duration calculated from the measured spectrum was about 220 fs at all measured pulse energies. Temporal Strehl ratio, which was defined as a ratio of the peak power of the pulse to the peak power of transform-limited pulse, was estimated to be 0.88 for 1  $\mu\text{J}$  and 0.61

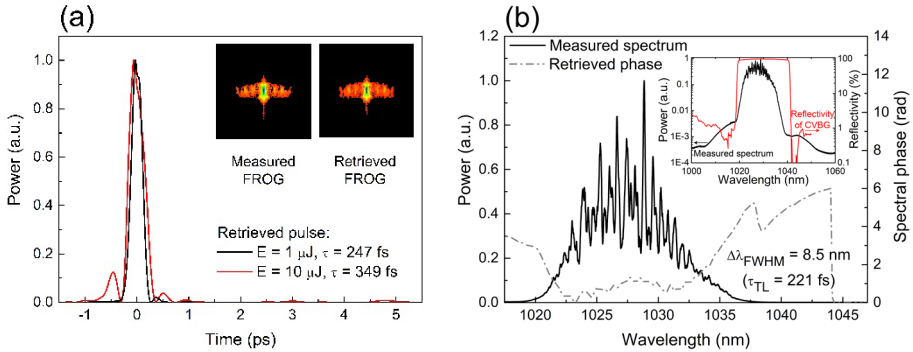


**Fig. 2.2.8.** a) Envelope of the compressed pulses retrieved from SHG FROG measurement at 1  $\mu\text{J}$  and 10  $\mu\text{J}$  pulse energies. Inset: measured and retrieved FROG traces at 10  $\mu\text{J}$  pulse energy. b) Measured pulse spectrum from the FCPA system at 10  $\mu\text{J}$  pulse energy along with retrieved spectral phase from a FROG measurement. Inset: measured pulse spectrum before CVBG compressor showed in a logarithmic scale together with a measured reflectivity profile of CVBG.

for 10  $\mu\text{J}$  pulse energy. Amplified spontaneous emission (ASE) power level was evaluated from the laser spectrum before the compressor at 10  $\mu\text{J}$  pulse energy (inset of Fig. 2.2.8(b)). After CVBG compressor, which also operated as a spectral filter, ASE accounted for  $\sim 2\%$  ( $\sim 7\text{ mW}$ ) of the total 359 mW output power. As it was mentioned before, modest pulse quality degradation can be attributed to the accumulated nonlinear phase-shift of  $1.4\pi$  rad in the small mode area ( $\sim 100\ \mu\text{m}^2$ ) fiber amplifier. This was also confirmed by a residual phase retrieved from FROG measurement shown in Fig. 2.2.8(b) along the measured spectrum. The enhancement of spectral modulations due to SPM was also observed (Fig. 2.2.8(b)). The initial spectral modulation could arise from group delay ripples of the CFBG stretcher or from the internal reflections in micro-optical components used in the FCPA system. It was previously shown that a small initial spectral modulation leads to pulse contrast degradation in nonlinear CPA system [109,110]. Small amplitude of  $\sim 1\%$  satellite pulses in the range of 3-5 ps from the main pulse can be seen in Fig. 2.2.8(a) at the case of 10  $\mu\text{J}$  pulse energy. The spacing of the satellite pulses matched well with modulation frequency of the spectrum.

Despite a large nonlinear phase-shift and a high pulse compression ratio of  $\sim 660$ , overall temporal quality of the compressed pulses at the highest energy was still quite good. Based on the FROG retrieval results, it was estimated that  $>85\%$  of the energy was stored in the main part of the pulse. This pulse energy ratio would significantly drop with the increased nonlinear phase-shift in the fiber amplifier. However, in this configuration of fiber amplifier, the demonstration of higher pulse energy was limited by the gain saturation in the fiber amplifier.

The length of the fiber amplifier and accumulated nonlinear phase-shift must be optimized to achieve high-quality ultrashort pulses at the output of high-energy fiber laser. This can be demonstrated by using fiber amplifiers of different lengths, which accumulated different nonlinear phase-shifts at the same pulse energy. Measured autocorrelation traces of compressed 1  $\mu\text{J}$  energy pulses using different, 0.9 m and 0.3 m lengths of 11  $\mu\text{m}$  core diameter Yb-doped fiber in the power amplifier are shown in Fig. 2.2.9. The case of the 0.3 m fiber length was chosen as an example of the optimized fiber amplifier which was already introduced in this chapter. High-quality 230 fs duration (326 fs ACF width) pulses were obtained after the pulse compression. Accumulated nonlinear phase-shift was estimated to be  $0.16\pi$  rad which was low enough and did not affect the compressed pulse

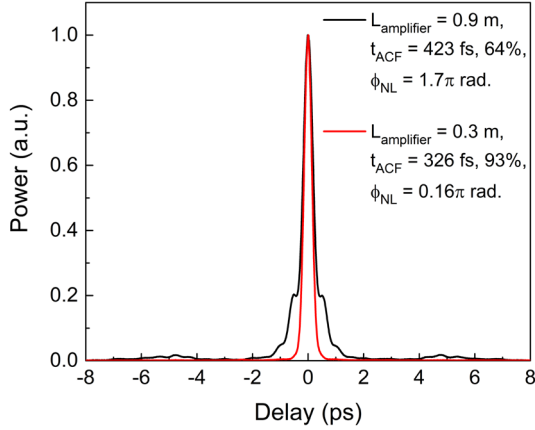


**Fig. 2.2.9.** Measured autocorrelation traces of compressed 1  $\mu\text{J}$  energy pulses using different length (0.9 m and 0.3 m) 11  $\mu\text{m}$  core diameter Yb-doped fiber amplifier.

quality. Pulse quality parameter evaluating the area under the curve of measured and approximated Gaussian-like pulses was accounted and equal to 93%. Significantly lower pulse quality was obtained by using a longer (0.9 m length) fiber amplifier. Accumulated nonlinear phase-shift was estimated to be  $\sim 1.7\pi$  rad which resulted in longer pulse duration of 300 fs (423 fs ACF width), increased uncompressed pulse pedestal and side pulses. It had the considerable impact to the decreased peak power of the pulse. For comparison, pulse quality parameter dropped to 64%.

## 2.2.4 High-energy FCPA system optimized for solid-state Yb:YAG amplifier

A very similar high-energy FCPA system with optimized output parameters for high-power high-energy femtosecond CPA laser system based on solid-state Yb:YAG amplifier was demonstrated. The Yb:YAG material has significantly narrow gain bandwidth compared to Yb:glass, so the seed source should have a narrower pulse spectrum than demonstrated in previous section (8.5 nm at FWHM) in order to achieve high gain efficiency.

Linearly up-chirped pulses of  $\sim 4$  ps duration and 3.93 nm spectrum bandwidth at FWHM were delivered from all-in-fiber seed source. A higher group delay dispersion of  $\beta_2 = -33.7 \text{ ps}^2$  of CFBG was used to stretch pulses to 220 ps duration. Dispersion profiles between CFBG stretcher and CVBG compressor were matched in this case as well in order to obtain high-quality ultrashort pulses at the output of the system. The whole schematic setup was the same as introduced in Fig. 2.2.1. Stretched pulses were amplified in

single-mode fiber amplifiers to 10  $\mu\text{J}$  pulse energy and examined using SHG FROG autocorrelation method. Pulse envelope retrieved by FROG algorithm and experimentally measured pulse spectrum along with the retrieved spectral phase are shown in Fig. 2.2.10.

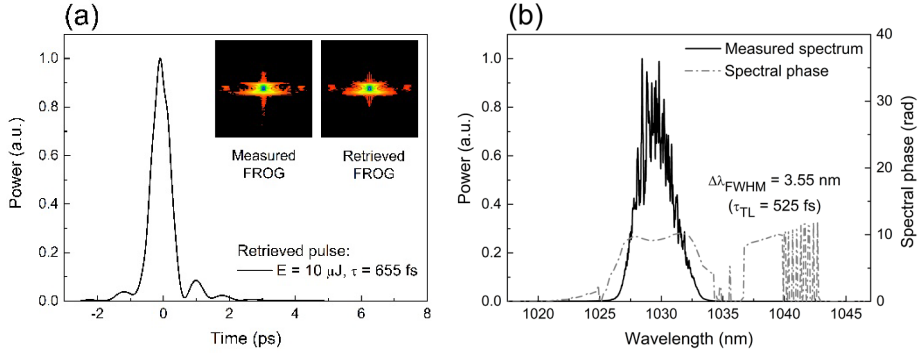


**Fig. 2.2.10.** High-energy FCPA system, which parameters was optimized for Yb:YAG amplifier. a) Envelope of the compressed pulse retrieved from SHG FROG measurement at 10  $\mu\text{J}$  pulse energy. Inset: measured and retrieved FROG traces. b) Measured pulse spectrum at 10  $\mu\text{J}$  pulse energy along with retrieved spectral phase from FROG measurement.

Retrieved pulse duration of 655 fs was obtained while Fourier transform-limited pulse duration calculated from the measured spectrum was about 525 fs. The energy stored in the main part of the pulse was estimated from FROG retrieval results and was equal to  $\sim 88\%$ , manifesting the high quality of the compressed pulses. Modest pulse quality degradation can be attributed to the similar level of accumulated nonlinear phase-shift of  $>1\pi$  rad in the small mode area fiber amplifiers as in previously demonstrated FCPA system. Such fiber laser was used as a seed source in a femtosecond CPA laser system based on a double-pass Yb:YAG free-space amplifier delivering 20 W of average power, 104  $\mu\text{J}$  energy and 764 fs duration pulses [93].

In conclusion, the accurate dispersion profile matching of the stretcher and compressor, together with the compensation mechanism of accumulated nonlinear phase-shift enabled the high-quality ultrashort pulse generation in the high-energy FCPA system.

### 2.2.5 Optimization of a single-mode fiber amplifier configuration and minimization of photodarkening effect

Robust and environmentally stable operation of high-energy femtosecond fiber laser is as important as the temporal and spectral quality of the compressed ultrashort pulses and spatial properties of the beam. The

photodarkening effect, recognized as a limiting factor of high-energy FCPA system pumped by high-intensity laser radiation, reduces the lifetime and reliability of Yb-doped fiber amplifiers. This undesired effect must be mitigated for a stable laser operation. How optimization of a fiber amplifier configuration which consisted of ytterbium-doped fibers with different concentrations reduced the effect of photodarkening is discussed in this section.

The use of a long low-ytterbium-doped fiber in an amplifier is undesirable because it would induce nonlinear effects and accumulate large nonlinear phase-shifts which would strongly affect the quality of compressed ultrashort pulses and limit the maximal achievable pulse energy (as it was demonstrated in Fig. 2.2.9). In order to avoid using long lengths of fiber, high doping level fiber amplifier is required. However, the usage of high-doping fiber amplifier, especially core-pumped with  $\sim 976$  nm laser radiation, is worst case scenario for the photodarkening. Light-induced optical losses result in the decrease of the output power of the fiber laser. This was also observed in the high-energy FCPA system, which is presented in this section. Dependence of average amplified signal power over time from FCPA system employing a little bit longer (38 cm in length) Yb-doped fiber core-pumped by  $\sim 1$  W of laser diode radiation at 976 nm and operating at 50 kHz pulse repetition rate is presented in Fig. 2.2.11 (black curve). A significant drop of the amplified signal power was observed at the beginning and then decreased to reach a stable power level.

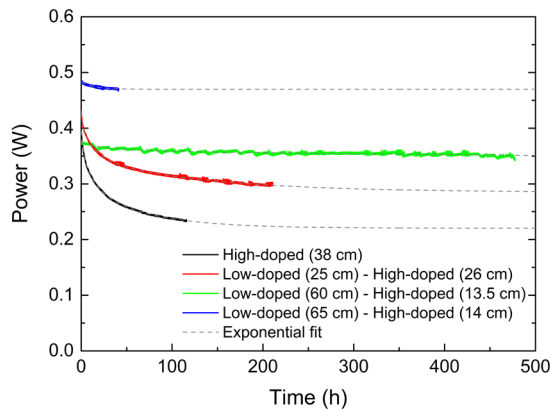


**Fig. 2.2.11.** Dependence of average amplified signal power from FCPA system at 50 kHz pulse repetition rate over time at four different configurations of fiber amplifiers.

The numerical simulations were performed to find an optimal configuration of fiber amplifier that would allow to achieve both - high pulse

energy operation and stable laser output power over time. A certain length of Yb-doped fiber is required for efficient amplification of laser pulses, but this length must be short enough obtaining accumulated nonlinear phase-shift as low as possible. A balance between the gain efficiency and the minimization of nonlinear effects must be achieved. For the optimization of fiber amplifier, two types of ytterbium-doped fibers with different concentrations were selected.

Low-doped (estimated ytterbium doping concentration of  $2 \cdot 10^{25} \text{ m}^{-3}$ ) 6  $\mu\text{m}$  core diameter fiber was used in first centimeters of the fiber amplifier to reduce the level of the gain in high-doped fiber, used further. The length of this fiber must be long enough to reduce the gain in the high-doped fiber, but short enough to avoid undesired nonlinear effects. High-doped (estimated ytterbium doping concentration of  $7 \cdot 10^{25} \text{ m}^{-3}$ ) 11  $\mu\text{m}$  core diameter fiber enabled the efficient amplification and reduced nonlinear effects due to larger diameter of the core. These two fibers were spliced together to ensure a monolithic design of the fiber amplifier. The results of numerically simulated evolution of amplified signal and absorbed pump power, together with nonlinear phase-shift per unit length along low-doped, high-doped and hybrid gain fibers at 50 kHz pulse repetition rate are presented in Fig. 2.2.12.

In a case of fiber amplifier which consisted of only a low-doped fiber (Fig. 2.2.12(a)), a sufficient gain and 0.8 W output power was obtained after 1.2 meters of Yb-doped fiber. Such output power at a pulse repetition rate of 50 kHz would correspond to a pulse energy of 16  $\mu\text{J}$ . However, the accumulated nonlinear phase-shift was over  $13\pi$  rad at that point, which would result in complete degradation of the compressed pulse or even the breakdown of the pulse. Experimentally such an amplifier has not even been tested to avoid major failures of a laser system. The power amplifier configuration consisting of 38 cm length high-doped fiber was numerically simulated to compare it with experimental results. The simulated output power was the direct power from the amplifier, while measured experimentally, was the power after the free-space isolator, used for the protection of the amplifier. By applying about 15% of losses to the simulated output power, the simulated and experimentally measured output powers had a pretty good agreement and was equal to  $\sim 0.4$  W. Accumulated nonlinear phase-shift was calculated to be about  $1.7\pi$  rad at that point. As previously mentioned, this experimentally demonstrated fiber amplifier was affected by a strong photodarkening effect (Fig. 2.2.11. (black curve)).

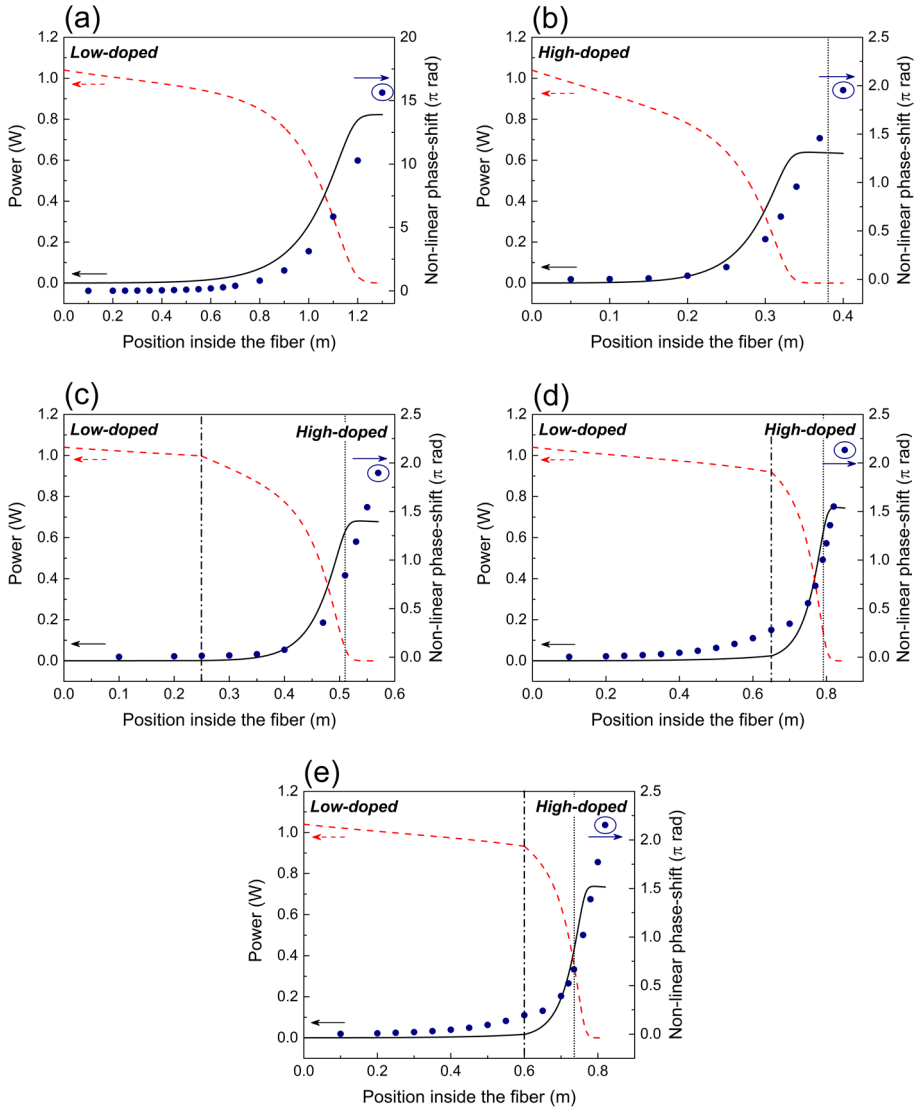


**Fig. 2.2.12.** Numerically simulated evolution of amplified signal (black solid curve) and absorbed pump (red dashed curve) power, nonlinear phase-shift (dots) per unit length along low-doped (a), high-doped (b), low-doped and high-doped hybrid gain fibers (c-e) at 50 kHz pulse repetition rate. Dot-dashed line implies the splice between low-doped and high-doped fibers. Dotted line implies the end of the experimentally demonstrated fiber amplifier. Ytterbium doping concentration was estimated to be about  $2 \cdot 10^{25} \text{ m}^{-3}$  for low-doped and  $7 \cdot 10^{25} \text{ m}^{-3}$  for high-doped fibers.

For the minimization of the photodarkening effect, a hybrid fiber amplifier consisting of 25 cm low-doped and 26 cm high-doped fibers was simulated (Fig. 2.2.12(c)). A simulated output power was similar as in

previous case and nonlinear phase-shift was equal to  $0.84\pi$  rad. Dependence of average power of amplified signal over time using this configuration of fiber amplifier is presented in Fig. 2.2.11 (red curve) along with other fiber configurations. The segment of low-doped fiber reduced the gain in the high-doped fiber. Light-induced optical losses were diminished as well which resulted in a smaller drop of the output power compared to the case of 38 cm length high-doped fiber amplifier.

To minimize the photodarkening effect, longer low-doped fiber and shorter high-doped fiber should be selected. In this case, fiber lengths of 65 cm and 14 cm were chosen accordingly (Fig. 2.2.12(d)). The effect of the photodarkening in the beginning of laser operation was reduced significantly (Fig. 2.2.11 (blue curve)). However, the simulated accumulated nonlinear phase-shift of  $1.1\pi$  rad was desired to be lower in order to maintain high-quality ultrashort laser pulses at the system output.

The lengths of Yb-doped fibers were optimized resulting in 60 cm low-doped fiber and 13.5 cm high-doped fiber final configuration of the fiber amplifier (Fig. 2.2.12(e)). The accumulated nonlinear phase-shift at the end of the amplifier was reduced and estimated to be about  $0.75\pi$  rad. This fiber amplifier configuration was experimentally demonstrated (Fig. 2.2.11 (green curve)). A typical power reduction due to photodarkening effect was not observed and a sufficiently stable laser operation was obtained over 500 hours. This amplifier was used for the construction of a high-energy FCPA system optimized for a femtosecond solid-state CPA laser system based on Yb:YAG amplifier, which was demonstrated in section 2.2.4. There the high-quality of the compressed ultrashort pulses was obtained.

Finally, these results of numerical simulation and experimental demonstration showed that such design of fiber amplifier, consisting of ytterbium-doped fibers with different concentrations, could be used for achieving both - high pulse energy and stable laser output power operation over time by minimizing the photodarkening effect.

## Summary of the results

In this work, a compact high-energy FCPA system employing the matched pair of CFBG stretcher and CVBG compressor was demonstrated. High temporal and spatial quality femtosecond laser pulses of 10  $\mu$ J pulse energy, 26 MW peak power and 349 fs pulse duration were obtained at the output of the system despite large accumulated nonlinear phase-shift of  $1.4\pi$  rad and high pulse compression ratio equal to  $\sim 660$ . Accumulated nonlinear phase-

shift due to SPM was partly compensated by the positive second-order dispersion and further compensated by the additionally applied third-order dispersion which was induced by temperature distribution along the CFBG stretcher. The results of numerical simulation of the single-mode fiber amplifier allowed to construct optimal configuration of the fiber amplifier which consisted of ytterbium-doped fibers with different concentrations. As a result, the photodarkening effect was minimized realizing stable operation of the high-energy fiber laser. This FCPA configuration paves the way for truly compact, robust and environmentally stable femtosecond fiber laser sources which could be used in applications where high peak power is required but moderate average power of sub-W level is sufficient.

## CHAPTER THREE

This chapter is dedicated to discuss the mostly used technologies and configurations of high-power fiber lasers. The literature review presents fiber technologies that enable average output power levels of tens and hundreds of Watts. The techniques, as multiplication of pulse repetition rate and formation of burst of pulses, allow to expand the regimes of the laser operation and thus to increase the burst energy level and to scale the average power. The main challenges and difficulties in designing high-power fiber laser systems are reviewed.

The experimental realization of high-power FCPA systems operating in single-pulse and burst of pulses regimes are presented in the experimental section of this chapter. The methods of pulse repetition rate multiplication, the formation of the pulse bursts and control of the shape of the burst envelope in time domain are introduced.

### 3.1 Literature review

#### 3.1.1 Fiber technology for high-power applications

The use of optical fiber amplifiers in the realization of high average power lasers rely on their exceptional properties comparing to other laser technologies. Good thermal management due to high surface area to volume ratio, low transmission losses, small quantum defect and high gain makes fiber technology suitable for high average power laser operation. Special fiber designs and high pump power storage are required for the construction of high-power fiber lasers.

Spectroscopic properties of Yb-doped silica glass make fiber amplifiers very attractive for ultrashort pulse and high-power operation. Broad emission spectrum enables ultrashort pulse amplification, wide wavelength coverage and tunability from around 980 nm to 1150 nm. Emission and absorption cross-sections of ytterbium-doped silica glass fiber are shown in Fig. 3.1.1. The absorption spectrum ranges from 850 nm to 1070 nm and has two peaks at ~910 nm and 975 nm. The broadband absorption spectrum enables the use of non-stabilized wavelength and lower cost laser diodes at ~910 nm for pumping. Efficient amplification and high gain coefficient are ensured by using this pumping configuration. However, the use of 975 nm narrowband wavelength stabilized laser diode radiation as a pump is

beneficial because the generation of amplified spontaneous emission at this wavelength is avoided.

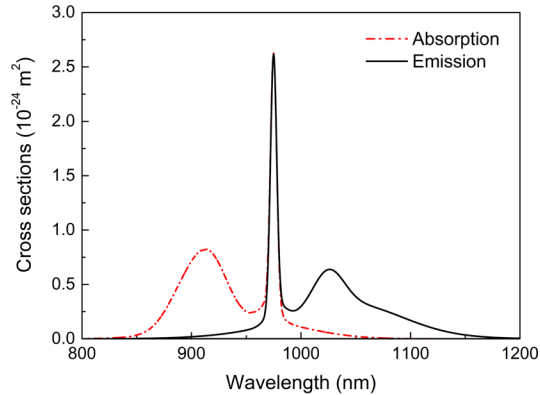


**Fig. 3.1.1.** Emission and absorption cross-sections of ytterbium-doped silica glass fiber [124].

The key component for the development of robust, high-power fiber lasers is high-power pumping source. High-power fiber lasers usually use fiber-coupled concept of pump laser diodes. It has several advantages compared with the direct laser diode emission. First of all, this approach allows the laser light to be delivered directly where it is needed. Moreover, it simplifies the maintenance of laser diodes as they can be easily replaced by splicing the fiber pigtailed and do not require alignment of the laser optics after this procedure. All-in-fiber solution and monolithic design is ensured by using only fiber-coupled components. Furthermore, laser diodes can be implemented separately from the main laser cavity and amplifiers allowing easier thermal management and flexible laser design.

Laser diodes can be fiber-coupled to single-mode or multimode optical fibers. The efficiency of fiber coupling strongly depends on many factors, such as the beam quality of laser diode, type of the fiber, the approach of the coupling light into the fiber and the structure of laser diode module. High-brightness laser radiation of only ~1 W of average power can be coupled into a single-mode 6  $\mu\text{m}$  diameter fiber. In order to reduce the requirements for the beam quality of laser diodes, prevent the damage of the fiber end-face and to achieve much higher coupling capacities, larger diameter (ranging from 105  $\mu\text{m}$  to 600  $\mu\text{m}$ ) multimode fibers with larger numerical apertures of ~0.12-0.22 were introduced. Pump laser modules of 155 W of average optical power coupled into a 105  $\mu\text{m}$  (numerical aperture of 0.15) fiber at 976 nm wavelength and over 363 W at 915 nm were demonstrated [125,126]. Electrical to optical efficiency exceeded 50%. Even

higher power levels are achieved by coupling laser radiation into multimode 200-600  $\mu\text{m}$  diameter fibers. However, the coupled pump power has limitations and cannot be increased indefinitely due to optical damage of the fiber end-face, nonlinear effects and practically achievable maximal values of numerical apertures of the fibers. Nevertheless, more powerful laser diodes are being developed, introduced and commercially available within time as it is desired for high-power laser systems and applications.

In order to efficiently couple the pump laser diode output radiation into high-power fiber amplifier, the specially designed double-clad structure fiber has been developed [127]. It consists of a core doped with rare earth ions, in which only fundamental mode is guided, surrounded by a first cladding of lower refractive index and a second cladding around the first one. Sufficiently large diameter (typically ranging from 105  $\mu\text{m}$  to 600  $\mu\text{m}$ ) first cladding supports a multimode waveguide for high-power pump radiation which now can be effectively coupled into the fiber. As it propagates down this cladding, pump radiation overlaps spatially with the rare-earth-ion-doped core and is absorbed gradually. The newly generated light is trapped in a core of a smaller size and a lower numerical aperture. In such way cladding-pumped fiber laser operates as a brightness converter which transforms lower brightness pump light into high brightness and intense laser radiation. Fiber-optic combiners are used for the coupling of pump and signal radiation into the fiber amplifier. Pump radiation can be coupled into the doped fiber by realizing end-pumping or side-pumping schemes [128–130]. Wavelength division multiplexers using series of bulk optics can be used for the combination of different wavelength laser radiation in end-pumping modules. In side-pumping configuration, pump fiber can be spliced or fused to the cladding of the signal fiber, making this device robust and insensitive to mechanical perturbations as it does not contain bulk elements. Multiple ports for pumping sources can be provided using pump-signal combiners in order to enhance the pump radiation and consequently the amplified signal power at the output of fiber amplifier.

Efficient uniform absorption of the pump in a small core volume, compared to a volume of the cladding, can be obtained by introducing various fiber designs. The overlap of the cladding modes with the doped core can be improved by the design of the cladding shape which breaks the circular symmetry of the fiber with a centered core and scrambles the propagating modes [131–134]. This was obtained in fibers of the offsetted core or rectangular, spiral, starlike and other demonstrated shapes of cladding cross sections. Higher absorbed pump power in fiber amplifiers

results in higher signal power at the output. In some cases, bend-induced pump loss must be avoided by introducing large diameter coiling of the fiber. Thermal handling and cooling technological solutions should be installed as well in order to eliminate the excess heating of the polymer.

In practice, the uniform absorption of pump power over the entire fiber length is not ensured just by breaking the symmetry of the cladding cross section. The cladding modes should be continuously mixed by perturbing the fiber along its entire length or introducing periodic fiber bending [135,136]. It was shown that the pump absorption was quite small and saturated quickly along the fiber length in the case without mode mixing. Mode mixing increased the pump absorption by  $\sim 20$  dB over the length of fiber amplifier [136]. Pump absorption can be increased to its limiting value in this case. The increased pump absorption can help to shorten the length of the fiber amplifier and thus to reduce nonlinear effects, which is crucial for ultrashort pulse laser operation.

A higher level of the absorbed pump power and an amplified signal power can be obtained by increasing the size of ytterbium-doped core of the fiber amplifier. Nonlinear effects occurring in the fiber amplifier are being reduced with the enlarged core, which is very beneficial in ultrashort pulse lasers pursuing high peak power and energy pulses. However, the core of large-mode-area (LMA) fiber cannot be increased as much as desired while maintaining a single-mode propagation. Single-mode operation has a limit for step-index fibers of about  $15\ \mu\text{m}$  in diameter, which are being kept straight [137]. The value of a core size that single-transverse-mode operation is obtained can be increased to  $25\ \mu\text{m}$  by properly bending and coiling the fiber [138]. However, bending improves output beam quality not in all cases, due to induced mode coupling, modal deformation and modal gain competition, and depends on the core radius and numerical aperture of the doped fiber [139]. In larger diameter fibers, higher order modes are excited affecting the quality of the output beam.

Large-mode-area fibers can be realized in a tapered configuration [140]. Such tapered fibers have different mode sizes at the ends of the fiber which operate as a mode converter between the two fibers and provide intrinsic mode scrambling mechanism and a lower insertion loss for the input signal.

Photonic crystal fiber (PCF) technology is used to enlarge the fiber core even more while maintaining a single-transverse-mode operation [141]. In such fibers a doped solid core is surrounded by a cladding consisting of a certain periodic microstructured arrangement of air gaps which modify the refractive index and the numerical aperture. Light propagation conditions are

determined by an effective air cladding structure. This fiber technology makes it possible to produce doped fibers with a large-diameter core, exceeding the limit of standard LMA fibers, and ensure the propagation of only the fundamental mode. By adjusting the spacing of the air-holes and the hole size around the large-mode-area doped core, fiber amplifiers of core diameters up to 100  $\mu\text{m}$  were demonstrated [142]. Photonic crystal fibers which contain cores larger than 50  $\mu\text{m}$  in diameter are particularly sensitive to bending, thus in practice are being kept straight. Such fibers are defined as rod-type.

Another technology that allows the realization of a single-mode operation in the LMA fiber, is based on higher order mode filtering and delocalization into the cladding of large-pitch fiber (LPF) [143]. The delocalization of higher order modes to undoped fiber cladding is obtained by the complex periodic structure of air holes similar to PCF. Higher order modes practically do not overlap with the doped core and are not amplified. This technology allowed the production of larger core fiber amplifiers, compared to aforementioned fiber technologies, with a core diameter of 135  $\mu\text{m}$ . LPF fibers are usually realized in rod-type configuration, so that single-mode operation would not be compromised. Nonlinear effects are suppressed due to extremely large core of the fiber amplifier, which allows the demonstration of record-high pulse energies in FCPA systems [19].

An alternative fiber design of higher order mode filtering is based on chirally-coupled core (CCC) fiber configuration, which provides resonant filtering of higher order modes and enables a single mode-operation [144]. The geometry of CCC fiber contains a central large-diameter core and at least one helical satellite core, wrapped around the central core. The main function of the satellite core is to filter the higher order modes from the central core allowing only fundamental mode to propagate. It is possible due to the fact that the fundamental mode and the higher order modes have different symmetries. CCC fibers with a central core diameter of up to 85  $\mu\text{m}$  were demonstrated [145].

However, moving towards high average powers in fiber lasers which incorporate large-mode-area fiber amplifiers, where higher order modes may exist, additional difficulties of transverse mode instabilities (TMI), currently considered as the most limiting factor for the maximum extractable average power in the fundamental-mode operation, are obtained [146]. TMI is described as sharp and rapid output beam deterioration above the certain output power threshold, which depends on a core diameter of the fiber. The larger the core diameter of fiber amplifier – the lower the output power

threshold for TMI. This phenomenon is observable in fiber amplifiers with core diameter above 20  $\mu\text{m}$ . Fiber power amplifier of 20  $\mu\text{m}$  core diameter showed no signs of TMI for  $>2$  kW output power [147]. This output power level threshold of TMI was reduced to 275 W in 1.3 m long LPF amplifier with a core diameter of 63  $\mu\text{m}$  [146]. This phenomenon was thoroughly investigated and it has been considered that the main cause of mode instabilities is attributed to the thermo-optically induced refractive-index gratings resulting from a periodic interference between the main mode and weak higher order modes [148]. It was proposed, that the threshold of mode instabilities depends on the thermal load of the fiber per unit length, so the threshold can be increased by increasing the fiber length [149]. However, the elongation of the fiber in high-energy ultrashort pulse FCPA systems is undesirable for the mitigation of nonlinear effects and maximization of the peak power of the amplified pulses.

In conclusion, the use of fiber-coupled high-power pump laser diode modules and special fiber designs of unique properties enable the realization of high-power fiber lasers. The brief review of the ultrashort pulse laser systems utilizing forementioned fiber technologies is provided in the next section of this chapter.

### **3.1.2 High-power fiber laser systems**

Output power and pulse energy can be increased in ultrashort pulse FCPA systems, by scaling the mode-field diameter, as discussed, and using special fiber designs, such as LMA fibers, tapered fibers, photonic crystal fibers (PCF), large-pitch fibers (LPF) or chirally-coupled-core (CCC) fibers in power amplifiers. Furthermore, in order to achieve gain saturation and therefore good pumping efficiency in large-mode-area doped fiber amplifiers, high average pump power has to be introduced. In this section, FCPA systems of different configurations utilizing high-power fiber technologies are briefly reviewed. The presented systems reveal the possibilities and potential of fiber technologies, but not necessarily show the limits of the achievable parameters from the fiber lasers.

Standard high-power LMA fiber amplifiers maintaining single-transverse-mode operation in ultrashort pulse systems are commonly used for average output power scaling to tens of Watts [150]. Pulse energy, in FCPA systems utilizing conventional LMA fiber amplifiers, is typically limited to  $\mu\text{J}$  level due to nonlinear effects in relatively small-mode-area of the fibers. The demonstrated ultrashort pulse Yb-doped fiber laser and

amplifier system produced  $>25$  W average power and high-quality 110 fs duration, 400 nJ energy pulses at the output [151]. Two stages of fiber amplifiers with a core diameter of 20  $\mu\text{m}$  and 40  $\mu\text{m}$  were used. The pulse energy could have been further increased by reducing the initial pulse repetition rate of 62 MHz.

LMA tapered fiber amplifier can be successfully implemented in high-power FCPA systems. The introduced laser utilizing double-clad LMA tapered fiber with a core diameter of 20  $\mu\text{m}$  at the narrow end and 110  $\mu\text{m}$  diameter at the large end delivered output power of 750 W, pumped by 915 nm wavelength radiation of  $\sim 1$  kW power, obtaining slope efficiency of 81.9% [152]. Achieved high signal power demonstrated the attractiveness of this technology for increasing the average output power from fiber amplifier. Unfortunately, due to the extremely large mode diameter of 110  $\mu\text{m}$  at the large end of the fiber, higher order modes may exist in the amplifier, which must be suppressed in order to achieve a good beam quality at the output of the system.

The use of PCF power amplifier of 40  $\mu\text{m}$  core diameter allowed to achieve high-energy and high-power laser operation [153]. Ytterbium-doped FCPA system delivered 100  $\mu\text{J}$  pulse energy and 90 W average power at 900 kHz pulse repetition rate. Stretched pulses of 1 ns duration were compressed to 500 fs. Moderate pulse quality degradation was attained due to phase distortions of some non-optimized optical components in the stretcher setup and accumulated nonlinear phase-shift of about  $3\pi$  rad. About 66% of the energy remained in the central peak of the compressed pulse, resulting in a pulse peak power of 120 MW. Diffraction-limited beam quality was ensured by the design of the fiber amplifier.

The pulse energy and average output power can be further increased by increasing the core diameter to 80  $\mu\text{m}$  of a Yb-doped rod-type PCF amplifier [19]. Average output power of more than 100 W was attained at 100 kHz pulse repetition rate corresponding to 1 mJ pulse energy and 1 GW peak power after the pulse compression. Sufficiently long stretched pulses of 2 ns were used to minimize nonlinear phase-shift to about  $2.2\pi$  rad, which ensured good quality of compressed 800 fs duration laser pulses.

The highest pulse energy from a single fiber amplifier was achieved in the FCPA system using a large-pitch fiber (LPF) with a 108  $\mu\text{m}$  core diameter in the main amplifier and active modulation of the initial pulse amplitude and phase before the amplification [154]. Pulse energy of 2.2 mJ with nearly transform-limited 480 fs pulse duration at 11 W average power was extracted from a fiber-based power amplifier. Diffraction grating pulse

stretcher and compressor configuration was used in the developed system. Stretched pulse duration of  $\sim 3$  ns in a combination with a reduction and compensation of the acquired nonlinear phase allowed to achieve high-quality compressed pulses of a record-high 3.8 GW peak power.

Other demonstrated FCPA system showed real potential of fiber technology in scaling the average output power with excellent beam quality [155]. The power of 830 W was achieved from the system utilizing single power amplifier of a water-cooled 8 meters long double-clad fiber with a  $27 \mu\text{m}$  mode-field-diameter. The pump power of nearly 1.5 kW at 976 nm wavelength was launched into the main amplifier. High pulse repetition rate of 76 MHz resulted to significantly low pulse energy of  $10.6 \mu\text{J}$  and a peak power of 12 MW. Ultrashort pulse duration of 640 fs was obtained after the pulse compression. A bending diameter of 1 m was chosen in order to sufficiently suppress higher order modes and to minimize fundamental mode losses.

Single-transverse-mode operation is maintained in ultrashort pulse fiber laser based on CCC fiber amplifier configuration which is designed to filter the higher order modes. CCC fiber amplifier with a  $33 \mu\text{m}$  diameter of the central core was used in Yb-doped FCPA system [156].  $50 \mu\text{J}$  energy pulses with the duration of 400 fs were obtained after pulse compression incorporating spectral filtering in a bulk diffraction grating compressor. The system was designed to demonstrate the highest achievable pulse energy from the system resulting in a pulse repetition rate of 100 kHz and average power of 5 W. The energy extraction from the power amplifier was limited by distortions in the pulse spectrum and degradation in polarization maintaining properties. The output beam quality was nearly diffraction-limited.

A big advantage of the demonstrated systems is that all were realized in polarization-maintaining fiber amplifier configurations, which ensured stable operation of the fiber lasers. Finally, presented fiber technologies of unique properties enabled average output power scalability to hundreds of Watts and pulse energy to a mJ level in Yb-doped ultrashort pulse FCPA systems.

### **3.1.3 Sophisticated techniques for realization of extremely-high average power levels in fiber laser systems**

Fiber-based ultrafast CPA systems are able to outreach kW level of average power while maintaining ultrashort pulse duration at the output. More sophisticated methods of coherent spatial laser beam combining and

temporal pulse stacking are used to achieve record-high parameters in such laser systems.

By combining laser radiation from several sources, it is desired not only to increase the output power, but also to keep the beam quality close to the diffraction-limited. The parameters such as wavelength, spectral line-width, beam phase and polarization of the individual high-power fiber laser sources have to be carefully controlled considering laser beam combination. Thus, the management of many parameters of the individual laser sources makes this task extremely difficult to realize.

High-power systems of multidimensional coherent combination, including special beam combining of separate amplifiers and temporal pulse combination, contain three main stages of beam splitting, amplification and then beam and pulse recombination [157]. Firstly, the initial signal from the seed source is split into multiple channels using a beam splitter before the amplification. After signal is amplified in individual fiber amplifiers, the different output beams are recombined using a beam combiner. It can be realized using intensity and polarization beam combination techniques by using various technological approaches of polarization beam splitters/combiners [158], diffractive-optical elements [159] or segmented mirror splitters [160]. All the beams have to be phased correctly in order to interfere constructively into one final laser beam. For that reason, the phase stabilization is performed by using a setup which consists of a detection scheme of the phase differences between the individual laser beams and actuators for the phase compensation.

In the case of pulsed laser operation, pulse propagation distances in separate channels must be precisely matched in order to achieve accurate pulse recombination at the output. The active stabilization, detection and feedback techniques in a laser setup have to be implemented because thermal and mechanical drifts in different channels are unavoidable during the laser system operation.

Furthermore, divided-pulse amplification (DPA) technique can be additionally implemented in the same multidimensional coherent combination laser system. In this case, additional temporal pulse splitting stage is implemented in the setup for the creation of multiple pulse replicas (burst of pulses) before the beam splitter. After amplification, a subsequent temporal pulse recombination is required resulting in extremely high peak power of the pulse at the output. Passive DPA, which does not require phase stabilization, can be realized using a method based on the Sagnac interferometer [161]. Using this technique, the pulse recombination is

accomplished by changing the polarization direction and reflecting back the burst of pulses through the setup. However, combination efficiency is sensitive to the mismatch of pulse amplitude inside the burst and is limited by the gain saturation which leads to the deformation of the pulse burst amplitude. The actively controlled DPA can reduce the negative impact of this effect [162].

An alternative method of coherent pulse stacking can be introduced by implementing Gires-Tournois interferometer [163]. Large number of equal-amplitude pulses can be stacked into one intense pulse using this technique. The cavity of the interferometer must be length matched to the pulse repetition rate of the seed source. Further, the amplitude and the phase of the pulses have to be matched as well to achieve a constructive interference.

Forementioned sophisticated techniques allowed the development and construction of ultrashort pulse fiber laser systems delivering extremely-high output power and high-energy of the pulses. A fiber-based ultrafast CPA system based on a coherent beam combination of 12 step-index fiber amplifiers was recently demonstrated delivering 10.4 kW average output power and maintaining ultrashort pulse operation [20]. Close to transform-limited compressed pulse duration of 254 fs was attained. Laser system operated at 80 MHz pulse repetition rate resulting to about 130  $\mu$ J energy of the combined pulses. This extremely-high power fiber-based CPA system demonstrated the highest average-power realized by an ultrafast laser system to the date of publication and showed the potential of average-power scalability to multi-kW power levels.

Another ultrafast kilowatt-class FCPA system using a spatial and temporal coherent pulse combination of eight amplifier channels and four pulse replicas demonstrated record-high pulse energy of a stacked pulse from fiber-based laser system [164]. Femtosecond pulses of 262 fs duration with a maximum pulse energy of 12 mJ, estimated peak power of 35 GW and an average power of 700 W were obtained. An excellent, nearly diffraction-limited beam quality at the output of the system was confirmed.

The techniques of coherent spatial laser beam combination and temporal pulse stacking allowed the development of multi-kW level ultrafast fiber-based CPA systems delivering ultrashort laser pulses exceeding the energy limits achieved by the individual fiber amplifiers. Sophisticated techniques and carefully tailored technological approaches are required and are being developed for the realization of the systems delivering record-high power and energy levels from the fiber lasers.

### 3.1.4 High-power high pulse repetition rate FCPA systems

New methods are being developed to achieve higher average power or pulse energy from the fiber laser and to improve the performance of certain applications. The increase of number of pulses in a closely packed bursts can provide the desired result. The method which allows to expand the regimes of the laser operation by delivering high repetition rate burst of pulses is presented in this section. Furthermore, the total (burst of pulses) energy is increased compared to the regime of a single pulse operation of the laser system.

Higher average output power from a fiber laser can be obtained by increasing the pulse repetition rate. Unfortunately, pulse repetition rate has practical upper limit which is related to the application of such laser sources and the maximum speed at which various translation and rotation stages used for scanning and beam delivery can be controlled. A pulse train of identical pulses with constant temporal spacing is not necessarily the best solution for some laser applications. Superior performance of the laser applications was obtained by forming a burst of closely and uniformly spaced pulses [165–167]. By using bursts, the signal-to-noise ratio was increased [165], better surface quality during material processing [166] or even better material removal results were provided [167]. Burst-mode operation regime can be beneficial in material processing for easier thermal management due to lower overall repetition rate but enhanced energy of the formed burst of high repetition rate pulses. The burst of closely packed pulses can be compared to the case of a single pulse which energy is similar to the one of entire burst during the interaction with the material [168].

Lasers operating at burst of pulses regimes, which also imitate higher pulse energy (enhance total energy of a burst), were being developed. The first fiber laser was designed to operate in the burst regime at a repetition rate of 1 kHz where laser pulses had 10 ns temporal spacing (100 MHz pulse repetition rate) inside the burst [169]. The highest total signal burst energy of 250  $\mu\text{J}$  and average individual pulse energy of 20  $\mu\text{J}$  were obtained. Compressed pulse duration of 400 fs was attained. Thus, the laser operation in burst regime allowed to scale the energy of the burst to 250  $\mu\text{J}$ , while the single pulse operation regime was limited to  $\sim 20$   $\mu\text{J}$  pulse energy. This regime of laser operation triggered the development of fiber laser systems for the applications that require burst of energetic ultrashort laser pulses.

GHz pulse repetition rate intra-burst regime was introduced in fiber laser system a little bit later [24]. The initial pulse repetition rate of 108 MHz

from fiber oscillator was converted to  $\sim 3.5$  GHz by a pulse multiplier consisting of six cascaded fiber couplers. The acousto-optic modulator was used to select desired width of the burst from a pulse train. The fiber laser system was able to deliver burst of pulses as short as 15 ns width, with intra-burst pulse repetition rate of 3.5 GHz and burst energy of 215  $\mu$ J at 1 kHz burst repetition rate. The shortest pulse duration inside the burst was estimated to be 450 fs after the pulse compression.

However, this pulse multiplication approach had several drawbacks. The minimal burst envelope width was limited to 15 ns by a rise and fall times of the acousto-optic modulator. Quite large mismatch of pulse amplitudes inside the burst was obtained due to the variation of splitting ratio of the fiber couplers. To reduce this effect additional losses had to be introduced in each of the fiber coupler output arms. The exact pulse spacing (pulse repetition period) was hardly realized by controlling the length of fiber pigtailed of each coupler. Furthermore, the compressed pulses inside the burst had significant variation in pulse duration due to the different acquired amount of GDD on broadband pulses traveling different distances in the fiber delay lines.

Nevertheless, this system was successfully used in demonstration of a new ablation-cooled laser material removal mechanism with bursts of ultrafast pulses, which allowed to achieve significantly higher ablation efficiency and to maintain the high quality of processed area [170].

This fiber-based technique of pulse multiplication and generation of GHz burst of pulses was implemented into the high-power and high-energy FCPA system which is investigated in the experimental part of this chapter. A detailed literature review on the realization of GHz bursts, various fiber-based techniques, technological limitations and possible applications will be provided in Chapter 4.

### **3.2 The realization of high-power FCPA systems**

Material related to this section was published in A3

The experimental realization of high-power FCPA systems operating in single-pulse and burst of pulses regimes incorporating two configurations of large-mode-area (LMA and PCF) cladding-pumped Yb-doped fiber power amplifiers are presented in this section. High-power FCPA system utilizing LMA fiber power amplifier operating in single-pulse regime delivered 1.5  $\mu$ J energy,  $\sim 680$  fs duration ultrashort pulses of a good pulse quality and 6 W of

average power at a pulse repetition rate of 4 MHz. Pulse repetition rate multiplier based on a cascaded 2x2 fiber coupler sequence with a splitting ratio of 50/50 allowed pulse repetition rate multiplication to 3.26 GHz. Two burst shaping layouts are introduced in this experimental setup obtaining desired burst shape by using one or two acousto-optic modulators controlled by an arbitrary waveform generator (AWG). Significantly high average power levels of 6 W (11  $\mu\text{m}$  core diameter LMA fiber power amplifier) and  $>20$  W (40  $\mu\text{m}$  core diameter PCF power amplifier) were achieved in a GHz intra-burst operation regime at 200 kHz burst repetition rate, which corresponded to a maximum energy of 30  $\mu\text{J}$  and  $>100$   $\mu\text{J}$  per burst respectively.

### 3.2.1 High-power FCPA system with LMA fiber power amplifier operating in a single-pulse regime

Schematic presentation of the high-power fiber chirped pulse amplification system utilizing LMA cladding-pumped Yb-doped fiber power amplifier and operating in a single-pulse (MHz pulse repetition rate) regime is illustrated in Fig. 3.2.1. The construction of a high-power FCPA system was based on the developed all-in-fiber seed source (passively mode-locked fiber oscillator and a stage of nonlinear pulse spectrum broadening) used as a front-end in the systems presented in previous chapters of this thesis.

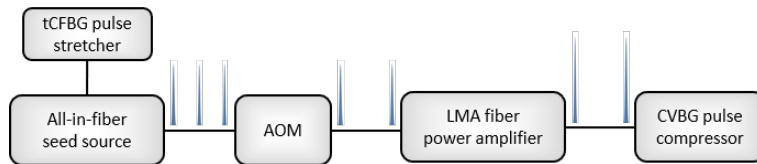


**Fig. 3.2.1.** Schematic presentation of the high-power FCPA system with LMA fiber power amplifier operating in a single pulse (MHz pulse repetition rate) regime. tCFBG – thermally tunable chirped fiber Bragg grating module, AOM – acousto-optic modulator, LMA – large mode area, CVBG – chirped volume Bragg grating.

All-in-fiber passively mode-locked oscillator was used for the generation of ultrashort laser pulses and operated at 1030.1 nm center wavelength and 50.93 MHz pulse repetition rate. The pulse spectrum was nonlinearly broadened to a bandwidth of 3.44 nm at FWHM (Fig. 3.2.2.) due to self-phase modulation in relatively long optical fiber. Pulse spectrum is broad enough to provide a pulse duration of few hundred femtoseconds at the output of the system after pulse compression.

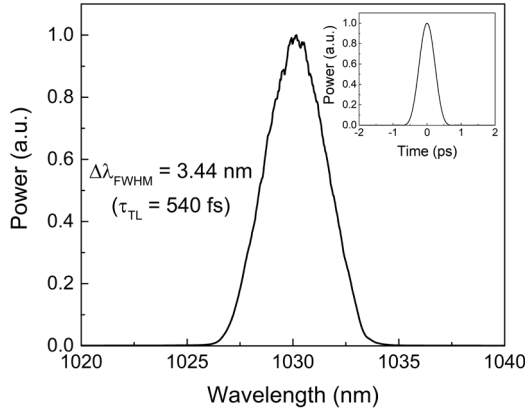


**Fig. 3.2.2.** Pulse spectrum from all-in-fiber seed source. Inset: an envelope of Fourier transform-limited pulse.

A Fourier transform-limited pulse duration derived from the spectrum was estimated to be about 540 fs. Pulses from the seed source were down-chirped to about 220 ps duration by using a chirped fiber Bragg grating stretcher with group delay dispersion of  $\beta_2 = -33.7 \text{ ps}^2$ . Thermal tuning of the CFBG was used for fine dispersion control. Furthermore, a system configuration consisting of CFBG stretcher and CVBG compressor with matched dispersion profiles was used to ensure high-quality ultrashort pulses at the output of the system. All-in-fiber seed source provided chirped laser pulses, which were amplified to 4 nJ energy in a core-pumped single-mode Yb-doped fiber amplifier pumped by 976 nm narrowband radiation from a single-mode laser diode. Pulse repetition rate was reduced by using fiber-coupled acousto-optic modulator before the power amplifier, enabling pulse amplification from  $\sim 2$  nJ pulse energy to microjoule energy level. The same Yb-doped LMA fiber (11  $\mu\text{m}$  core diameter), as in the high-energy FCPA system introduced in section 2.2.1, was used for the development of high average power fiber system. In this case, high-power pumping radiation was inserted into the cladding of 125  $\mu\text{m}$  diameter and 1.3 m long fiber amplifier which enabled high output power operation. Amplified pulses were compressed in a robust and compact CVBG compressor.

Pulse compression quality was examined at different output pulse energies using a second harmonic non-collinear autocorrelator (Fig. 3.2.3(a)).

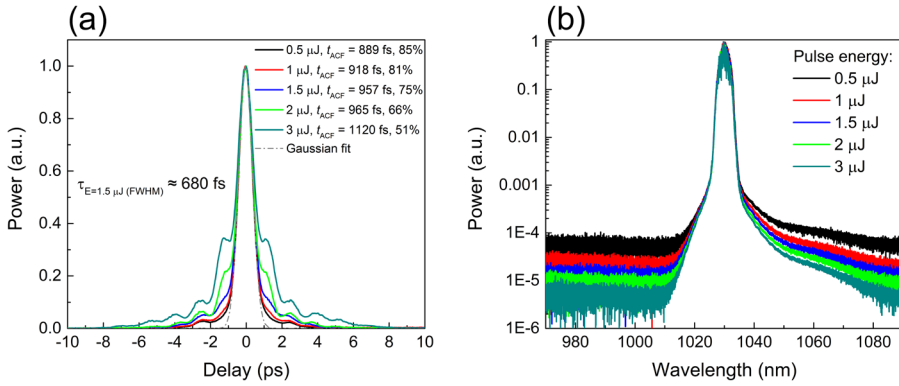


**Fig. 3.2.3.** Measured autocorrelation traces of compressed pulses (a) and pulse spectra before the CVBG compressor (b) at the output of the FCPA system at different (0.5-3 μJ) pulse energies.

The quality parameter of the compressed pulse, defined comparing the areas under the autocorrelation trace and the Gaussian-like envelope of the approximation, is provided in the same graph at different output pulse energies. For the ultrashort pulses of 1.5 μJ energy, this pulse quality parameter was equal to 75%. Significant pulse quality degradation was attained above 1.5 μJ output pulse energy and could be attributed to the accumulation of nonlinear phase-shift which cannot be completely compensated in the system. Compressed pulses of 3 μJ energy had a picosecond temporal pedestal which contained large amount of the pulse energy. To sum up, introduced high-power FCPA system operating in a single-pulse regime delivered 1.5 μJ energy, ~680 fs duration ultrashort pulses of a good pulse quality and 6 W of average power at a pulse repetition rate of 4 MHz.

Measured pulse spectra before the CVBG compressor from the FCPA system at different pulse energies are shown in Fig. 3.2.3(b) and manifests an extremely low level of amplified spontaneous emission in the amplified signal, which was further reduced by the CVBG compressor. CVBG had a reflection spectrum bandwidth of only 8 nm and operated as a spectral filter.

Beam quality at the output of the system was measured by performing z-scan (Fig. 3.2.4.). Measured beam quality parameter of  $M^2 \sim 1.05$  was close to the diffraction limit indicating excellent beam spatial properties as it could be expected from a fiber amplifier maintaining a single-mode operation. Furthermore, it confirmed the good quality of the end-cap which was used to expand laser beam at the surface on air/glass interface and to protect the output of the fiber from the optical damage.

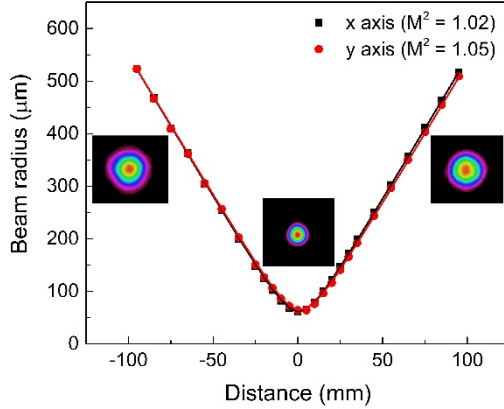


**Fig. 3.2.4.** The measurement of the beam quality parameter  $M^2$  at the output of the high-power FCPA system. Insets: beam intensity profiles at three different positions from the waist location.

### 3.2.2 Pulse repetition rate multiplier and GHz burst formation

The technique of pulse repetition rate (PRR) multiplication must be introduced in laser system in order to obtain GHz PRR levels. In this work, GHz pulse repetition rate was achieved using a cascaded 2x2 fiber coupler sequence with a splitting ratio of 50/50 as shown in Fig. 3.2.5. Input pulses

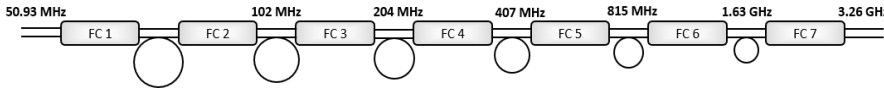


**Fig. 3.2.5.** Schematic presentation of a high pulse repetition rate multiplier. FC – fiber coupler of 50/50 splitting ratio.

were split into two output arms in the first fiber coupler and then combined in the subsequent fiber coupler. Each coupler had output arms of different lengths and the length difference introduced a delay between two pulse replicas equal to a half of the signal inter-pulse period at the input of that coupler. Such pulse repetition rate multiplier doubled PRR at each stage, starting with the second coupler. Therefore, after 6 fiber couplers the pulse repetition rate was multiplied by  $2^5$  and after 7 couplers -  $2^6$ . The initial pulse repetition rate of 50.93 MHz from the oscillator was multiplied to 1.63 GHz and 3.26 GHz pulse repetition rates using PRR multiplier which consisted of 6 and 7 fiber couplers respectively (Fig. 3.2.6(a-b)). Quite large mismatch of

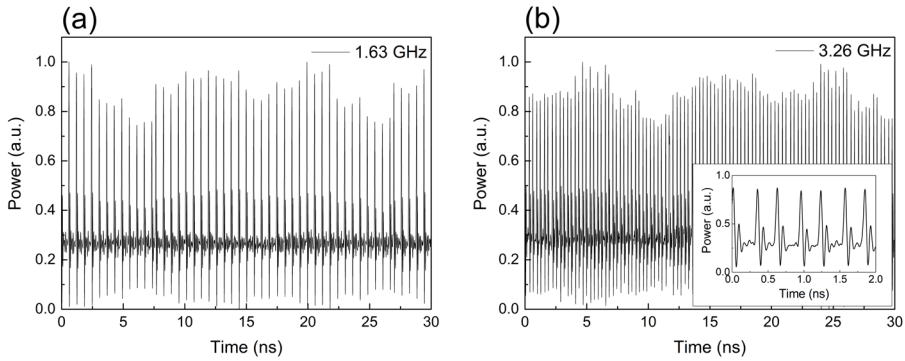


**Fig. 3.2.6.** Measured pulse train after the PRR multiplier containing 6 (a) and 7 (b) fiber couplers, resulting in 1.63 GHz and 3.26 GHz pulse repetition rates respectively. Inset: pulse train of 3.26 GHz PRR using a modified time scale for a clearer representation of the pulse period.

pulse amplitudes was observed due to the variation of splitting ratio of the fiber couplers. This pulse amplitude mismatch could have been reduced by introducing losses in each of the fiber coupler output arms, however it was not performed in this work since it was not critical for a successive pulse amplification. Furthermore, the exact pulse spacing between pulse replicas (pulse repetition period) was hardly realized using this PRR multiplication technique. Nevertheless, the control of the length of fiber pigtailed of each coupler was performed with quite high precision resulting in a  $\sim 10\%$  variation in pulse repetition period between the pulse replicas (inset of Fig. 3.2.6(b)). Since the proposed ablation-cooled laser material removal mechanism [170] do not require very high similarity of pulse amplitudes and pulse repetition period, this result was considered sufficient for the demonstration of a high-power GHz pulse repetition rate FCPA system.

Two burst formation configurations were introduced in the experimental setup in order to obtain the desired GHz burst shape. The first demonstrated configuration contained of all-in-fiber seed source, PRR multiplier of seven cascaded fiber couplers for pulse repetition rate multiplication and one acousto-optic modulator for burst formation (Fig. 3.2.7). Firstly, initial pulse repetition rate of 50.93 MHz from the seed source was multiplied in PRR multiplier to 3.26 GHz. The burst of GHz pulses was formed by picking the pulse packet of desired width from the GHz pulse train using an acousto-optic modulator after the PRR multiplier. The temporal profile of the burst

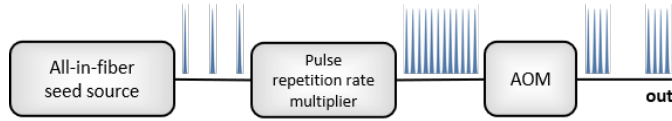


**Fig. 3.2.7.** Schematic presentation of high pulse repetition rate multiplication and burst formation from the GHz pulse train using one acousto-optic modulator (AOM).

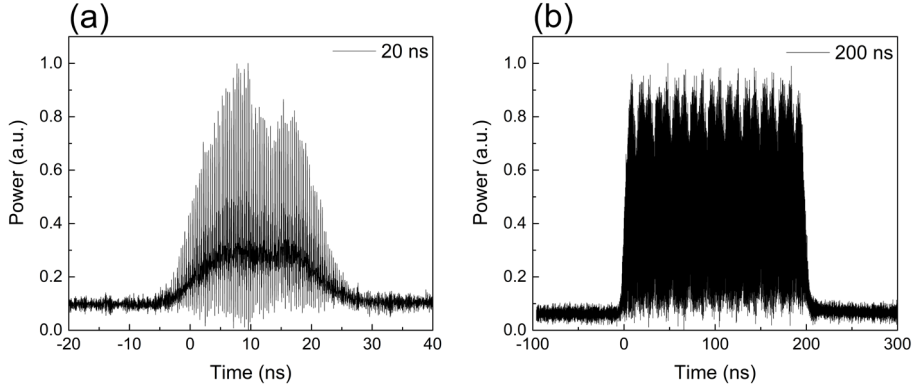


**Fig. 3.2.8.** Experimentally measured 20 ns (a) and 200 ns (b) width 3.26 GHz PRR bursts containing approximately 64 and 640 pulses respectively.

depended on the AOM performance (rise and fall times) which could be well illustrated by a Gaussian-like envelope of the shortest possible width burst of 20 ns in Fig. 3.2.8(a). The laser system was able to produce arbitrarily long rectangular-like bursts of 500 ns width, containing approximately 1600 pulses. The burst train of 200 ns width is shown in Fig. 3.2.8(b).

The second demonstrated burst formation configuration contained one additional acousto-optic modulator in the setup (Fig. 3.2.9.). The initial pulse train from the seed source was modified by using the first AOM creating the burst of MHz pulses. PRR multiplier converted these MHz pulses into GHz bursts at the output of the multiplier. The second AOM was used for additional GHz burst shaping together with an implemented arbitrary waveform generator. In this configuration, rectangular-like bursts were obtained at a minimum packet width of 20 ns and did not depend on the performance of AOM (Fig. 3.2.10(a)). For certain applications it may be important to have short bursts in which the ultrashort pulses have similar amplitude. Steeper slopes were also obtained for arbitrarily long bursts. However, the shape of longer burst (Fig. 3.2.10(b)) is similar to the one achieved in previous system modification (Fig. 3.2.8(b)).

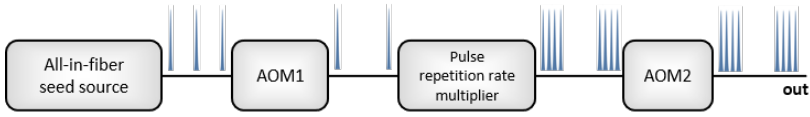


**Fig. 3.2.9.** Schematic presentation of high pulse repetition rate multiplication and GHz burst formation using two acousto-optic modulators (AOM1 and AOM2).

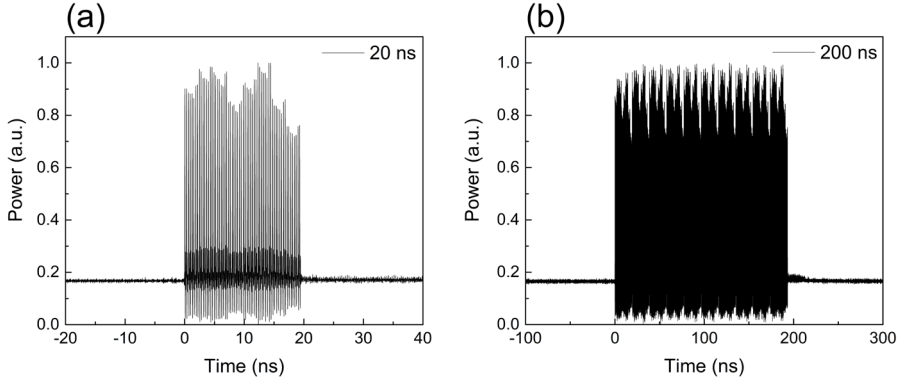


**Fig. 3.2.10.** Experimentally measured 20 ns (a) and 200 ns (b) width 3.26 GHz PRR bursts containing approximately 64 and 640 pulses respectively.

To sum up, presented technique of pulse repetition rate multiplication based on a cascaded fiber coupler sequence allowed to achieve very high PRR of 3.26 GHz. Two demonstrated configurations of the setup enabled burst formation and system operation in the GHz burst regime. In the following section, burst amplification in LMA fiber power amplifier and demonstration of high-power GHz intra-burst repetition rate FCPA system is presented.

### 3.2.3 High-power GHz intra-burst repetition rate FCPA system with LMA fiber power amplifier

The experimental realization of high-power FCPA system operating in burst of pulses regime with two configurations of large-mode-area (LMA and PCF) cladding-pumped Yb-doped fiber power amplifiers is presented in this section.

The layout of the developed high-power FCPA system operating in GHz intra-burst regime is illustrated in Fig. 3.2.11. The whole scheme of the experiment was similar to that of the system operating in a single-pulse regime introduced in section 3.2.1. In this case, PRR multiplier and the second acousto-optic modulator was additionally implemented into the system. As a reminder, all-in-fiber seed source provided chirped laser pulses

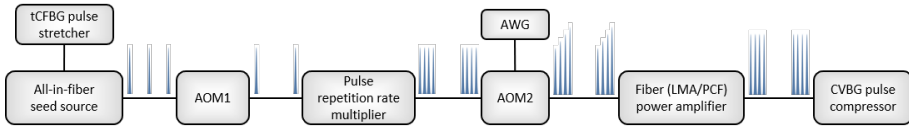


**Fig. 3.2.11.** Schematic presentation of the high-power FCPA system operating in GHz intra-burst pulse regime. tCFBG – thermally tunable chirped fiber Bragg grating module, AOM – acousto-optic modulator, AWG – arbitrary waveform generator, LMA – large mode area fiber amplifier, PCF – photonic crystal fiber amplifier, CVBG – chirped volume Bragg grating.

of about 220 ps duration and 3.44 nm bandwidth at 1030.1 nm center wavelength (pulse spectrum was depicted in Fig. 3.2.2.). A relatively narrow pulse spectrum was selected in this work so that the material dispersion would have a smaller impact on the pulse duration after the propagation through sufficiently long fiber delay lines (the total length difference between fiber coupler output arms was about 4 meters) in the pulse repetition rate multiplier. At the same time, it was broad enough to support few hundreds of femtoseconds pulse duration at the output of the system.

The bursts of GHz pulses were produced using the setup containing two acousto-optic modulators and pulse repetition rate multiplier based on cascaded fiber-based delay lines and controlled using the second acousto-optic modulator and an arbitrary waveform generator to obtain desired burst shape after amplification. In the first experimental realization, burst of pulses were amplified in a cladding-pumped single-mode LMA (core diameter of 11  $\mu\text{m}$ ) Yb-doped fiber amplifier at 200 kHz burst repetition rate up to  $\sim 6$  W

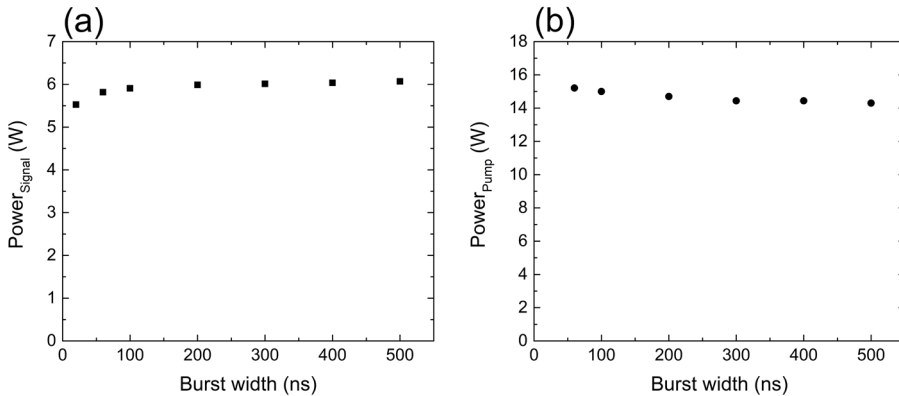


**Fig. 3.2.12.** a) The dependence of average output power on burst width at the constant pump power of 12.5 W without burst pre-shaping using AWG. b) The dependence of pump power on burst width required for constant amplified signal power of 6 W using burst pre-shaping technique controlled by AWG before the power amplifier for desired rectangular-like burst shape at the output of the system.

of average power after the pulse compressor. The dependence of average output power on burst width at constant pump power of 12.5 W without burst pre-shaping using AWG is shown in Fig. 3.2.12(a). At 20 ns burst width average output power was reduced by less than 10% to 5.53 W, though seed power before the power amplifier was reduced nearly two times from 129 mW at 500 ns burst width to 69 mW at 20 ns. Weak dependence of average output power on seed input power manifested high level of saturation in the power amplifier.

Yb-doped glass is defined by a high saturation fluence which results in the capability of superior energy storage. However, the pulse amplification up to  $\mu\text{J}$  level in a small mode-area fiber amplifier leads to saturation induced pulse deformations of sufficiently long pulses at certain pulse energies. This effect also strongly limits the amplification of closely packed burst of pulses as most of the power is extracted by the front part of the burst. An exponentially decaying burst shape was observed after amplification due to the reduction of the inversion for the trailing part of the non-pre-shaped burst as shown in Fig. 3.2.13.

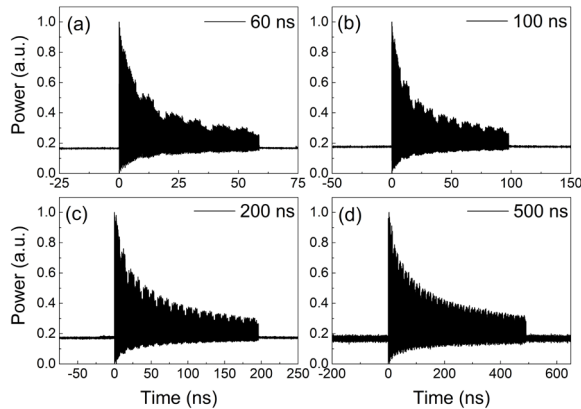


**Fig. 3.2.13.** Experimentally measured 3.26 GHz PRR bursts of 60-500 ns width (a-d) without burst pre-shaping using an arbitrary waveform generator before the power amplifier.

One of the main intentions of this work was to achieve rectangular-like burst of GHz pulses with a constant output signal power over all burst widths. In order to reduce the influence of the gain saturation, a burst pre-shaping technique was used before the pulse amplification in the LMA fiber power amplifier. An exponentially increasing burst shape was produced by using second acousto-optic modulator controlled by an arbitrary waveform generator. The dependence of pump power on burst width required for constant output power of 6 W using burst pre-shaping technique for desired

rectangular-like burst shape at the output of the system is shown in Fig. 3.2.12(b). The pump power was increased from 14.3 W at 500 ns burst width to 15.2 W at 60 ns. Experimentally measured 3.26 GHz bursts of 60-500 ns width using burst pre-shaping technique before the power amplifier for desired rectangular-like burst shape at the output of the system is depicted in Fig. 3.2.14. The burst energy of 30  $\mu\text{J}$  was achieved at 200 kHz burst repetition rate and 6 W of average output power. Individual pulse energy in the GHz burst was obtained of  $\sim 0.16 \mu\text{J}$  at 60 ns burst width and  $\sim 19 \text{ nJ}$  at 500 ns burst width.

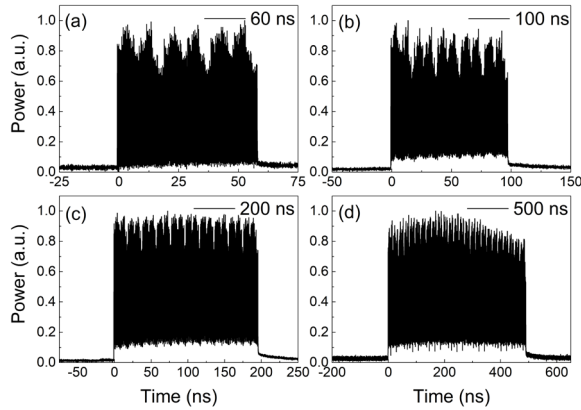


**Fig. 3.2.14.** Experimentally measured 3.26 GHz PRR burst of 60-500 ns width (a-d) at the output of the system. In this case burst pre-shaping technique was used in order to obtain desired rectangular-like burst shape.

Amplified bursts of pulses were compressed in the free-space CVBG compressor. Pulse compression quality was examined at different width of GHz bursts using second harmonic non-collinear autocorrelator. Significant pulse quality degradation was not observed since the energy of the individual pulses in the bursts was low enough and nonlinear effects did not limit pulse amplification in the power amplifier (Fig. 3.2.15(a)). The average duration of the compressed pulses was about 640 fs (FWHM for Gaussian-like pulse) and was slightly longer than the bandwidth-limited duration due to the impact of the dispersion of sufficiently long fiber delay lines in the PRR multiplier. The quality parameter of the compressed pulses, comparing the areas under the measured autocorrelation trace and Gaussian-like approximation, was estimated to be about 83%, declaring the high quality of the compressed ultrashort pulses.

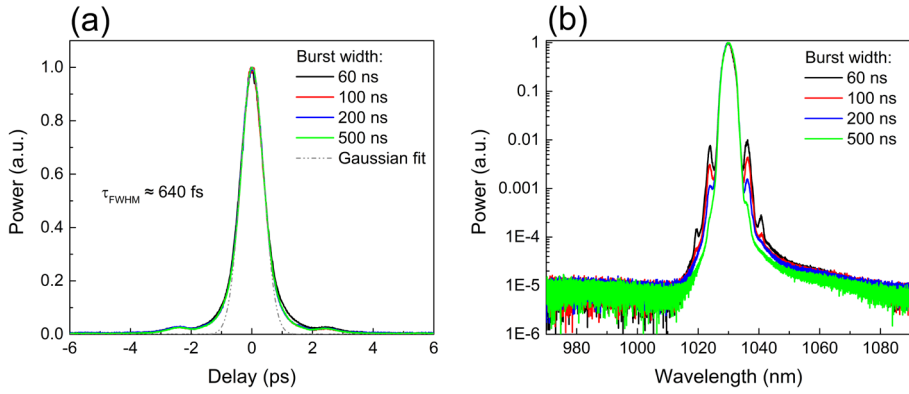


**Fig. 3.2.15.** The measured autocorrelation traces of compressed pulses (a) and pulse spectra before the CVBG compressor (b) of GHz bursts at different (60-500 ns) burst widths at the output of the FCPA system utilizing LMA fiber power amplifier.

Measured pulse spectra from the FCPA system before the CVBG compressor at different burst widths are shown in a log scale in Fig. 3.2.15(b). These spectra show an extremely low level of amplified spontaneous emission in the amplified signal, which was further reduced by the CVBG compressor, as in previously presented FCPA system operating in a single-pulse regime.

The second realization of high-power FCPA system operating at GHz burst regime was based on the implementation of larger core diameter fiber power amplifier instead of the 11  $\mu\text{m}$  core diameter LMA fiber which was used in previous experiments. Photonic crystal fiber (PCF) power amplifier of 40  $\mu\text{m}$  core diameter and 1.8 m length was used to achieve average output power levels higher than 20 W. In this configuration of the fiber amplifier, 60 W of pump power was coupled into the cladding of 200  $\mu\text{m}$  diameter of the fiber amplifier in the backward direction to the seed signal. Burst pre-shaping technique was used for the minimization of gain saturation and the achievement of rectangular-like GHz bursts. The dependence of average amplified signal power on burst width at constant pump power of 60 W using burst pre-shaping technique for desired rectangular-like burst shape is shown in Fig. 3.2.16. Amplified signal power levels of >20 W were achieved at all burst widths at 200 kHz burst repetition rate resulting in burst energies of >100  $\mu\text{J}$ . Individual pulse energy in the GHz burst was obtained of  $\sim 0.57 \mu\text{J}$  at 60 ns burst width and  $\sim 72 \text{ nJ}$  at 500 ns burst width.

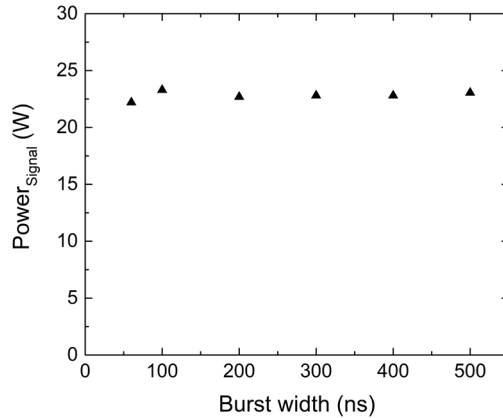


**Fig. 3.2.16.** The dependence of average output power on burst width at the constant pump power of 60 W using burst pre-shaping technique controlled by AWG before power amplifier for desired rectangular-like burst shape at the output of the system.

Pulse compression quality at different widths of GHz bursts was examined as well. No significant pulse quality degradation was observed, as individual energy of the pulses was low enough to be limited by the nonlinear effects (Fig. 3.2.17(a)). The high quality 630 fs duration ultrashort pulses were obtained, as the quality parameter of the compressed pulses was estimated to be about 87% at all measured burst widths. Measured pulse spectra from the FCPA system before the CVBG compressor at different burst widths are shown in a log scale in Fig. 3.2.17(b) and was defined by an extremely low level of ASE.

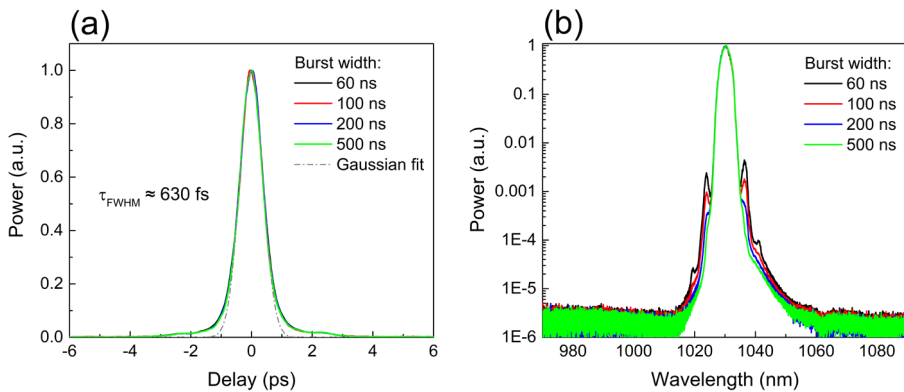


**Fig. 3.2.17.** The measured autocorrelation traces of the compressed pulses (a) and pulse spectra before the CVBG compressor (b) of GHz bursts at different (60-500 ns) burst widths at the output of the FCPA system utilizing PCF power amplifier.

In conclusion, the usage of LMA fiber power amplifier of 11  $\mu\text{m}$  core diameter, PCF power amplifier of 40  $\mu\text{m}$  core diameter and high pump

power laser diode modules, allowed to achieve significantly high average power levels of 6 W and >20 W, respectively. FCPA systems operating in the GHz intra-burst operation regime at 200 kHz burst repetition rate, delivered maximum burst energies of 30  $\mu\text{J}$  (the configuration of LMA fiber power amplifier) and >100  $\mu\text{J}$  (the configuration of PCF fiber power amplifier) per burst, exceeding the pulse energies of the single-pulse operation.

## Summary of the results

High power FCPA system utilizing cladding-pumped LMA (11  $\mu\text{m}$  core diameter) Yb-doped fiber power amplifier operating in a single-pulse (MHz pulse repetition rate) regime, which produced 1.5  $\mu\text{J}$  energy,  $\sim$ 680 fs duration ultrashort pulses of a good pulse quality and 6 W of average output power at a pulse repetition rate of 4 MHz was presented. FCPA system operation in a GHz burst regime was introduced for the comparison to the single-pulse operation.

GHz pulse train was obtained using pulse repetition rate multiplier based on a cascaded 2x2 fiber coupler sequence with a splitting ratio of 50/50. Two burst shaping layouts were introduced in this experimental setup to obtain desired burst shape using one or two AOMs controlled by an AWG. Certain application may select most suitable burst shape obtained by introduced burst shaping layouts.

High-power FCPA system produced bursts of laser pulses at 3.26 GHz intra-burst repetition rate and 200 kHz burst repetition rate. Burst amplification was demonstrated using two configurations of large-mode-area (LMA and PCF) cladding-pumped Yb-doped fiber power amplifiers. Both amplifiers operated in well saturated regime and produced high output power of 6 W (11  $\mu\text{m}$  core LMA fiber power amplifier) and more than 20 W (40  $\mu\text{m}$  core PCF power amplifier) which corresponded to a maximum energy of 30  $\mu\text{J}$  and 100  $\mu\text{J}$  per burst respectively. The energy level of 30  $\mu\text{J}$  in the burst exceeded the pulse energy of 1.5  $\mu\text{J}$  achieved in FCPA system operating at the single-pulse regime. Rectangular-like shaped bursts of 60-500 ns widths (containing from  $\sim$ 192 to 1600 pulses) were obtained by means of burst pre-shaping using acousto-optic modulator driven by an arbitrary waveform generator. The high quality of the compressed pulses was examined and declared since nonlinear effects did not limit the pulse amplification in power amplifiers. The average duration of the compressed pulses was about 640 fs and was slightly longer than the bandwidth-limited

duration due to the impact of the dispersion of sufficiently long fiber delay lines in the PRR multiplier.

Developed high-power ultrashort pulse FCPA systems operating in a single-pulse and burst of pulses regimes could be successfully used in laser applications for material processing which require high output power and  $\mu\text{J}$  level pulse energy or bursts of energetic ultrashort laser pulses.

## CHAPTER FOUR

The literature review of this chapter is dedicated to discuss of proposed various fiber-based techniques, laser system configurations and technological limitations for the realization of high repetition rate pulse trains and bursts of laser pulses. The applications and future prospects for the usage of GHz bursts of laser pulses are also reviewed.

A new method to synthesize ultra-high repetition rate bursts of ultrashort laser pulses, which allows to overcome many limitations encountered in other techniques is introduced in the experimental section of this chapter. This new method, based on the use of active fiber loop, enabled to synthesize bursts of ultrashort laser pulses containing any number of pulses in a burst with identical pulse separation and adjustable amplitude.

### **4.1 Literature review**

#### **4.1.1 Applications of the laser systems generating high repetition rate bursts of laser pulses**

Ultrashort light pulses are highly applicable in science, medicine and industry [171–174]. The usage of GHz bursts of laser pulses can open new avenues not only in material processing but in various bio-imaging applications as well.

Many micro- and nano- machining applications require picosecond or femtosecond lasers due to its high performance, superior precision and small heat-affected zone provided by ultrashort light pulses [173,175–177]. Some beneficial material processing mechanisms are triggered only by femtosecond pulses [178–181]. Ultrafast fiber lasers ensure high processing quality, yet sufficiently low ablation efficiency per single pulse can be obtained. Therefore, the enhancement of the processing speed was made by increasing the pulse repetition rate [182–184]. Small temporal separation between sequential laser pulses enhanced certain processes or provided better quality of the processed site and its surroundings [185–187]. The demonstrated ablation-cooled laser material removal mechanism using bursts of high repetition rate ultrashort laser pulses, allowed to achieve significantly higher ablation efficiency maintaining high quality of ultrafast laser material processing [170]. The ablation efficiency was increased not only by a higher number of pulses within a certain time interval, but also because less of the deposited laser energy was lost to heat diffusion. Furthermore, the lower

pulse energy was required to achieve the same efficiency at high pulse repetition rates. A number of studies have been performed comparing different laser operation regimes for processing various materials [188–191]. A proper set of parameters was material dependent for the desired optimal processing result. In the demonstrated experiments, higher micromachining throughput was obtained using the GHz burst mode, wherein sequences of pulses with a predetermined number and separation were formed, as compared to the results of the conventional operation regimes at kHz and MHz pulse repetition rates. Nevertheless, more research has to be performed investigating the behavior of different materials affected by GHz bursts of ultrashort laser pulses in order to generalize the advantage of each operation regime.

The result of material processing using bursts of high repetition rate ultrashort laser pulses depends on the main predefined parameters of the laser source, such as burst width, burst and individual pulse energy, number of pulses and pulse repetition rate within a burst, pulse duration and a wavelength of the laser radiation. Fortunately, micro-machining applications do not require the exact pulse spacing (pulse repetition period) and very accurately matched pulse amplitudes inside the burst, which make the development of such laser sources easier. The whole material processing mechanism using burst of closely packed pulses can be defined by the effective absorption of the laser radiation and compared to the case of a single pulse whose energy is similar to the one of entire burst during the interaction with material.

High repetition rate (GHz) bursts of laser pulses can be used for developing new laser systems operating at mid-infrared (around 3-5  $\mu\text{m}$ ) wavelengths. Such laser sources are successfully applied in spectroscopy and free-space communication [192,193]. In these applications, high pulse repetition rate and high peak power can help to enhance processing speed and to increase signal-to-noise ratio. In the demonstrated systems, high repetition rate burst of pulses (1.5 GHz and 1.1 GHz) were used to quasi-synchronously pump mid-infrared picosecond optical parametric oscillators (OPO) based on the use of nonlinear crystal with quasi-periodically poled structure [194,195]. Sufficiently long pump pulse durations of 37 ps and 200 ps and different number (30 and 480) of pulses within a burst were used in the demonstrated experiments. System, using bursts of 37 ps duration pulses, provided tunable idler wavelength in the range of 2.26-3.57  $\mu\text{m}$  [194]. OPO system pumped by long bursts, containing up to 480 pulses (200 ps duration of individual pulse), provided maximum average

output power of 7.9 W at 3.8  $\mu\text{m}$  wavelength [195]. Compared to the conventional OPO systems pumped by long pulses, the approach using bursts of pulses enabled the improvement of pump-to-idler conversion efficiency by 40%. In both cases, the GHz pulse repetition rate within a burst allowed to shorten the cavity length of the OPO and to make it very compact and robust.

GHz bursts were implemented in the synchronously pumped broadband picosecond Raman laser [196]. In the presented system, the pump source generated 532 nm wavelength bursts consisting of 6 pulses at a burst repetition rate of 1 kHz, and 1.25 GHz PRR within the burst. Total width of the burst was equal to 4 ns, and the duration of individual pulses - 30 ps. The compact ring type cavity design of synchronously pumped Raman laser was realized in extremely short length of only 70 mm, since the pulse period inside the burst was 800 ps. The investigated system produced 270 mW output power covering the spectra from 532 nm to 800 nm wavelength. Developed compact scheme can be applied to far-infrared or ultraviolet laser sources where synchronously pumped stimulated Raman scattering technology is used.

High PRR ultrashort pulse bursts can be used for realization of a compact Raman laser generating ultrashort pulses in a spectral range from 1.1  $\mu\text{m}$  to 1.5  $\mu\text{m}$  suitable for bio-imaging applications. Full description of ultrashort pulse Raman laser system, implemented methods and laser technology are proposed in patent P2. The GHz burst formation was based on the newly developed method which is presented in the experimental part of this chapter and patent P1. The Raman laser system consists of fiber laser, providing high PRR burst of ultrashort pulses, and external synchronously pumped Raman cavity containing highly nonlinear crystal for wavelength shifting to 1.1-1.5  $\mu\text{m}$  region. The output pulse duration could be obtained from under 100 fs to 1 ps at the  $\mu\text{J}$ -level pulse energy, resulting in a very high peak intensity of the pulse. Laser system may operate at about 100 kHz burst repetition rate and PRR of 0.5-3 GHz within a burst which allows to significantly increase signal-to-noise ratio and enhance processing speed of the imaging process. This technique of wavelength conversion can open new avenues in building compact, reliable and efficient laser systems which will provide superior performance in nonlinear microscopy [197].

The presented laser systems containing external resonator for wavelength conversion require exact pulse repetition period within a burst which must be matched to the geometrical length of the cavity. The precise control of pulse

amplitudes can be necessary as well. The developed laser system has to meet these predefined requirements for creating suitable burst of laser pulses.

The technique of temporal pulse stacking (already introduced in section 3.1.3) uses GHz bursts of pulses in order to obtain extremely high pulse energy from ultrafast FCPA system [163]. Using this technique large number of equal-amplitude equidistant pulses can be stacked into one extremely-high output power and high-energy laser pulse exceeding the energy limit achieved by the individual pulse amplification [164]. This technique requires exact pulse repetition period between the pulses which must be matched to the cavity of the interferometer used in the system. Furthermore, the amplitude and the phase of the pulses have to be matched and precisely controlled to achieve constructive interference during the pulse stacking.

To sum up, development of new techniques which use GHz burst of pulses attracted a lot of attention in science and industry, demonstrating superior performance of laser systems. That encouraged the development of new methods and laser technologies capable to generate high PRR bursts, and demonstration of laser systems that provide the desired unique parameters of the laser radiation.

#### **4.1.2 Techniques providing high repetition rate bursts of laser pulses**

The generation and multiplication techniques of pulse trains as high as gigahertz repetition rates are reviewed in this section. There are many methods producing GHz bursts of laser pulses, however, fiber-based pulse multiplication techniques have the highest interest as it could be easily implemented in FCPA systems.

A typical pulse repetition rate of periodic pulse trains generated by mode-locked fiber oscillators is in the range from tens to hundreds of MHz. The highest possible PRR obtained from the fiber oscillator is limited by the length of the resonator which cannot be extremely short. Direct generation of pulses at multi-GHz repetition rates may be a challenging task. Conventional methods based on modulation instability, referred as a physical process that leads to a spontaneous breakup of intense continuous wave into a periodic pulsing even without any mode-locking element in a laser cavity, can provide pulse repetition rates usually higher than 100 GHz [198,199]. However, stable pulse trains with repetition rate of several or tens of GHz cannot be generated and, therefore, are not suitable for the industrial

application of such laser source. A method based on the cavity-induced modulation instability can greatly alter the phase matching condition and provide a generation mechanism of a highly stable pulse train up to tens of GHz from a ring cavity fiber laser [200]. The demonstrated system generated stable pulses of about 60 pJ pulse energy from 3 GHz to ~32 GHz PRR at 1.58  $\mu\text{m}$  center wavelength. However, at certain conditions laser operation was disturbed by the conventional modulation instability effect which had a higher pulse repetition rate and was unstable. Furthermore, using this technique PRR depends on cavity parameters and cannot be controlled independently from pulse temporal and spectral properties which makes the applicability of such laser source in FCPA systems complicated.

Comprehensive theoretical and experimental study investigated the operation of passively mode-locked Er/Yb-doped fiber oscillators at GHz PRR range and 1.53  $\mu\text{m}$  center wavelength [201]. The developed theoretical model predicted the requirements for a stable passive mode-locking at PRR above 1 GHz. Theoretical results were validated experimentally demonstrating a fiber cavity which generated laser pulses at 1-2.2 GHz PRR. The demonstration of higher PRR (5-10 GHz) was limited by the possible optical damage of the SESAM and gain conditions for mode-locking regime, due to extremely short fiber cavity of only few centimeters. Long term operation of more than thousand hours was not yet confirmed and can be the limiting factor for the oscillator to be used into industrial laser systems. Moreover, output pulse parameters depended on the PRR of the fiber cavity.

There are numerous methods which let to obtain higher PRR than fiber oscillators typically generate [24,183,184] [202–211]. Among these methods, pulse repetition rate can be multiplied by simply delaying laser pulses coming from the oscillator [24,185] [204–211]. These techniques could be more convenient as conventional oscillators operating in MHz PRR regime can be used for multiplication of GHz level pulse trains.

Interferometer-alike free-space arrangements [204,205] are limited in smallest achievable pulse separation due to the geometry of layouts and the size of optical elements. Furthermore, complexity and size of the free-space arrangements grow with the number of pulses within a burst. Passive Fabry-Perot cavities [185] are attractive because they are small in size, permit generation of small delays (up to 100 GHz intra-burst PRR) and can be adjustable. However, an exponentially decaying burst amplitude envelope is hardly useful in applications as it requires additional amplification and pulse train shaping. Using this technique, the pulse separation within a burst depends on the alignment precision of Fabry-Perot cavity.

Fiber solutions for PRR multiplication [24,184,207–211] are more attractive and have higher interest due to compactness, robustness and easy implementation in all-in-fiber laser systems. One fiber based PRR multiplication technique was introduced in section 3.1.4., where initial pulse repetition rate of 108 MHz from fiber oscillator was converted to  $\sim 3.5$  GHz by a pulse multiplier based on cascaded fiber couplers [24]. The approach of cascaded fiber couplers of 50/50 splitting ratio in combination with fiber delay lines allow to double pulse repetition rate after each fiber coupler.  $2^N$  times multiplication of the PRR requires  $(N+1)$  fiber couplers and  $N$  fiber delay lines. However, one of the drawbacks of this PRR multiplication technique is the difficulty to maintain equal pulse energies (pulse amplitudes) and equal temporal separations between the pulses due to coupling efficiency asymmetries of the fiber couplers and the difficulty to ensure precise fiber lengths. Another disadvantage is ultrashort pulse duration variation within a burst since dispersion is not controlled in this solution. Broadband ultrashort pulses that propagate the shortest optical path within the PRR multiplier undergo lowest dispersion, while pulses that propagate the longest optical path, undergo highest dispersion. The more PRR cascades are used, the higher pulse temporal distortion is obtained for broadband radiation. In the presented system, the acousto-optic modulator was used after the PRR multiplier to select desired width of the burst from a GHz pulse train. Minimal width of the bursts was limited by a response (rise and fall times) of the AOM. Therefore, the minimal burst width of 15 ns consisting of 50 pulses was demonstrated.

A modified solution was suggested of the aforementioned technique in which the cascaded fiber couplers with different arm lengths were used [183]. The delay between two pulse replicas after the first fiber coupler was not equal and much smaller than the half of the period of the input pulse train ( $\Delta T_1 \ll T_0$ ). The delays between adjacent pulses were halved after every stage in the following fiber delay lines. With  $N$  fiber delay lines, the pulse train with  $\Delta T_1/2^{N-1}$  distance between pulses was generated. In this case, quite short bursts of pulses of nearly equal amplitude were shaped and a burst-mode with an intra-burst repetition rate of  $\sim 4$  GHz was obtained. The disadvantages of this approach are similar to those of the previous method: generation of long bursts requires many stages of pulse multiplication; the absence of dispersion control results in pulse duration variation within a burst; pulse separation precision depends on a precision of fiber splicing procedure.

Another modification proposed the dispersion management capability by using fibers with different dispersion parameters inside the fiber delay lines [208]. In this case, the dispersion of different length fibers in each pulse multiplication stage was compensated and an equal pulse durations of laser pulses within a burst was obtained. Precisely selected dispersion parameters and lengths of the fibers were required for the desired optimal result. However, this solution only solved the issue of pulse duration variation inside the burst, but all the other aforementioned drawbacks remained.

Pulse repetition rate can be increased by using the pulse multiplication technique based on the configuration of passive fiber loops [209–211]. Using this method, the initial pulse from the laser source is coupled in the passive fiber loop which is formed by connecting one input and one output port of the 2x2 fiber coupler. The pulse circulates inside the loop while its energy is steadily reduced by the fiber coupler resulting in a formation of burst of pulses with decaying amplitude at the output of the passive fiber loop. A temporal separation between pulse replicas of coupled pulse from the laser source and emerged from the second output port of the fiber coupler is determined by the length of the fiber loop.

Different number of passive fiber loops can be connected sequentially to form bursts which contain several pulses [210,211]. A burst of 6 pulses was formed using two cascaded passive fiber loops, connected via 2x2 fiber couplers of 70/30 and 60/40 splitting ratios [210]. The temporal delay provided by the first fiber loop was more than three times lower than the initial pulse period of the pulse train coming from the fiber oscillator ( $T_1 < 3 * T_0$ ). The second fiber loop was half shorter than the first fiber loop ( $T_2 = T_1/2$ ). In this way, a pulse delayed by the first fiber loop after one round-trip exactly coincided in time with a pulse delayed by the second fiber loop after two round-trips. Therefore, the cascade of two fiber loops formed a burst of 6 pulses of different amplitudes where the third pulse had the highest amplitude. The energy of all consequent pulses was negligible due to the fast decay of the burst amplitude. In the presented system, the initial 2.67 MHz pulse train was transformed into a pulse train containing bursts of 6 pulses with 16 MHz intra-burst PRR.

A demonstration of three cascaded passive fiber loops, where  $T_1 \ll T_0$ ,  $T_2 = T_1/2$ ,  $T_3 = T_2/2$ , provided bursts of 13 pulses [211]. The synthesized burst was a sum of pulse replicas circulating multiple round-trips inside the three passive fiber loops of different lengths. The intra-burst pulse repetition rate of 793 MHz was demonstrated and defined by the length of the third fiber loop. The final pulse duration was not affected by the dispersion inside

the fiber loops as narrow bandwidth laser radiation (800 ps duration pulses) was used in the demonstrated system.

The pulse multiplication methods of multiple passive fiber loops with no additional elements have several drawbacks. The synthesized bursts contain laser pulses of unequal amplitudes, which can be hardly matched. The burst envelope is adjusted only by selecting the splitting ratios of the fiber couplers. No other control of pulse amplitudes is provided. Two or three pulses of small amplitude instead of one pulse can be formed by the inaccurate lengths of the fiber loops, which are not strictly in multiple. This technique is not suitable for synthesizing burst of ultrashort pulses as broadband radiation circulating many round-trips inside the fiber loops would experience the influence of the dispersion which would lead to the pulse duration variation inside the burst. Furthermore, the highest possible PRR that can be achieved by the aforementioned approach is about 2 GHz as it is defined by the length of the shortest fiber loop and a minimum length of two fiber pigtailed (approximately 5 cm each) that is required to accomplish the splicing with a fiber splicing machine. Therefore, ultra-high PRR can be defined to be above this value.

In the next section, a modified method to synthesize ultra-high PRR (>2 GHz) bursts of ultrashort laser pulses with identical pulse separation and adjustable amplitude is presented. The developed new technique based on the use of active fiber loop allows to overcome many limitations encountered by other techniques.

## **4.2 The development of the technique to synthesize ultra-high PRR burst of ultrashort pulses**

Material related to this section was published in A4 and described in patent P1

A method to synthesize ultra-high repetition rate bursts of ultrashort laser pulses containing any number of pulses within a burst with identical pulse separation and adjustable amplitude is presented in this section. The key element of this development which allowed to synthesize the GHz bursts of pulses was an active fiber loop. This technique was implemented in the FCPA system in order to demonstrate the performance. Bursts containing 20 pulses with a 2.65 GHz intra-burst pulse repetition rate and 500 kHz burst repetition rate were amplified to 72 nJ energy in a single-mode Yb-doped fiber amplifier. The bursts were not further amplified to a higher energy level as it was not the aim of this work. The dispersion compensation

mechanism used in active fiber loop ensured a mean 570 fs duration of pulse within the bursts after pulse compression.

This type of an active fiber loop can synthesize bursts of laser pulses with any desired pulse repetition rate from initial pulse train. A demonstration of 217 GHz intra-burst PRR showed the capability of this technique.

#### 4.2.1 The description and operation of the active fiber loop

The technique based on the active fiber loop is a very versatile method suitable to synthesize bursts of ultrashort laser pulses. The full description of this invention is presented in patent P1. In this section, the main focus is devoted on the configuration of the active fiber loop providing ultra-high PRR ( $>2$  GHz) ultrashort laser pulses within a burst.

The burst synthesizing element - an active fiber loop is depicted in Fig. 4.2.1. The active fiber loop comprises a fiber coupler which has two input and two output ports with the splitting ratio of 50/50, optical circulator, ytterbium doped fiber, chirped fiber Bragg grating, laser diode, acousto-optic modulator and a segment of a passive optical fiber. The loop is formed by connecting one input and one output port of the fiber coupler (*IN2* and *OUT2* ports in Fig. 4.2.1.) together with all containing components realizing a monolithic design. All fiber-optic components and optical fibers are polarization maintaining and single-mode.

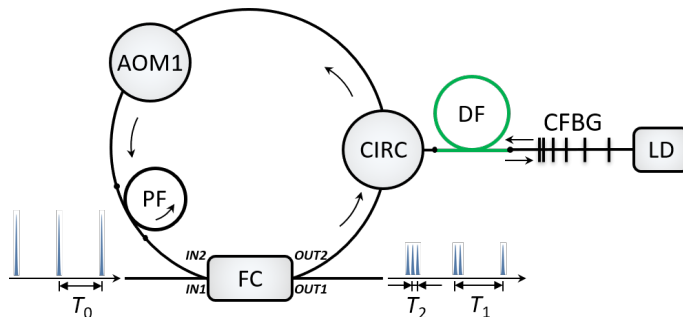


**Fig. 4.2.1.** Schematic setup of an active fiber loop. FC - 2x2 fiber coupler (50/50 splitting ratio), CIRC - optical circulator, DF - ytterbium doped fiber, CFBG - chirped fiber Bragg grating, LD - single-mode laser diode, AOM1 - acousto-optic modulator, PF - a segment of a passive optical fiber. *IN1,2* - input ports of the fiber coupler, *OUT1,2* - output ports of the fiber coupler. Time delays:  $T_0$  - between input pulses,  $T_1$  - between a delayed replica of an input pulse and an undelayed replica of the pulse,  $T_2$  - intra-burst pulse separation. Adapted with permission from [A4].

The active fiber loop can synthesize bursts of laser pulses with any desired pulse repetition rate. Though, an ultra-high intra-burst pulse

repetition rate of  $>2$  GHz was preferred in this demonstration. A delay  $T_1$  inside the active fiber loop is determined from a pulse period  $T_0$  of an initial pulse train and a desired intra-burst pulse separation  $T_2$  of the synthesized bursts as follows:  $T_1 = T_0 + T_2$ . A required total optical path length of the active fiber loop is estimated from  $T_1$ . In order to obtain the ultra-high intra-burst PRR, a physical length of the loop should be slightly longer than the cavity length of the master oscillator. The segment of the passive fiber is inserted into the loop in order to achieve the required total length for the desired intra-burst PRR. Thus, any arbitrary intra-burst pulse repetition rate can be formed, independently from the initial PRR.

The whole operation and burst formation can be explained by observing the propagation of single pulses with pulse separation  $T_0$  of the initial pulse train. The first pulse from the initial pulse train coupled into the fiber coupler is divided into two replicas. One pulse is outcoupled through the first output port *OUT1* and another replica of the pulse is delivered into the active fiber loop through the second output port *OUT2*. The pulse replica propagating through the active fiber loop returns to the fiber coupler a little bit later (time delay  $T_2$ ) than the second pulse from the initial pulse train arrives. They form the first burst containing two pulses. Further, one replica of the pair of pulses is outcoupled through the first output port and another replica containing two pulses is delivered into the loop again. After the second round-trip, a burst containing three pulses will be formed. After  $N$  round-trips, the burst of  $N+1$  pulses will be formed at the output of the active fiber loop. Thus, arbitrarily long bursts up to a few hundred nanosecond widths can be synthesized using the described method along with an additional temporal modulation of the initial pulse train.

The number of pulses within bursts is controlled using acousto-optic modulator (AOM1) inside the active fiber loop. When a desired number of pulses in the burst is formed, the acousto-optic modulator is turned off (zero transmission of radiation), and circulation of laser pulses inside the active fiber loop is interrupted. The formation of the bursts is restarted when the acousto-optic modulator is turned on again (the highest transmission of radiation).

The amplitude of pulses within a burst is controlled by amplification conditions in the ytterbium doped fiber. Pump radiation from a single-mode laser diode was coupled into the amplifier through the chirped fiber Bragg grating in this case. It is possible to provide a constant amplitude of the pulses within a burst among the whole train of bursts (Fig. 4.2.2.). The gain in the doped fiber must compensate the losses of all elements of the active

fiber loop. A total transmission of the demonstrated setup was around 2%. Therefore, amplification of 50 times was required in order to obtain a constant amplitude of the pulses within a burst, as shown in Fig. 4.2.2.

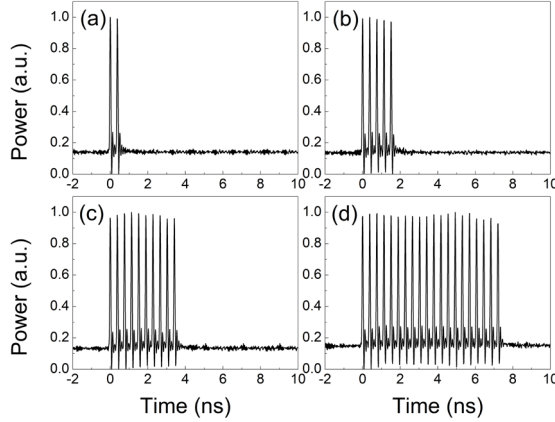


**Fig. 4.2.2.** Experimentally measured 2.65 GHz intra-burst PRR burst of pulses containing different number of ultrashort pulses: (a) 2, (b) 5, (c) 10, and (d) 20. Adapted with permission from [A4].

Arbitrarily long bursts which are longer than  $T_0$  may be synthesized using the described method along with a temporal modulation of the initial pulse train. The additional optical switch has to be inserted before the active fiber loop. The first stage of burst formation is the same as it was described above. When a certain number of pulses that circulate inside the active fiber loop fill the entire length of the loop, the optical switch blocks the subsequent input pulse. Pulses circulating inside the loop are outcoupled during the next optical cycle and are added to the previous cycle thus making a continuous burst of pulses which is roughly two times longer than the previous burst. Bursts up to a few hundred nanosecond widths can be formed by keeping the input pulses blocked. Therefore, time interval needed for long burst formation is approximately equal to a time that is needed to fill the active fiber loop with pulses. Experimentally measured 200 ns and 400 ns width 2.65 GHz PRR bursts, containing approximately 500 and 1000 pulses, respectively, are shown in Fig. 4.2.3. By synthesizing long bursts, the temporal profile of the burst was affected by the gain saturation resulting in the reduced amplitude of the trailing pulses. Furthermore, the rear front of the burst was restricted by a closing time of the acousto-optic modulator which was placed inside the loop.

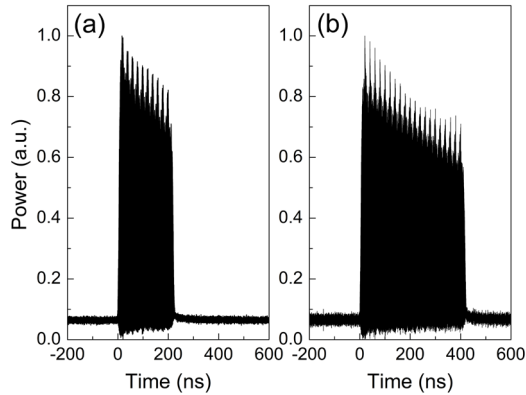


**Fig. 4.2.3.** Experimentally measured 200 ns (a) and 400 ns (b) width 2.65 GHz PRR bursts, which were synthesized using active fiber loop along with an additional temporal modulation of the initial pulse train, containing approximately 500 and 1000 pulses respectively.

The active fiber loop has a property to form a desired shape of amplitude envelope of a burst as long as it is not limited by the effect of the gain saturation. A decaying amplitude envelope of a burst is obtained (Fig. 4.2.4(a)) if the gain of the doped fiber is lower than the level of total losses of the elements. Moreover, a rising amplitude envelope of a burst is obtained (Fig. 4.2.4(b)) if the gain is greater than the losses. Any arbitrary shape of the amplitude envelope, with a resolution of a single pulse, can be obtained by actively modulating gain (LD current) or losses (AOM1 transmission) of the active fiber loop. At the output of the active fiber loop, an additional gate (acousto-optic or electro-optic) which selects bursts with a necessary number of pulses should be placed. For the case of long burst formation, three optical switches in total are required in the laser setup.

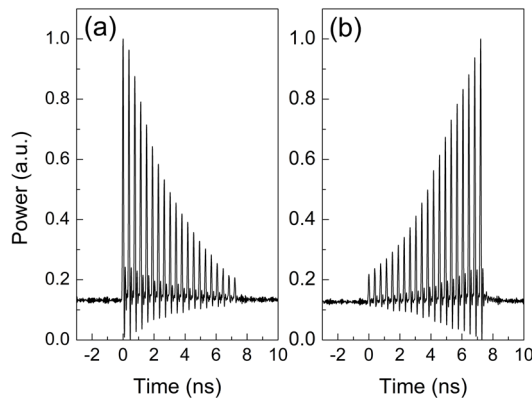


**Fig. 4.2.4.** Experimental representation of burst amplitude envelope shaping inside the active fiber loop: (a) decaying amplitude, (b) rising amplitude of pulses. Adapted with permission from [A4].

In order to obtain GHz bursts from the initial pulse train of  $\sim 50$  MHz pulse repetition rate, a total optical path length of the active fiber loop is around 4 meters. The dispersion may have sufficiently big impact on the pulse duration for broadband radiation after the propagation through a long active fiber loop. Due to chromatic dispersion, various spectral components undergo different phase shifts. As a result, the duration of delayed pulses may be changed. Every consequent pulse of the bursts propagates a longer path and, without dispersion control, a difference of spectral phases is accumulated. That means that a second pulse of the burst will differ from the first pulse, a third pulse will have different duration than the second and the first pulse, etc. In order to compensate the differences in spectral phases and to obtain bursts of pulses with identical durations, the element with an opposite dispersion to that of the fibers within the active fiber loop is required. A low dispersion (group delay dispersion of  $\beta_2 = -0.0816$  ps<sup>2</sup> at 1030 nm) chirped fiber Bragg grating was used as a dispersion compensation element which operated as a mirror in the presented system. Dispersion compensation element was designed to compensate the chromatic dispersion of the active fiber loop at each round-trip. At an ideal compensation case, pulse duration at the end of the loop is identical to that of the pulse that is outcoupled without propagation through the active fiber loop. Dispersion compensation is preferred for synthesizing GHz bursts of a broadband radiation and attaining a few hundred femtosecond pulse duration at the output of the system.

## 4.2.2 FCPA system with implemented active fiber loop

The realization of bursts of ultrashort laser pulses was demonstrated by implementing dispersion compensation mechanism into the active fiber loop which was used in FCPA system. A layout of the FCPA system which provided GHz bursts of nJ level ultrashort pulses is shown in Fig. 4.2.5.



**Fig. 4.2.5.** Schematic diagram of the laser system synthesizing GHz bursts of equidistant ultrashort pulses. AOM2 - second acousto-optic modulator in the experimental setup, tCFBG - thermally tunable chirped fiber Bragg grating, CVBG - chirped volume Bragg grating. Adapted with permission from [A4].

The laser system consisted of an all-in-fiber seed source with a temporal pulse stretcher, active fiber loop, additional acousto-optic modulator (AOM2), fiber power amplifier and pulse compressor. All-in-fiber passively mode-locked seed source operated at 1029.9 nm center wavelength, 50.8 MHz pulse repetition rate and provided pulse parameters similar to those of the system described in Chapter 1 of this thesis. Initial 22 pJ energy laser pulses were down-chirped to about 230 ps duration by using a chirped fiber Bragg grating (tCFBG) stretcher with group delay dispersion of  $\beta_2 = -33.7 \text{ ps}^2$ . Thermal tuning of the tCFBG was used for dispersion fine control and optimization of the pulse compression. Stretched pulses were sent to the active fiber loop in order to decrease pulse intensity and ensure that self-phase modulation does not distort the spectral phase of the pulses due to amplification. Pulse spectrum from the seed source is shown in Fig. 4.2.6.

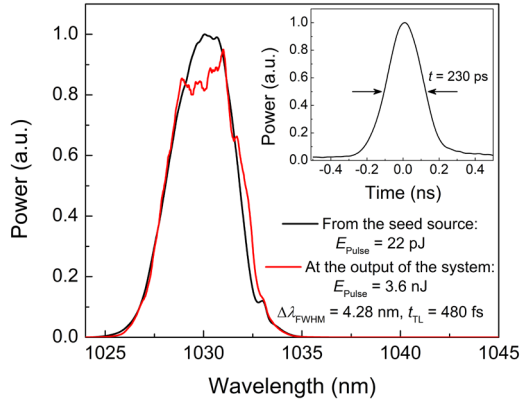


**Fig. 4.2.6.** Pulse spectrum from the seed source and at the output of the system. Inset: temporal envelope of the stretched pulses. Adapted with permission from [A4].

The active fiber loop produced the train of bursts with a different number of pulses and 2.65 GHz intra-burst PRR. The second acousto-optic modulator (AOM2) was used as a pulse picker to select only those bursts with an equal number of pulses. The GHz bursts of 500 kHz burst repetition rate containing 20 pulses were amplified in a core-pumped single-mode Yb-doped fiber power amplifier up to 72 nJ burst energy (3.6 nJ individual pulse energy). Rectangular-like burst amplitude (as in Fig. 4.2.2(d)) was obtained at the output of the system by adjusting amplification conditions of the fiber amplifier inside the active fiber loop. Rising amplitude of pulses in the bursts after the active fiber loop were required in order to achieve rectangular-like burst amplitude after the power amplifier because trailing part of the burst had smaller gain due to the gain saturation. Pulse spectrum after the power

amplifier is shown in Fig. 4.2.6 along with the one from the seed source. A Fourier-transform-limited pulse duration derived from the measured pulse spectrum (Fig. 4.2.6 (red curve)) was about 480 fs. The formation of a burst containing 20 pulses required 19 round-trips in the active fiber loop which corresponded to a propagation of the first replicated pulse in a 78.8-meters long optical fiber. Without dispersion compensation inside the active fiber loop, a broadband pulse (spectrum width of 4.28 nm at FWHM) would elongate up to 9 ps by propagating in 78.8 meters of the optical fiber.

Pulse compression was performed in a chirped volume Bragg grating (CVBG) compressor. The quality of compressed pulses was examined using a second harmonic noncollinear autocorrelator. Autocorrelation trace of the compressed pulses operating at GHz burst regime (burst containing 20 pulses) was compared to the single pulse regime and depicted in Fig. 4.2.7.

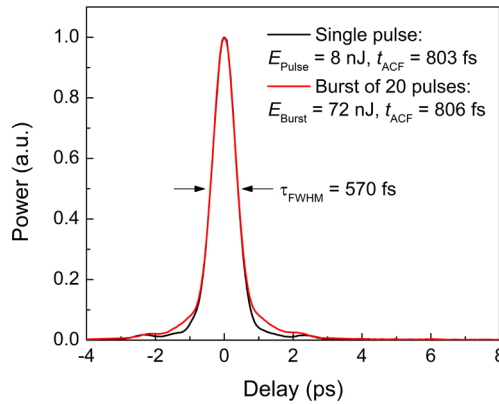


**Fig. 4.2.7.** Measured autocorrelation traces of the compressed pulses: single pulse regime, ultra-high PRR burst regime (20 pulses). Adapted with permission from [A4].

Measured autocorrelation trace had a width of  $\sim 806$  fs (FWHM) which corresponded to  $\sim 570$  fs pulse duration for Gaussian shaped pulses. Close match between GHz burst and single pulse regimes proved that the dispersion of the active fiber loop was successfully compensated by the low dispersion CFBG element. No pulse quality degradation was observed since the 3.6 nJ energy of the individual pulses in the bursts was small enough, and nonlinear effects did not limit the pulse amplification in the power amplifier, as well as, in the single pulse regime (individual pulse energy of 8 nJ). A slight difference in the autocorrelation traces may be resulted by the higher order dispersion in the active fiber loop since just the second order dispersion was compensated by the CFBG element. Furthermore, the difference in compressed pulse duration (570 fs) and Fourier-transform-

limited pulse duration (480 fs) can be attributed to a dispersion matching error between the CFBG stretcher and CVBG compressor.

### 4.2.3 The demonstration of 217 GHz intra-burst PRR burst

As already mentioned, one of the main advantages of the technique based on the use of active fiber loop is the capability to synthesize burst of laser pulses containing any number of pulses within a burst with identical pulse separation. Active fiber loop allows to adjust the amplitude envelope of the burst and maintain ultrashort pulse duration within a burst by implementing dispersion compensation mechanism. Furthermore, this technique enables burst formation of any arbitrary intra-burst PRR which do not depend on the initial pulse repetition rate. A presented demonstration of 217 GHz intra-burst PRR, which was achieved from the initial 50 MHz pulse train delivered from the fiber oscillator, show the versatility of this technique.

The principles of the burst formation of any desired PRR within a burst were fully described in section 4.2.1. In order to obtain the ultra-high intra-burst PRR, a physical length of the active fiber loop should be slightly longer than the cavity length of the fiber oscillator. The length of the segment of the passive fiber and corresponding time delay  $T_2$  (see Fig. 4.2.1.) predetermine pulse repetition rate within the synthesized burst. In the demonstration of  $>200$  GHz PRR within a burst, this segment of passive fiber was chosen to be extremely short of only  $\sim 0.95$  mm in length.

The exact pulse separation within a burst of compressed pulses was examined using a second harmonic noncollinear autocorrelator, as a response time of the conventional semiconductor detectors are too low for time delays of only few picoseconds. Measured autocorrelation trace of the compressed burst of pulses is shown in Fig. 4.2.8. The pulse separation between the pulses within a burst was estimated to be about 4.6 ps which corresponded to a 217 GHz intra-burst PRR. The ultrashort pulse duration of the individual pulses was maintained and equal to  $\sim 550$  fs.

This demonstration of 217 GHz intra-burst PRR showed the feasibility of this technique. By selecting an even shorter length of the passive fiber segment of only 0.2 mm and a temporal delay of 1 ps, the burst of laser pulses of 1 THz PRR can be synthesized. The development of the laser source which provide burst of ultrashort laser pulses at THz-level PRR can open new avenues in science and technology [212,213].

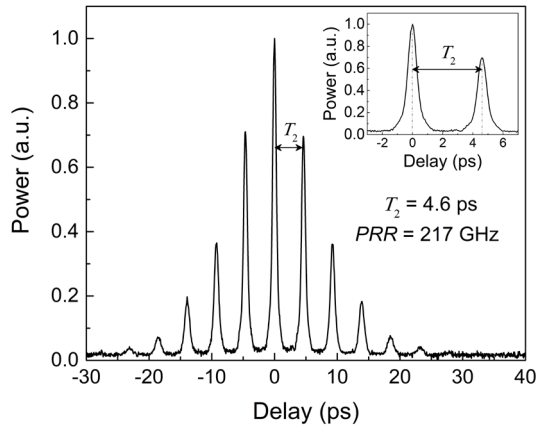


**Fig. 4.2.8.** Measured autocorrelation trace of compressed burst of pulses of 217 GHz PRR. Inset: measured autocorrelation trace with a modified time scale for a clearer representation of the pulse period ( $T_2 = 4.6$  ps) between the compressed pulses.

## Summary of the results

In this work, a novel technique to synthesize ultra-high repetition rate ( $>2$  GHz) bursts of ultrashort laser pulses with identical pulse separation and adjustable amplitude was presented. A single active fiber loop was able to synthesize bursts of laser pulses containing any number of pulses. Bursts containing from 2 to approximately 1000 pulses were demonstrated. One of the main advantages of the developed method over other fiber-based PRR multiplication techniques was the ability to synthesize bursts of laser pulses with any desired PRR which do not depend on the initial pulse repetition rate.

The constructed experimental fiber chirped pulse amplification system provided bursts of 2.65 GHz intra-burst PRR and 500 kHz burst repetition rate. Dispersion compensation mechanism was successfully implemented in the active fiber loop which allowed to obtain identical pulse durations within the GHz burst. At the output of the system, 570 fs pulse duration of Gaussian shaped pulses was attained within the 72 nJ-energy burst of 20 pulses.

The demonstration of 217 GHz intra-burst PRR showed the feasibility and versatility of this technique as burst of laser pulses of THz-level PRR can be synthesized. This technology can open new avenues in science and technology by building fiber lasers which will be able to provide superior performance over other laser sources.

## CONCLUSIONS

1. Implementation of fiber chirped Bragg grating stretcher and chirped volume Bragg grating compressor with matched dispersion profiles in a fiber chirped pulse amplification system enables the generation of 208 fs duration ultrashort laser pulses at high compression ratio of  $\sim 1100$ . Excellent pulse contrast of 90%, defined as the ratio of energy in the Fourier transform-limited pulse to the energy of experimentally measured pulse, can be achieved and only be limited by residual fiber chirped Bragg grating group delay irregularities caused by manufacturing precision.
2. Ultrashort pulses of 349 fs duration, 10  $\mu\text{J}$  energy and 26 MW peak power can be realized in a compact femtosecond fiber chirped pulse amplification system despite the accumulated large  $1.4\pi$  rad nonlinear phase-shift which is partly compensated by the positive second-order dispersion induced by linear temperature distribution along the CFBG stretcher. This could be further improved by applying a nonlinear temperature gradient along the CFBG. Numerical simulation and experimental investigation proved that a sufficient method for the minimization of a photodarkening effect in a single-mode fiber amplifier is a proper selection of ytterbium doped fibers of two different concentrations and lengths.
3. All-in-fiber pulse repetition rate multiplier based on a cascaded fiber coupler sequence, the formation of the bursts and the control of the shape of the burst amplitude envelope by using acousto-optic modulators expands the regimes of the laser operation. The implementation of such technique in FCPA system utilizing single-mode cladding-pumped large-mode-area (11  $\mu\text{m}$  core diameter) Yb-doped fiber power amplifier allows to increase the pulse/burst energies from 1.5  $\mu\text{J}$  in single-pulse operation regime to 30  $\mu\text{J}$  in burst regime. This technique had several drawbacks. First of all, a minimal burst envelope width was limited to 20 ns by a rise and fall times of the acousto-optic modulator. Secondly, quite large mismatch of pulse amplitudes inside the burst was obtained due to the variation of splitting ratio of the fiber couplers. Furthermore, the exact pulse spacing (pulse repetition period) was hardly realized by controlling the length of fiber pigtails of each coupler. Nevertheless, a successful demonstration of the laser system providing 3.26 GHz intra-burst

repetition rate ultrashort (640 fs) burst of pulses was presented. This straightforward approach is usable for laser machining of materials, which is not very sensitive to variations of the energy of individual pulses in the GHz train more than 10%.

4. A new method based on the use of an active fiber loop allows to synthesize ultra-high repetition rate bursts of ultrashort laser pulses containing any number of pulses in a burst with identical pulse separation and adjustable amplitude as it was demonstrated in FCPA system providing ultrashort pulse (570 fs) bursts of 2.65 GHz and 217 GHz pulse repetition rates. The developed method has the advantage over other fiber-based PRR multiplication techniques as it allows to synthesize bursts of laser pulses with any desired PRR which do not depend on the initial pulse repetition rate. Low dispersion CFBG implemented in an active fiber loop for proper chromatic dispersion compensation of the optical fiber enables pulse duration matching within the GHz burst.

# SANTRAUKA

## Ižanga

Šviesolaidiniai lazeriai pasižymi keliomis savybėmis, išskiriančiomis juos iš kitų lazerinių technologijų. Šio tipo lazeriai, dėl didelio šviesolaidžių paviršiaus ploto ir tūrio santykio, pasižymi geromis šiluminėmis savybėmis, užtikrinančiomis efektyvų lazerinės terpės aušinimą. Bangolaidinis lazerinės spinduliuotės sklidimas sąlygoja puikią erdvinę pluošto kokybę, sumažindamas arba visiškai pašalindamas šiluminių efektų sukeltus iškraipymus. Nehomogeniškai išplitę aktyviųjų jonų spinduliuotės ir sugerties spektrai leidžia šviesolaidiniams lazeriams veikti tiek nuolatinės veikos, tiek itin trumpų impulsų generacijos režimuose bei pasižymėti bangos ilgio keitimo galimybe pakankamai plačiose ribose. Maži spinduliuotės sklidimo nuostoliai, nedidelis kvantinis defektas bei didelis stiprinimas leidžia šviesolaidiniams lazeriams pasiekti itin dideles spinduliuotės vidutines galias, siekiančias kelių kilovatų lygį vienos skersinės modos režime [1], ir rekordinius elektros vertimo lazerine spinduliuote efektyvumus [2,3]. Be to, įvairiapusiška ir lanksti šviesolaidžių technologija leidžia suprojektuoti kompaktiškus lazerių dizainus, nes dažniausiai naudojami šviesolaidžiai yra lankstūs ir gali būti suvynioti.

Šviesolaidiniai lazeriniai šaltiniai yra paklausūs įvairiose taikymo srityse tiek moksle, tiek ir pramonėje, dėl minėtų išskirtinių jų savybių. Pramonėje didelės vidutinės galios šviesolaidiniai lazeriai dažniausiai naudojami įvairiems medžiagų apdirbimams. Pavyzdžiui suvirinimui, gręžimui ir pjovimui, naudojami kilovatinės klasės nuolatinės veikos [4] arba impulsiniai kokybės moduliacijos lazeriai, generuojantys intensyvius nanosekundinės trukmės impulsus [5]. Daugelis metrologinių taikymų, tokių kaip tikslus optinis atstumo nustatymas [6] ar žadinimo-zondavimo eksperimentas [7], reikalauja trumpų (ps eilės) impulso trukmių. Mikroskopiniai metodai, pagrįsti dviejų arba daugelio fotonų sužadinimo fluorescencija biologinių audinių vaizdinimui, reikalauja itin trumpos (kelių šimtų fs eilės) impulso trukmės ir santykinai mažos, nanodžiaulių lygio, impulso energijos [8,9]. Panašių parametrų (impulso trukmė ir energija) lazerio spinduliuotė naudojama ir plačiaujustės terahercinės spinduliuotės generavimui [10].

Daugybė pažangių taikymų, tokių kaip lazerinis medžiagų mikroapdirbimas [11], netiesinė spektroskopija [12], rentgeno spinduliuotės generavimas [13] ir efektyvus parametrinis bangos ilgio keitimas [14,15],

reikalauja didesnių lazerio spinduliuotės vidutinių galių, siekiančių dešimtis vatų, ir impulsų energijų, nuo dešimčių iki šimtų mikrodžaulių. Didesnę šviesolaidinio lazerio vidutinę galią galima pasiekti įdiegus didelės galios kaupinimo šaltinių modulius ir naujus stiprinimo terpės dizainus [16] arba koherentiškai apjungiant kelis lazerio pluoštus [17].

Skirtingos didelės galios šviesolaidinės lazerinės sistemos, veikiančios nuolatinės veikos ar ultratrumpųjų impulsų generavimo režimuose, atitinkamai susiduria su skirtingais efektais, ribojančiais maksimalius lazerio parametrus. Didelės energijos ultratrumpųjų impulsų realizacija šviesolaidiniuose lazeriuose yra ribota dėl mažos soties energijos, lyginant su kietojo kūno lazeriais. Didelės impulsų smailinės galios šviesolaidinių lazerių kūrimas yra sudėtingas dėl netiesinių efektų, ribojančių ultratrumpųjų impulsų stiprinimą aktyviais jonais legiruotuose šviesolaidiniuose stiprintuvuose, dėl ilgo spinduliuotės ir medžiagos sąveikos ilgio ir mažo šviesolaidžio šerdies ploto. Fazės moduliavimasis yra labiausiai dominuojantis netiesinis efektas, kuris, kartu su kitais netiesiniais efektais, tokiais kaip savifokusacija ir Ramano sklaida, turi būti sumažintas, norint išvengti nepageidaujamų impulso gaubtinės iškraipymų. Sukurta faziškai moduluotų impulsų stiprinimo technologija leido sumažinti šių žalingų efektų įtaką [18].

Faziškai moduluotų impulsų stiprinimo technologijos bei didelio modos ploto šviesolaidžių panaudojimas ultratrumpųjų impulsų šviesolaidinėse lazerinėse sistemose leido pasiekti šioms sistemoms rekordiškai dideles energijas, siekiančias 1 mJ [19]. Neseniai buvo pristatyta 10.4 kW vidutinės galios šviesolaidinė faziškai moduluotų impulsų stiprinimo (*angl. trump.: FCPA*) sistema, generuojanti itin trumpus 254 fs trukmės impulsus [20]. Iki publikacijos paskelbimo datos, šios sistemos spinduliuotės vidutinė galia buvo didžiausia, kurią buvo pasiekusi ultratrumpųjų impulsų lazerinė sistema. Ši demonstracija parodė didelės galios šviesolaidinių faziškai moduluotų impulsų stiprinimo sistemų, naudojančių koherentinį lazerio pluoštų apjungimą, tinkamumą ir technologines galimybes bei perspektyvas realizuoti dar didesnes vidutinės spinduliuotės galias, siekiančias 100 kW lygį. Tokios sistemos ateityje galėtų būti taikomos dalelių greitinimo sistemose [21,22]. Nauji šviesolaidinių lazerių spinduliuotės vidutinių galių bei generuojamų impulsų energijos rekordai yra pasiekiami tobulinant šviesolaidines technologijas, išrandant naujus metodus bei vengiant žalingo netiesinių efektų poveikio.

Vienas pagrindinių šios disertacijos tikslų buvo kompaktiškos ir patikimos didelės energijos (mikrodžaulių lygio) femtosekundinės

šviesolaidinės faziškai moduluotų impulsų stiprinimo sistemos sukūrimas, naudojančios į šerdį kaupinamą vienamodį poliarizaciją išlaikantį iterbio jonais legiruotą šviesolaidinį stiprintuvą, ir veikiančios ties  $1.03 \mu\text{m}$  centriniu bangos ilgiu. Ypatingas dėmesys buvo skirtas kompaktiško lazerio dizaino išlaikymui, įgyvendinant visiškai šviesolaidinio lazerio konfigūraciją ir naują šviesolaidinės faziškai moduluotų impulsų stiprinimo sistemos schemą, pagrįstą čirpuotos šviesolaidinės Brego gardelės (*angl. trump.: CFBG*) impulsų plėstuvu ir itin mažų matmenų čirpuotos tūrinės Brego gardelės (*angl. trump.: CVBG*) impulsų spaustuvu. Šių dispersinių elementų dispersijos profiliai buvo suderinti tarpusavyje, tam kad sistemos išėjime būtų realizuoti aukštos laikinės kokybės spektriškai riboti ultratrumpieji lazerio impulsai. Šiame darbe pristatomas sistemos optimizavimas ir sukaupto netiesinės fazės pokyčio kompensavimas leido pasiekti didelės energijos ( $10 \mu\text{J}$ ) lazerio impulsus. Fototamsėjimo efektas yra laikomas vienu pagrindinių veiksnių, ribojančių šviesolaidinių stiprintuvų, kaupinamų didelio intensyvumo spinduliuote, tarnavimo laiką ir patikimumą. Šiame darbe atlikti skaitinio modeliavimo ir eksperimentiniai tyrimai leido sumažinti fototamsėjimo efekto įtaką šviesolaidiniame stiprintuve, užtikrinant stabilų šviesolaidinio lazerio veikimą. Sukaupta patirtis buvo panaudota konstruojant didelės galios ultratrumpųjų impulsų šviesolaidinį lazerį. Impulsų energija, tiesiogiai gaunama iš didelio modos ploto šviesolaidinio stiprintuvo, turi pakankamai aiškią technologinę ribą, nes šviesolaidžio šerdies negalima padidinti iki itin didelių diametrų. Taigi, sukurti lazerio veikimo režimai, leido imituoti didesnes impulsų energijas, generuojant MHz [23] ir GHz [24] impulsų pasikartojimo dažnio impulsų paketus. Šiame darbe pristatomas naujas metodas, generuojantis gigahercinio impulsų pasikartojimo dažnio impulsų paketus bei leidžiantis išplėsti lazerio veikimo režimus. Šis metodas gali būti panaudotas vystant naujus lazerinius šaltinius, kurie būtų pritaikyti įvairiose mokslo ir pramonės srityse.

## **Mokslinis naujumas**

Šio darbo mokslinis naujumas slypi sėkmingai pademonstruotose lazerinėse technologijose, kurių įdiegimas leido realizuoti kompaktiškas šviesolaidines faziškai moduluotų impulsų stiprinimo sistemas generuojančias didelės energijos ultratrumpuosius impulsus ir impulsų paketus:

1. Pasiūlyta ir eksperimentiškai pademonstruota kompaktiška faziškai moduluotų impulsų stiprinimo sistema, naudojanti čirpuotos

šviesolaidinės Brego gardelės impulsų plėstuvą ir čirpuotą tūrinės Brego gardelės impulsų spaustuvą su suderintais dispersijos profiliais, generavo aukštos kokybės spektriškai ribotus ultratrumpuosius impulsus lazerinės sistemos išėjime. Tokia aukšta suspausto impulso laikinė kokybė buvo pasiekta pirmą kartą, naudojant šią impulsų plėtimo ir suspaudimo konfigūraciją. Ši faziškai moduluotų impulsų stiprinimo sistemos konfigūracija atveria kelią itin kompaktiškų ir patikimų didelės energijos femtosekundinių šviesolaidinių lazerių kūrimui.

2. Didelė 10  $\mu\text{J}$  impulsų energija buvo pasiekta kompaktiškoje visiškai šviesolaidinėje faziškai moduluotų impulsų stiprinimo sistemoje, naudojančioje hibridinį šviesolaidinį stiprintuvą, sudarytą iš skirtingomis koncentracijomis iterbio jonais legiruotų vienamodžių šviesolaidžių.
3. Didelės galios ultratrumpųjų impulsų šviesolaidinis lazeris, generuojantis gigahercinio impulsų pasikartojimo dažnio impulsų paketus, buvo realizuotas remiantis kaskadiniu šviesolaidinių daliklių impulsų daugintuvu bei didelio modos ploto į apvaskalą kaupinamais iterbio jonais legiruotais šviesolaidiniais stiprintuvais. Šie technologiniai sprendimai leido išplėsti lazerio veikimo režimus ir taip padidinti generuojamų impulsų paketų energijas bei vidutinę galią iš šviesolaidinės lazerinės sistemos.
4. Sukurtas ir pirmą kartą eksperimentiškai pademonstruotas naujas metodas, skirtas itin didelio pasikartojimo dažnio ultratrumpųjų lazerio impulsų paketų sintezavimui. Šis metodas leidžia išgauti impulsų paketus, turinčius bet kokį impulsų skaičių pakete, identišką impulsų laikinį atskyrimą bei gali valdyti pavienių impulsų amplitudę pakete.

### **Praktinė nauda**

Šviesolaidinių technologijų tobulinimas ir naujų metodų vystymas leidžia sukurti naujas lazerių architektūras bei realizuoti kompaktiškus, patikimus ir industrinius reikalavimus atitinkančius ultratrumpųjų impulsų šviesolaidinius lazerius. Be to, nauji metodai leidžia išplėsti lazerio veikimo režimus bei pritaikyti šiuos lazerinius šaltinius tiek moksle, tiek pramonėje.

Šis darbas praktiškai vertingas keliais aspektais:

1. Žymus ultratrumpųjų impulsų laikinės kokybės pagerinimas šviesolaidinėje faziškai moduluotų impulsų stiprinimo sistemoje, paremtoje čirpuotos šviesolaidinės Brego gardelės impulsų plėstuvo ir čirpuotos tūrinės Brego gardelės impulsų spaustuvo su suderintais dispersijos profiliais panaudojimu, leidžia šią technologiją įdiegti įmonės „Ekspla“ gaminamose lazerinėse sistemose.
2. Šviesolaidinių stiprintuvų optimizavimas leido realizuoti didelės energijos šviesolaidinį lazerį, kuris įmonėje „Ekspla“ buvo panaudotas, kaip užkrato šaltinis konstruojant didelės galios ir energijos hibridinį lazerį, paremtą šviesolaidinėmis ir kietojo kūno lazerinėmis technologijomis.
3. Sėkmingai sukonstruotas ir pademonstruotas naujas metodas, skirtas itin didelio pasikartojimo dažnio ultratrumpųjų lazerio impulsų paketų sintezavimui leido vystyti naujus lazerinius šaltinius, skirtus lazeriniam medžiagų mikroapdirbimui ir derinamo bangos ilgio lazerinių sistemų kaupinimui.

### **Ginamieji teiginiai**

- S1. Dispersinių elementų (čirpuotos šviesolaidinės Brego gardelės plėstuvo ir čirpuotos tūrinės Brego gardelės spaustuvo) su suderintais dispersijos profiliais panaudojimas šviesolaidinėje faziškai moduluotų impulsų stiprinimo sistemoje leidžia generuoti aukštos laikinės kokybės mažesnės nei 300 fs trukmės impulsus, net ir esant dideliame impulsų plėtimo ir spaudimo santykiui, siekiančiam 1100 kartų.
- S2. Vienamodis šviesolaidinis stiprintuvas, sudarytas iš dviejų šviesolaidžių, kurie skiriasi iterbio jonų legiravimo laipsniu ir ilgiu, leidžia minimizuoti fototamsėjimo efektą šviesolaidiniame stiprintuve bei pasiekti itin didelę 10  $\mu$ J impulsų energiją ir 26 MW smailinį intensyvumą kompaktiškoje femtosekundinėje šviesolaidinėje faziškai moduluotų impulsų stiprinimo sistemoje, nepaisant sukaupto didelio ( $>1\pi$  rad) netiesinės fazės pokyčio.
- S3. Gigahercinio impulsų pasikartojimo dažnio impulsų paketų realizacija bei paketų amplitudinės gaubtinės formavimas ir valdymas leidžia praplėsti lazerio veikimo režimus bei tokiu būdu padidina šviesolaidinio lazerio generuojamas impulsų (paketų) energijas, nuo

1.5  $\mu\text{J}$  pavienių impulsų stiprinimo režime iki 30  $\mu\text{J}$  impulsų paketų stiprinimo atveju, šviesolaidinėje lazerinėje sistemoje, naudojančioje didelio modos ploto (11  $\mu\text{m}$  šerdies diametro) į apvaskalą kaupinamą iterbio jonais legiruotą šviesolaidinį stiprintuvą.

- S4. Itin didelio impulsų pasikartojimo dažnio ( $>2$  GHz) ultratrumpųjų lazerio impulsų paketai, turintys bet kokią impulsų kiekį pakete, identišką laikinį atstumą tarp impulsų bei reguliuojamą amplitudę, gali būti sintezuojami nauja metodika, paremta aktyvios šviesolaidinės kilpos panaudojimu.

### **Autoriaus indėlis**

Autorius sukonstravo visas lazerines sistemas, aprašytas A1-A4 mokslinėse publikacijose ir P1 patentinėje paraiškoje. Taip pat prisidėjo prie eksperimentinių tyrimų rengiant P2 patentinę paraišką. Autorius pasiūlė vertingų idėjų atliekant eksperimentinių sistemų realizavimą, kurios pristatytos A3 mokslinėje publikacijoje, bei pasiūlė techninius sprendimus naujo metodo vystymui, skirto itin didelio impulsų pasikartojimo dažnio ultratrumpųjų lazerio impulsų paketų sintezavimui, kuris aprašytas A4 mokslinėse publikacijose ir P1 patentinėje paraiškoje. Autorius parengė A1-A4 mokslinių publikacijų rankraščius. Taip pat, autorius atliko skaitinio modeliavimo ir teorinės analizės darbus pateiktus pristatytose mokslinėse publikacijose ir šioje disertacijoje.

### **Diskusija ir rezultatų apžvalga**

#### **Kompaktiška FCPA sistema, naudojanti CFBG impulsų plėstuvą ir CVBG impulsų spaustuvą su suderintais dispersijos profiliais**

Skyriuje pateikta medžiaga publikuota A1

Daugeliui industrinių taikymų ir mokslinių tyrimų krypčių yra svarbi gera lazerinio pluošto bei impulsų laikinė kokybė, didelė impulsų energija ir vidutinė galia, lazerio patikimumas. Šviesolaidinis lazeris gali būti puikus pasirinkimas, užtikrinantis šiuos keliamus reikalavimus. Pasiūlyta faziškai moduluotų impulsų stiprinimo technologija [18], leido sumažinti neigiamą netiesinių efektų įtaką, bloginančią suspaustų impulsų laikinę kokybę bei ribojančią maksimalius lazerio energetinius parametrus.

Faziškai moduluotų impulsų stiprinimo technologija yra paremta impulsų plėtimu laike, sumažinant smailinį impulsų intensyvumą bei netiesinių efektų įtaką, išplėstų impulsų stiprinimu lazeriniame stiprintuve ir impulsų suspaudimu iki pradinės ar netgi mažesnės impulsų trukmės (itin didelio smailinio intensyvumo). Impulsų plėtimas ir suspaudimas šviesolaidinėse faziškai moduluotų impulsų stiprinimo sistemose gali būti realizuojamas naudojant difrakcines gardeles [67,68]. Šis technologinis sprendimas turi privalumą, jog tinkamai suprojektuotas plėstuvai ir spaustuvas turi tiksliai sukompensuotą dispersijos profilį. Taip pat, naudojant šią technologiją, pradiniai impulsai gali būti išplėsti iki kelių nanosekundžių trukmės. Tai leidžia sumažinti netiesinių efektų įtaką bei pasiekti šioms sistemoms rekordiškai dideles energijas [19]. Tačiau impulsus plečiant laike iki kelių šimtų pikosekundžių ar ilgesnės trukmės, difrakcinių gardelių pagrindu sukurta FCPA sistema tampa gana didelė. Be to, difrakcinių gardelių plėstuvai ir spaustuvas yra jautrūs mechaniniam ir šiluminiam poveikiui, o laikinė suspausto impulso gaubtinė bei erdvinis pluošto profilis stipriai priklauso nuo tikslaus optinių elementų suderinimo [69]. Dėl šių priežasčių difrakcinių gardelių technologija pagrįstos šviesolaidinės lazerinės sistemos praranda pakankamai svarbų kompaktiškumą bei patikimumo privalumą.

Svarbus pasiekimas leidęs sumažinti FCPA sistemų matmenis buvo pasiektas difrakcinių gardelių impulsų plėstuvą pakeitus itin kompaktišku čirpuotos šviesolaidinės Brego gardelės impulsų plėstuvu [72]. Šis technologinis sprendimas leido realizuoti visiškai skaidulinę faziškai moduluotų impulsų stiprinimo sistemą, impulsus spaudžiant išoriniame difrakcinių gardelių kompresoriuje. CFBG plėstuvai gali būti pagaminti taip, jog turėtų dispersijos profilį priderintą prie impulsų spaustuvo konfigūracijos, užtikrinant aukštą suspaustų impulsų laikinę kokybę.

Dar vienas proveržis šviesolaidinių faziškai moduluotų impulsų stiprinimo sistemų srityje įvyko tobulėjant alternatyviai impulsų plėtimo bei spaudimo technologijai – čirpuotai tūrinei Brego gardelei [73–77]. Čirpuotos tūrinės Brego gardelės, kurių matmenys (ilgis) gali siekti tik kelis centimetrus, gali išplėsti impulsus iki kelių šimtų pikosekundžių trukmės ir vėl juos suspausti iki kelių šimtų femtosekundžių trukmės. Čirpuotų tūrinių Brego gardelių panaudojimas impulsų plėtimui ir spaudimui turi praktinį privalumą prieš difrakcinių gardelių plėstuvus ir spaustuvas dėl mažų matmenų (kompaktiškumo), paprasto derinimo ir patikimumo. Panaudojant šviesolaidinę čirpuotą Brego gardelę impulsų plėtimui bei čirpuotą tūrinę Brego gardelę impulsų spaudimui, buvo pademonstruota naujo tipo faziškai

moduliuotų impulsų stiprinimo sistemos koncepcija [83,84]. Deja, dėl netikslaus dispersijos kompensavimo tarp CFBG plėstuvo ir CVBG spaustuvo, pristatytose sistemose suspausti impulsai nebuvo spektriškai ribotos trukmės, pasižymėjo pakankamai dideliu pikosekundiniu laikiniu pjedestalu, kuriame sukaupta pakankamai didelė impulso energijos dalis. Šiame darbe pristatoma šviesolaidinė faziškai moduliuotų impulsų stiprinimo sistema, paremta čirpuotos šviesolaidinės Brego gardelės impulsų plėstuvu ir čirpuotos tūrinės Brego gardelės impulsų spaustuvu su suderintais dispersijos profiliais, užtikrinanti aukštą suspaustų impulsų laikinę kokybę sistemos išėjime.

Gaminamos čirpuotos tūrinės Brego gardelės, skirtos ultratrumpųjų impulsų sistemoms, pasižymi ne visiškai tiesiniu dispersijos profiliu lazerio spinduliuojamų bangos ilgių srityje. Dėl šios priežasties, čirpuotos šviesolaidinės Brego gardelės plėstuvo dispersijos profilis turi būti priderintas prie spaustuvo, tam kad plataus impulsų spektro skirtingo bangos ilgio komponentės būtų sufazuotos ir pasiekta itin aukšta laikinė suspaustų impulsų kokybė. Skaitinio modeliavimo rezultatai, remiantis eksperimentiškai išmatuotomis dispersinių elementų grupinio vėlinimo kreivėmis, parodė, jog dispersijos profilių derinimo atveju gaunami aukštos laikinės kokybės spektriškai riboti impulsai sistemos išėjime. Jeigu dispersijos profiliai tarp CFBG ir CVBG elementų nebūtų derinami, atlikus impulsų spaudimą, būtų gaunami prastesnės laikinės kokybės impulsai, pasižymintys šalutiniais impulsais bei beveik 30% mažesniu smailiniu intensyvumu.

Lazerinės sistemos, paremtos dispersiškai suderintų CFBG ir CVBG elementų panaudojimu, koncepcijos patvirtinimui buvo sukonstruota šviesolaidinė faziškai moduliuotų impulsų stiprinimo sistema, kurią sudarė visiškai šviesolaidinis užkrato šaltinis, CFBG impulsų plėstuvai, šviesolaidinis stiprintuvas, kaupinimo modulis bei CVBG impulsų spaustuvas. Impulsai buvo generuojami visiškai šviesolaidinio pasyvios modų sinchronizacijos osciliatoriaus, veikiančio 53 MHz impulsų pasikartojimo dažniu ties 1029.4 nm centriniu bangos ilgiu. Impulsų spektras išplėstas iki 10.6 nm pločio (pusės maksimalaus intensyvumo lygyje) dėl fazės moduliavimosi, impulsams sklindant pakankamai ilgame pasyviame šviesolaidyje. Toliau impulsai buvo plečiami laike iki 230 ps trukmės, panaudojus čirpuotos šviesolaidinės Brego gardelės plėstuvą, kurio grupinio vėlinimo dispersijos vertė buvo lygi  $-13.65 \text{ ps}^2$ . Faziškai moduliuoti impulsai buvo pastiprinti iki 4.85 nJ impulsų energijos ir spaudžiami čirpuotos tūrinės Brego gardelės impulsų spaustuve. Temperatūrinis CFBG dispersijos

reguliuojamas leido lengvai optimizuoti impulsų suspaudimą. Ši procedūra buvo atliekama keičiant temperatūros pasiskirstymą išilgai čirpuotos šviesolaidinės Brego gardelės ir nereikalavo nepatogaus tikslaus šviesolaidžio ilgio parinkimo sistemoje ir virinimo stebint suspaustų impulsų trukmę. Optimaliai suspaustų impulsų kokybė charakterizuota atliekant antros harmonikos dažninės skyros optinės sklendės (*angl. trump.: FROG*) matavimą. Atkurto impulso trukmė buvo lygi 208 fs. Spektriškai ribotų impulsų trukmė įvertinta iš spektro buvo lygi 203 fs. Artimos išmatuotos ir įvertintos trukmių vertės, įrodo, jog CFBG dispersijos profilis buvo tiksliai suderintas su CVBG spaustuvo dispersijos profiliu. Tai parodo ir maža likutinė spektrinė fazė atkurta iš FROG matavimų bei daugiau nei 90% siekiantis impulsų kontrastas, apibrėžiamas energijos santykiu tarp pagrindinio impulso ir šalutinių impulsų. Puiki laikinė impulsų kokybė buvo gauta nepaisant itin didelio impulsų spaudimo santykio siekusio ~1100 kartų.

Ši nauja šviesolaidinė faziškai moduluotų impulsų stiprinimo sistemos konfigūracija atveria kelią itin kompaktiškų, patikimų didelės energijos femtosekundinių šviesolaidinių lazerių kūrimui.

### **Kompaktiškas didelės energijos femtosekundinis šviesolaidinis lazeris su CFBG impulsų plėstuvu ir CVBG impulsų spaustuvu**

Skyriuje pateikta medžiaga publikuota A2

Sėkmingai pademonstruota šviesolaidinė faziškai moduluotų impulsų stiprinimo sistema, naudojanti CFBG impulsų plėstuvą ir CVBG impulsų spaustuva su suderintais dispersijos profiliais, leido kurti didesnės energijos (apie 10  $\mu\text{J}$ ) bei mažesnės nei 1 W vidutinės galios kompaktišką femtosekundinį (apie 300 fs trukmės) šviesolaidinį lazerį. Toks lazeris, gali būti pritaikytas netiesiniuose taikymuose, tokiuose kaip, efektyvus parametrinis bangos ilgio keitimas [92] ar biologinių audinių vaizdinimas [88–91], kur didelė vidutinė lazerio galia nėra reikalinga ar netgi yra žalinga. Taip pat, toks šviesolaidinis lazeris gali būti panaudotas, kaip užkrato šaltinis didelės galios ir energijos femtosekundinėje lazerinėje sistemoje [93].

Pastaruoju metu, buvo pristatytos įvairios šviesolaidinės sistemos, generuojančios panašius impulsų parametrus [81,94–98]. Šios sistemos generavo nuo 0.5  $\mu\text{J}$  iki 5  $\mu\text{J}$  energijos impulsus, kurių trukmė siekė nuo 160 fs iki 711 fs. Vidutinė lazerinės spinduliuotės galia buvo registruota nuo

0.5 W iki 21 W. Visos šios sistemos buvo paremtos faziškai moduluotų impulsų stiprinimo technologija ir naudojo pakankamai didelės vidutinės galios (dešimčių vatų eilės) daugiamodžius mažo skaičiaus lazerinius diodus šviesolaidinių stiprintuvų kaupinimui. Dėl šios priežasties pademonstruotos sistemos buvo pakankamai sudėtingos, joms trūko kompaktiškumo ir paprastumo, kurių pageidaujama iš šviesolaidinių lazerinių sistemų. Didelės galios kaupinimo diodų panaudojimas FCPA sistemose [81,96–98], kurios spinduliavo tik 0.5 W vidutinės galios lazerinę spinduliuotę, nėra optimalus pasirinkimas. Šioje disertacijoje pristatytame darbe buvo siekiama sukurti kompaktišką femtosekundinį šviesolaidinį lazerį, kuriame būtų panaudoti mažų matmenų didelio skaičiaus vienamodžiai lazeriniai diodai, kurie į šerdį kaupintų vienamodį iterbio jonais legiruatą šviesolaidinį stiprintuvą. Pagrindiniai iššūkiai su kuriais teko susidurti konstruojant tokią lazerinę sistemą, buvo sukaupto netiesinės fazės pokyčio valdymas ir kompensavimas bei fototamsėjimo efekto sumažinimas šviesolaidiniame stiprintuve.

Didelės energijos femtosekundinio šviesolaidinio lazerio realizavimas buvo paremtas sėkmingai pademonstruota šviesolaidine sistema, apžvelgta praeitame skyrelyje. Tam, kad faziškai moduluoti 230 ps trukmės ir 7.8 nJ energijos impulsai, būtų pastiprinti iki mikrodžiaulius siekiančios energijos, impulsų pasikartojimo dažnis buvo sumažintas, panaudojant šviesolaidinį akustooptinį moduliatorių prieš impulsų stiprinimą 11  $\mu\text{m}$  šerdies diametro šviesolaidiniame galios stiprintuve. Šis stiprintuvas buvo kaupinamas 976 nm bangos ilgio, 1.4 W vidutinės galios spinduliuote, kuri buvo gauta poliarizaciniu būdu apjungiant du vienamodžius didelio ryškio lazerinius diodus. Bendras kaupinimo spinduliuotės ryškis siekė  $\sim 3 \text{ MW/cm}^2$ . Maksimali 10  $\mu\text{J}$  impulsų energija buvo pasiekta prie 35 kHz impulsų pasikartojimo dažnio, esant 359 mW išvadinei lazerio galiai.

Didelės smailinės galios impulsams sklindant sąlyginai mažo modos ploto ( $\sim 100 \mu\text{m}^2$ ) šviesolaidiniame stiprintuve, dėl fazės moduliavimosi yra kaupiamas netiesinės fazės pokytis, kuris blogina suspaustų impulsų laikinę kokybę, sąlygojančią smailinio intensyvumo sumažėjimą bei padidėjusią impulso trukmę. Šis efektas turi būti kompensuotas norint pagerinti šiuos suspausto impulso parametrus. Šiame darbe pristatytas dalinis netiesinės fazės pokyčio kompensavimo mechanizmas naudojant antros ir trečios eilės dispersiją, kurią sukelia temperatūros pasiskirstymas išilgai CFBG plėstuvo. Didžiausią įtaką netiesinės fazės kompensavimui turėjo antros eilės dispersijos pokytis. 10  $\mu\text{J}$  impulsų energijos atveju buvo sukauptas  $1.4\pi$  rad netiesinės fazės pokytis, kuris dalinai kompensuotas antros eilės dispersijos

pokyčiu ( $\Delta GDD = 0.077 \text{ ps}^2$ ). Suspaustų impulsų trukmė sumažėjo nuo  $\sim 800 \text{ fs}$  iki  $349 \text{ fs}$  trukmės, taikant šį kompensavimo mechanizmą. Pademonstruotas netiesinės fazės kompensavimas, papildomai įvedant trečios eilės dispersijos pokytį, lygų  $\Delta TOD = 0.0142 \text{ ps}^3$ , sąlygojo papildomą suspausto impulso trukmės sumažėjimą bei laikinio kontrasto pagerėjimą, atitinkamai  $\sim 7\%$  ir  $4\%$ .

Optimaliai suspaustų impulsų kokybė buvo papildomai charakterizuota atliekant FROG matavimus. Atkurto  $10 \mu\text{J}$  energijos impulso trukmė buvo lygi  $349 \text{ fs}$ , o įvertinta spektriškai riboto impulso trukmė buvo lygi  $221 \text{ fs}$ . Pagrindinis suspaustų impulsų kokybės sumažėjimas prie didesnės impulsų energijos buvo siejamas su netiesinės fazės kaupimu mažo modos ploto šviesolaidiniuose stiprintuvuose ir nepilnu jos kompensavimu.

Lazeriniam šaltiniui yra svarbu ne tik užsibrėžti spinduliuotės parametrai, tačiau ir ilgas veikimo laikas ir patikimumas. Fototamsėjimo efektas, riboja šviesolaidinių stiprintuvų, kaupinamų didelio intensyvumo spinduliuote, tarnavimo laiką ir patikimumą. Šio efekto sumažinimas šiame darbe buvo tiriamas tiek skaitiniu, tiek eksperimentiniu būdu. Skaitinis modeliavimas atliktas panaudojant dviejų tipų aktyviaisiais jonais legiruotus šviesolaidžius. Naudojant žemo legiravimo lygio (iterbio jonų koncentracija –  $2 \cdot 10^{25} \text{ m}^{-3}$ )  $6 \mu\text{m}$  šerdies diametro šviesolaidinį stiprintuvą, galima pasiekti norimą išvadinės spinduliuotės galią, tačiau netiesiniai efektai pasireiškia itin stipriai, iškraipydami laikinę suspaustų impulsų gaubtinę. Naudojant aukšto legiravimo lygio (iterbio jonų koncentracija –  $7 \cdot 10^{25} \text{ m}^{-3}$ )  $11 \mu\text{m}$  šerdies diametro šviesolaidinį stiprintuvą stipriai pasireiškė tamsėjimo efektas, tačiau buvo sumažinama netiesinių efektų įtaka. Skaitinio modeliavimo metu, surasta optimali šviesolaidinio stiprintuvo kombinacija, sudaryto iš skirtingomis koncentracijomis iterbio jonais legiruotų šviesolaidžių, kuri sumažino netiesinių efektų įtaką bei tamsėjimo efektą. Šie tyrimo rezultatai buvo patvirtinti eksperimentiškai.

Šiame darbe pademonstruotas sukaupto netiesinės fazės pokyčio dalinis kompensavimas bei fototamsėjimo efekto sumažinimas vienamodžiam šviesolaidiniame stiprintuve leido sukonstruoti stabilaus veikimo didelės energijos femtosekundinę šviesolaidinę lazerinę sistemą. Ši sistema realizuota kompaktiškoje lazerio konfigūracijoje – visa lazerinė sistema, kartu su ją valdančia elektronika ir maitinimo šaltiniais buvo sutalpinta  $45 \times 43.6 \times 13.3 \text{ cm}^3$  matmenų korpuse.

## Didelės vidutinės galios šviesolaidinis lazeris

Skyriuje pateikta medžiaga publikuota A3

Praeitame skyrelyje apžvelgta šviesolaidinė lazerinė sistema generavo didelės ( $10 \mu\text{J}$ ) energijos impulsus, tačiau išvadinė spinduliuotės galia siekė tik kelis šimtus milivatų. Dėl šios priežasties sistemos panaudojimas yra apribotas taikymuose, kurie reikalauja didelės vidutinės lazerinės spinduliuotės galios.

Didelė (dešimčių vatų) spinduliuotės galia šviesolaidiniuose lazeriuose įprastai pasiekama naudojant didelės galios lazerinius kaupinimo diodus bei įvairių dizainų didelio modos ploto dvigubo apvalkalo šviesolaidinius stiprintuvus [16,127,140,141,143,144]. Šiuose stiprintuvuose kaupinimo spinduliuotė yra įvedama į šviesolaidžio apvalkalą, kuriuo sklisdama palaipsniui yra sugerama aktyviaisiais jonais legiruotoje šerdyje. Tuo tarpu impulsų energija, tiesiogiai gaunama iš didelio modos ploto šviesolaidinio stiprintuvo, turi pakankamai aiškia technologinę ribą, susijusią su šviesolaidžio šerdies diametro didinimu bei netiesinių efektų poveikio mažinimu. Taigi, kuriami nauji lazerio veikimo režimai, imituojantys didesnes impulsų energijas, generuojant didelio impulsų pasikartojimo dažnio impulsų paketus [23,24]. Šie režimai gali išplėsti lazerinių sistemų panaudojimo sritis įvairiose mokslo ir pramonės srityse [170]. Šio darbo pagrindinis tikslas buvo sukurti didelės galios šviesolaidinį lazerį, generuojantį didelės energijos ultratrumpuosius impulsus ir impulsų paketus.

Sukonstruota didelės vidutinės galios šviesolaidinė faziškai moduluotų impulsų stiprinimo sistema, naudojanti didelio modos ploto ( $11 \mu\text{m}$  šerdies diametro) į apvalkalą kaupinamą iterbio jonais legiruotą šviesolaidinį stiprintuvą. Šioje sistemoje panaudotas to paties tipo iterbio jonais legiruotas šviesolaidis, kaip praeitame skyrelyje pristatyme lazeryje, tik šiuo atveju daugiamodžio lazerinio diodo kaupinimo spinduliuotė buvo įvedama ne į šviesolaidžio šerdį, o į apvalkalą. Lazeris generavo  $1.5 \mu\text{J}$  energijos pakankamai aukštos laikinės kokybės  $\sim 680$  fs trukmės impulsus. Fazės moduliavimosi sukeltas netiesinės fazės pokytis, buvo pagrindinis veiksnys ribojantis maksimalią impulsų energiją šviesolaidinėje sistemoje. Esant  $4$  MHz impulsų pasikartojimo dažniui buvo pasiekta  $6$  W išvadinė spinduliuotės galia.

Lazerio veikimo režimas buvo išplėstas generuojant gigahercinio impulsų pasikartojimo dažnio impulsų paketus. Taigi, tradicinėje faziškai moduluotų impulsų stiprinimo sistemoje buvo įdiegtas papildomas impulsų dauginimo

modulis, paremtas kaskadine šviesolaidinių daliklių seka, didinančia impulsų pasikartojimo dažnį. Šis daugintuvas leido pasiekti 3.26 GHz impulsų pasikartojimo dažnį, esant pradiniam 50.93 MHz impulsų pasikartojimo dažniui. Pademonstruotos dvi sistemos konfigūracijos skirtos paketų amplitudinės gaubtinės formavimui ir valdymui. Šių metodų pagalba buvo formuojami stačiakampės formos impulsų paketai sistemos išėjime. Itin didelio impulsų pasikartojimo dažnio impulsų paketų stiprinimas FCPA sistemoje buvo pademonstruotas panaudojus du skirtingus šviesolaidinius galios stiprintuvus.

11  $\mu\text{m}$  šerdies diametro stiprintuvo atveju, esant 6 W spinduliuotės vidutinei galiai, pasiekta 30  $\mu\text{J}$  impulsų paketų energija. Taigi, GHz impulsų paketų realizacija leido praplėsti lazerio veikimo režimą bei tokiu būdu padidinti šviesolaidinio lazerio generuojamas impulsų (paketų) energijas nuo 1.5  $\mu\text{J}$  pavienių impulsų režime iki 30  $\mu\text{J}$  impulsų paketų stiprinimo atveju. Vidutinė pavienių impulsų trukmė impulsų pakete buvo apie 640 fs. Paketų plotis buvo valdomas nuo 60 ns iki 500 ns, taip keičiant impulsų kiekį pakete nuo ~200 iki 1600 impulsų. Taigi, 60 ns paketo pločio atveju, pavienių impulsų energija pakete buvo lygi 150 nJ. Ši energija buvo sąlyginai maža, taigi netiesiniai efektai šviesolaidiniame stiprintuve nedarė didelės įtakos suspaustų impulsų laikinei kokybei.

Žymiai didesnė GHz impulsų paketų energija, siekianti net 100  $\mu\text{J}$ , ir daugiau nei 20 W lazerio spinduliuotės vidutinė galia buvo realizuota sistemos konfigūracijoje naudojančioje fotoninių kristalų šviesolaidinį (40  $\mu\text{m}$  šerdies diametro) stiprintuvą.

### **Gigahercinio impulsų pasikartojimo dažnio ultratrumpųjų impulsų paketų sintezavimo metodas**

Skyriuje pateikta medžiaga publikuota A4 bei aprašyta patentinėje paraiškoje P1

Ultratrumpųjų impulsų lazeriniai šaltiniai plačiai naudojami medicinoje, įvairiose mokslinių tyrimų srityse bei pramonėje [171–174]. Lazerinės sistemos, generuojančios gigahercinio impulsų pasikartojimo dažnio impulsų paketus, gali atverti naujas galimybes panaudojus jas medžiagų mikroapdirbimo taikymuose [170,188–191] ar derinamo bangos ilgio lazerinių sistemų kaupinimui [194–197], kurios taikomos įvairių biologinių audinių vaizdinimui. Didelis susidomėjimas tokiomis lazerinėmis sistemomis skatina kurti naujus medotus bei tobulinti lazerines technologijas skirtas GHz impulsų paketų generavimui. Pakankamai daug yra pristatytų

įvairių šviesolaidinių impulsų pasikartojimo dažnio dauginimo technologinių sprendimų [24,184,207–211], kurie gali būti įdiegti šviesolaidinėse faziškai moduluotų impulsų stiprinimo sistemose. Tačiau dauguma jų pasižymi tam tikrais trūkumais, ribojančiais šių metodų ir lazerinių sistemų panaudojimą. Maksimalus realizuojamas impulsų pasikartojimo dažnis, impulsų kiekio valdymas, skirtinga impulsų amplitudė (impulsų energija) ir impulsų trukmė, netolygus impulsų periodas impulsų pakete – pagrindiniai veiksniai, kurie gali netenkinti impulsų paketui keliamų reikalavimų tam tikram taikymui. Šio darbo tikslas buvo naujo šviesolaidinio metodo sukūrimas, kuris leistų įveikti daugelį apribojimų ir būtų pranašesnis prieš kitas šviesolaidines impulsų dauginimo technologijas.

Šio darbo metu buvo sukurtas ir eksperimentiškai realizuotas naujas metodas, paremtas aktyvios šviesolaidinės kilpos panaudojimu, leido sintezuoti itin didelio impulsų pasikartojimo dažnio ( $>2$  GHz) ultratrumpųjų lazerio impulsų paketus, turinčius bet kokią impulsų kiekį pakete, identišką laikinį atstumą tarp impulsų bei reguliuojamą amplitudę. Impulsų paketai, turintys nuo 2 iki maždaug 1000 impulsų, buvo pademonstruoti šiame darbe. Šis metodas leido sintezuoti impulsų paketus, kuriuose impulsų pasikartojimo dažnis gali būti laisvai pasirinktas, nepriklausomai nuo pradinio (užkrato šaltinio generuojamo) impulsų pasikartojimo dažnio. Eksperimentiškai pademonstruotas impulsų paketas, kuriame impulsų pasikartojimo dažnis buvo lygus net 217 GHz. Taigi, šis metodas leido sintezuoti impulsų paketus, kuriuose impulsų pasikartojimo dažnis siekė THz lygį. Tokia, itin didelio impulsų pasikartojimo dažnio, impulsų paketų sintezavimo galimybė parodė šios metodikos lankstumą bei unikalumą. Kituose šviesolaidiniuose metoduose, paremtuose pasyvios šviesolaidinės kilpos panaudojimu, minimalus kilpos ilgis sąlygoja maksimalų impulsų pasikartojimo dažnį, kuris lygus  $\sim 2$  GHz. Taigi, šios savybės parodė naujai sukurtos metodikos lankstumą, patrauklumą bei pranašumą prieš kitas šviesolaidines impulsų dauginimo technologijas.

Aktyvi šviesolaidinė kilpa, kurioje įdiegtas dispersijos kompensavimo mechanizmas, leido sintezuoti ultratrumpuosius impulsų paketus, kuriuose užtikrinta vienoda pavienių impulsų trukmė. Ši aktyvi šviesolaidinė kilpa buvo panaudota šviesolaidinėje faziškai moduluotų impulsų stiprinimo sistemoje demonstruojančioje šios metodikos bei sistemos galimybes. FCPA sistemos išėjime buvo gauti 72 nJ energijos 2.65 GHz impulsų pasikartojimo dažnio impulsų paketai, sudaryti iš 20 impulsų, kurių trukmė buvo lygi 570 fs. Dispersijos kompensavimo mechanizmas buvo sėkmingai įdiegtas, kadangi pavienių impulsų trukmė pakete, buvo artima spektriškai ribotai

impulsų trukmei. Jeigu aktyvioje šviesolaidinėje kilpoje dispersija nebūtų kompensuota, impulsų paketas būtų sudarytas iš impulsų, kurių trukmė kistų nuo 570 fs iki  $\sim 9$  ps.

Šis unikalus impulsų paketų sintezavimo metodas leidžia sėkmingai jį taikyti šviesolaidinėse sistemose bei vystyti naujus lazerinius šaltinius, skirtus lazeriniam medžiagų mikroapdirbimui ir derinamo bangos ilgio lazerinių sistemų kaupinimui.

## Išvados

1. Čirpuotos šviesolaidinės Brego gardelės impulsų plėstuvo ir čirpuotos tūrinės Brego gardelės impulsų spaustuvo su suderintais dispersijos profiliais panaudojimas šviesolaidinėje faziškai moduluotų impulsų stiprinimo sistemoje leido generuoti 208 fs trukmės ultratrumpuosius lazerio impulsus esant dideliame impulsų plėtimo ir spaudimo santykiui siekiamam net  $\sim 1100$  kartų. Didesnis nei 90% impulsų kontrastas, apibrėžtas pagrindinio impulso ir šalutinių impulsų energijos santykiu, gali būti pasiektas ir ribojamas tik liekamųjų čirpuotos šviesolaidinės Brego gardelės grupinio vėlinimo netolygumų, kuriuos lemia nepakankamas gamybos tikslumas.
2. Ultratrumpieji 349 fs trukmės lazerio impulsai, kurių energija –  $10 \mu\text{J}$  ir 26 MW smailinis intensyvumas, gali būti generuojami kompaktiškoje faziškai moduluotų impulsų stiprinimo sistemoje, nepaisant sukaupto didelio  $1.4\pi$  rad netiesinės fazės pokyčio, kuris yra dalinai kompensuojamas teigiamos antros eilės dispersijos pokyčiu, sukuriant tiesinį temperatūros pasiskirstymą išilgai CFBG plėstuvo. Šį rezultatą galima pagerinti taikant netiesinį temperatūros gradientą išilgai CFBG. Skaitinio modeliavimo ir eksperimentinių tyrimų rezultatai įrodė, jog tinkamas dviejų šviesolaidžių, kurie skiriasi iterbio jonų legiravimo laipsniu ir ilgiu, pasirinkimas leidžia sumažinti fototamsėjimo efektą, pasireiškiantį vienamodžiam šviesolaidiniame stiprintuve.
3. Impulsų pasikartojimo dažnio daugintuvas, paremtas kaskadiniu šviesolaidinių daliklių panaudojimu, impulsų paketų amplitudinės gaubtinės formavimas ir valdymas, naudojant akustooptinius moduliatorius, leido praplėsti lazerio veikimo režimus. Šios metodikos įgyvendinimas FCPA sistemoje, naudojančioje didelio modos ploto ( $11 \mu\text{m}$  šerdies diametro) į apvaskalą kaupinamą iterbio jonais

legiruotą šviesolaidinį stiprintuvą leido padidinti šviesolaidinio lazerio generuojamas impulsų (paketų) energijas nuo 1.5  $\mu\text{J}$  pavienių impulsų režime iki 30  $\mu\text{J}$  impulsų paketų stiprinimo atveju. Ši metodika pasižymėjo keletu trūkumų. Pirmiausia, minimalų (20 ns) impulsų paketo plotį ribojo akustoptinio modulatoriaus atsidarymo ir užsidarymo laikas. Šviesolaidinių daliklių dalinimo santykio neatitikimas sąlygojo pakankamai didelį impulsų amplitudės kitimą impulsų pakete. Taip pat, kontroliuojant kiekvienos pakopos šviesolaidinių vėlinimo linijų ilgį, identiškas impulsų periodo realizavimas impulsų pakete buvo sunkiai pasiekiamas. Nepaisant to, šviesolaidinė lazerinė sistema, generuojanti 3.26 GHz pasikartojimo dažnio ultratrumpųjų (640 fs) impulsų paketus, buvo sėkmingai pademonstruota. Pristatytas šviesolaidinis metodas bei lazerinė sistema yra tinkami lazeriniam medžiagų apdirbimui, kuris nėra labai jautrus impulsų energijos pokyčiams (didesniems nei 10%) GHz impulsų pakete.

4. Naujas metodas, paremtas aktyvios šviesolaidinės kilpos panaudojimu, leidžia sintezuoti itin didelio impulsų pasikartojimo dažnio ultratrumpųjų lazerio impulsų paketus, turinčius bet kokią impulsų kiekį pakete, identišką laikiną atstumą tarp impulsų bei reguliuojamą amplitudę. Eksperimentiškai realizuota FCPA sistema generavo ultratrumpųjų (570 fs) impulsų paketus, kuriuose impulsų pasikartojimo dažnis siekė 2.65 GHz ir 217 GHz. Sukurtas metodas yra pranašesnis prieš kitus šviesolaidinius impulsų pasikartojimo dažnio dauginimo metodus, kadangi impulsų pasikartojimo dažnį galima laisvai pasirinkti, nepriklausomai nuo pradinio, užkrato šaltinio generuojamo, impulsų pasikartojimo dažnio. Mažos dispersijos CFBG panaudojimas aktyvioje šviesolaidinėje kilpoje leidžia kompensuoti šviesolaidžio chromatinę dispersiją, tam kad būtų pasiekti panašios trukmės impulsai GHz impulsų pakete.

## CURRICULUM VITAE

### **About the author**

Tadas Bartulevičius was born in 1991 in Alytus, Lithuania. In 2010 he graduated from Likiskeliu secondary school in Alytus. In 2014 he received his bachelor degree in Physics at Faculty of Physics, Vilnius University. In 2016 he received his master degree in Laser Physics and Optical Technologies at Faculty of Physics, Vilnius University. In 2016 he started doctoral studies in Center for Physical Sciences and Technology. From 2014 he has been working as an engineer in the department of Research and Development of the laser manufacturing company UAB Ekspla.

### **Apie autorių**

Tadas Bartulevičius gimė 1991 metais Alytuje. 2010 metais baigė Alytaus Likiškėlių vidurinę mokyklą. 2014 metais baigė Fizikos bakalauro studijų programą Vilniaus universiteto Fizikos fakultete. 2016 metais baigė Lazerinės fizikos ir optinių technologijų magistro studijų programą Vilniaus universiteto Fizikos fakultete. 2016 metais buvo priimtas į doktorantūros studijas Fizinių ir technologijos mokslų centre. Nuo 2014 metų dirba inžinieriumi lazerių gamybos įmonėje UAB „Ekspla“ naujų produktų kūrimo skyriuje.

## BIBLIOGRAPHY

- [1] F. Beier, C. Hupel, S. Kuhn, S. Hein, J. Nold, F. Proske, B. Sattler, A. Liem, C. Jauregui, J. Limpert, N. Haarlammert, T. Schreiber, R. Eberhardt, and A. Tünnermann, "Single mode 4.3 kW output power from a diode-pumped Yb-doped fiber amplifier," *Opt. Express* **25**, 14892–14899 (2017).
- [2] V. Gapontsev, V. Fomin, E. Scherbakov, A. Ovtchinnikov, A. Ferin, and A. Abramov, "High power high efficiency fiber laser and method for optimizing wall plug efficiency thereof," U.S. patent US10615570B2 (2020).
- [3] V. Gapontsev, E. Shcherbakov, V. Fomin, A. Abramov, M. Abramov, A. Ferin, V. Mironov, and A. Doronkin, "Multi-kilowatt CW fiber laser systems with record wall-plug efficiency exceeding 50%," in *17th International Conference of Laser Optics* (2016).
- [4] A. Kratky, D. Schuöcker, and G. Liedl, "Processing with kW fibre lasers: advantages and limits," *Proc. SPIE* **7131**, 71311X (2009).
- [5] T. Westphäling, "Pulsed fiber lasers from ns to ms range and their applications," *Phys. Procedia* **5**, 125–136 (2010).
- [6] J. Lee, K. Lee, S. Lee, S. W. Kim, and Y. J. Kim, "High precision laser ranging by time-of-flight measurement of femtosecond pulses," *Meas. Sci. Technol.* **23**, 065203 (2012).
- [7] W. S. Capinski and H. J. Maris, "Improved apparatus for picosecond pump-and-probe optical measurements," *Rev. Sci. Instrum.* **67**, 2720–2726 (1996).
- [8] Á. Krolopp, A. Csákányi, D. Haluszka, D. Csáti, L. Vass, A. Kolonics, N. Wikonkál, and R. Szipőcs, "Handheld nonlinear microscope system comprising a 2 MHz repetition rate, mode-locked Yb-fiber laser for in vivo biomedical imaging," *Biomed. Opt. Express* **7**, 3531–3542 (2016).
- [9] S. Tang, J. Liu, T. B. Krasieva, Z. Chen, and B. J. Tromberg, "Developing compact multiphoton systems using femtosecond fiber lasers," *J. Biomed. Opt.* **14**, 030508 (2009).
- [10] G. Matthäus, T. Schreiber, J. Limpert, S. Nolte, G. Torosyan, R. Beigang, S. Riehemann, G. Notni, and A. Tünnermann, "Surface-emitted THz generation using a compact ultrashort pulse fiber amplifier at 1060 nm," *Opt. Commun.* **261**, 114–117 (2006).
- [11] L. Shah, M. E. Fermann, J. W. Dawson, and C. P. J. Barty, "Micromachining with a 50 W, 50  $\mu$ J, subpicosecond fiber laser

- system," *Opt. Express* **14**, 12546–12551 (2006).
- [12] R. Berera, R. van Grondelle, and J. T. M. Kennis, "Ultrafast transient absorption spectroscopy: Principles and application to photosynthetic systems," *Photosynth. Res.* **101**, 105–118 (2009).
- [13] K.-H. Liao, A. G. Mordovanakis, B. Hou, G. Chang, M. Rever, G. A. Mourou, J. Nees, and A. Galvanauskas, "Generation of hard X-rays using an ultrafast fiber laser system," *Opt. Express* **15**, 13942–13948 (2007).
- [14] F. Köttig, F. Tani, C. M. Biersach, J. C. Travers, and P. S. J. Russell, "Generation of microjoule pulses in the deep ultraviolet at megahertz repetition rates," *Optica* **4**, 1272–1276 (2017).
- [15] A. Alismail, H. Wang, N. Altwaijry, and H. Fattahi, "Carrier-envelope phase stable, 5.4  $\mu$ J, broadband, mid-infrared pulse generation from a 1-ps, Yb:YAG thin-disk laser," *Appl. Opt.* **56**, 4990–4994 (2017).
- [16] J. M. Fini, "Design of solid and microstructure fibers for suppression of higher-order modes," *Opt. Express* **13**, 3477–3490 (2005).
- [17] Z. Liu, P. Zhou, X. Xu, X. Wang, and Y. Ma, "Coherent beam combining of high power fiber lasers: Progress and prospect," *Sci. China Technol. Sci.* **56**, 1597–1606 (2013).
- [18] D. Strickland and G. Mourou, "Compression of amplified chirped optical pulses," *Opt. Commun.* **56**, 219–221 (1985).
- [19] F. Röser, T. Eidam, J. Rothhardt, O. Schmidt, D. N. Schimpf, J. Limpert, and A. Tünnermann, "Millijoule pulse energy high repetition rate femtosecond fiber chirped-pulse amplification system," *Opt. Lett.* **32**, 3495–3497 (2007).
- [20] M. Müller, C. Aleshire, A. Klenke, E. Haddad, F. Légaré, A. Tünnermann, and J. Limpert, "10.4 kW coherently combined ultrafast fiber laser," *Opt. Lett.* **45**, 3083–3086 (2020).
- [21] W. Leemans, "White paper of the ICFA ICUIL joint task force - high power laser technology for accelerators," *ICFA beam Dyn. newsletters* **56**, 10–88 (2011).
- [22] G. Mourou, B. Brocklesby, T. Tajima, and J. Limpert, "The future is fibre accelerators," *Nat. Photonics* **7**, 258–261 (2013).
- [23] H. Kalaycıoğlu, Ö. Akçaalan, S. Yavaş, Y. B. Eldeniz, and F. Ö. Ilday, "Burst-mode Yb-doped fiber amplifier system optimized for low-repetition-rate operation," *J. Opt. Soc. Am. B* **32**, 900–906 (2015).

- [24] C. Kerse, H. Kalaycıođlu, P. Elahi, Ö. Akçaalan, and F. Ö. Ilday, "3.5-GHz intra-burst repetition rate ultrafast Yb-doped fiber laser," *Opt. Commun.* **366**, 404–409 (2016).
- [25] O. Katz and Y. Sintov, "Strictly all-fiber picosecond ytterbium fiber laser utilizing chirped-fiber-Bragg-gratings for dispersion control," *Opt. Commun.* **281**, 2874–2878 (2008).
- [26] I. N. Duling, "All-fiber ring soliton laser mode locked with a nonlinear mirror," *Opt. Lett.* **16**, 539–541 (1991).
- [27] K. Regelskis, J. Želudevičius, K. Viskontas, and G. Račiukaitis, "Ytterbium-doped fiber ultrashort pulse generator based on self-phase modulation and alternating spectral filtering," *Opt. Lett.* **40**, 5255–5258 (2015).
- [28] Z. Liu, Z. M. Ziegler, L. G. Wright, and F. W. Wise, "Megawatt peak power from a Mamyshev oscillator," *Optica* **4**, 649–654 (2017).
- [29] V. J. Matsas, T. P. Newson, D. J. Richardson, and D. N. Payne, "Selfstarting passively mode-locked fibre ring soliton laser exploiting nonlinear polarisation rotation," *Electron. Lett.* **28**, 1391–1393 (1992).
- [30] P. Bowen, H. Singh, A. Runge, R. Provo, and N. G. R. Broderick, "Mode-locked femtosecond all-normal all-PM Yb-doped fiber laser at 1060 nm," *Opt. Commun.* **364**, 181–184 (2016).
- [31] J. Szczepanek, T. M. Kardaś, C. Radzewicz, and Y. Stepanenko, "Ultrafast laser mode-locked using nonlinear polarization evolution in polarization maintaining fibers," *Opt. Lett.* **42**, 575–578 (2017).
- [32] J. Szczepanek, T. M. Kardaś, C. Radzewicz, and Y. Stepanenko, "Nonlinear polarization evolution of ultrashort pulses in polarization maintaining fibers," *Opt. Express* **26**, 13590–13604 (2018).
- [33] P. V. Mamyshev, "All-optical data regeneration based on self-phase modulation effect," in *24th European Conference on Optical Communication (ECOC '98)* (1998).
- [34] W. Fu, L. G. Wright, P. Sidorenko, S. Backus, and F. W. Wise, "Several new directions for ultrafast fiber lasers [Invited]," *Opt. Express* **26**, 9432–9463 (2018).
- [35] W. Liu, R. Liao, J. Zhao, J. Cui, Y. Song, C. Wang, and M. Hu, "Femtosecond Mamyshev oscillator with 10-MW-level peak power," *Optica* **6**, 194–197 (2019).
- [36] I. Samartsev, A. Bordenyuk, and V. Gapontsev, "Environmentally stable seed source for high power ultrafast laser," *Proc. SPIE* **10085**, 100850S (2017).

- [37] V. Boulanger, M. Olivier, F. Guilbert-Savary, F. Trépanier, M. Bernier, and M. Piché, "All-fiber Mamyshev oscillator enabled by chirped fiber Bragg gratings," *Opt. Lett.* **45**, 3317–3320 (2020).
- [38] P. Sidorenko, W. Fu, L. G. Wright, M. Olivier, and F. W. Wise, "Self-seeded, multi-megawatt, Mamyshev oscillator," *Opt. Lett.* **43**, 2672–2675 (2018).
- [39] S. Y. Set, H. Yaguchi, Y. Tanaka, and M. Jablonski, "Laser mode locking using a saturable absorber incorporating carbon nanotubes," *J. Light. Technol.* **22**, 51–56 (2004).
- [40] Q. Bao, H. Zhang, Y. Wang, Z. Ni, Y. Yan, Z. X. Shen, K. P. Loh, and D. Y. Tang, "Atomic-layer graphene as a saturable absorber for ultrafast pulsed lasers," *Adv. Funct. Mater.* **19**, 3077–3083 (2009).
- [41] S. Hong, F. Lédée, J. Park, S. Song, H. Lee, Y. S. Lee, B. Kim, D. Il Yeom, E. Deleporte, and K. Oh, "Mode-locking of all-fiber lasers operating at both anomalous and normal dispersion regimes in the C- and L-bands using thin film of 2D perovskite crystallites," *Laser Photonics Rev.* **12**, 1800118 (2018).
- [42] R. I. Woodward and E. J. R. Kelleher, "2D saturable absorbers for fibre lasers," *Appl. Sci.* **5**, 1440–1456 (2015).
- [43] W. Liu, L. Pang, H. Han, W. Tian, H. Chen, M. Lei, P. Yan, and Z. Wei, "70-fs mode-locked erbium-doped fiber laser with topological insulator," *Sci. Rep.* **6**, 19997 (2016).
- [44] U. Keller, K. J. Weingarten, F. X. Kärtner, D. Kopf, B. Braun, I. D. Jung, R. Fluck, C. Hönninger, N. Matuschek, and J. Aus Der Au, "Semiconductor saturable absorber mirrors (SESAM's) for femtosecond to nanosecond pulse generation in solid-state lasers," *IEEE J. Sel. Top. Quantum Electron.* **2**, 435–453 (1996).
- [45] O. Okhotnikov, A. Grudinin, and M. Pessa, "Ultra-fast fibre laser systems based on SESAM technology: New horizons and applications," *New J. Phys.* **6**, 177 (2004).
- [46] K. Viskontas, K. Regelskis, and N. Rusteika, "Slow and fast optical degradation of the SESAM for fiber laser mode-locking at 1  $\mu\text{m}$ ," *Lith. J. Phys.* **54**, 127–135 (2014).
- [47] A. Chong, J. R. Buckley, W. H. Renninger, and F. W. Wise, "All-normal-dispersion femtosecond fiber laser," *Opt. Express* **14**, 10095–10100 (2006).
- [48] M. Baumgartl, C. Lecaplain, A. Hideur, J. Limpert, and A. Tünnermann, "66 W average power from a microjoule-class sub-100 fs fiber oscillator," *Opt. Lett.* **37**, 1640–1642 (2012).

- [49] K. Özgören and F. Ö. Ilday, "All-fiber all-normal dispersion laser with an in-fiber Lyot filter," *Opt. Lett.* **35**, 1296–1298 (2010).
- [50] J.-B. Lecourt, C. Duterte, F. Narbonne, D. Kinet, Y. Hernandez, and D. Giannone, "All-normal dispersion, all-fibered PM laser mode-locked by SESAM," *Opt. Express* **20**, 11918–11923 (2012).
- [51] F. Ö. Ilday, J. R. Buckley, W. G. Clark, and F. W. Wise, "Self-similar evolution of parabolic pulses in a laser," *Phys. Rev. Lett.* **92**, 213902 (2004).
- [52] C. K. Nielsen, B. Ortac, T. Schreiber, J. Limpert, R. Hohmuth, W. Richter, and A. Tünnermann, "Self-starting self-similar all-polarization maintaining Yb-doped fiber laser," *Opt. Express* **13**, 9346–9351 (2005).
- [53] D. N. Papadopoulos, Y. Zaouter, M. Hanna, F. Druon, E. Mottay, E. Cormier, and P. Georges, "Generation of 63 fs 41 MW peak power pulses from a parabolic fiber amplifier operated beyond the gain bandwidth limit," *Opt. Lett.* **32**, 2520–2522 (2007).
- [54] M. E. Fermann, V. I. Kruglov, B. C. Thomsen, J. M. Dudley, and J. D. Harvey, "Self-similar propagation and amplification of parabolic pulses in optical fibers," *Phys. Rev. Lett.* **84**, 6010–6013 (2000).
- [55] H. Lim, F. Ö. Ilday, and F. W. Wise, "Generation of 2-nJ pulses from a femtosecond ytterbium fiber laser," *Opt. Lett.* **28**, 660–662 (2003).
- [56] X. Zhou, D. Yoshitomi, Y. Kobayashi, and K. Torizuka, "Generation of 28-fs pulses from a mode-locked ytterbium fiber oscillator," *Opt. Express* **16**, 7055–7059 (2008).
- [57] C. K. Nielsen, K. G. Jespersen, and S. R. Keiding, "A 158 fs 5.3 nJ fiber-laser system at 1  $\mu\text{m}$  using photonic bandgap fibers for dispersion control and pulse compression," *Opt. Express* **14**, 6063–6068 (2006).
- [58] O. Katz, Y. Sintov, Y. Nafcha, and Y. Glick, "Passively mode-locked ytterbium fiber laser utilizing chirped-fiber-Bragg-gratings for dispersion control," *Opt. Commun.* **269**, 156–165 (2007).
- [59] W. J. Tomlinson, R. H. Stolen, and C. V. Shank, "Compression of optical pulses chirped by self-phase modulation in fibers," *J. Opt. Soc. Am. B* **1**, 139–149 (1984).
- [60] M. D. Perry, T. Ditmire, and B. C. Stuart, "Self-phase modulation in chirped-pulse amplification," *Opt. Lett.* **19**, 2149–2151 (1994).
- [61] A. E. Siegman, *Lasers*, revised ed (University Science Books, 1986).
- [62] S. Frankinas, T. Bartulevicius, A. Michailovas, and N. Rusteika,

- "Investigation of all-in-fiber Yb doped femtosecond fiber oscillator for generation of parabolic pulses in normal dispersion fiber amplifier," *Opt. Fiber Technol.* **36**, 366–369 (2017).
- [63] D. N. Schimpf, J. Limpert, and A. Tünnermann, "Controlling the influence of SPM in fiber-based chirped-pulse amplification systems by using an actively shaped parabolic spectrum," *Opt. Express* **15**, 16945–16953 (2007).
- [64] R. Banici and D. Ursescu, "Spectral combination of ultrashort laser pulses," *Europhys. Lett.* **94**, 44002 (2011).
- [65] W. Z. Chang, T. Zhou, L. A. Siiman, and A. Galvanauskas, "Femtosecond pulse spectral synthesis using coherently combined multi-channel fiber chirped pulse amplifiers," *Opt. Express* **21**, 3897–3910 (2013).
- [66] K. Michailovas, A. Baltuska, A. Pugzlys, V. Smilgevicius, A. Michailovas, A. Zaukevicius, R. Danilevicius, S. Frankinas, and N. Rusteika, "Combined Yb/Nd driver for optical parametric chirped pulse amplifiers," *Opt. Express* **24**, 22261–22271 (2016).
- [67] E. B. Treacy, "Optical pulse compression with diffraction gratings," *IEEE J. Quantum Electron.* **5**, 454–458 (1969).
- [68] O. E. Martinez, J. P. Gordon, and R. L. Fork, "Negative group-velocity dispersion using refraction," *J. Opt. Soc. Am. A* **1**, 1003–1006 (1984).
- [69] B. Webb, M. J. Guardalben, C. Dorrer, S. Bucht, and J. Bromage, "Simulation of grating-compressor misalignment tolerances and mitigation strategies for chirped-pulse-amplification systems of varying bandwidth and beam size," *Appl. Opt.* **58**, 234–243 (2019).
- [70] J. Limpert, T. Clausnitzer, A. Liem, T. Schreiber, H.-J. Fuchs, H. Zellmer, E.-B. Kley, and A. Tünnermann, "High-average-power femtosecond fiber chirped-pulse amplification system," *Opt. Lett.* **28**, 1984–1986 (2003).
- [71] J. Limpert, T. Schreiber, S. H. Nolte, A. Zellmer, and A. Tünnermann, "All fiber chirped-pulse amplification system based on compression in air-guiding photonic bandgap fiber," *Opt. Express* **11**, 3332–3337 (2003).
- [72] G. Imeshev, I. Hartl, and M. E. Fermann, "Chirped pulse amplification with a nonlinearly chirped fiber Bragg grating matched to the Treacy compressor," *Opt. Lett.* **29**, 679–681 (2004).
- [73] A. Galvanauskas, A. Heaney, I. Erdogan, and D. Harter, "Use of volume chirped Bragg gratings for compact high-energy chirped

- pulse amplification circuits," in *Conference on Lasers and Electro-Optics* (1998), Vol. 6, p. 362.
- [74] A. Galvanauskas and M. Fermann, "Optical pulse amplification using chirped Bragg grating," U.S. patent 5,499,143 (1996).
  - [75] K.-H. Liao, M.-Y. Cheng, E. Flecher, V. I. Smirnov, L. B. Glebov, and A. Galvanauskas, "Large-aperture chirped volume Bragg grating based fiber CPA system," *Opt. Express* **15**, 4876–4882 (2007).
  - [76] L. Glebov, V. Smirnov, E. Rotari, I. Cohanoschi, L. Glebova, O. Smolski, J. Lumeau, C. Lantigua, and A. Glebov, "Volume-chirped Bragg gratings: monolithic components for stretching and compression of ultrashort laser pulses," *Opt. Eng.* **53**, 051514 (2014).
  - [77] G. Chang, M. Rever, V. Smirnov, L. Glebov, and A. Galvanauskas, "Femtosecond Yb-fiber chirped-pulse-amplification system based on chirped-volume Bragg gratings," *Opt. Lett.* **34**, 2952–2954 (2009).
  - [78] R. Sun, D. Jin, F. Tan, S. Wei, C. Hong, J. Xu, J. Liu, and P. Wang, "High-power all-fiber femtosecond chirped pulse amplification based on dispersive wave and chirped-volume Bragg grating," *Opt. Express* **24**, 22806–22812 (2016).
  - [79] G. Sobon, K. Krzempek, J. Taka, and J. Sotor, "Compact, all-PM fiber-CPA system based on a chirped volume Bragg grating," *Laser Phys.* **26**, 015106 (2016).
  - [80] R. A. Sims, P. Kadwani, H. Ebendorff-Heideprems, L. Shah, T. M. Monro, and M. Richardson, "Chirped pulse amplification in single mode Tm: fiber using a chirped Bragg grating," *Appl. Phys. B Lasers Opt.* **111**, 299–304 (2013).
  - [81] H. Hoogland and R. Holzwarth, "Compact polarization-maintaining 2.05- $\mu\text{m}$  fiber laser at 1-MHz and 1-MW peak power," *Opt. Lett.* **40**, 3520–3523 (2015).
  - [82] D. Sanchez, J. Biegert, G. Matras, and C. Simon-Boisson, "High energy high repetition rate compact picosecond Holmium YLF laser for mid-IR OPCPA pumping," *Proc. SPIE* **10082**, 100820N (2017).
  - [83] S. Frankinas, A. Michailovas, N. Rusteika, V. Smirnov, R. Vasilieu, and A. L. Glebov, "Efficient ultrafast fiber laser using chirped fiber Bragg grating and chirped volume Bragg grating stretcher/compressor configuration," *Proc. SPIE* **9730**, 973017 (2016).
  - [84] A. Yusim, I. Samartsev, O. Shkurikhin, D. Myasnikov, A. Bordenyuk, N. Platonov, V. Kancharla, and V. Gapontsev, "New generation of high average power industry grade ultrafast ytterbium

- fiber lasers," Proc. SPIE **9728**, 972839 (2016).
- [85] M. J. F. Digonnet, *Rare-Earth-Doped Fiber Lasers and Amplifiers, Second Edition, Revised and Expanded* (Marcel Dekker, Inc., 2001).
- [86] B. Stuart, M. Feit, S. Herman, A. Rubenchik, B. Shore, and M. Perry, "Nanosecond-to-femtosecond laser-induced breakdown in dielectrics," Phys. Rev. B **53**, 1749–1761 (1996).
- [87] A. Galvanauskas, D. J. Harter, M. E. Fermann, and F. Raksi, "Microchip-Yb fiber hybrid optical amplifier for micro-machining and marking," U.S. patent 7,492,508 B2 (2009).
- [88] J. Squier and M. Müller, "High resolution nonlinear microscopy: A review of sources and methods for achieving optimal imaging," Rev. Sci. Instrum. **72**, 2855–2867 (2001).
- [89] C. Xu and F. W. Wise, "Recent advances in fiber lasers for nonlinear microscopy," Nat. Photonics **7**, 875–882 (2013).
- [90] C. Macias-Romero, M. E. P. Didier, P. Jourdain, P. Marquet, P. Magistretti, O. B. Tarun, V. Zubkovs, A. Radenovic, and S. Roke, "High throughput second harmonic imaging for label-free biological applications," Opt. Express **22**, 31102–31112 (2014).
- [91] C. Macias-Romero, V. Zubkovs, S. Wang, and S. Roke, "Wide-field medium-repetition-rate multiphoton microscopy reduces photodamage of living cells," Biomed. Opt. Express **7**, 1458–1467 (2016).
- [92] T. V. Andersen, O. Schmidt, J. Limpert, C. Aguergaray, E. Cormier, and A. Tünnermann, "High repetition rate tunable femtosecond pulses from fiber laser pumped parametric amplifier," Opt. Express **14**, 4765–4773 (2006).
- [93] L. Veselis, T. Bartulevicius, K. Madeikis, A. Michailovas, and N. Rusteika, "Compact 20 W femtosecond laser system based on fiber laser seeder, Yb:YAG rod amplifier and chirped volume Bragg grating compressor," Opt. Express **26**, 31873–31879 (2018).
- [94] T. Schreiber, C. K. Nielsen, B. Ortac, J. Limpert, and A. Tünnermann, "Microjoule-level all-polarization-maintaining femtosecond fiber source," Opt. Lett. **31**, 574–576 (2006).
- [95] B. Ortac, M. Baumgartl, J. Limpert, and A. Tünnermann, "Approaching microjoule-level pulse energy with mode-locked femtosecond fiber lasers," Opt. Lett. **34**, 1585–1587 (2009).
- [96] A. Fernández, K. Jespersen, L. Zhu, L. Grüner-Nielsen, A. Baltuška, A. Galvanauskas, and A. J. Verhoef, "High-fidelity, 160 fs, 5  $\mu$ J pulses from an integrated Yb-fiber laser system with a fiber stretcher

- matching a simple grating compressor," *Opt. Lett.* **37**, 927–929 (2012).
- [97] S. Pavlova, H. Rezaei, I. Pavlov, H. Kalaycıoğlu, and F. Ö. Ilday, "Generation of 2- $\mu$ J 410-fs pulses from a single-mode chirped-pulse fiber laser operating at 1550 nm," *Appl. Phys. B* **124**, 201 (2018).
- [98] F. Morin, F. Druon, M. Hanna, and P. Georges, "Microjoule femtosecond fiber laser at 1.6  $\mu$ m for corneal surgery applications," *Opt. Lett.* **34**, 1991–1993 (2009).
- [99] D. Schimpf, E. Seise, J. Limpert, and A. Tünnermann, "Self-phase modulation compensated by positive dispersion in chirped-pulse systems," *Opt. Express* **17**, 4997–5007 (2009).
- [100] A. Chong, L. Kuznetsova, and F. W. Wise, "Theoretical optimization of nonlinear chirped-pulse fiber amplifiers," *J. Opt. Soc. Am. B* **24**, 1815–1823 (2007).
- [101] S. Zhou, L. Kuznetsova, A. Chong, and F. W. Wise, "Compensation of nonlinear phase shifts with third-order dispersion in short-pulse fiber amplifiers," *Opt. Express* **13**, 4869–4877 (2005).
- [102] L. Kuznetsova and F. W. Wise, "Scaling of femtosecond Yb-doped fiber amplifiers to tens of microjoule pulse energy via nonlinear chirped pulse amplification," *Opt. Lett.* **32**, 2671–2673 (2007).
- [103] L. Shah, Z. Liu, I. Hartl, G. Imeshev, G. C. Cho, and M. E. Fermann, "High energy femtosecond Yb cubicon fiber amplifier," *Opt. Express* **13**, 4717–4722 (2005).
- [104] H. Song, B. Liu, L. Wen, C. Wang, and M. Hu, "Optimization of nonlinear compensation in a high-energy femtosecond fiber CPA system by negative TOD fiber," *IEEE Photonics J.* **9**, 3200110 (2017).
- [105] J. Želudevičius, R. Danilevičius, and K. Regelskis, "Optimization of pulse compression in a fiber chirped pulse amplification system by adjusting dispersion parameters of a temperature-tuned chirped fiber Bragg grating stretcher," *J. Opt. Soc. Am. B* **32**, 812–817 (2015).
- [106] F. He, H. S. S. Hung, J. H. V. Price, N. K. Daga, N. Naz, J. Prawiharjo, D. C. Hanna, D. P. Shepherd, D. J. Richardson, J. W. Dawson, C. W. Siders, and C. P. J. Barty, "High energy femtosecond fiber chirped pulse amplification system with adaptive phase control," *Opt. Express* **16**, 5813–5821 (2008).
- [107] J. Prawiharjo, N. K. Daga, R. Geng, J. H. V. Price, D. C. Hanna, D. J. Richardson, and D. P. Shepherd, "High fidelity femtosecond pulses from an ultrafast fiber laser system via adaptive amplitude and phase

- pre-shaping," *Opt. Express* **16**, 15074–15089 (2008).
- [108] F. Verluise, V. Laude, Z. Cheng, C. Spielmann, and P. Tournois, "Amplitude and phase control of ultrashort pulses by use of an acousto-optic programmable dispersive filter: pulse compression and shaping," *Opt. Lett.* **25**, 575–577 (2000).
- [109] D. Schimpf, E. Seise, J. Limpert, and A. Tünnermann, "Decrease of pulse-contrast in nonlinear chirped-pulse amplification systems due to high-frequency spectral phase ripples," *Opt. Express* **16**, 8876–8886 (2008).
- [110] D. N. Schimpf, E. Seise, J. Limpert, and A. Tünnermann, "The impact of spectral modulations on the contrast of pulses of nonlinear chirped-pulse amplification systems," *Opt. Express* **16**, 10664–10674 (2008).
- [111] C. Dorrer and J. Bromage, "Impact of high-frequency spectral phase modulation on the temporal profile of short optical pulses," *Opt. Express* **16**, 3058–3068 (2008).
- [112] J. Limpert, F. Röser, D. N. Schimpf, E. Seise, T. Eidam, S. Hädrich, J. Rothhardt, C. J. Mias, and A. Tünnermann, "High repetition rate gigawatt peak power fiber laser systems: Challenges, design, and experiment," *IEEE J. Sel. Top. Quantum Electron.* **15**, 159–169 (2009).
- [113] J. Buldt, M. Mueller, R. Klas, T. Eidam, J. Limpert, and A. Tünnermann, "Temporal contrast enhancement of energetic laser pulses by filtered self-phase-modulation-broadened spectra," *Opt. Lett.* **42**, 3761–3764 (2017).
- [114] S. Jetschke, S. Unger, U. Röpke, and J. Kirchhof, "Photodarkening in Yb doped fibers: experimental evidence of equilibrium states depending on the pump power," *Opt. Express* **15**, 14838–14843 (2007).
- [115] M. Hotoleanu, J. Koponen, T. Kokki, and M. Laurila, "Experimental verification of spatial distribution of photodarkening in large mode area ytterbium doped fibers," in *Conference on Lasers and Electro-Optics/Quantum Electronics and Laser Science Conference and Photonic Applications Systems Technologies* (2008).
- [116] M. N. Zervas, F. Ghiringhelli, M. K. Durkin, and I. Crowe, "Distribution of photodarkening-induced loss in Yb-doped fiber amplifiers," *Proc. SPIE* **7914**, 79140L (2011).
- [117] S. Jetschke, S. Unger, A. Schwuchow, M. Leich, and J. Kirchhof, "Efficient Yb laser fibers with low photodarkening by optimization of

- the core composition," *Opt. Express* **16**, 15540–15545 (2008).
- [118] S. Jetschke, S. Unger, M. Leich, and J. Kirchhof, "Photodarkening kinetics as a function of Yb concentration and the role of Al codoping," *Appl. Opt.* **51**, 7758–7764 (2012).
- [119] M. Engholm, P. Jelger, F. Laurell, and L. Norin, "Improved photodarkening resistivity in ytterbium-doped fiber lasers by cerium codoping," *Opt. Lett.* **34**, 1285–1287 (2009).
- [120] N. Zhao, Y. Liu, M. Li, J. Li, J. Peng, L. Yang, N. Dai, H. Li, and J. Li, "Mitigation of photodarkening effect in Yb-doped fiber through Na<sup>+</sup> ions doping," *Opt. Express* **25**, 18191–18196 (2017).
- [121] B. Morasse, S. Chatigny, É. Gagnon, C. Hovington, J.-P. Martin, and J.-P. de Sandro, "Low photodarkening single cladding ytterbium fibre amplifier," *Proc. SPIE* **6453**, 64530H (2007).
- [122] I. Manek-Höninger, J. Boulet, T. Cardinal, F. Guillen, S. Ermeneux, M. Podgorski, R. Bello Doua, and F. Salin, "Photodarkening and photobleaching of an ytterbium-doped silica double-clad LMA fiber," *Opt. Express* **15**, 1606–1611 (2007).
- [123] J. Jasapara, M. Andrejco, D. DiGiovanni, and R. Windeler, "Effect of heat and H<sub>2</sub> gas on the photo-darkening of Yb<sup>3+</sup> fibers," in *Conference on Lasers and Electro-Optics/Quantum Electronics and Laser Science Conference and Photonic Applications Systems Technologies 2006, Technical Digest* (2006).
- [124] R. Paschotta, J. Nilsson, A. C. Tropper, and D. C. Hanna, "Ytterbium-doped fiber amplifiers," *IEEE J. Quantum Electron.* **33**, 1049–1056 (1997).
- [125] D. M. Hemenway, Z. Chen, M. Kanskar, W. Urbanek, D. Dawson, L. Bao, M. DeFranza, M. DeVito, K. Fortier, R. Martinsen, and K. Welch, "976nm high brightness fiber-coupled laser Modules for ytterbium fiber laser pumping," *Proc. SPIE* **10900**, 109000D (2019).
- [126] M. Kanskar, C. Bai, L. Bao, Z. Chen, C. Chiong, M. DeFranza, K. Fortier, M. Hemenway, S. Li, E. Martin, J. Small, B. Tomakian, W. Urbanek, B. Wilkins, and J. Zhang, "High brightness diodes and 600W 62% efficient low SWaP fiber-coupled package," *Proc. SPIE* **11262**, 112620A (2020).
- [127] E. Snitzer, H. Po, F. Hakimi, R. Tumminelli, and B. C. McCollum, "Double-clad, offset core Nd fiber laser," *Proc. Conf. Opt. Fiber Sensors* **PD5**, 533–536 (1988).
- [128] T. Y. Fan, "Efficient coupling of multiple diode laser arrays to an optical fiber by geometric multiplexing," *Appl. Opt.* **30**, 630–632

(1991).

- [129] A. Kosterin, V. Temyanko, M. Fallahi, and M. Mansuripur, "Tapered fiber bundles for combining high-power diode lasers," *Appl. Opt.* **43**, 3893–3900 (2004).
- [130] P. Polynkin, V. Temyanko, M. Mansuripur, and N. Peyghambarian, "Efficient and scalable side pumping scheme for short high-power optical fiber lasers and amplifiers," *IEEE Photonics Technol. Lett.* **16**, 2024–2026 (2004).
- [131] D. Kouznetsov, J. V. Moloney, and E. M. Wright, "Efficiency of pump absorption in double-clad fiber amplifiers. I. Fiber with circular symmetry," *J. Opt. Soc. Am. B* **18**, 743–749 (2001).
- [132] D. Kouznetsov and J. V. Moloney, "Efficiency of pump absorption in double-clad fiber amplifiers. II. Broken circular symmetry," *J. Opt. Soc. Am. B* **19**, 1259–1263 (2002).
- [133] A. Liu and K. Ueda, "The absorption characteristics of circular, offset, and rectangular double-clad fibers," *Opt. Commun.* **132**, 511–518 (1996).
- [134] P. Leproux, S. Février, V. Doya, P. Roy, and D. Pagnoux, "Modeling and optimization of double-clad fiber amplifiers using chaotic propagation of the pump," *Opt. Fiber Technol.* **6**, 324–339 (2001).
- [135] D. Gloge, "Bending loss in multimode fibers with graded and ungraded core index," *Appl. Opt.* **11**, 2506–2513 (1972).
- [136] M. N. Zervas, A. Marshall, and J. Kim, "Effective absorption in cladding-pumped fibers," *Proc. SPIE* **7914**, 79141T (2011).
- [137] D. J. Richardson, J. Nilsson, and W. A. Clarkson, "High power fiber lasers: current status and future perspectives [Invited]," *J. Opt. Soc. Am. B* **27**, B63–B92 (2010).
- [138] J. P. Koplow, D. A. V. Kliner, and L. Goldberg, "Single-mode operation of a coiled multimode fiber amplifier," *Opt. Lett.* **25**, 442–444 (2000).
- [139] R. T. Schermer, "Mode scalability in bent optical fibers," *Opt. Express* **15**, 15674–15701 (2007).
- [140] V. Filippov, Y. Chamorovskii, J. Kerttula, K. Golant, M. Pessa, and O. G. Okhotnikov, "Double clad tapered fiber for high power applications," *Opt. Express* **16**, 1929–1944 (2008).
- [141] S. Arismar Cerqueira, "Recent progress and novel applications of photonic crystal fibers," *Reports Prog. Phys.* **73**, 024401 (2010).
- [142] F. Di Teodoro, M. K. Hemmat, J. Morais, and E. C. Cheung, "High

- peak power operation of a 100 $\mu\text{m}$ -core Yb-doped rod-type photonic crystal fiber amplifier," Proc. SPIE **7580**, 758006 (2010).
- [143] J. Limpert, F. Stutzki, F. Jansen, H. J. Otto, T. Eidam, C. Jauregui, and A. Tünnermann, "Yb-doped large-pitch fibres: Effective single-mode operation based on higher-order mode delocalisation," Light Sci. Appl. **1**, 1–5 (2012).
- [144] X. Ma, C. Zhu, I.-N. Hu, A. Kaplan, and A. Galvanauskas, "Single-mode chirally-coupled-core fibers with larger than 50 $\mu\text{m}$  diameter cores," Opt. Express **22**, 9206–9219 (2014).
- [145] H. Pei, J. Ruppe, S. Chen, M. Sheikhsola, J. Nees, and A. Galvanauskas, "Multi-mJ ultrashort pulse coherent pulse stacking amplification in a Yb-doped 85 $\mu\text{m}$  CCC fiber based system," in *Conference on Lasers and Electro-Optics* (2017), p. SM1L.2.
- [146] T. Eidam, C. Wirth, C. Jauregui, F. Stutzki, F. Jansen, H.-J. Otto, O. Schmidt, T. Schreiber, J. Limpert, and A. Tünnermann, "Experimental observations of the threshold-like onset of mode instabilities in high power fiber amplifiers," Opt. Express **19**, 13218–13224 (2011).
- [147] L. Huang, W. Wang, J. Leng, S. Guo, X. Xu, and X. Cheng, "Experimental investigation on evolution of the beam quality in a 2-kW high power fiber amplifier," IEEE Photonics Technol. Lett. **26**, 33–36 (2014).
- [148] C. Jauregui, T. Eidam, H. J. Otto, F. Stutzki, F. Jansen, J. Limpert, and A. Tünnermann, "Physical origin of mode instabilities in high-power fiber laser systems," Opt. Express **20**, 12912–12925 (2012).
- [149] C. Jauregui, H.-J. Otto, S. Bretkopf, J. Limpert, and A. Tünnermann, "Optimizing high-power Yb-doped fiber amplifier systems in the presence of transverse mode instabilities," Opt. Express **24**, 7879–7892 (2016).
- [150] L. Shah and M. Fermann, "High-power ultrashort-pulse fiber amplifiers," IEEE J. Sel. Top. Quantum Electron. **22**, 552–558 (2007).
- [151] A. Malinowski, A. Piper, J. H. V Price, K. Furusawa, Y. Jeong, J. Nilsson, and D. J. Richardson, "Ultrashort-pulse Yb<sup>3+</sup>-fiber-based laser and amplifier system producing >25-W average power," Opt. Lett. **29**, 2073–2075 (2004).
- [152] V. Filippov, J. Kerttula, Y. Chamorovskii, K. Golant, and O. G. Okhotnikov, "Highly efficient 750 W tapered double-clad ytterbium fiber laser," Opt. Express **18**, 12499 (2010).

- [153] F. Röser, D. Schimpf, O. Schmidt, B. Ortaç, K. Rademaker, J. Limpert, and A. Tünnermann, "90 W average power 100  $\mu$ J energy femtosecond fiber chirped-pulse amplification system," *Opt. Lett.* **32**, 2230–2232 (2007).
- [154] T. Eidam, J. Rothhardt, F. Stutzki, F. Jansen, S. Hädrich, H. Carstens, C. Jauregui, J. Limpert, and A. Tünnermann, "Fiber chirped-pulse amplification system emitting 3.8 GW peak power," *Opt. Express* **19**, 255–260 (2011).
- [155] T. Eidam, S. Hanf, E. Seise, T. V. Andersen, T. Gabler, C. Wirth, T. Schreiber, J. Limpert, and A. Tünnermann, "Femtosecond fiber CPA system emitting 830 W average output power," *Opt. Lett.* **35**, 94–96 (2010).
- [156] J. Želudevičius, R. Danilevičius, K. Viskontas, N. Rusteika, and K. Regelskis, "Femtosecond fiber CPA system based on picosecond master oscillator and power amplifier with CCC fiber," *Opt. Express* **21**, 5338–5345 (2013).
- [157] A. Klenke, M. Muller, H. Stark, M. Kienel, C. Jauregui, A. Tünnermann, and J. Limpert, "Coherent beam combination of ultrafast fiber lasers," *IEEE J. Sel. Top. Quantum Electron.* **24**, 0902709 (2018).
- [158] R. Uberna, A. Bratcher, and B. G. Tiemann, "Coherent polarization beam combination," *IEEE J. Quantum Electron.* **46**, 1191–1196 (2010).
- [159] E. C. Cheung, J. G. Ho, G. D. Goodno, R. R. Rice, J. Rothenberg, P. Thielen, M. Weber, and M. Wickham, "Diffractive-optics-based beam combination of a phase-locked fiber laser array," *Opt. Lett.* **33**, 354–356 (2008).
- [160] R. Harney and J. Schipper, "Passive and active pulse stacking scheme for pulse shaping," U.S. patent 4,059,759 (1977).
- [161] L. Daniault, M. Hanna, D. N. Papadopoulos, Y. Zaouter, E. Mottay, F. Druon, and P. Georges, "Passive coherent beam combining of two femtosecond fiber chirped-pulse amplifiers," *Opt. Lett.* **36**, 4023–4025 (2011).
- [162] M. Kienel, A. Klenke, T. Eidam, S. Hädrich, J. Limpert, and A. Tünnermann, "Energy scaling of femtosecond amplifiers using actively controlled divided-pulse amplification," *Opt. Lett.* **39**, 1049–1052 (2014).
- [163] T. Zhou, J. Ruppe, C. Zhu, I.-N. Hu, J. Nees, and A. Galvanauskas, "Coherent pulse stacking amplification using low-finesse Gires-

- Tournois interferometers," *Opt. Express* **23**, 7442–7462 (2015).
- [164] M. Kienel, M. Müller, A. Klenke, J. Limpert, and A. Tünnermann, "12 mJ kW-class ultrafast fiber laser system using multidimensional coherent pulse addition," *Opt. Lett.* **41**, 3343–3346 (2016).
- [165] T. Liu, J. Wang, G. I. Petrov, V. V. Yakovlev, and H. F. Zhang, "Photoacoustic generation by multiple picosecond pulse excitation," *Med. Phys.* **37**, 1518–1521 (2010).
- [166] M. Murakami, B. Liu, Z. Hu, Z. Liu, Y. Uehara, and Y. Che, "Burst-mode femtosecond pulsed laser deposition for control of thin film morphology and material ablation," *Appl. Phys. Express* **2**, 042501 (2009).
- [167] R. Knappe, H. Haloui, A. Seifert, A. Weis, and A. Nebel, "Scaling ablation rates for picosecond lasers using burst micromachining," *Proc. SPIE* **7585**, 75850H (2010).
- [168] W. Hu, Y. C. Shin, and G. King, "Modeling of multi-burst mode pico-second laser ablation for improved material removal rate," *Appl. Phys. A* **98**, 407–415 (2010).
- [169] H. Kalaycioglu, K. Eken, and F. Ö. Ilday, "Fiber amplification of pulse bursts up to 20  $\mu$ J pulse energy at 1 kHz repetition rate," *Opt. Lett.* **36**, 3383–3385 (2011).
- [170] C. Kerse, H. Kalaycioglu, P. Elahi, B. Çetin, D. K. Kesim, Ö. Akçaalan, S. Yavaş, M. D. Aşlk, B. Öktem, H. Hoogland, R. Holzwarth, and F. Ö. Ilday, "Ablation-cooled material removal with ultrafast bursts of pulses," *Nature* **537**, 84–88 (2016).
- [171] N. A. of S. E. and Medicine, *Opportunities in Intense Ultrafast Lasers: Reaching for the Brightest Light* (The National Academies, 2018).
- [172] K. Sugioka and Y. Cheng, "Femtosecond laser three-dimensional micro- and nanofabrication," *Appl. Phys. Rev.* **1**, 041303 (2014).
- [173] K. Sugioka, "Progress in ultrafast laser processing and future prospects," *Nanophotonics* **6**, 393–413 (2017).
- [174] M. Malinauskas, A. Žukauskas, S. Hasegawa, Y. Hayasaki, V. Mizeikis, R. Buividas, and S. Juodkazis, "Ultrafast laser processing of materials: from science to industry," *Light Sci. Appl.* **5**, e16133 (2016).
- [175] B. N. Chichkov, C. Momma, S. Nolte, F. Von Alvensleben, and A. Tünnermann, "Femtosecond, picosecond and nanosecond laser ablation of solids," *Appl. Phys. A* **63**, 109–115 (1996).

- [176] M. Gedvilas, S. Indrišiunas, B. Voisiat, E. Stankevičius, A. Selskis, and G. Račiukaitis, "Nanoscale thermal diffusion during the laser interference ablation using femto-, pico-, and nanosecond pulses in silicon," *Phys. Chem. Chem. Phys.* **20**, 12166–12174 (2018).
- [177] S. Gao and H. Huang, "Recent advances in micro- and nano-machining technologies," *Front. Mech. Eng.* **12**, 18–32 (2017).
- [178] A. Borowiec and H. K. Haugen, "Subwavelength ripple formation on the surfaces of compound semiconductors irradiated with femtosecond laser pulses," *Appl. Phys. Lett.* **82**, 4462–4464 (2003).
- [179] M. Malinauskas, M. Farsari, A. Piskarskas, and S. Juodkazis, "Ultrafast laser nanostructuring of photopolymers: a decade of advances," *Phys. Rep.* **533**, 1–31 (2013).
- [180] M. Beresna, M. Gecevičius, and P. G. Kazansky, "Ultrafast laser direct writing and nanostructuring in transparent materials," *Adv. Opt. Photonics* **6**, 293–339 (2014).
- [181] C. Corbari, A. Champion, M. Gecevičius, M. Beresna, Y. Bellouard, and P. G. Kazansky, "Femtosecond versus picosecond laser machining of nano-gratings and micro-channels in silica glass," *Opt. Express* **21**, 3946–3958 (2013).
- [182] P. Elahi, Ö. Akçaalan, C. Ertek, K. Eken, F. Ö. Ilday, and H. Kalaycoğlu, "High-power Yb-based all-fiber laser delivering 300 fs pulses for high-speed ablation-cooled material removal," *Opt. Lett.* **43**, 535–538 (2018).
- [183] J. Liu, X. Li, S. Zhang, M. Han, H. Han, and Z. Yang, "Wavelength-tunable burst-mode pulse with controllable pulse numbers and pulse intervals," *IEEE J. Sel. Top. Quantum Electron.* **25**, 1–6 (2019).
- [184] X. Wolters, G. Bonamis, K. Mishchick, E. Audouard, C. Hönninger, and E. Mottay, "High power GHz femtosecond laser for ablation efficiency increase," *Procedia Manuf.* **36**, 200–207 (2019).
- [185] A. Okhrimchuk, S. Fedotov, I. Glebov, V. Sigaev, and P. Kazansky, "Single shot laser writing with sub-nanosecond and nanosecond bursts of femtosecond pulses," *Sci. Rep.* **7**, 16563 (2017).
- [186] I. Miyamoto, K. Cvecek, and M. Schmidt, "Crack-free conditions in welding of glass by ultrashort laser pulse," *Opt. Express* **21**, 14291–14302 (2013).
- [187] F. Zimmermann, S. Richter, S. Döring, A. Tünnermann, and S. Nolte, "Ultrastable bonding of glass with femtosecond laser bursts," *Appl. Opt.* **52**, 1149–1154 (2013).
- [188] G. Bonamis, K. Mishchick, E. Audouard, C. Hönninger, E. Mottay, J.

- Lopez, and I. Manek-Hönninger, "High efficiency femtosecond laser ablation with gigahertz level bursts," *J. Laser Appl.* **31**, 022205 (2019).
- [189] A. Žemaitis, P. Gečys, M. Barkauskas, G. Račiukaitis, and M. Gedvilas, "Highly-efficient laser ablation of copper by bursts of ultrashort tuneable (fs-ps) pulses," *Sci. Rep.* **9**, 12280 (2019).
- [190] S. Butkus, V. Jukna, D. Paipulas, M. Barkauskas, and V. Sirutkaitis, "Micromachining of invar foils with GHz, MHz and kHz femtosecond burst modes," *Micromachines* **11**, 733 (2020).
- [191] S. M. Remund, M. Gafner, M. V. Chaja, A. Urniezius, S. Butkus, and B. Neuenschwander, "Milling applications with GHz burst: Investigations concerning the removal rate and machining quality," *Procedia CIRP* **94**, 850–855 (2020).
- [192] M. W. Sigrist, "Mid-infrared laser-spectroscopic sensing of chemical species," *J. Adv. Res.* **6**, 529–533 (2015).
- [193] Y. Su, W. Wang, X. Hu, H. Hu, X. Huang, Y. Wang, J. Si, X. Xie, B. Han, H. Feng, Q. Hao, G. Zhu, T. Duan, and W. Zhao, "10 Gbps DPSK transmission over free-space link in the mid-infrared," *Opt. Express* **26**, 34515–34528 (2018).
- [194] Y. Wu, S. Liang, Q. Fu, L. Xu, and D. J. Richardson, "Compact picosecond mid-IR PPLN OPO with controllable peak powers," *OSA Contin.* **3**, 2741–2748 (2020).
- [195] S. Cai, M. Ruan, B. Wu, Y. Shen, and P. Jiang, "High conversion efficiency, mid-infrared pulses generated via burst-mode fiber laser pumped optical parametric oscillator," *IEEE Access* **8**, 64725–64729 (2020).
- [196] X. Q. Gao, M. L. Long, and C. Meng, "Compact KGd(WO<sub>4</sub>)<sub>2</sub> picosecond pulse-train synchronously pumped broadband Raman laser," *Appl. Opt.* **55**, 6554–6558 (2016).
- [197] L. M. G. van Huizen, N. V. Kuzmin, E. Barbé, S. van der Velde, E. A. te Velde, and M. L. Groot, "Second and third harmonic generation microscopy visualizes key structural components in fresh unprocessed healthy human breast tissue," *J. Biophotonics* **12**, e201800297 (2019).
- [198] C. J. S. de Matos, D. A. Chestnut, and J. R. Taylor, "Low-threshold self-induced modulational instability ring laser in highly nonlinear fiber yielding a continuous-wave 262-GHz soliton train," *Opt. Lett.* **27**, 915–917 (2002).
- [199] Y. Gong, P. Shum, D. Tang, C. Lu, and X. Guo, "660 GHz solitons

- source based on modulation instability in short cavity," *Opt. Express* **11**, 2480–2485 (2003).
- [200] D. Y. Tang, J. Guo, Y. F. Song, L. Li, L. M. Zhao, and D. Y. Shen, "GHz pulse train generation in fiber lasers by cavity induced modulation instability," *Opt. Fiber Technol.* **20**, 610–614 (2014).
- [201] H. Muñoz-Marco, J. Abreu-Afonso, G. Sardiello, and P. Pérez-Millán, "Theoretical and experimental comprehensive study of GHz-range passively mode-locked fiber lasers," *Appl. Opt.* **59**, 6817–6827 (2020).
- [202] R. Maram, L. R. Cortés, J. Van Howe, and J. Azaña, "Energy-preserving arbitrary repetition-rate control of periodic pulse trains using temporal Talbot effects," *J. Light. Technol.* **35**, 658–668 (2017).
- [203] T. Flöry, G. Andriukaitis, M. Barkauskas, E. Kaksis, I. Astrauskas, A. Pugžlys, A. Baltuška, R. Danielius, A. Galvanauskas, and T. Balčiūnas, "High repetition rate fs pulse burst generation using the vernier effect," in *Conference on Lasers and Electro-Optics* (2017), p. SM4I.5.
- [204] C. W. Siders, J. L. W. Siders, A. J. Taylor, S.-G. Park, and A. M. Weiner, "Efficient high-energy pulse-train generation using a  $2^n$ -pulse Michelson interferometer," *Appl. Opt.* **37**, 5302–5305 (1998).
- [205] H. Matsumoto, Z. Lin, and J. Kleinert, "Ultrafast laser ablation of copper with ~GHz bursts," *Proc. SPIE* **10519**, 1 (2018).
- [206] B. Dromey, M. Zepf, M. Landreman, K. O’Keeffe, T. Robinson, and S. M. Hooker, "Generation of a train of ultrashort pulses from a compact birefringent crystal array," *Appl. Opt.* **46**, 5142–5146 (2007).
- [207] S. sik Min, Y. Zhao, and S. Fleming, "Repetition rate multiplication in figure-eight fibre laser with 3 dB couplers," *Opt. Commun.* **277**, 411–413 (2007).
- [208] T. Eidam and B. Limpert, "Generating laser pulses in a burst mode," *Deutchl. Pat. DE102016124087B3* (2016).
- [209] Y. Zhao, S. Min, H. Wang, and S. Fleming, "High-power figure-of-eight fiber laser with passive sub-ring loops for repetition rate control," *Opt. Express* **14**, 10475–10480 (2006).
- [210] K. Wei, P. Wu, R. Wen, J. Song, Y. Guo, and X. Lai, "High power burst-mode operated sub-nanosecond fiber laser based on 20/125  $\mu\text{m}$  highly doped Yb fiber," *Laser Phys.* **26**, 25104 (2016).
- [211] K. H. Wei, P. P. Jiang, B. Wu, T. Chen, and Y. H. Shen, "Fiber laser

- pumped burst-mode operated picosecond mid-infrared laser," *Chinese Phys. B* **24**, 024217 (2015).
- [212] A. Wang, A. Das, and D. Grojo, "Internal structuring of silicon using THz-repetition-rate trains of ultrashort pulses," in *Conference on Lasers and Electro-Optics, OSA Technical Digest* (2020), p. ATu3K.4.
- [213] V. Stummer, T. Flöry, G. Krizsán, G. Polónyi, E. Kaksis, A. Pugžlys, J. A. Fülöp, and A. Baltuška, "Programmable generation of terahertz bursts in chirped-pulse laser amplification," *Optica* **7**, 1758–1763 (2020).

## COPIES OF PUBLICATIONS

A1

COMPACT FIBER CPA SYSTEM BASED ON A CFBG STRETCHER  
AND CVBG COMPRESSOR WITH MATCHED DISPERSION PROFILE

**T. Bartulevicius**, S. Frankinas, A. Michailovas, R. Vasilyeu,  
V. Smirnov, F. Trepanier, and N. Rusteika

Opt. Express **25**, 19856-19862 (2017)

Preprint version reprinted with permission from © The Optical Society

The publication may also be viewed on the official OSA Publishing website  
DOI: 10.1364/OE.25.019856

# Compact fiber CPA system based on CFBG stretcher and CVBG compressor with matched dispersion profile

TADAS BARTULEVICIUS,<sup>1,2,\*</sup> SAULIUS FRANKINAS,<sup>1,2</sup> ANDREJUS MICHAILOVAS,<sup>1,2</sup> RUSLAN VASILYEU,<sup>3</sup> VADIM SMIRNOV,<sup>3</sup> FRANCOIS TREPANIER,<sup>4</sup> AND NERIJUS RUSTEIKA<sup>1,2</sup>

<sup>1</sup> Ekspla Ltd., Savanoriu ave. 237, LT-02300 Vilnius, Lithuania

<sup>2</sup> Center for Physical Sciences and Technology, Savanoriu ave. 231, LT-02300, Vilnius, Lithuania

<sup>3</sup> OptiGrate Corp., 562 South Econ Circle, Oviedo, Florida 32765-4311, USA

<sup>4</sup> TeraXion Inc., 2716 Einstein, Quebec, Qc G1P 4S8, Canada

\* [t.bartulevicius@ekspla.com](mailto:t.bartulevicius@ekspla.com)

**Abstract:** In this work, compact fiber chirped pulse amplification system exploiting tandem of chirped fiber Bragg grating stretcher and chirped volume Bragg grating compressor with matched chromatic dispersion is presented. Chirped pulses of 230 ps duration were amplified in Yb-doped fiber amplifier and re-compressed to 208 fs duration with good fidelity. Compressed pulse duration was fine-tuned by temperature gradient along the fiber Bragg grating stretcher.

© 2017 Optical Society of America

**OCIS codes:** (320.7090) Ultrafast lasers; (060.3510) Lasers, fiber; (140.3615) Lasers, ytterbium; (320.5520) Pulse compression; (050.7330) Volume gratings.

---

## References and links

1. L. Shah, M. E. Fermann, J. W. Dawson, and C. P. J. Barty, "Micromachining with a 50 W, 50  $\mu$ J, sub-picosecond fiber laser system," *Opt. Express* **14**, 12546-12551 (2006).
2. J. Squier and M. Müller, "High resolution nonlinear microscopy: A review of sources and methods for achieving optimal imaging," *Rev. Sci. Instrum.* **72**, 2855-2867 (2001).
3. R. Berera, R. van Grondelle, and J. T. M. Kennis, "Ultrafast transient absorption spectroscopy: principles and application to photosynthetic systems," *Photosynth. Res.* **101**, 105-118 (2009).
4. G. Matthäus, T. Schreiber, J. Limpert, S. Nolte, G. Torosyan, R. Beigang, S. Riehemann, G. Notni, and A. Tünnermann, "Surface-emitted THz generation using a compact ultrashort pulse fiber amplifier at 1060 nm," *Opt. Commun.* **261**, 114-117 (2006).
5. K. H. Liao, A. G. Mordovanakis, B. Hou, G. Q. Chang, M. Rever, G. A. Mourou, J. Nees, and A. Galvanauskas, "Generation of hard X-rays using an ultrafast fiber laser system," *Opt. Express* **15**, 13942-13948 (2007).
6. D. Strickland and G. Mourou, "Compression of amplified chirped optical pulses," *Opt. Commun.* **56**, 219-221 (1985).
7. E. Treacy, "Optical pulse compression with diffraction gratings," *IEEE J. Quantum Electron.* **5**, 454-458 (1969).
8. O. E. Martinez, J. P. Gordon, and R. L. Fork, "Negative group-velocity dispersion using refraction," *J. Opt. Soc. Am. A* **1**, 1003-1006 (1984).
9. G. Imeshev, I. Hartl, and M. E. Fermann, "Chirped pulse amplification with a nonlinearly chirped fiber Bragg grating matched to the Treacy compressor," *Opt. Lett.* **29**, 679-681 (2004).
10. A. Galvanauskas, A. Heaney, I. Erdogan, and D. Harter, "Use of volume chirped Bragg gratings for compact high-energy chirped pulse amplification circuits," *Conf. on Lasers and Electro-Optics* **6**, 362 (1998).
11. K-H Liao, M-Y Cheng, E. Flecher, V. Smirnov, L. B. Glebov, and A. Galvanauskas, "Large-aperture chirped volume Bragg grating based fiber CPA system," *Opt. Express* **15**, 4876-4882 (2007).
12. L. B. Glebov, V. Smirnov, E. Rotari, I. Cohanoschi, L. Glebova, O. V. Smolski, J. Lumeau, C. Lantigua, and A. Glebov, "Volume-chirped Bragg gratings: monolithic components for stretching and compression of ultrashort laser pulses," *Opt. Eng.* **53**, 051514 (2014).
13. G. Chang, M. Rever, V. Smirnov, L. Glebov, and A. Galvanauskas, "Femtosecond Yb-fiber chirped-pulse-amplification system based on chirped-volume Bragg gratings," *Opt. Lett.* **34**, 2952-2954 (2009).
14. R. Sun, D. Jin, F. Tan, S. Wei, C. Hong, J. Xu, J. Liu, and P. Wang, "High-power all-fiber femtosecond chirped pulse amplification based on dispersive wave and chirped-volume Bragg grating," *Opt. Express* **24**, 22806-22812 (2016).
15. G. Sobon, K. Krzempek, J. Taka, and J. Sotor, "Compact, all-PM fiber-CPA system based on chirped volume Bragg grating," *Laser Phys.* **26**, 015106 (2016).

16. R. A. Sims, P. Kadwani, H. Ebendorff-Heidepre, L. Shah, T. M. Monro, and M. Richardson, "Chirped pulse amplification in single mode Tm: fiber using a chirped Bragg grating," *Appl. Phys. B* **111**, 299–304 (2013).
  17. H. Hoogland and R. Holzwarth, "Compact polarization-maintaining 2.05- $\mu\text{m}$  fiber laser at 1-MHz and 1-MW peak power," *Opt. Lett.* **40**, 3520–3523 (2015).
  18. A. Galvanauskas and M. Fermann, "Optical pulse amplification using chirped Bragg grating," US Patent 5,499,143 (1996).
  19. D. Sanchez, G. Matras, J. Biagetti, C. Simon-Boisson, "High energy high repetition rate compact picosecond Holmium YLF laser for mid-IR OPCPA pumping," *Proc. SPIE* 10082-22 (2017).
  20. S. Frankinas, A. Michailovas, N. Ruseika, V. Smirnov, R. Vasilyeu, A. L. Glebov, "Efficient ultrafast fiber laser using chirped fiber Bragg grating and chirped volume Bragg grating stretcher/compressor configuration," *Proc. SPIE* **9730**, 973017 (2016).
  21. A. Yusim, I. Samartsev, O. Shkurikhin, D. Myasnikov, A. Bordenyuk, N. Platonov, V. Kancharla, V. Gapontsev, "New generation of high average power industry grade ultrafast ytterbium fiber lasers," *Proc. SPIE* **9728**, 972839 (2016).
- 

## 1. Introduction

Fiber laser sources offer many advantages compared to solid state laser counterparts. Excellent beam quality, reliability, maintenance-free operation, high output power makes fiber lasers attractive for a wide array of applications. A number of advanced applications require ultrashort laser pulses with high peak power, e.g. laser material micro-processing [1], nonlinear microscopy [2] and spectroscopy [3], generation of terahertz [4] and X-ray radiation [5]. However, direct amplification of high energy ultrashort pulses in fiber amplifiers is limited by nonlinear effects such as self-phase modulation, self-focusing, Raman scattering etc. To mitigate nonlinear effects in solid state lasers the chirped pulse amplification (CPA) technique was proposed [6]. Pulse stretching and compression in CPA systems can be conveniently realized using diffraction gratings [7,8]. This approach has advantage that properly designed stretcher and compressor have exactly compensated chromatic dispersion profile. However, when pulses are chirped to hundreds of picoseconds or longer duration, diffraction grating based CPA system becomes quite bulky. Furthermore, diffraction grating based pulse stretcher and compressor are susceptible to mechanical and thermal perturbations. A quality of compressed pulse temporal profile as well as spatial beam profile strongly depends on precise alignment of the optical elements. Therefore when applied to fiber laser systems diffraction grating based CPA approach negates their important advantage in compactness and robustness.

Major achievement in miniaturization of the fiber CPA (FCPA) systems was a substitute of diffraction grating based pulse stretcher by chirped fiber Bragg grating (CFBG) [9]. Diffraction grating compressor however remained the limiting factor in realization of truly compact and robust FCPA system. Another breakthrough was achieved when large aperture chirped volume Bragg gratings (CVBG) were introduced as pulse stretcher and compressor in femtosecond FCPA system [10]. Chirped volume Bragg grating can stretch pulses to a few hundreds of picoseconds in duration and recompress them to femtosecond duration in only a few centimeters of glass. The use of CVBG as pulse stretcher and compressor has practical advantage over the diffraction grating based systems due to compactness, simplicity of alignment, efficiency and robustness [11–13]. In recent years, several CVBG based FCPA systems for the most common wavelengths, such as 1  $\mu\text{m}$  (Yb doped fiber) [13,14], 1.56  $\mu\text{m}$  (Er doped fiber) [12,15], 2.05  $\mu\text{m}$  (Tm/Ho doped fiber) [16,17], were demonstrated.

It was mentioned that usage of CVBGs based stretcher/compressor allows designing compact and robust ultra-short pulsed lasers. This idea was proposed long time ago by Galvanauskas and Fermann [18]. However due to lack of holographic materials it was not implemented until volume Bragg gratings (VBGs) based on Photo-Thermo-Refractive (PTR) glass were developed [11]. VBGs holographically fabricated in PTR glass have several key advantages: unrestricted life time, stability to harsh environmental conditions and high diffraction efficiency. On top of it PTR glass has a low absorption coefficient that enables its usage for compression of high power/energy pulses. Over last several years parameters of

CVBGs were significantly improved [12], which led in an increased efficiency of CVBGs combined with nearly diffraction limited beam quality. All above triggered extensive development of novel laser designs. Two historic milestones were recently achieved for PTR glass based CVBGs: compression of more than 100 W power beam [14] and 100 mJ pulses [19].

However, CVBG based FCPA systems require additional dispersion compensation to eliminate the residual dispersion of the fiber [13]. Compensation of the dispersion in the system is inconvenient and requires addition of the fiber with opposite sign of dispersion. To minimize the recompressed pulse duration a cut back of the fiber while monitoring pulse duration is required.

To overcome the limitations of FCPA systems based solely on CVBG, an alternative ultrafast fiber laser configuration using CFBG as pulse stretcher and CVBG as pulse compressor was proposed [20, 21]. However, compressed pulses were not transform-limited and had temporal pedestal due to the imprecise dispersion compensation between CFBG and CVBG. In this work, we present compact FCPA system consisting of CVBG compressor and CFBG stretcher which was manufactured with matched chromatic dispersion profile to achieve high fidelity femtosecond pulses. Dispersion of the FCPA system was fine-tuned by using temperature distribution along the CFBG stretcher.

## 2. Experimental setup and results

Schematic representation of the experimental FCPA system is depicted in Fig. 1. The main parts of the system were all-in-fiber seed source, CFBG stretcher, power amplification stage and CVBG compressor. Linearly up-chirped pulses of 13 ps duration and 10.6 nm bandwidth were generated by commercially available all-in-fiber passively mode-locked seed source (FFS100CHI, *Ekspla*) operating at 1029.4 nm center wavelength and 53 MHz pulse repetition rate. Initial pulse spectrum from the seed source is shown in Fig. 2. Pulses from the seed source were down-chirped to about 230 ps duration by using CFBG stretcher (*TeraXion*) with group velocity dispersion (GVD) of  $\beta_2 = -13.65 \text{ ps}^2$ .

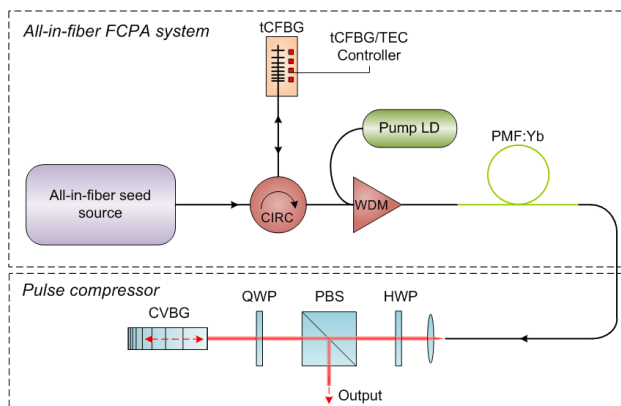


Fig. 1. Schematic representation of the experimental FCPA system with CFBG stretcher and CVBG pulse compressor. CIRC - optical circulator, tCFBG - thermally tunable CFBG module, WDM - wavelength-division multiplexer, LD - laser diode, PMF:Yb - Ytterbium doped polarization maintaining single-mode fiber, HWP - half-wave plate, PBS - polarization beam splitter, QWP - quarter-wave plate, CVBG - chirped volume Bragg grating.

Temporal envelope of the stretched pulses was measured using a photodiode with 35 ps response time and an oscilloscope with 20 GHz bandwidth. Spectrum and temporal shape of the stretched pulses are shown in Fig. 2.

After CFBG chirped laser pulses were combined with pump radiation from the single mode laser diode (976 nm) by wavelength-division multiplexer and amplified in a single-mode Yb-doped fiber amplifier. Seed source, CFBG stretcher and fiber amplifier were spliced

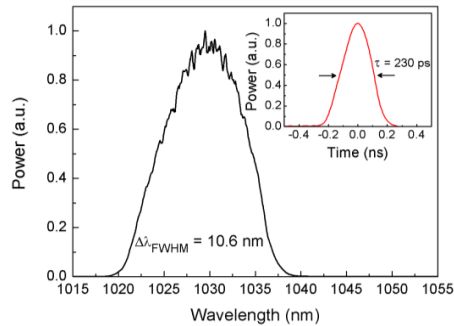


Fig. 2. Spectrum of the stretched pulses after CFBG. Inset: temporal envelope of the stretched pulses.

to a monolithic FCPA system. Chirped laser pulses were amplified up to 4.85 nJ energy (257 mW average power). Total power gain of the system was 13.3 dB. After the amplifier pulses were compressed in free space by CVBG compressor (*OptiGrate*). The output of the system was arranged by separating incident and reflected beams using quarter wave-plate (QWP) and polarizing beam splitter (PBS), as shown in the Fig. 1. Average power of the system after pulse compression was 223 mW, which corresponds to 87% efficiency of CVBG compressor. A few nanojoule pulse energy was sufficient for further pulse characterization and was not limited by nonlinear effects in the fiber amplifier. Demonstration of the microjoule level pulses from such system will be a subject of future work.

The key novelty in the described FCPA system is the use of FCBG and CVBG elements in tandem as well as dispersion matching between these elements. Below the details of producing these elements will be described.

CVBG was designed for this application aiming at several important points: efficiency above >85%, spectral bandwidth supporting pulses <300 fs along with stretching up to ~500 ps. Manufactured grating had diffraction efficiency >85% for more than 20 nm spectral bandwidth (Fig. 3). It also had linear stretching factor of ~22 ps/nm. Nearly diffraction limited beam quality was measured by reflection from both sides of this grating. It confirms that CVBG can be used in both orientations providing positive and negative dispersion.

The mismatch of chromatic dispersion profiles between stretcher and compressor might lead to temporal distortion of compressed pulses. In this work, a custom CFBG stretcher was produced with its dispersion profile designed to compensate dispersion profile of CVBG as well as residual dispersion of the FCPA system approximately equal to 1 ps<sup>2</sup> (equivalent to 50 m of fused silica fiber). First, dispersion profile of CVBG element with clear aperture of 5x5 mm was measured by using a homemade high resolution interferometric group delay measurement system. From this dispersion profile and estimated additional dispersion in the FCPA system, the matched CFBG design was computed and the parameters were sent to a UV based CFBG writing station. Following inscription of the CFBG in the fiber, its dispersion profile was measured and compared against the target dispersion to validate its performance. Measured group delay (GD) traces of CVBG and CFBG, as well as their net GD trace are presented in Fig. 3. The delay of the different spectral components has close to linear dependence on wavelength for both CFBG and CVBG. Total GD for CVBG was ~500 ps in its reflection bandwidth range of 1019-1041 nm with shorter wavelengths being delayed in respect to the longer ones (normal dispersion). CFBG had similar total GD in the same

bandwidth but with opposite sign (anomalous dispersion). Net GD curve has slight rising slope (anomalous dispersion) to compensate residual dispersion of the FCPA system.

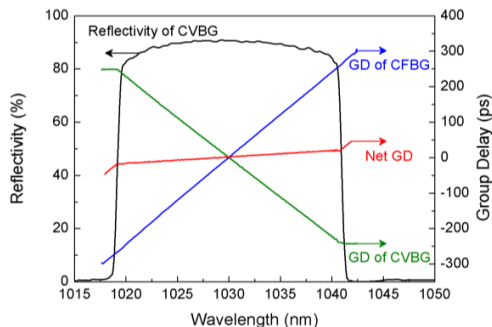


Fig. 3. Experimentally measured and smoothed ( $\sim 0.3$  nm smoothing) GD traces of CVBG (green line), CFBG (blue line) and their net GD trace (red line). The black curve shows measured reflectivity profile of CVBG.

Dispersion-matched CFBG was placed in thermal platform (produced by *TeraXion*) for dispersion fine-tuning. Temperature distribution along CFBG was controlled by thermoelectric cooler (TEC) elements which enabled the tunability of GVD and optimization of compressed pulse duration without requirement to change length of the fiber in the system.

At first, pulse compression was investigated when the temperature along CFBG was set constant ( $60^\circ\text{C}$ ). Measured autocorrelation trace had a width of 1.42 ps (FWHM), which corresponds to 1.01 ps pulse duration for Gaussian shaped pulses. Then TEC temperatures along CFBG were optimized to minimize pulse duration after the compressor. Only linear temperature gradient was required to reach minimal width of the autocorrelation function of 301 fs. Both autocorrelation traces are shown in Fig. 4 with corresponding temperature distributions along CFBG depicted in the inset of the figure. Additionally induced GVD due to thermal gradient of  $15^\circ\text{C}$  per 50 mm of CFBG length was estimated around  $0.072$  ps<sup>2</sup> (equivalent to 3.6 m of fused silica fiber).

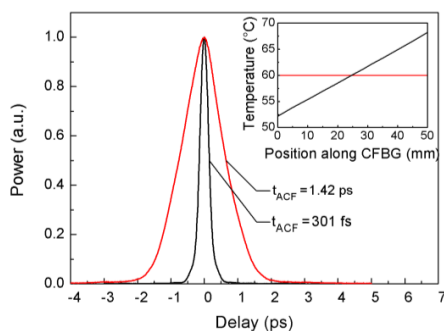


Fig. 4. Measured autocorrelation traces of compressed pulses after CVBG with a constant nominal temperature along CFBG (red line) and with an optimized temperature gradient applied along CFBG (black line). Inset: corresponding temperature distributions along CFBG.

Optimally compressed pulses were further characterized using second harmonic generation (SHG) frequency-resolved optical gating (FROG) autocorrelation method. The pulse duration retrieved by FROG algorithm (*Swamp Optics*) was equal to 208 fs (Fig. 5(a)). FROG retrieval was performed on a  $256 \times 256$  grid and yielded an error of 0.19%. Measured pulse spectrum after the FCPA system is depicted in Fig. 5(b) along with spectrum and its phase retrieved

from FROG. Transform-limited pulse duration derived from the spectrum was 203 fs. Close match between transform-limited and retrieved pulse duration proves that CFBG dispersion profile was successfully matched to this of CVBG. That is also confirmed by a small residual phase ( $< \pm 0.5$  rad) retrieved from FROG. Pulse contrast defined as the ratio of energy in main pulse to the energy of side pulses was  $>90\%$ . Excellent temporal quality of the compressed pulses was achieved despite high pulse compression ratio of  $\sim 1100$  in the described FCPA system.

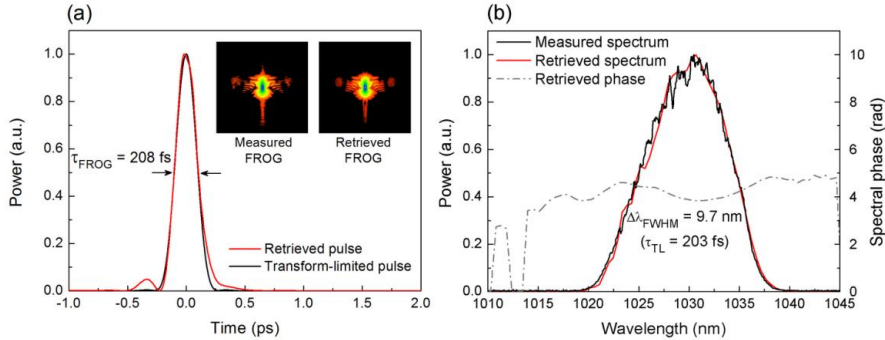


Fig. 5. a) Envelope of the compressed pulses retrieved from SHG FROG measurement in comparison with transform-limited pulse shape derived from the measured spectrum. Inset: measured and retrieved FROG traces. b) Measured pulse spectrum from the FCPA system in comparison with retrieved spectrum and retrieved spectral phase from FROG.

Beam quality at the output of the system was measured by performing Z-scan of the beam. The beam quality parameter  $M^2$  was estimated from the beam radius change along the propagation axis with best fit yielding  $M^2 \sim 1.06$ , indicating excellent beam quality (Fig. 6). This was achieved due to high optical homogeneity of photo-thermo-refractive glass of CVBG as well as precise control of Bragg grating geometry.

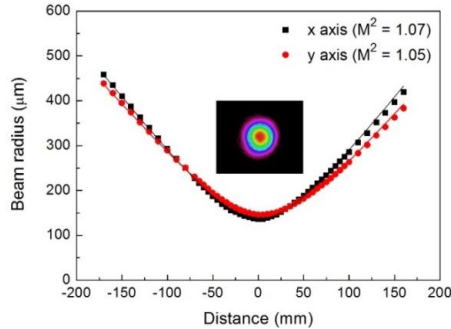


Fig. 6. Dependence of  $4\sigma$  beam radius at the output of the FCPA system versus the distance from the waist location for both directions perpendicular to the axis of propagation. Inset: beam profile at the waist position.

### 3. Conclusion

In this work we have demonstrated compact fiber chirped pulse amplification (FCPA) system exploiting tandem of chirped volume Bragg grating (CVBG) compressor and chirped fiber Bragg grating (CFBG) stretcher with matched chromatic dispersion. Chirped pulses of 230 ps duration were amplified in Yb-doped fiber amplifier and compressed to high fidelity 208 fs duration pulses corresponding to compression ratio of  $\sim 1100$ . GVD in the system was fine-

tuned by changing temperature gradient along CFBG stretcher. This novel FCPA configuration opens path to truly compact and robust high energy femtosecond fiber lasers.

**Funding**

Research Council of Lithuania (LAT-10/2016).

A2

COMPACT FEMTOSECOND 10  $\mu$ J PULSE ENERGY FIBER LASER  
WITH A CFBG STRETCHER AND CVBG COMPRESSOR

**T. Bartulevicius**, L. Veselis, K. Madeikis, A. Michailovas, and N. Rusteika

Opt. Fiber Technol. **45**, 77-80 (2018)

Reprinted with permission from ScienceDirect

The publication may also be viewed on the official ScienceDirect website

DOI: 10.1016/j.yofte.2018.06.006



## Regular Articles

Compact femtosecond 10  $\mu$ J pulse energy fiber laser with a CFBG stretcher and CVBG compressorT. Bartulevicius<sup>a,b,\*</sup>, L. Veselis<sup>a,b</sup>, K. Madeikis<sup>a,b</sup>, A. Michailovas<sup>a,b</sup>, N. Rusteika<sup>a,b</sup><sup>a</sup> Ekspla Ltd., Savanoriu Ave. 237, LT-02300 Vilnius, Lithuania<sup>b</sup> Center for Physical Sciences and Technology, Savanoriu Ave. 231, LT-02300, Vilnius, Lithuania

## ARTICLE INFO

## Keywords:

Ultrafast lasers  
Ytterbium fiber laser  
Fiber chirped pulse amplification  
Pulse compression  
Volume gratings

## ABSTRACT

In this work, a compact high energy fiber chirped pulse amplification system with matched pair of a chirped fiber Bragg grating stretcher and a chirped volume Bragg grating compressor is presented. Chirped pulses of 230 ps duration were amplified in a single mode Yb-doped fiber amplifiers to 10  $\mu$ J pulse energy and re-compressed to 349 fs duration corresponding to the peak power of 26 MW. Gain saturation was demonstrated when pumping with tandem of single mode laser diodes due to small mode area of the single mode fiber. Such laser source could be used in applications where high peak power is required but moderate average power is sufficient.

## 1. Introduction

Fiber laser sources offer excellent beam quality, maintenance-free operation, reliability and stability. Efficient heat dissipation and guided light propagation in optical fibers make fiber lasers attractive for average output power scaling to multi-kW level in the single transverse mode regime [1]. However much higher multi-MW level peak power and ultrashort (< 10 ps) pulse duration is needed for efficient laser frequency conversion from deep-UV to MIR spectral regions [2,3] to significantly extend the application areas of the ultrafast fiber lasers to technology [4] or applied science [5]. Megawatt and higher peak power levels and wavelength tunability are especially attractive for selective plane illumination microscopy as high energy wide field illumination enables faster data acquisition [6,7]. Nonlinear effects (e.g. self-phase modulation (SPM), self-focusing, stimulated Raman scattering) however, limit the amplification of ultrashort optical pulses in fiber amplifiers due to long interaction length and small mode area of the gain fibers. Chirped pulse amplification (CPA) is a powerful technique to mitigate nonlinear effects [8,9]. Fiber CPA (FCPA) technique allows achieving significantly higher pulse energies by reducing nonlinear effects in a gain fiber by stretching initial pulse and de-chirping the pulse after the amplification. The temporal stretching of the pulses is typically limited to hundreds of picoseconds as stretching and compressing beyond this duration becomes impractical due to large dimensions of diffraction gratings in stretcher and compressor of CPA system.

Quite commonly diffraction gratings are used in the compressor of the FCPA systems. However diffraction grating based compressor

negates important advantage in compactness and robustness of fiber laser systems. The development of large aperture chirped volume Bragg gratings (CVBG) provided an alternative solution of novel ultrashort pulsed laser design [10–14]. The use of CVBG has practical advantage over the diffraction grating based systems due to compactness, robustness and simplicity of alignment. However FCPA systems, based solely on CVBG stretcher and compressor, require additional dispersion management mechanism to eliminate residual dispersion of the fiber. An alternative FCPA system configuration using chirped fiber Bragg grating (CFBG) as pulse stretcher and chirped volume Bragg grating as pulse compressor was proposed to solve this issue [15,16]. Compact FCPA system consisting of CVBG compressor and CFBG stretcher with matched chromatic dispersion profile and the implementation of pulse duration tunability using temperature distribution along CFBG stretcher was presented in our previous work [17], where generation of nanojoule energy level high fidelity femtosecond pulses was demonstrated.

To further increase pulse energy and peak power in FCPA systems, scaling of mode-field diameter using special fiber designs, such as large mode area (LMA) fibers [18,19], photonic crystal fibers (PCF) [20,21], chirally-coupled-core (CCC) fibers [22,23] or tapered fibers [24,25] has been implemented. However in large mode area doped fiber amplifiers in order to achieve gain saturation and therefore good pumping efficiency, large average pump power has to be used, increasing system complexity, dimensions and price. For nonlinear applications, in particular bio-imaging, where high average power is not required and is even harmful [26–29] it limits practicality of the laser source and how widely certain application can be implemented.

In this work we used a core-pumped single mode polarization

\* Corresponding author at: Ekspla Ltd., Savanoriu Ave. 237, LT-02300 Vilnius, Lithuania.  
E-mail address: [t.bartulevicius@ekspla.com](mailto:t.bartulevicius@ekspla.com) (T. Bartulevicius).

<https://doi.org/10.1016/j.yofte.2018.06.006>

Received 21 March 2018; Received in revised form 9 May 2018; Accepted 10 June 2018  
1068-5200/ © 2018 Elsevier Inc. All rights reserved.

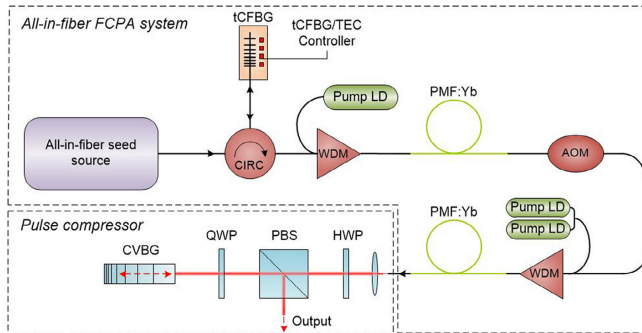


Fig. 1. Schematic presentation of the high energy FCPA system. CIRC – optical circulator, iCFBG – thermally tunable CFBG module, WDM – wavelength-division multiplexer, LD – laser diode, PMF:Yb – Ytterbium doped polarization maintaining single-mode fiber, AOM – acousto-optic modulator, HWP – half-wave plate, PBS – polarization beam splitter, QWP – quarter-wave plate, CVBG – chirped volume Bragg grating.

maintaining Yb-doped fiber amplifier, as well as a novel CPA scheme based on CFBG stretcher and CVBG compressor to build a compact 10  $\mu\text{J}$  energy sub-W average power femtosecond FCPA system which could be used for efficient parametric wavelength conversion [30], various imaging applications requiring moderate average power [26–29] and as a seed source in high power high energy femtosecond CPA laser systems.

2. Experimental setup and results

The experimental setup of the developed FCPA system is illustrated in Fig. 1. The main parts of the system were all-in-fiber seed source (FFS100CHI, Ekspla), CFBG stretcher (TeraXion), two fiber amplification stages and CVBG compressor (IPG Photonics). Linearly up-chirped pulses of 13 ps duration from the seed source (1029.4 nm center wavelength and 53 MHz pulse repetition rate) were down-chirped to about 230 ps duration by using CFBG stretcher with group velocity dispersion (GVD) of  $\beta_2 = -13.65 \text{ ps}^2$ . Thermal tuning of the CFBG was used in this work for fine dispersion control. Chirped laser pulses were combined with pump radiation from a single mode laser diode (976 nm) by wavelength-division multiplexer and amplified in a core pumped single-mode Yb-doped fiber amplifier up to 7.8 nJ energy. More details about fiber seed source can be found in our previous work [17]. Spectrum of the stretched pulses after CFBG is shown in Fig. 2.

Pulse repetition rate was reduced using fiber-coupled acousto-optic modulator (AOM) before the power amplifier. Incoherent polarization beam combining was used to double the brightness of pump radiation from two single mode laser diodes. Resulting 1.4 W pump power was

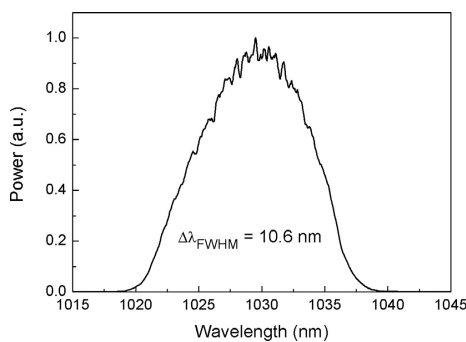


Fig. 2. Spectrum of the stretched pulses after CFBG.

coupled to the 11  $\mu\text{m}$  core of the Yb-doped truly single mode fiber by wavelength-division multiplexer. Length of the fiber amplifier was 0.3 m and Yb doping concentration was estimated to be about  $7 \cdot 10^{25} \text{ m}^{-3}$ . All FCPA laser system except the compressor was monolithically spliced. Amplified pulses were compressed in the free space CVBG compressor and out-coupled from the laser by separating incident and reflected beams using quarter wave-plate (QWP) and polarizing beam splitter (PBS), as shown in Fig. 1.

Dependence of average output power and pulse energy on the pulse repetition rate is shown in Fig. 3. At 10.6 MHz repetition rate average power of 658 mW was measured after compressor corresponding to 62 nJ pulse energy. At 35 kHz pulse repetition rate average output power was reduced by less than two times to 359 mW though seed power after AOM coupled to the amplifier was reduced from 47 mW at 10.6 MHz to 0.16 mW at 35 kHz. Weak dependence of average output power on seed input power manifests high level of saturation in the amplifier. Highest pulse energy of 10  $\mu\text{J}$  after the compressor was obtained at 35 kHz repetition rate corresponding to 26 MW peak power and a total gain of 34.8 dB in the power amplifier.

Pulse compression quality was examined for different output pulse energies using second harmonic non-collinear autocorrelator. Measured widths (FWHM) of autocorrelation functions (ACF) for different pulse energies are shown in Fig. 4(a). ACF widths of the transform-limited pulses were calculated from experimental pulse spectra and are shown at the same graph. For pulse energies below 2  $\mu\text{J}$ , transform limited and measured ACF widths were similar,  $\sim 300 \text{ fs}$  and  $\sim 330 \text{ fs}$  respectively. Assuming Gaussian pulse shape at low pulse energies, this corresponds

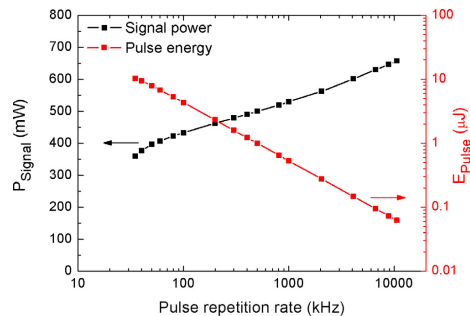


Fig. 3. Dependence of average amplified signal power (left axis) and pulse energy (right axis) after pulse compressor on pulse repetition rate. At lowest repetition rate of 35 kHz pulse energy was 10  $\mu\text{J}$ .

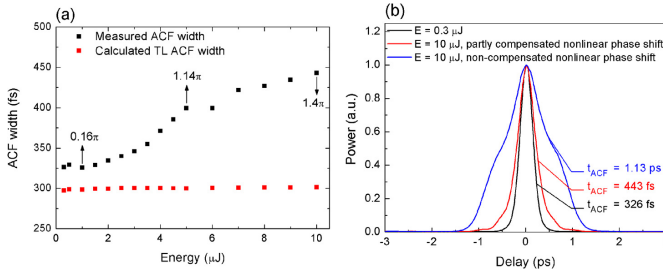


Fig. 4. a) Width (FWHM) of autocorrelation function of laser pulses at different energies in comparison with transform-limited pulse autocorrelation function width. Accumulated nonlinear phase-shift in a single-mode amplification stage at three different energies is indicated in the picture. b) Measured autocorrelation traces of compressed pulses with non-compensated nonlinear phase (blue line) and partly compensated nonlinear phase (red line) at 10 μJ pulse energy in comparison with measured 0.3 μJ pulse energy autocorrelation trace (black line). (For interpretation of the references to colour in this figure legend, the reader is referred to the web version of this article.)

to measured pulse duration of ~240 fs. For pulse energies above 2 μJ, transform-limited and measured ACF widths differ significantly. This could be attributed to the accumulation of nonlinear phase which cannot be completely compensated in the system. Accumulated nonlinear phase was partly compensated by changing dispersion of CFBG stretcher. When pulse energy was increased, a linear temperature gradient of 13 °C per 50 mm of CFBG length was applied to achieve shortest pulse duration. Optimal thermally induced GVD was estimated to be 0.077 ps<sup>2</sup> for 10 μJ pulse energy. When the dispersion curve of the CFBG is changed by the temperature gradient along the CFBG length, the third order dispersion (TOD) of the CFBG is changed too. However, the change of the TOD with the linear temperature distribution implemented in this work was very low, estimated to be -0.00012 ps<sup>3</sup> and does not affect the compressed pulse. Accumulated nonlinear phase-shift is characterized by B-integral, which was estimated to be 1.4π rad for 10 μJ pulse energy using phase-compensation relation derived in Ref. [31]. Accumulated nonlinear phase shift, estimated using the compensating gradient values for three different energies is indicated in Fig. 4(a) by arrows. Measured autocorrelation traces of compressed pulses after CVBG with non-compensated nonlinear phase and partly compensated nonlinear phase at 10 μJ pulse energy is shown in Fig. 4(b). The partially compensated nonlinear phase enables for higher temporal pulse quality and higher peak power. Residual nonlinear phase shift can also be compensated by TOD [32] or could be used to compensate the dispersion mismatch in the system [33] to improve the pulse quality.

The output pulse duration after the CVBG compressor was also measured using second harmonic generation (SHG) frequency-resolved optical gating (FROG) autocorrelation method for 1 μJ and 10 μJ pulse energies. Pulse envelopes retrieved by FROG algorithm (*Swamp Optics*) are shown in Fig. 5(a). FROG retrieval yielded a retrieval error of 0.1%

and was performed on a 1024 × 1024 grid. Retrieved pulse durations were 247 fs for 1 μJ and 349 fs for 10 μJ pulses energies.

Transform-limited pulse duration calculated from measured spectrum was about 220 fs at all measured pulse energies. Temporal Strehl ratio, which is defined as ratio of the peak power of the pulse to the peak power of transform-limited pulse, was estimated to be 0.88 for 1 μJ and 0.61 for 10 μJ pulse energy. Amplified spontaneous emission (ASE) power level was estimated from the laser spectrum before the compressor at 10 μJ pulse energy (inset of Fig. 5(b)). After CVBG compressor ASE accounted for about 2% (~7 mW) of the total (359 mW) output power. As it was mentioned, modest pulse quality degradation can be attributed to the nonlinear phase (~1.4π rad) in the small mode area (~100 μm<sup>2</sup>) fiber amplifier. This is also confirmed by a residual phase retrieved from FROG shown in Fig. 5(b) along the measured spectrum. The enhancement of spectral modulations due to SPM was also observed (Fig. 5(b)). The initial spectral modulation could arise from group delay ripples of the CFBG stretcher or from the internal reflections in micro-optical components used in the FCPA system. It was previously shown that small initial spectral modulation leads to pulse contrast degradation in nonlinear CPA system [34,35]. Small amplitude (~1%) satellite pulses in the range of 3–5 ps from the main pulse can be seen in Fig. 5(a). The spacing of the satellite pulses matches well with modulation frequency of the spectrum. Despite large nonlinear phase and high pulse compression ratio (~660), overall temporal quality of the compressed pulses at highest energy was still quite good.

Incident beam diameter at the input of the CVBG was about 1.1 mm (at 1/e<sup>2</sup> level). Beam quality at the output of the system was measured by performing z-scan at 10 μJ pulse energy. Measured beam quality parameter M<sup>2</sup> ~1.06 in directions perpendicular to the propagation axis was close to the diffraction limit indicating excellent beam spatial

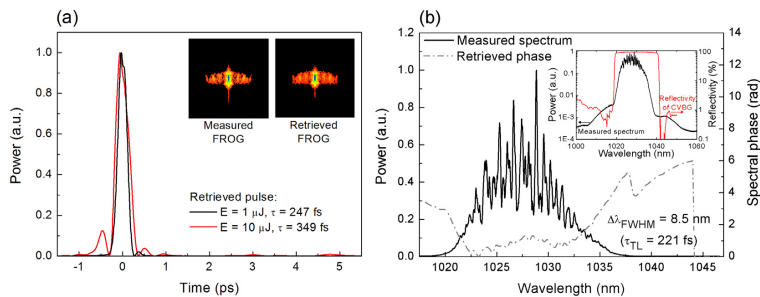


Fig. 5. a) Envelope of the compressed pulses retrieved from SHG FROG measurement for 1 μJ and 10 μJ pulse energies. Inset: measured and retrieved FROG traces for 10 μJ pulse energy. b) Measured pulse spectrum from the FCPA system at 10 μJ pulse energy along with retrieved spectral phase from FROG. Inset: Measured pulse spectrum before CVBG compressor showed in logarithmic scale together with measured reflectivity profile of CVBG.

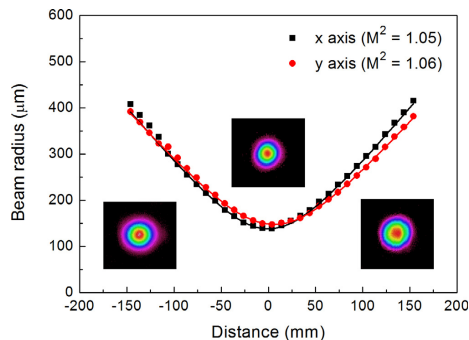


Fig. 6. The measurement of the beam quality parameter  $M^2$  ( $4\sigma$ ) for both directions perpendicular to the axis of propagation at the output of the high energy FCPA system. Insets: beam intensity profiles at three different positions from the waist location.

properties (Fig. 6), as it could be expected from a single mode fiber amplifier. This also indicates good optical homogeneity of photo-thermo-refractive glass as well as precise control of geometry of the holographically recorded chirped Bragg grating.

### 3. Conclusion

In this work we presented compact FCPA system employing the matched pair of CFBG stretcher and CVBG compressor. High temporal and spatial quality femtosecond laser pulses with 10  $\mu$ J pulse energy were generated at the output of the system despite large nonlinear phase-shift and high pulse compression ratio. Accumulated nonlinear phase-shift due to SPM was partly compensated by positive dispersion which was induced by temperature distribution along the CFBG stretcher. This FCPA configuration paves the way for truly compact, robust and environmentally stable femtosecond fiber laser sources with high peak and modest average power suitable for many nonlinear optical applications.

### Funding

This work has been funded by Research Council of Lithuania under contract LAT-10/2016.

### References

- [1] F. Beier, C. Hupel, S. Kuhn, S. Hein, J. Nold, F. Proske, B. Sattler, A. Liem, C. Jauregui, J. Limpert, N. Haarlammert, T. Schreiber, R. Eberhardt, A. Tünnermann, Single mode 4.3 kW output power from a diode-pumped Yb-doped fiber amplifier, *Opt. Express* 25 (2017) 14892–14899, <http://dx.doi.org/10.1364/OE.25.014892>.
- [2] F. Köttig, F. Tani, C.M. Biersach, J.C. Travers, P.S.J. Russell, Generation of microjoule pulses in the deep ultraviolet at megahertz repetition rates, *Optica* 4 (2017) 1272–1276, <http://dx.doi.org/10.1364/OPTICA.4.001272>.
- [3] A. Alismail, H. Wang, N. Altawirjy, H. Fattahi, Carrier-envelope phase stable, 5.4  $\mu$ J, broadband, mid-infrared pulse generation from a 1-ps, Yb:YAG thin-disk laser, *Appl. Opt.* 56 (2017) 4990–4994, <http://dx.doi.org/10.1364/AO.56.004990>.
- [4] K. Jain, C.G. Willson, B.J. Lin, Ultrafast deep UV lithography with excimer lasers, *IEEE Electron Dev. Lett.* 3 (1982) 53–55, <http://dx.doi.org/10.1109/EDL.1982.25476>.
- [5] L. Velarde, H.-F. Wang, Unified treatment and measurement of the spectral resolution and temporal effects in frequency-resolved sum-frequency generation vibrational spectroscopy (SFG-VS), *PCP* 15 (2013) 19970, <http://dx.doi.org/10.1039/C3CP2577E>.
- [6] E.H.K. Stelzer, Light-sheet fluorescence microscopy for quantitative biology, *Nat. Methods* 12 (2015) 23–26, <http://dx.doi.org/10.1038/nmeth.3219>.
- [7] J. Huisken, D.Y.R. Stainier, Selective plane illumination microscopy techniques in developmental biology, *Development* 136 (2009) 1963–1975, <http://dx.doi.org/10.1242/dev.022426>.
- [8] D. Strickland, G. Mourou, Compression of amplified chirped optical pulses, *Opt.*

- Commun. 56 (1985) 219–221, [http://dx.doi.org/10.1016/0030-4018\(85\)90120-8](http://dx.doi.org/10.1016/0030-4018(85)90120-8).
- [9] G. Imeshev, I. Hartl, M.E. Fermann, Chirped pulse amplification with a nonlinearly chirped fiber Bragg grating matched to the Treacy compressor, *Opt. Lett.* 29 (2004) 679–681, <http://dx.doi.org/10.1364/OL.29.00679>.
- [10] A. Galvanauskas, M. Fermann, Optical pulse amplification using chirped Bragg grating, US Patent 5,499,143 (1996).
- [11] A. Galvanauskas, A. Heaney, I. Erdogan, D. Harter, Use of volume chirped Bragg gratings for compact high-energy chirped pulse amplification circuits, *Conf. on Lasers and Electro-Optics* 6 (1998) 362, <http://dx.doi.org/10.1109/CLEO.1998.676304>.
- [12] K.-H. Liao, M.-Y. Cheng, E. Flecher, V. Smirnov, L.B. Glebov, A. Galvanauskas, Large-aperture chirped volume Bragg grating based fiber CPA system, *Opt. Express* 15 (2007) 4876–4882, <http://dx.doi.org/10.1364/OE.15.004876>.
- [13] L.B. Glebov, V. Smirnov, E. Rotari, I. Cohanoschi, I. Glebova, O.V. Smolitski, J. Lumeau, C. Lanigua, A. Glebov, Volume-chirped Bragg gratings: monolithic components for stretching and compression of ultrashort laser pulses, *Proc. Opt. Eng.* 53 (2014) 051514, <http://dx.doi.org/10.1117/1.0.53.5.051514>.
- [14] G. Chang, M. Reyer, V. Smirnov, L. Glebov, A. Galvanauskas, Femtosecond Yb-fiber chirped-pulse amplification system based on chirped-volume Bragg gratings, *Opt. Lett.* 34 (2009) 2952–2954, <http://dx.doi.org/10.1364/OL.34.002952>.
- [15] S. Frankinas, A. Michailovas, N. Rusteika, V. Smirnov, R. Vasilyeu, A.L. Glebov, Efficient ultrafast fiber laser using chirped fiber Bragg grating and chirped volume Bragg grating stretcher/compressor configuration, *Proc. SPIE* 9730 (2016) 973017, <http://dx.doi.org/10.1117/12.2214720>.
- [16] A. Yustin, I. Samartsev, O. Shkurikhin, D. Myasnikov, A. Bordenyuk, N. Platonov, V. Kancharla, V. Gaponov, New generation of high average power industry grade ultrafast ytterbium fiber lasers, *Proc. SPIE* 9728 (2016) 972839, <http://dx.doi.org/10.1117/12.2212916>.
- [17] T. Bartulevičius, S. Frankinas, A. Michailovas, R. Vasilyeu, V. Smirnov, F. Trepanier, N. Rusteika, Compact fiber CPA system based on a CFBG stretcher and CVBG compressor with matched dispersion profile, *Opt. Express* 25 (2017) 19856–19862, <http://dx.doi.org/10.1364/OE.25.019856>.
- [18] A. Galvanauskas, Mode-scalable fiber-based chirped pulse amplification systems, *IEEE J. Sel. Top. Quantum Electron.* 7 (2001) 504, <http://dx.doi.org/10.1109/2944.974221>.
- [19] A. Galvanauskas, M.Y. Cheng, K.C. Hou, K.H. Liao, High peak power pulse amplification in large core Yb-doped fiber amplifiers, *IEEE J. Sel. Top. Quantum Electron.* 13 (2007) 559–566, <http://dx.doi.org/10.1109/JSTQE.2007.899145>.
- [20] F. Röser, D. Schimpf, O. Schmidt, B. Ortaç, K. Rademaker, J. Limpert, A. Tünnermann, 90 W average power 100  $\mu$ J energy femtosecond fiber chirped-pulse amplification system, *Opt. Lett.* 32 (2007) 2230–2232, <http://dx.doi.org/10.1364/OL.32.002230>.
- [21] J. Limpert, N. Deguil-Robin, I. Manek-Höninger, F. Salin, F. Röser, A. Liem, T. Schreiber, S. Nolte, H. Zellmer, A. Tünnermann, J. Broeng, A. Petersson, C. Jakobsen, High-power rod-type photonic crystal fiber laser, *Opt. Express* 13 (2005) 1055–1058, <http://dx.doi.org/10.1364/OPEX.13.001055>.
- [22] X. Ma, C. Zhu, I. Hu, A. Kaplan, A. Galvanauskas, Single-mode chirally-coupled-core fibers with larger than 50  $\mu$ m diameter cores, *Opt. Express* 22 (2014) 9206–9219, <http://dx.doi.org/10.1364/OE.22.009206>.
- [23] J. Želudevičius, R. Danilevičius, K. Viskontas, N. Rusteika, K. Regelskis, Femtosecond fiber CPA system based on picosecond master oscillator and power amplifier with CCC fiber, *Opt. Express* 21 (2013) 5338–5345, <http://dx.doi.org/10.1364/OE.21.005338>.
- [24] V. Filippov, Yu. Chamorovskii, J. Kertulla, K. Golant, M. Pessa, O.G. Okhotnikov, Double clad tapered fiber for high power applications, *Opt. Express* 16 (2008) 1929–1944, <http://dx.doi.org/10.1364/OE.16.001929>.
- [25] V. Filippov, J. Kertulla, Y. Chamorovskii, K. Golant, O.G. Okhotnikov, Highly efficient 750 W tapered double-clad ytterbium fiber laser, *Opt. Express* 18 (2010) 12499–12512, <http://dx.doi.org/10.1364/OE.18.012499>.
- [26] J. Squier, M. Müller, High resolution nonlinear microscopy: a review of sources and methods for achieving optimal imaging, *Rev. Sci. Instrum.* 72 (2001) 2855–2867, <http://dx.doi.org/10.1063/1.1379598>.
- [27] C. Xu, F.W. Wise, Recent advances in fiber lasers for nonlinear microscopy, *Nat. Photon.* 7 (2013) 875–882, <http://dx.doi.org/10.1038/nphoton.2013.284>.
- [28] C. Macias-Romero, M.E.P. Didier, P. Jourdain, P. Marquet, P. Magistretti, O.B. Tarun, V. Zubkova, A. Radenovic, S. Roke, High throughput second harmonic imaging for label-free biological applications, *Opt. Express* 22 (2014) 31102–31112, <http://dx.doi.org/10.1364/OE.22.031102>.
- [29] C. Macias-Romero, V. Zubkova, S. Wang, S. Roke, Wide-field medium-repetition-rate multiphoton microscopy reduces photodamage of living cells, *Biomed. Opt. Express* 7 (2016) 1458–1467, <http://dx.doi.org/10.1364/BOE.7.001458>.
- [30] T.V. Andersen, O. Schmidt, C. Bruchmann, J. Limpert, C. Aguerregaray, E. Cormier, A. Tünnermann, High repetition rate tunable femtosecond pulses and broadband amplification from fiber laser pumped parametric amplifier, *Opt. Express* 14 (2006) 4765–4773, <http://dx.doi.org/10.1364/OE.14.004765>.
- [31] D.N. Schimpf, E. Seise, J. Limpert, A. Tünnermann, Self-phase modulation compensated by positive dispersion in chirped-pulse systems, *Opt. Express* 17 (2009) 4997–5007, <http://dx.doi.org/10.1364/OE.17.004997>.
- [32] A. Chong, L. Kummetsova, F.W. Wise, Theoretical optimization of nonlinear chirped-pulse fiber amplifiers, *J. Opt. Soc. Am. B* 24 (2007) 1815–1823, <http://dx.doi.org/10.1364/JOSAB.24.001815>.
- [33] H. Song, B. Liu, L. Wen, C. Wang, M. Hu, Optimization of nonlinear compensation in a high-energy femtosecond fiber CPA system by negative TOD filter, *IEEE Photon. J.* 9 (2017) 3200110, <http://dx.doi.org/10.1109/JPHOT.2017.2681704>.
- [34] D.N. Schimpf, E. Seise, J. Limpert, A. Tünnermann, Decrease of pulse-contrast in nonlinear chirped-pulse amplification systems due to high-frequency spectral phase ripples, *Opt. Express* 16 (2008) 8876–8886, <http://dx.doi.org/10.1364/OE.16.008876>.
- [35] D.N. Schimpf, E. Seise, J. Limpert, A. Tünnermann, The impact of spectral modulations on the contrast of pulses of nonlinear chirped-pulse amplification systems, *Opt. Express* 16 (2008) 10664–10674, <http://dx.doi.org/10.1364/OE.16.010664>.

A3

COMPACT HIGH-POWER GHZ INTRA-BURST REPETITION RATE  
ALL-IN-FIBER CPA SYSTEM WITH LMA FIBER POWER AMPLIFIER

**T. Bartulevičius**, K. Madeikis, L. Veselis, A. Michailovas

Proc. SPIE **11260**, 112602F (2020)

Reprinted with permission from SPIE

The publication may also be viewed on the official SPIE Digital Library  
DOI: 10.1117/12.2545665

# PROCEEDINGS OF SPIE

[SPIDigitalLibrary.org/conference-proceedings-of-spie](https://spiedigitallibrary.org/conference-proceedings-of-spie)

## Compact high-power GHz intra-burst repetition rate all-in-fiber CPA system with LMA fiber power amplifier

Bartulevičius, Tadas, Madeikis, Karolis, Veselis, Laurynas, Michailovas, Andrejus

Tadas Bartulevičius, Karolis Madeikis, Laurynas Veselis, Andrejus Michailovas, "Compact high-power GHz intra-burst repetition rate all-in-fiber CPA system with LMA fiber power amplifier," Proc. SPIE 11260, Fiber Lasers XVII: Technology and Systems, 112602F (21 February 2020); doi: 10.1117/12.2545665

**SPIE.**

Event: SPIE LASE, 2020, San Francisco, California, United States

Downloaded From: <https://www.spiedigitallibrary.org/conference-proceedings-of-spie> on 05 Mar 2020 Terms of Use: <https://www.spiedigitallibrary.org/terms-of-use>

# Compact high-power GHz intra-burst repetition rate all-in-fiber CPA system with LMA fiber power amplifier

Tadas Bartulevičius<sup>\*a,b</sup>, Karolis Madeikis<sup>a,b</sup>, Laurynas Veselis<sup>a,b</sup>, Andrejus Michailovas<sup>a,b</sup>  
<sup>a</sup>Ekspla Ltd, Savanoriu Ave. 237, LT-02300 Vilnius, Lithuania; <sup>b</sup>Center for Physical Sciences and Technology, Savanoriu Ave. 231, LT-02300, Vilnius, Lithuania

## ABSTRACT

A compact high-power femtosecond (~640 fs) GHz intra-burst repetition rate all-in-fiber CPA system operating at 3.26 GHz intra-burst and 200 kHz burst repetition rate regime with two configurations of large mode area (LMA and PCF) cladding-pumped Yb-doped fiber power amplifiers were presented in this work. Significantly high average power levels of 6 W (LMA fiber power amplifier) and >20 W (PCF power amplifier) were achieved which corresponded to a maximum energy of 30 μJ and >100 μJ per burst respectively.

Two burst shaping layouts were introduced in this experimental setup obtaining desired burst shape using one or two acousto-optic modulators, pulse repetition rate multiplier based on a cascaded 2x2 fiber coupler sequence with a splitting ratio of 50/50 and controlled using arbitrary waveform generator.

High power all-in-fiber CPA system with LMA fiber power amplifier operating at GHz burst regime was compared to the system operating at MHz pulse repetition rate regime which allowed to achieve 1.5 μJ energy pulses of good pulse quality at the output of the laser system at a repetition rate of 4 MHz.

**Keywords:** Ultrafast fiber laser, high power, GHz intra-burst repetition rate, femtosecond pulses, LMA fiber amplifier

## 1. INTRODUCTION

High energy ultrashort pulse fiber chirped pulse amplification (FCPA) systems are attractive for micromachining applications because of their reliability, excellent beam quality and high output power. These applications require carefully tailored output parameters of the laser system. The amplification of ultrashort optical pulses in fiber amplifiers is limited by nonlinear effects due to long interaction length and small mode area of the gain fibers. Chirped pulse amplification technique allows to reduce the nonlinear effects and to achieve significantly higher pulse energies up to tens of μJ from single mode fiber amplifiers<sup>1</sup>.

In our previous work, we presented a compact femtosecond FCPA system producing 10 μJ energy pulses and sub-W average power, with a core-pumped single mode (11 μm) polarization maintaining Yb-doped fiber amplifier, suitable for precise microfabrication or various bio-imaging applications requiring moderate average power<sup>2</sup>. However, a number of advanced applications needs to scale the average power to tens of Watts power levels. To increase output power of the FCPA systems, scaling of mode-field diameter using special fiber designs, such as large mode area (LMA) fibers<sup>3,4</sup>, photonic crystal fibers (PCF)<sup>5,6</sup>, chirally-coupled-core (CCC) fibers<sup>7,8</sup> or tapered fibers<sup>9,10</sup> and high-power pump is used.

Recently demonstrated new material removal mechanism with bursts of ultrafast pulses, called ablation-cooled laser material removal mechanism, allowed to achieve significantly higher ablation efficiency and to maintain the high quality of ultrafast laser ablation<sup>11</sup>. This material processing regime requires tens to hundreds of microjoules energies per burst of laser pulses and ~tens of Watts of average power. In this system, GHz pulse repetition rates in the bursts were achieved using repetition rate multiplier based on cascaded fiber couplers<sup>12</sup>. GHz pulse trains suitable for burst shaping could be generated in fiber laser systems by several alternative methods<sup>13,14</sup>.

In this work we present two burst shaping layouts which allowed to obtain desired burst shape using one or two acousto-optic modulators, pulse repetition rate multiplier based on a cascaded 2x2 fiber coupler sequence and controlled using arbitrary waveform generator. A compact high-power femtosecond GHz intra-burst repetition rate all-in-fiber CPA system

\*t.bartulevicius@ekspla.com; phone 370 5 264 96 29; fax 370 5 264 18 09; ekspla.com

operating at 3.26 GHz intra-burst and 200 kHz burst repetition rate regime with two configurations of large mode area (LMA and PCF) cladding-pumped Yb-doped fiber power amplifiers is presented.

## 2. EXPERIMENTAL SETUP AND RESULTS

### 2.1 Pulse repetition rate multiplier and burst formation

In this work, GHz pulse repetition rates were achieved using a cascaded 2x2 fiber coupler (FC) sequence with a splitting ratio of 50/50 (Fig. 1(a)). Input pulses were split in to two output arms and then combined in the next fiber coupler. Each coupler had output arms of different lengths, and the length difference introduces a delay between two replicas equal to a half of the signal inter-pulse period at the input of that coupler. Such pulse repetition rate (PRR) multiplier doubled PRR at each stage, beginning with the second coupler. Therefore, after 6 fiber couplers the pulse repetition rate was multiplied by  $2^5$  and after 7 couplers -  $2^6$ . The initial pulse repetition rate of 50.93 MHz from the oscillator were multiplied to 1.63 GHz and 3.26 GHz pulse repetition rates using multiplier which consisted of 6 and 7 fiber couplers respectively (Fig. 1(a-b)). Quite large variation in pulse amplitudes was observed due to the variation of splitting ratio of the fiber couplers. These pulse amplitude variations could be reduced by introducing losses in each of the fiber coupler output arms, however it was not performed in this work since it was not critical for successive amplification.

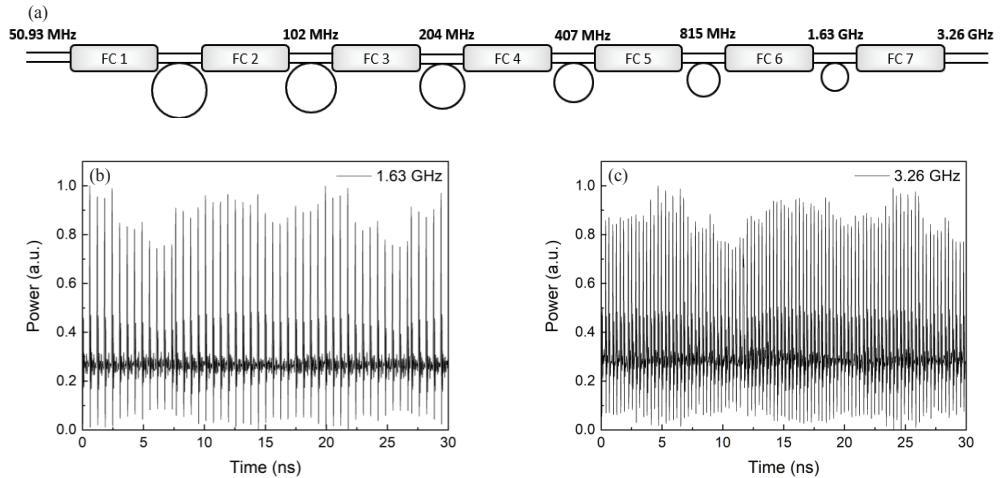


Figure 1. a) Schematic presentation of high pulse repetition rate multiplier. FC – fiber coupler (50/50 splitting ratio). b-c) Pulse train measured after the pulse repetition rate multiplier containing 6 and 7 fiber couplers and resulting 1.63 GHz and 3.26 GHz pulse repetition rates respectively.

Two burst formation configurations were introduced in the experimental setup to obtain desired burst shape. In the first configuration pulse repetition rate of 50.93 MHz from the all-in-fiber seed source were multiplied in repetition rate multiplier to 3.26 GHz (Fig. 2(a)). The burst of GHz pulses was formed using one acousto-optic modulator (AOM) after the multiplier and by picking the packet of desired width from the GHz pulse train. The temporal profile of the burst depends on the AOM performance (rise/fall time) and is well illustrated by a Gaussian-like envelope of the burst of the shortest possible width of 20 ns in Fig. 2(b). The laser system was also able to produce arbitrarily long rectangular shape bursts of 500 ns width, containing approximately 1600 of pulses. The burst train of 200 ns width is shown in Fig. 2(c).

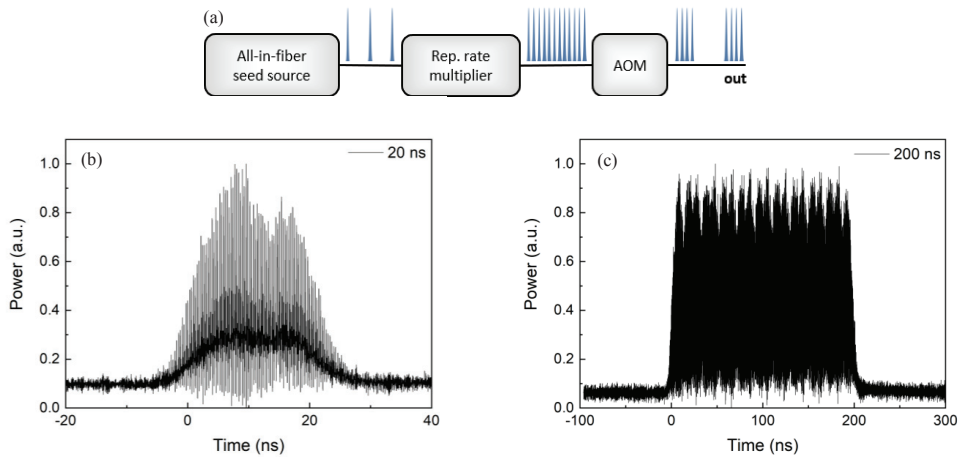


Figure 2. a) Schematic presentation of high pulse repetition rate burst formation using one acousto-optic modulator (AOM). b-c) Experimentally measured 20 ns and 200 ns width 3.26 GHz burst train containing approximately 64 and 640 pulses respectively.

In the second configuration pulse repetition rate from the seed source was decreased using first AOM by forming MHz repetition rate train (Fig. 3(a)). Pulse repetition rate multiplier multiplied these MHz pulses transforming them to GHz burst at the output of the multiplier. The second AOM was used in the further system for additional GHz burst shaping together with arbitrary waveform generator. In this case, rectangular-like bursts were obtained at a minimum packet width of 20 ns and were independent of the AOM performance (Fig. 3(b)). Steeper slopes were also obtained for arbitrarily long bursts however this advantage diminishes for longer bursts (Fig. 3(c)).

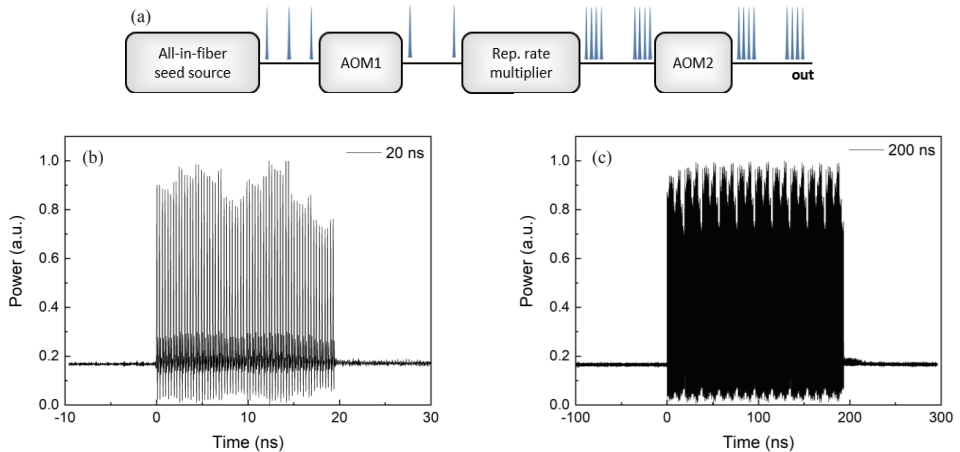


Figure 3. a) Schematic presentation of high pulse repetition rate burst formation using two acousto-optic modulators (AOM1 and AOM2). b-c) Experimentally measured 20 ns and 200 ns width 3.26 GHz burst train with steeper slopes containing approximately 64 and 640 pulses respectively.

## 2.2 High-power GHz intra-burst repetition rate all-in-fiber CPA system with LMA fiber power amplifier

Schematic presentation of the developed high-power fiber chirped pulse amplification (FCPA) system operating at GHz intra-burst regime is illustrated in Fig. 4. Pulses from the seed source generated by passively mode-locked all-in-fiber oscillator operating at average soliton pulse regime (1029.4 nm center wavelength and 50.93 MHz pulse repetition rate) were down-chirped to about 220 ps duration by using chirped fiber Bragg grating (CFBG) stretcher with group delay dispersion (GDD) of  $\beta_2 = -33.7 \text{ ps}^2$ . Thermal tuning of the CFBG was used for fine dispersion control.

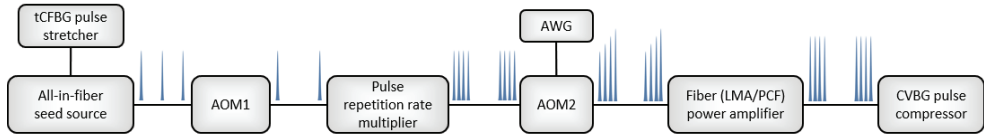


Figure 4. Schematic presentation of the high power FCPA system operating at GHz intra-burst regime. tCFBG – thermally tunable chirped fiber Bragg grating module, AOM – acousto-optic modulator, AWG – arbitrary waveform generator, LMA – large mode area fiber amplifier, PCF – photonic crystal fiber amplifier, CVBG – chirped volume Bragg grating.

Spectrum of the stretched pulses from the all-in-fiber seed source is shown in Figure 5. A relatively narrow spectrum of the pulses (3.44 nm at full width at half maximum (FWHM)) was selected in this work so that the dispersion would have a smaller impact on the pulse duration after spread through sufficiently long fiber delay lines in the pulse repetition rate multiplier. At the same time, it was enough to support femtosecond pulse duration at the output of the system. A Fourier-transform-limited pulse duration derived from the spectrum was about 540 fs.

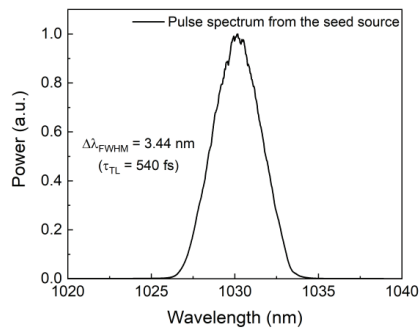


Figure 5. Spectrum of the stretched seed pulses.

The burst of GHz pulses was produced using setup of two acousto-optic modulators and pulse repetition rate multiplier based on cascaded fiber-based delay lines and controlled using second acousto-optic modulator and arbitrary waveform generator (AWG) to obtain desired burst shape after amplification. Burst of pulses at 200 kHz burst repetition rate were amplified in a cladding pumped single-mode (core diameter of 11  $\mu\text{m}$ ) Yb-doped fiber amplifier up to  $\sim 6 \text{ W}$  of average power after pulse compressor. Dependence of average output power after pulse compressor on burst width at constant pump power (12.5 W) without burst pre-shaping is shown in Fig. 6(a). At 20 ns burst width average output power was reduced by less than 10% to 5.53 W though seed power before the power amplifier was reduced nearly two times from 129 mW at 500 ns burst width to 69 mW at 20 ns. Weak dependence of average output power on seed input power manifests high level of the saturation in the power amplifier.

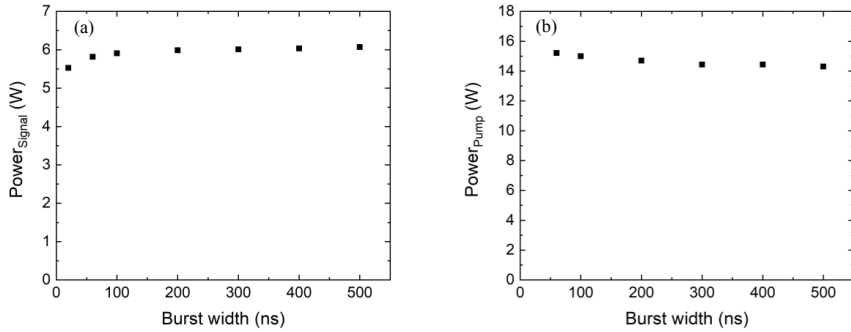


Figure 6. a) Dependence of average power after pulse compressor on burst width at constant pump power (12.5 W) without burst pre-shaping using AWG. b) Dependence of pump power on burst width required for constant amplified signal power after pulse compressor (6 W) with burst pre-shaping using AWG before power amplifier for desired rectangular-like burst shape at the output of the system.

An exponentially falling burst shape was observed after amplification due to the reduction of the inversion for the trailing part of the non-pre-shaped burst as shown in Fig. 7(Left). The purpose of this work was to achieve rectangular-like burst of GHz pulses with a constant output signal power. The dependence of pump power on burst width required for constant output power after pulse compressor (6 W) with burst pre-shaping using AWG for desired rectangular-like burst shape at the output of the system is shown in Fig. 6(b). The pump power was increased from 14.3 W at 500 ns burst width to 15.2 W at 60 ns. Experimentally measured 3.26 GHz burst trains of 60-500 ns width with burst pre-shaping using arbitrary waveform generator before power amplifier for desired rectangular-like burst shape at the output of the system is depicted in Fig. 7(Right). GHz burst energy of 30  $\mu$ J was achieved at the output of the system at 200 kHz burst repetition rate and 6 W of output power. Single pulse energy in the GHz burst was obtained of  $\sim 0.16$   $\mu$ J at 60 ns burst width and  $\sim 19$  nJ at 500 ns burst width.

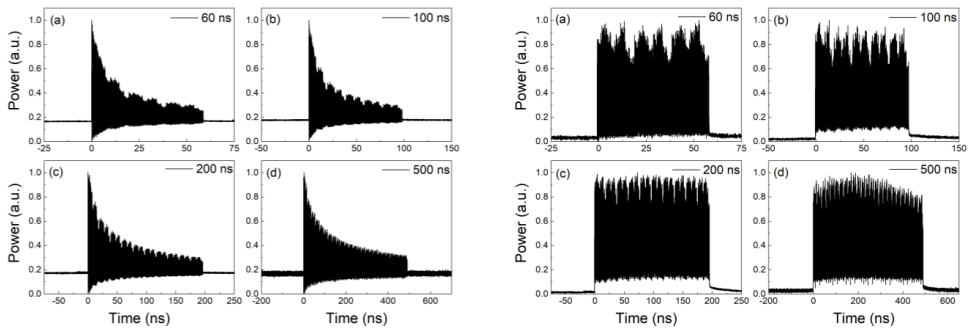


Figure 7. Left: Experimentally measured 3.26 GHz burst trains of 60-500 ns (a-d) width without burst pre-shaping using arbitrary waveform generator before power amplifier. Right: Experimentally measured 3.26 GHz burst trains of 60-500 ns (a-d) width with burst pre-shaping using arbitrary waveform generator before power amplifier for desired rectangular-like burst shape at the output of the system.

Amplified bursts of pulses were compressed in the free space chirped volume Bragg grating (CVBG) compressor. The use of matched pair of a CFBG stretcher and a CVBG compressor in FCPA system allows to build a very compact and robust fiber laser source. Pulse compression quality was examined for different width of GHz bursts using second harmonic non-collinear autocorrelator. No pulse quality degradation was observed since the energy of the individual pulses in the bursts was small enough and nonlinear effects did not limit the amplification of the ultrashort pulses in the power amplifier (Fig. 8(a)). The average duration of the compressed pulses was 640 fs (FWHM for Gaussian-like pulse) and was slightly longer than the bandwidth-limited duration due to the impact of the dispersion of sufficiently long fiber delay lines in the PRR multiplier. Measured pulse spectra from the FCPA system before the CVBG compressor at different burst width are shown in log scale in Fig. 8(b). These spectra show an extremely low level of amplified spontaneous emission (ASE) in the amplified signal, which is further reduced by the CVBG compressor, which has a reflection spectrum bandwidth of 8 nm. The rest of the radiation is filtered off.

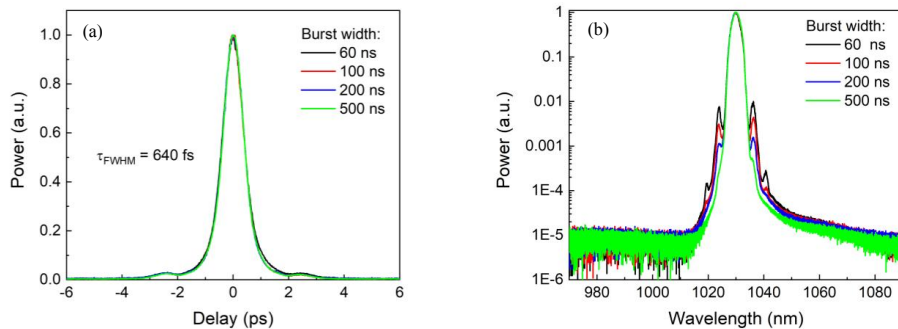


Figure 8. The measured autocorrelation traces of compressed output pulses (a) and pulse spectra before the CVBG compressor (b) of GHz burst of pulses at the output of the FCPA system for different (60-500 ns) burst widths.

Photonic crystal fiber (PCF) power amplifier with 40  $\mu\text{m}$  core diameter was used to achieve average output power levels higher than 20 W. 60 W of pump power was used in this configuration of the system and coupled to the cladding of the fiber amplifier in the backward direction to the seed signal. Rectangular-like bursts of GHz pulses were achieved using burst pre-shaping technique. Dependence of average amplified signal power after pulse compressor on burst width at constant pump power (60 W) with burst pre-shaping using AWG before power amplifier for desired rectangular-like burst shape at the output of the system is shown in Fig. 9(a). Amplified signal power levels of  $>20$  W were achieved at all burst width at 200 kHz burst PRR resulting burst energies of  $>100$   $\mu\text{J}$ . Single pulse energy in the GHz burst was obtained of  $\sim 0.57$   $\mu\text{J}$  at 60 ns burst width and  $\sim 72$  nJ at 500 ns burst width.

Pulse compression quality for different width of GHz bursts was also examined and no pulse quality degradation was observed (Fig. 9(b)). Measured pulse spectra from the FCPA system before the CVBG compressor at different burst width are shown in log scale in Fig. 9(c) and manifests an extremely low level of amplified spontaneous emission in the amplified signal as well.

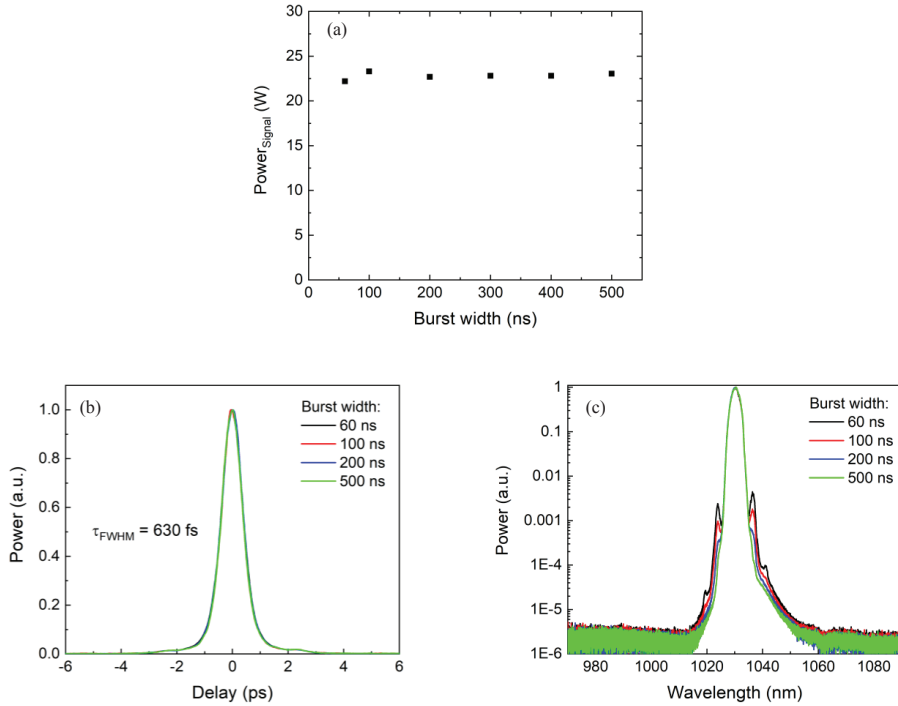


Figure 9. a) Dependence of average power after pulse compressor on burst width at constant pump power (60 W) with burst pre-shaping using AWG before power amplifier for desired rectangular-like burst shape at the output of the system. The measured autocorrelation traces of compressed output pulses (b) and pulse spectra before the CVBG compressor (c) of GHz burst of pulses at the output of the FCPA system for different (60-500 ns) burst widths.

### 2.3 High-power MHz repetition rate all-in-fiber CPA system with LMA fiber power amplifier

In previous sections we presented high power FCPA systems operating at GHz intra-burst regime with LMA/PCF fiber amplifiers corresponding output power levels of 6 W/>20 W and burst energies of 30  $\mu$ J/>100  $\mu$ J respectively. In this section we present amplification results of the same 11  $\mu$ m core diameter LMA fiber power amplifier operating in non-burst (single pulse) regime for comparison to GHz burst amplification mode. A schematic diagram of the experimental setup is presented in Fig. 10.

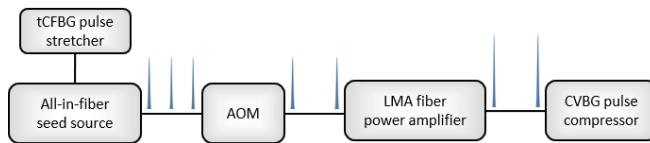


Figure 10. Layout of the high power FCPA system with LMA fiber power amplifier operating at MHz pulse repetition rate regime. tCFBG – thermally tunable chirped fiber Bragg grating module, AOM – acousto-optic modulator, LMA – large mode area fiber amplifier, CVBG – chirped volume Bragg grating.

The whole scheme of the experiment is similar to depicted in Figure 4 but PRR multiplier was missing in this configuration. Initial pulse repetition rate from the seed source was reduced using fiber-coupled acousto-optic modulator before the power amplifier. Chirped laser pulses of 2 nJ energy after AOM were amplified up to  $\mu\text{J}$  level pulse energies in the power amplifier at 1 MHz pulse repetition rate.

Pulse compression quality was examined for different output pulse energies (Fig. 11(a)). Significant pulse quality degradation was visible from 1.5  $\mu\text{J}$  output pulses energies and could be attributed to the accumulation of nonlinear phase which cannot be completely compensated in the system. Compressed pulses of 3  $\mu\text{J}$  energy had a picosecond temporal pedestal which contained sufficiently large amount of the pulse energy. Thus, introduced high power FCPA system should operate at a pulse repetition rate of 4 MHz, which corresponds to maximum output power of 6 W while ensuring good pulse quality (1.5  $\mu\text{J}$  pulse energy).

Measured pulse spectra (before the CVBG compressor) from the FCPA system operating at MHz PRR regime at different pulse energies are shown in Fig. 11(b) and manifests an extremely low level of ASE in the amplified signal as in previously described FCPA systems operating at GHz bursts regime.

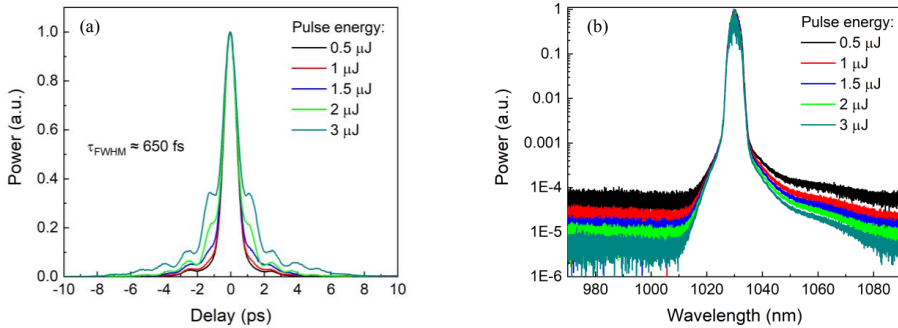


Figure 11. The measured autocorrelation traces of compressed output pulses (a) and pulse spectra before the CVBG compressor (b) of the pulses at the output of the FCPA system for different (0.5-3  $\mu\text{J}$ ) pulse energies.

Beam quality at the output of the system was measured by performing z-scan (Fig. 12). Measured beam quality parameter of  $M^2 \sim 1.05$  was close to the diffraction limit indicating excellent beam spatial properties as it could be expected from a single mode fiber amplifier.

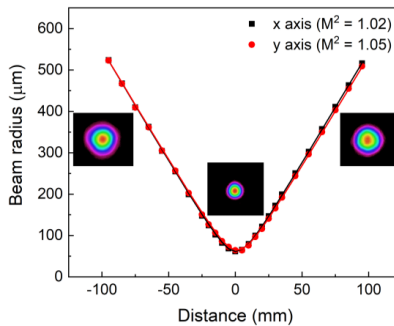


Figure 12. The measurement of the beam quality parameter  $M^2$  at the output of the high power FCPA system. Insets: beam intensity profiles at three different positions from the waist location.

### 3. CONCLUSION

In this work we presented a compact high-power all-in-fiber CPA system producing bursts of laser pulses at 3.26 GHz intra-burst repetition rate and 200 kHz burst repetition rate. These bursts were amplified using two configurations of large mode area (LMA and PCF) cladding-pumped Yb-doped fiber power amplifiers. Both amplifiers operated in well saturated regime and produced high power output of 6 W (11  $\mu\text{m}$  core LMA fiber power amplifier) and more than 20 W (40  $\mu\text{m}$  core PCF power amplifier) which corresponded to a maximum energy of 30  $\mu\text{J}$  and 100  $\mu\text{J}$  per burst respectively. Rectangular-like shaped bursts with durations from 60 ns to 500 ns (containing from  $\sim$ 192 to 1600 pulses) was obtained by means of burst pre-shaping using acousto-optical modulator driven by AWG. The quality of the compressed pulses was examined and proved to be excellent since nonlinear effects did not limit the amplification of the ultrashort pulses in the power amplifier. The average duration of the compressed pulses was about 640 fs (FWHM for Gaussian-like pulse).

GHz pulse train was obtained using pulse repetition rate multiplier based on a cascaded 2x2 fiber coupler sequence with a splitting ratio of 50/50. Furthermore, two burst shaping layouts were introduced in this experimental setup to obtain desired burst shape using one or two acousto-optic modulators and controlled using arbitrary waveform generator.

High power FCPA system with LMA fiber power amplifier operating at GHz burst regime was compared to the system operating at MHz pulse repetition rate regime, which produced 1.5  $\mu\text{J}$  energy pulses of good pulse quality at the output of a laser system at a repetition rate of 4 MHz. This energy level is much lower as compared to GHz burst energy of 30  $\mu\text{J}$ . At higher bursts energies one could achieve higher laser machining productivity. Developed FCPA system could be successfully used in ablation-cooled laser material removal experiments.

### REFERENCES

- [1] Strickland, D., Mourou, G., "Compression of amplified chirped optical pulses," *Opt. Commun.* 56, 219–221 (1985).
- [2] Bartulevicius, T., Veselis, L., Madeikis, K., Michailovas, A. and Rusteika, N., "Compact femtosecond 10  $\mu\text{J}$  pulse energy fiber laser with a CFBG stretcher and CVBG compressor," *Opt. Fiber Technol.* 45, 77–80 (2018).
- [3] Galvanauskas, A., "Mode-scalable fiber-based chirped pulse amplification systems," *IEEE J. Sel. Top. Quantum Electron.* 7, 504–517 (2001).
- [4] Galvanauskas, A., Cheng, M. Y., Hou, K. C., Liao, K. H., "High peak power pulse amplification in large core Yb-doped fiber amplifiers," *IEEE J. Sel. Top. Quantum Electron.* 13, 559–566 (2007).
- [5] Röser, F., Schimpf, D., Schmidt, O., Ortaç, B., Rademaker, K., Limpert, J., Tünnermann, A., "90 W average power 100  $\mu\text{J}$  energy femtosecond fiber chirped-pulse amplification system," *Opt. Lett.* 32, 2230–2232 (2007).
- [6] Limpert, J., Deguil-Robin, N., Manek-Hönninger, I., Salin, F., Röser, F., Liem, A., Schreiber, T., Nolte, S., Zellmer, H., Tünnermann, A., Broeng, J., Petersson, A., Jakobsen, C., "High-power rod-type photonic crystal fiber laser," *Opt. Express* 13, 1055–1058 (2005).
- [7] Ma, X., Zhu, C., Hu, L., Kaplan, A., Galvanauskas, A., "Single-mode chirally-coupled-core fibers with larger than 50  $\mu\text{m}$  diameter cores," *Opt. Express* 22, 9206–9219 (2014).
- [8] Želudevičius, J., Danilevičius, R., Viskontas, K., Rusteika, N., Regelskis, K., "Femtosecond fiber CPA system based on picosecond master oscillator and power amplifier with CCC fiber," *Opt. Express* 21, 5338–5345 (2013).
- [9] Filippov, V., Chamorovskii, Yu., Kerttula, J., Golant, K., Pessa, M., Okhotnikov, O. G., "Double clad tapered fiber for high power applications," *Opt. Express* 16, 1929–1944 (2008).
- [10] Filippov, V., Kerttula, J., Chamorovskii, Y., Golant, K., Okhotnikov, O. G., "Highly efficient 750 W tapered double-clad ytterbium fiber laser," *Opt. Express* 18, 12499–12512 (2010).
- [11] Kerse, C., Kalaycıoğlu, H., Elahi, P., Çetin, B., Kesim, D. K., Akçaalan, Ö., Yavaş, S., Aşık, M. D., Öktem, B., Hoogland, H., Holzwarth, R., Ilday, F. Ö., "Ablation-cooled material removal with ultrafast bursts of pulses," *Nature* 537, 84–88 (2016).
- [12] Kerse, C., Kalaycıoğlu, H., Elahi, P., Akçaalan Ö. and Ilday, F. Ö., "3.5-GHz intra-burst repetition rate ultrafast Yb-doped fiber laser," *Opt. Commun.* 366, 404–409 (2016).
- [13] Tang, D. Y., Guo, J., Song, Y. F., Li, L., Zhao, L. M. and Shen, D. Y., "GHz pulse train generation in fiber lasers by cavity induced modulation instability," *Opt. Fiber Technol.* 20, 610–614 (2014).
- [14] Liu, J., Li, X., Zhang, S., Han, M., Han, H. and Yang, Z., "Wavelength-tunable burst-mode pulse with controllable pulse numbers and pulse intervals," *IEEE J. Sel. Top. Quantum Electron.* 25, 8900106 (2019).

A4

ACTIVE FIBER LOOP FOR SYNTHESIZING GHZ BURSTS OF  
EQUIDISTANT ULTRASHORT PULSES

**T. Bartulevicius**, K. Madeikis, L. Veselis, V. Petrauskiene, and  
A. Michailovas

Opt. Express **28**, 13059-13067 (2020)

Reprinted with permission from © The Optical Society

The publication may also be viewed on the official OSA Publishing website  
DOI: 10.1364/OE.389056



# Active fiber loop for synthesizing GHz bursts of equidistant ultrashort pulses

TADAS BARTULEVICIUS,<sup>1,2,\*</sup> KAROLIS MADEIKIS,<sup>1,2</sup> LAURYNAS VESELIS,<sup>1,2</sup> VIRGINIJA PETRAUSKIENE,<sup>1</sup> AND ANDREJUS MICHAILOVAS<sup>1,2</sup>

<sup>1</sup>*Ekspla UAB, Savanoriu Ave. 237, LT-02300 Vilnius, Lithuania*

<sup>2</sup>*Center for Physical Sciences and Technology, Savanoriu Ave. 231, LT-02300 Vilnius, Lithuania*  
*\*t.bartulevicius@ekspla.com*

**Abstract:** We demonstrate a method to synthesize ultra-high repetition rate bursts of ultrashort laser pulses containing any number of pulses within a burst with identical pulse separation and adjustable amplitude. The key element to synthesize the GHz bursts of ultrashort laser pulses is an active fiber loop. The method was implemented in the fiber chirped pulse amplification system to obtain 72 nJ-energy bursts of 20 pulses with a 2.65 GHz intra-burst pulse repetition rate and a 500 kHz burst repetition rate. The dispersion compensation mechanism ensured a mean pulse duration of 570 fs within the bursts.

© 2020 Optical Society of America under the terms of the [OSA Open Access Publishing Agreement](#)

## 1. Introduction

Sources of ultrashort light pulses opened new avenues in science, medicine and industry [1–4]. Picosecond and femtosecond lasers are particularly desirable in material micro- and nanomachining due to superior precision and small heat-affected zone [3,5–7]. Some processing mechanisms are triggered only by femtosecond pulses [8–11]. Machining with ultrafast fiber lasers is attractive for industry due to robustness and small size of the source. They ensure high processing quality, yet at lower ablation efficiency per single pulse. Thus, efforts are made to increase the processing speed by multiplying the pulse repetition rate (PRR) [12–14]. Small separation between consecutive pulses enhances certain processes or provides better quality of the processed site and surroundings [15–17]. High PRR increases the ablation efficiency not only because a number of pulses increases within a certain time interval, but also because less of the deposited laser energy is lost to heat diffusion [18]. On the other hand, the lower energy of pulses is required to achieve the same efficiency at high repetition rates. A proper set of parameters is material dependent.

Highest throughputs of micro-processing are achieved with pulse trains of as high as gigahertz (GHz) repetition rates [12,18,19]. The most desired mode of operation of lasers intended for laser technology is a burst mode, wherein sequences of pulses with a predetermined number and separation of pulses are formed. Bursts of pulses with GHz pulse repetition rate are particularly desirable [12,14,15,20,21].

There are many methods for producing GHz bursts of laser pulses. A typical PRR of pulse trains generated by mode-locked fiber oscillators is in the range from tens up to hundreds of MHz. Direct generation of femtosecond pulses at multi-GHz repetition rates is challenging and impractical [22]. Among numerous pulse repetition rate multiplication techniques [13,14,23–32] there are techniques based on simple delaying a part of radiation coming from the oscillator [15,25–32].

Interferometer-like free-space arrangements [25,26] are limited in smallest achievable pulse separation due to geometry of optical elements. Complexity and size of the free-space arrangements grows with the number of pulses within a burst.

Passive Fabry-Perot cavities [15] are attractive because are small in size, permit generation of small delays (up to 100 GHz intra-burst PRR) and can be adjustable. An exponentially decaying burst amplitude envelope is hardly useful in applications as it requires additional amplification and train shaping.

Fiber solutions [14,28–32] are more attractive as all-fiber laser systems are compact and robust. Cascaded 50/50 fiber couplers in combination with fiber delay lines allow to double pulse repetition rate after each fiber coupler  $2^N$  times. The multiplication of the PRR requires  $(N+1)$  fiber couplers and  $N$  fiber delay lines. The disadvantage of this PRR multiplication approach is the difficulty to maintain equal pulse energies and equal temporal separations due to coupling efficiency asymmetries of the couplers and the difficulty to get precise fiber lengths. Another disadvantage is ultrashort pulse duration variation within a burst since dispersion is not controlled in this solution. Broadband ultrashort pulses that propagate the shortest optical path within the PRR multiplier undergo lowest dispersion, while pulses that propagate the longest optical path, undergo highest dispersion. The more PRR cascades are used, the higher pulse temporal distortion is obtained for broadband radiation. An acousto-optic modulators (AOM) were placed after the PRR multiplier for bursts cutting from the high-PRR pulse train [14,28]. Therefore, minimal width of the bursts was limited by a response time of the AOM. The shortest bell-shaped burst of 15 ns consisting of 50 pulses was demonstrated by S.-s. Min *et al.* [28]. Intra-burst PRR was achieved as high as 3.5 GHz [29].

Liu *et al.* [13] suggested a modified version of the aforementioned method in which the cascade of  $2 \times 2$  50/50 fiber couplers with different arm lengths was used. The delay between two pulse replicas after the first fiber coupler is not equal and much smaller than the half of the period of the input pulse train ( $\Delta T_1 \ll T_0$ ). In the following delay lines, the delays between adjacent pulses are halved after every stage. With  $N$  fiber delay lines the pulse train with  $\Delta T_1/2^{N-1}$  distance between pulses is generated. In this way, quite short bursts of pulses of nearly equal amplitude were shaped. The disadvantages of this approach are similar to those of the previous method: long bursts generation requires many pulse multiplication stages; the absence of dispersion control; pulse separation precision depends on fibers cutting and splicing precision.

Another approach to increase pulse repetition rate is based on the use of the passive fiber loops demonstrated in [30–32]. The seed pulse is injected in the fiber loop through one of input ports of  $2 \times 2$  fiber coupler, and another input port is connected to the one of output ports. The pulse in the loop will circulate while its energy is steadily lost at the fiber coupler. An output of the passive fiber loop consists of pulses with decaying amplitude. The length of the loop determines a delay between replicas of input pulse emerging from the second output port of the fiber coupler.

Wei *et al.* used two [31] and three [32] passive fiber loops to form bursts of several pulses. Using two cascaded passive fiber loops, connected via  $2 \times 2$  fiber couplers with 70/30 and 60/40 splitting ratios, authors of Ref. [31] synthesized a burst of 6 pulses (energy of the seventh and all consequent pulses was negligible). The delay of the first fiber loop was less than a period of pulse train of the fiber oscillator by more than three times ( $T_1 < 3 * T_0$ ), the second fiber loop is half shorter than the first fiber loop ( $T_2 = T_1/2$ ). A pulse delayed by the first loop after one round-trip exactly coincides in time with a pulse delayed by the second loop after two round-trips. Therefore, the cascade of the two fiber loops form a burst of six pulses of different amplitudes, and the third pulse has the highest amplitude. Further pulses are hardly observable because the amplitude of the burst decays fast. The final PRR is defined by the length of the second fiber loop. 16 MHz PRR was demonstrated.

In Ref. [32], three cascaded passive fiber loops ( $T_1 \ll T_0$ ,  $T_2 = T_1/2$ ,  $T_3 = T_2/2$ ) synthesized a burst of 13 pulses. The synthesized burst is a sum of pulse parts circulating multiple round-trips inside the three passive fiber loops of different lengths. The intra-burst pulse repetition rate of 793 MHz was demonstrated and defined by the length of the third fiber loop. Despite a broad

bandwidth of seed radiation, duration of the pulses was preserved because relatively short fibers (104 cm, 52 cm and 26 cm) were used and only a few round-trips were performed.

Solutions with multiple passive fiber loops and no additional elements have several drawbacks. It is impossible to form equal amplitudes of the pulses within the synthesized burst. The burst profile is adjusted only by selection of the splitting ratios of the fiber couplers. No other control of amplitudes is provided. Inaccurate lengths of the loops, which are not strictly in multiple, lead to formation of two or three pulses of small amplitude instead of one pulse. The ultrashort pulse (broadband radiation) circulating many round-trips experiences duration variation and it may depend on an amplitude of the pulse. The third drawback is as follows. The shortest time interval between adjacent intra-burst pulses is defined by the optical length of the shortest fiber loop. There is a minimum length of two fiber pigtailed (approximately 5 cm each) that is needed to accomplish the splicing with a fusion machine. It limits the minimum length of the delay line. Thus, the highest possible PRR that can be achieved by the aforementioned approach is about 2 GHz.

In this work, we present a modified method to synthesize bursts of ultrashort laser pulses with identical pulse separation and adjustable amplitude.

## 2. Experimental setup and results

The burst synthesizing element is an active fiber loop depicted in Fig. 1. The active fiber loop comprises: a fiber coupler which has two input ports and two output ports with the splitting ratio of 50/50, optical circulator, ytterbium doped fiber, chirped fiber Bragg grating, laser diode, acousto-optic modulator and a segment of a passive optical fiber. The loop is formed by connecting one input and one output port (*IN2* and *OUT2* ports in Fig. 1) together with all containing components. All fiber-optic components and optical fiber are polarization maintaining single-mode.

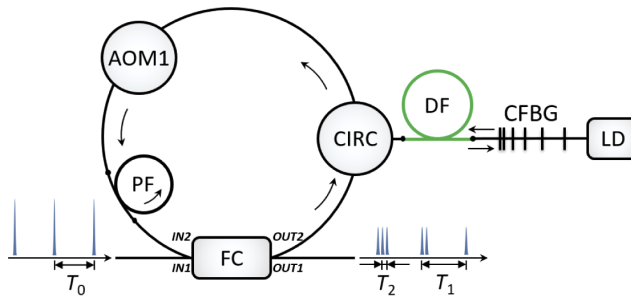


**Fig. 1.** Schematic setup of an active fiber loop. FC – 2x2 fiber coupler (50/50 splitting ratio), CIRC – optical circulator, DF – ytterbium doped fiber, CFBG – chirped fiber Bragg grating, LD – single-mode laser diode, AOM1 – acousto-optic modulator, PF – a segment of a passive optical fiber. *IN1,2* – input ports of the fiber coupler, *OUT1,2* – output ports of the fiber coupler. Time delays:  $T_0$  – between single input pulses,  $T_1$  – between a delayed replica of an input pulse and an undelayed replica of the pulse,  $T_2$  – intra-burst pulse separation of the formed bursts.

The active fiber loop can synthesize bursts of laser pulses with an ultra-high intra-burst pulse repetition rate ( $>2$  GHz) or any desired pulse repetition rate (PRR). A delay  $T_1$  inside the active fiber loop is determined from a pulse period  $T_0$  of an initial pulse train and a desired intra-burst pulse separation  $T_2$  of the synthesized bursts as follows:  $T_1 = T_0 + T_2$ . A required total optical path length of the active fiber loop is estimated from  $T_1$ . In order to obtain the ultra-high intra-burst PRR, a physical length of the loop should be slightly longer than the cavity length of

the master oscillator. The segment of the passive fiber (PF) is inserted into the loop in order to achieve the required total length for the desired intra-burst PRR. Thus, any arbitrary intra-burst pulse repetition rate can be formed, independently from the initial PRR.

The whole operation and burst formation can be explained by observing the propagation of single pulses with pulse separation  $T_0$  of the initial pulse train. The first pulse from the initial pulse train coupled into the fiber coupler is divided into two replicas. One pulse is outcoupled through the first output port *OUT1* and another replica of the pulse is delivered into the active fiber loop through the second output port *OUT2*. The pulse replica propagating through the active fiber loop returns to the fiber coupler a little bit later (time delay  $T_2$ ) than the second pulse from the initial pulse train. They form the first burst containing two pulses. Further, one replica of the pair of pulses is outcoupled through the first output port and another replica of the two pulses is delivered into the active fiber loop again. After the second round-trip, a burst containing three pulses will be formed. After  $N$  round-trips, the burst of  $N+1$  pulses will be formed at the output of the active fiber loop. Thus, arbitrarily long bursts up to a few hundred nanosecond widths can be synthesized using the described method along with an additional temporal modulation of the initial pulse train.

The acousto-optic modulator (AOM1) inside the active fiber loop is used to control the number of pulses within bursts. When a desired number of pulses in the burst is formed, the acousto-optic modulator is turned off (zero transmission of radiation), and circulation of radiation inside the active fiber loop is interrupted. The formation of the bursts is restarted when the acousto-optic modulator is turned on again (the highest transmission of radiation).

Amplitude of pulses is controlled by amplification conditions in the ytterbium doped fiber (DF). Pump radiation from the single-mode laser diode (LD) is coupled to the amplifier through the chirped fiber Bragg grating (CFBG) in this case. It is possible to provide a constant amplitude of the pulses within a burst among the whole train of bursts (Fig. 2). The gain of the doped fiber must compensate the losses of all elements of active fiber loop. It has a property to form a desired shape of amplitude envelope of a burst as well. A decaying amplitude envelope of a burst is obtained [Fig. 3(a)] if the gain of the doped fiber is lower than the level of total losses of the elements. Also, a rising amplitude envelope of a burst is obtained [Fig. 3(b)] if the gain is greater than the losses. Any arbitrary shape of the amplitude envelope – with the resolution of a single

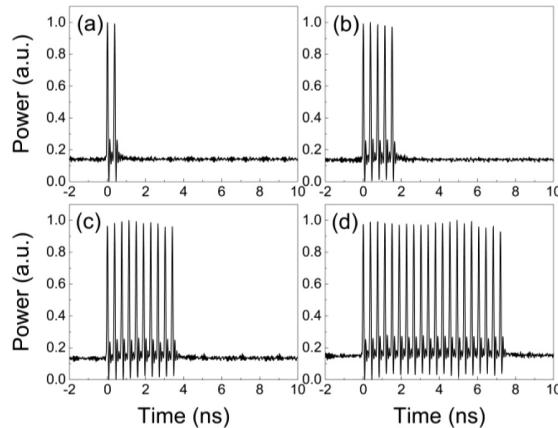


**Fig. 2.** Experimentally measured 2.65 GHz intra-burst PRR burst of pulses containing different number of ultrashort pulses: (a) 2, (b) 5, (c) 10, and (d) 20.

pulse amplitude – can be obtained by actively modulating gain (LD current) or losses (AOM1 transmission) of the active fiber loop. At the output of the active fiber loop, an additional gate (acousto-optic or electro-optic) is placed which selects bursts with a necessary number of pulses.

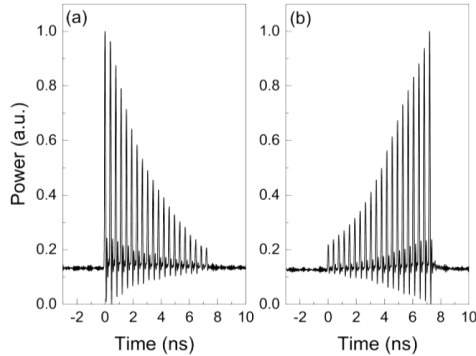


**Fig. 3.** Experimental representation of burst amplitude envelope shaping inside the active fiber loop: (a) decaying amplitude, (b) rising amplitude of pulses.

In order to obtain GHz bursts from the initial pulse train of  $\sim 50$  MHz repetition rate, a total optical path length of the active fiber loop is around 4 meters. The dispersion may have sufficiently big impact on the pulse duration after the propagation through the long active fiber loop. Due to chromatic dispersion, various spectral components undergo different shifts of their phases. As a result, duration of the delayed pulses may be changed. Every consequent pulse of the bursts propagates a longer path and, without dispersion control, a difference of spectral phases is accumulated. That means that a second pulse of the burst will differ from the first pulse, a third pulse will be different from the second and the first pulse, etc. In order to compensate the differences in spectral phases and to obtain bursts of pulses with identical durations, the element with an opposite dispersion to that of the fibers within the active fiber loop is required. A low dispersion (group delay dispersion of  $\beta_2 = -0.0816$  ps<sup>2</sup> at 1030 nm) chirped fiber Bragg grating (CFBG) was used as a dispersion compensation element which operates as a mirror in the presented system. Dispersion compensation element is designed to compensate the chromatic dispersion of the active fiber loop at each round-trip. At an ideal compensation case, pulse duration at the end of the loop is identical to that of the pulse that is outcoupled without propagation through the active fiber loop. Dispersion compensation is preferred for synthesizing GHz bursts of broadband radiation and attaining a few hundred femtosecond pulse duration at the output of the system. A total transmission of the active fiber loop is around 2%. Therefore,

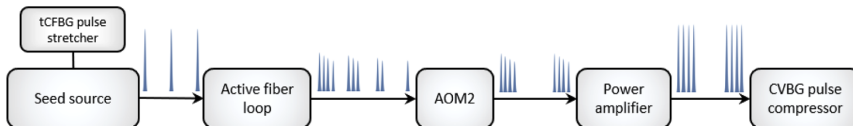


**Fig. 4.** Schematic diagram of the laser system synthesizing GHz bursts of equidistant ultrashort pulses. AOM2 – second acousto-optic modulator in the experimental setup, tCFBG – thermally tunable chirped fiber Bragg grating, CVBG – chirped volume Bragg grating.

amplification of 50 times is required in order to obtain a constant amplitude of the pulses within a burst (as shown in Fig. 2).

The described method was used in the fiber chirped pulse amplification (FCPA) system which provided GHz bursts of nJ level femtosecond pulses. A layout of the laser system is shown in Fig. 4.

The laser system consisted of an all-in-fiber seed source, active fiber loop, additional acousto-optic modulator (AOM2), fiber power amplifier and pulse compressor. Pulses were generated by all-in-fiber passively mode-locked seed source (FFS100CHI, *Ekspla*) operating at 1029.9 nm center wavelength and 50.8 MHz pulse repetition rate. Initial 22 pJ energy laser pulses were down-chirped to about 230 ps duration by using a chirped fiber Bragg grating (tCFBG) stretcher (*TeraXion*) with group delay dispersion (GDD) of  $\beta_2 = -33.7 \text{ ps}^2$ . Thermal tuning of the tCFBG was used for dispersion fine control. Stretched pulses were sent to the active fiber loop in order to ensure that self-phase modulation (SPM) does not distort the spectral phase of the pulses due to amplification. Pulse spectrum from the seed source is shown in Fig. 5.

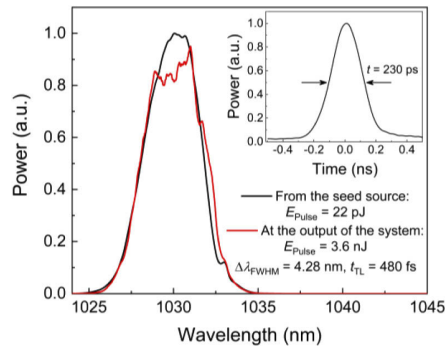


**Fig. 5.** Pulse spectrum from the seed source and at the output of the system. Inset: temporal envelope of the stretched pulses.

The active fiber loop produced the train of bursts with a different number of pulses and 2.65 GHz intra-burst PRR. The second acousto-optic modulator (AOM2) was used as a pulse picker to select only those bursts with an equal number of pulses. The GHz bursts of 500 kHz burst repetition rate containing 20 pulses were amplified in a core-pumped single-mode Yb-doped fiber power amplifier up to 72 nJ burst energy (3.6 nJ individual pulse energy). Rectangular-like burst amplitude [as in Fig. 2(d)] was obtained at the output of the system by adjusting amplification conditions of the fiber amplifier inside the active fiber loop. Rising amplitude of pulses in the bursts after the active fiber loop were required in order to achieve rectangular-like burst amplitude after the power amplifier because trailing part of the burst has smaller gain due to the gain saturation. Pulse spectrum after the power amplifier is compared to the one from the seed source and shown in Fig. 5. A Fourier-transform-limited pulse duration – derived from the measured pulse spectrum [Fig. 5 (red curve)] – was about 480 fs. The formation of the 20 pulses burst required 19 round-trips in the active fiber loop. That corresponds to a propagation of the first replicated pulse in a 78.8-meter long optical fiber. Without dispersion compensation inside the active fiber loop, a broadband pulse [spectrum width of 4.28 nm at full width at half maximum (FWHM)] would elongate up to 9 ps propagating in 78.8 meters of the optical fiber.

Pulse compression was performed in a chirped volume Bragg grating (CVBG) compressor (*OptiGrate*). The quality of compressed pulses was examined using a second harmonic non-collinear autocorrelator. Autocorrelation trace of the compressed pulses operating at GHz burst

regime (burst containing 20 pulses) was compared to the single pulse regime and depicted in Fig. 6. Measured autocorrelation trace had a width of  $\sim 806$  fs (FWHM) which corresponds to  $\sim 570$  fs pulse duration for Gaussian shaped pulses. Close match between GHz burst and single pulse regimes proves that the dispersion of the active fiber loop was successfully compensated by the low dispersion CFBG element. No pulse quality degradation was observed since the 3.6 nJ energy of the individual pulses in the bursts was small enough, and nonlinear effects did not limit the amplification of the ultrashort pulses in the power amplifier as well as in the single pulse regime (individual pulse energy of 8 nJ). A slight difference in the autocorrelation traces may be resulted by the higher order dispersion in the active fiber loop since just the second order dispersion was compensated by the CFBG element. As well as, the difference in compressed pulse duration (570 fs) and Fourier-transform-limited pulse duration (480 fs) can be attributed to a dispersion matching error between the CFBG stretcher and CVBG compressor.

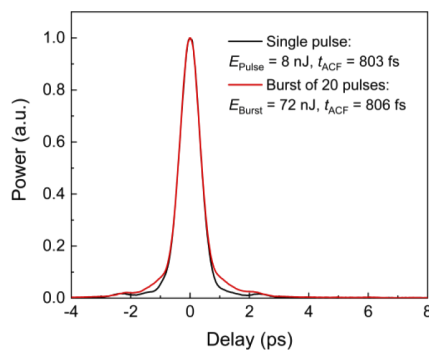


**Fig. 6.** Measured autocorrelation traces of compressed pulses: single pulse regime, ultra-high PRR burst regime (20 pulses).

### 3. Conclusion

We have demonstrated a new method to synthesize ultra-high repetition rate bursts of ultrashort laser pulses with identical pulse separation and adjustable amplitude. A single active fiber loop is able to synthesize bursts of laser pulses containing any number of pulses. Arbitrarily long bursts of a few hundred nanosecond width containing several thousand pulses are possible. The experimental fiber chirped pulse amplification system provided bursts of 2.65 GHz intra-burst PRR and 500 kHz burst repetition rate. Dispersion compensation mechanism was successfully implemented in the active fiber loop to obtain identical pulse durations within the GHz bursts. At the output of the system, 570 fs pulse duration of Gaussian shaped pulses were attained within the 72 nJ-energy burst of 20 pulses.

### Funding

Eurostars (E!12870).

### Disclosures

The authors declare no conflicts of interest.

### References

1. National Academies of Sciences, Engineering, and Medicine, Opportunities in Intense Ultrafast Lasers: Reaching for the Brightest Light (The National Academies, 2018).

2. K. Sugioka and Y. Cheng, "Femtosecond laser three-dimensional micro- and nanofabrication," *Appl. Phys. Rev.* **1**(4), 041303 (2014).
3. K. Sugioka, "Progress in ultrafast laser processing and future prospects," *Nanophotonics* **6**(2), 393–413 (2017).
4. M. Malinauskas, A. Žukauskas, S. Hasegawa, Y. Hayasaki, V. Mizeikis, R. Buividas, and S. Juodkazis, "Ultrafast laser processing of materials: from science to industry," *Light: Sci. Appl.* **5**(8), e16133 (2016).
5. B. N. Chichkov, C. Momma, S. Nolte, F. von Alvensleben, and A. Tünnermann, "Femtosecond, picosecond and nanosecond laser ablation of solids," *Appl. Phys. A* **63**(2), 109–115 (1996).
6. M. Gedvilas, S. Indrišūnas, B. Voisiat, E. Stankevičius, A. Selskis, and G. Račiukaitis, "Nanoscale thermal diffusion during the laser interference ablation using femto-, pico-, and nanosecond pulses in silicon," *Phys. Chem. Chem. Phys.* **20**(17), 12166–12174 (2018).
7. S. Gao and H. Huang, "Recent advances in micro- and nano-machining technologies," *Front. Mech. Eng.* **12**(1), 18–32 (2017).
8. A. Borowiec and H. K. Haugen, "Subwavelength ripple formation on the surfaces of compound semiconductors irradiated with femtosecond laser pulses," *Appl. Phys. Lett.* **82**(25), 4462–4464 (2003).
9. M. Malinauskas, M. Farsari, A. Piskarskas, and S. Juodkazis, "Ultrafast laser nanostructuring of photopolymers: A decade of advances," *Phys. Rep.* **533**(1), 1–31 (2013).
10. M. Beresna, M. Gecevičius, and P. G. Kazansky, "Ultrafast laser direct writing and nanostructuring in transparent materials," *Adv. Opt. Photonics* **6**(3), 293–339 (2014).
11. C. Corbari, A. Champion, M. Gecevičius, M. Beresna, Y. Bellouard, and P. G. Kazansky, "Femtosecond versus picosecond laser machining of nano-gratings and micro-channels in silica glass," *Opt. Express* **21**(4), 3946–3958 (2013).
12. P. Elahi, Ö. Akçaalan, C. Ertek, K. Eken, F. Ö. İlday, and H. Kalaycıoğlu, "High-power Yb-based all-fiber laser delivering 300 fs pulses for high-speed ablation-cooled material removal," *Opt. Lett.* **43**(3), 535–538 (2018).
13. J. Liu, X. Li, S. Zhang, M. Han, H. Han, and Z. Yang, "Wavelength-tunable burst-mode pulse with controllable pulse numbers and pulse intervals," *IEEE J. Sel. Top. Quantum Electron.* **25**(4), 1–6 (2019).
14. X. Wolters, G. Bonamis, K. Mishchick, E. Audouard, C. Hönninger, and E. Mottay, "High power GHz femtosecond laser for ablation efficiency increase," *Procedia Manuf.* **36**, 200–207 (2019).
15. A. Okhrimchuk, S. Fedotov, I. Glebov, V. Sigaev, and P. Kazansky, "Single shot laser writing with sub-nanosecond and nanosecond bursts of femtosecond pulses," *Sci. Rep.* **7**(1), 16563–11 (2017).
16. I. Miyamoto, K. Cvecek, and M. Schmidt, "Crack-free conditions in welding of glass by ultrashort laser pulse," *Opt. Express* **21**(12), 14291–14302 (2013).
17. F. Zimmermann, S. Richter, S. Döring, A. Tünnermann, and S. Nolte, "Ultrastable bonding of glass with femtosecond laser bursts," *Appl. Opt.* **52**(6), 1149–1154 (2013).
18. C. Kerse, H. Kalaycıoğlu, P. Elahi, B. Çetin, D. K. Kesim, Ö. Akçaalan, S. Yavaş, M. D. Aşık, B. Öktem, H. Hoogland, R. Holzwarth, and F. Ö. İlday, "Ablation-cooled material removal with ultrafast bursts of pulses," *Nature* **537**(7618), 84–88 (2016).
19. G. Bonamis, K. Mishchick, E. Audouard, C. Hönninger, E. Mottay, J. Lopez, and I. Manek-Hönninger, "High efficiency femtosecond laser ablation with gigahertz level bursts," *J. Laser Appl.* **31**(2), 022205 (2019).
20. P. Deladurantaye, A. Cournoyer, M. Drolet, L. Desbiens, D. Lemieux, M. Briand, and Y. Taillon, "Material micromachining using bursts of high repetition rate picosecond pulses from a fiber laser source," *Proc. SPIE* **7914**, 791404 (2011).
21. C. Gaudio, G. Giannuzzi, A. Volpe, P. M. Lugarà, I. Choquet, and A. Ancona, "Incubation during laser ablation with bursts of femtosecond pulses with picosecond delays," *Opt. Express* **26**(4), 3801–3813 (2018).
22. D. Y. Tang, J. Guo, Y. F. Song, L. Li, L. M. Zhao, and D. Y. Shen, "GHz pulse train generation in fiber lasers by cavity induced modulation instability," *Opt. Fiber Technol.* **20**(6), 610–614 (2014).
23. R. Maram, L. R. Cortés, J. van Howe, and J. Azaña, "Energy-preserving arbitrary repetition-rate control of periodic pulse trains using temporal talbot effects," *J. Lightwave Technol.* **35**(4), 658–668 (2017).
24. T. Flöry, G. Andriukaitis, M. Barkauskas, E. Kaksis, I. Astrauskas, A. Pugžlys, A. Baltuška, R. Danielius, A. Galvanuskas, and T. Balčiūnas, "High repetition rate fs pulse burst generation using the vernier effect," in *Conference on Lasers and Electro-Optics (2017)* (Optical Society of America, 2017), p. SM4I.5.
25. C. W. Siders, J. L. W. Siders, A. J. Taylor, S.-G. Park, and A. M. Weiner, "Efficient high-energy pulse-train generation using a 2<sup>n</sup>-pulse michelson interferometer," *Appl. Opt.* **37**(22), 5302–5305 (1998).
26. H. Matsumoto, Z. Lin, and J. Kleinert, "Ultrafast laser ablation of copper with ~GHz bursts," *Proc. SPIE* **10519**, 1 (2018).
27. B. Dromey, M. Zepf, M. Landreman, K. O'Keefe, T. Robinson, and S. M. Hooker, "Generation of a train of ultrashort pulses from a compact birefringent crystal array," *Appl. Opt.* **46**(22), 5142–5146 (2007).
28. S.-s. Min, Y. Zhao, and S. Fleming, "Repetition rate multiplication in figure-eight fiber laser with 3 dB couplers," *Opt. Commun.* **277**(2), 411–413 (2007).
29. C. Kerse, H. Kalaycıoğlu, P. Elahi, Ö. Akçaalan, and F. Ö. İlday, "3.5-GHz intra-burst repetition rate ultrafast Yb-doped fiber laser," *Opt. Commun.* **366**, 404–409 (2016).
30. Y. Zhao, S.-s. Min, H.-c. Wang, and S. Fleming, "High-power figure-of-eight fiber laser with passive sub-ring loops for repetition rate control," *Opt. Express* **14**(22), 10475–10480 (2006).

31. K. Wei, P. Wu, R. Wen, J. Song, Y. Guo, and X. Lai, "High power burst-mode operated sub-nanosecond fiber laser based on 20/125 $\mu\text{m}$  highly doped Yb fiber," *Laser Phys.* **26**(2), 025104 (2016).
32. K.-H. Wei, P.-P. Jiang, B. Wu, T. Chen, and Y.-H. Shen, "Fiber laser pumped burst-mode operated picosecond mid-infrared laser," *Chin. Phys. B* **24**(2), 024217 (2015).

## NOTES

## NOTES

Vilniaus universiteto leidykla  
Saulėtekio al. 9, III rūmai, LT-10222 Vilnius  
El. p.: [info@leidykla.vu.lt](mailto:info@leidykla.vu.lt), [www.leidykla.vu.lt](http://www.leidykla.vu.lt)  
Tiražas 20 egz.